TECHNISCHE UNIVERSITÄT MÜNCHEN

The Custodially Protected Randall-Sundrum Model: Global Features and Distinct Flavor Signatures

Dissertation

von

Björn Duling

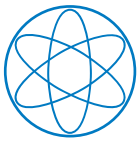

PHYSIK DEPARTMENT

Prof. Dr. Andrzej J. Buras

TECHNISCHE UNIVERSITÄT MÜNCHEN

Lehrstuhl T31 Prof. A. J. Buras
Physik Department
James-Franck-Straße
85748 Garching

The Custodially Protected Randall-Sundrum Model: Global Features and Distinct Flavor Signatures

Björn Duling

Vollständiger Abdruck der von der Fakultät für Physik der Technischen Universität München zur Erlangung des akademischen Grades eines

Doktors der Naturwissenschaften (Dr. rer. nat.)

genehmigten Dissertation.

Vorsitzender: Univ.-Prof. Dr. Lothar Oberauer

Prüfer der Dissertation:

1. Univ.-Prof. Dr. Andrzej J. Buras
2. Hon.-Prof. Dr. Wolfgang F.L. Hollik

Die Dissertation wurde am 25. März 2010 bei der Technischen Universität München eingereicht und durch die Fakultät für Physik am 19. April 2010 angenommen.

Preface

Abstract

Models with a warped extra dimension as first proposed by Randall and Sundrum offer possible solutions to the gauge hierarchy and flavor hierarchy problems. In this thesis we concentrate on the particularly well-motivated Randall-Sundrum model with custodial protection of the T parameter and the $Zb_L\bar{b}_L$ vertex and carefully work out its flavor structure. Based on these results we study how the presence of additional Kaluza-Klein states affects particle-antiparticle oscillations and rare decays and derive analytic expressions for the most relevant K and B physics observables. In the course of the ensuing global numerical analysis we confirm the stringent bound on the Kaluza-Klein mass scale which is imposed by indirect CP violation in $K^0 - \bar{K}^0$ oscillations. Yet, we are able to show that agreement with all available data on $\Delta F = 2$ observables can be obtained for TeV-scale Kaluza-Klein masses without significant fine tuning. Furthermore we find large possible effects in CP violation in $B_s - \bar{B}_s$ oscillations as well as in rare K decays, which however are mutually exclusive. The impact on rare decay branching ratios of B mesons on the other hand turns out to be small and very challenging to measure in the near future. In addition we identify a number of distinct correlations between different observables and find that a very specific pattern of flavor violation is present. This pattern can be used to distinguish the model under consideration from other frameworks of new physics, as we demonstrate explicitly for the Littlest Higgs model with T-parity and the Standard Model with a sequential fourth generation of quarks and leptons.

Zusammenfassung

Modelle mit einer gekrümmten zusätzlichen Raumdimension, wie sie zuerst von Randall und Sundrum vorgeschlagen wurden, ermöglichen sowohl eine Lösung des Hierarchieproblems als auch des Flavorproblems. In der vorliegenden Arbeit konzentrieren wir uns auf ein besonders fundiertes Randall-Sundrum Modell, in dem der T-Parameter und die $Zb_L\bar{b}_L$ Kopplung vor großen Korrekturen geschützt sind, und erarbeiten sorgfältig seine Flavorstruktur. Ausgehend hiervon untersuchen wir, wie die Existenz zusätzlicher, massiver Kaluza-Klein-Zustände die Meson-Antimeson Mischung und seltene Mesonenzerfälle beeinflusst und leiten hierzu analytische Ausdrücke für die wichtigsten Ober-

vablen in den K und B Mesonensystemen ab. Im Laufe der anschließend durchgeführten globalen numerischen Analyse bestätigen wir zunächst den strengen Mindestwert für die Massenskala der Kaluza-Klein-Zustände, welcher durch die indirekte CP-Verletzung in der Mischung von $K^0 - \bar{K}^0$ Mesonen notwendig gemacht wird. Zugleich gelingt es uns aber zu zeigen, dass auch für Kaluza-Klein-Massen von der Größenordung der TeV-Skala eine Übereinstimmung der Modellvorhersagen mit allen verfügbaren experimentellen $\Delta F = 2$ Resultaten ohne großes Feintuning möglich ist. Darüber hinaus finden wir eine potentiell große CP-Verletzung in der Mischung von $B_s - \bar{B}_s$ Mesonen sowie große Effekte in seltenen Kaon-Zerfällen, wobei jedoch beide Effekte nicht gleichzeitig auftreten können. Die Auswirkungen auf die seltenen Zerfälle von B-Mesonen erweisen sich als deutlich kleiner und ihre Messung stellt in naher Zukunft eine große Herausforderung dar. Zusätzlich zeigen wir eine Reihe von deutlichen Korrelationen zwischen verschiedenen Observablen auf und folgern, dass die Flavorverletzung im vorliegenden Fall einem charakteristischen Muster folgt. Mit Hilfe dieses Musters ist es möglich, das betrachtete Modell von anderen Modellen neuer Physik zu unterscheiden, wie wir konkret am Beispiel des Littlest Higgs Modells mit T-Parität und des Standardmodells mit einer vierten Generation von Quarks und Leptonen demonstrieren.

Danksagung

An dieser Stelle möchte ich all jenen herzlich danken, die zum Gelingen dieser Arbeit maßgeblich beigetragen haben.

Zuallererst danke ich meinem Betreuer und Doktorvater Prof. Andrzej Buras für die Möglichkeit, in seiner Arbeitsgruppe diese Dissertation anzufertigen, für die enge persönliche Betreuung während der vergangenen vier Jahre, für die einmalige Chance, weitestgehend frei zu forschen und an einer Vielzahl von Konferenzen und Workshops aktiv teilzunehmen und für den gemeinsamen Forschungsaufenthalt an der Cornell University in Ithaca, während dessen ich viel gelernt habe und, mindestens genauso wichtig, eine sehr schöne Zeit verbracht habe. Zuletzt halte ich Dein großzügiges Angebot, mich über die Zeit meiner Promotion hinaus an Deinem Lehrstuhl weiterzubeschäftigen keinesfalls für selbstverständlich und bin aufrichtig dankbar dafür. Danke, Andrzej.

Für die finanzielle Unterstützung durch ein Promotionsstipendium danke ich dem Graduiertenkolleg GRK 1054, *Teilchenphysik im Energiebereich neuer Phänomene*, und in diesem Zusammenhang besonders Prof. Ottmar Biebel, dem Sprecher des Graduiertenkollegs. Weiterhin danke ich der Technischen Universität München, der Universität Heidelberg und dem Institute for Advanced Study der TU München für die Finanzierung einzelner Dienstreisen.

Die vorliegende Dissertation ist aus einer Reihe von Veröffentlichungen erwachsen, und ich bin meinen Kollegen, mit denen zusammen ich an diesen Veröffentlichungen gear-

beitet habe, zu großem Dank verpflichtet. Im Einzelnen sind dies Michaela Albrecht, Monika Blanke, Andrzej Buras, Katrin Gemmler, Stefania Gori und nicht zuletzt Andreas Weiler, dessen anfängliche Hilfe bei der Einarbeitung in die komplexe Materie der RS-Modelle sehr zum Gelingen der vorliegenden Arbeit beigetragen hat.

Ferner möchte ich mich herzlich bei allen Kollegen bedanken, mit denen ich gemeinsam an Veröffentlichungen gearbeitet habe, die keinen Eingang in diese Dissertation gefunden haben. Hier ist die Zusammenarbeit mit Monika Blanke, Andrzej Buras, Anton Poschenrieder, Stefan Recksiegel und Cecilia Tarantino im Rahmen der Untersuchung des Littlest Higgs Modells zu nennen, sowie die Zusammenarbeit mit Andrzej Buras, Thorsten Feldmann, Tillmann Heidsieck, Christoph Promberger und Stefan Recksiegel im Rahmen des 4-Generationen-Projekts. Bei der Arbeit an beiden Projekten habe ich ungemein von den ganz verschiedenen Spezialfähigkeiten meiner Kollegen profitiert.

Spezieller Dank gilt auch meinen Kollegen, mit denen ich über die Jahre ein Büro geteilt habe. Danke, Anton. Für die harmonische und unaufgeregte Zusammenarbeit schon zu Beginn meiner Diplomarbeit, die sicherlich entscheidend dazu beigetragen hat, mich in die Arbeitsgruppe einzuleben. In den unzähligen Diskussionen mit Dir habe ich viele Einsichten über Physik, aber auch über das Leben und den Wissenschaftsbetrieb gewonnen.
Danke, Monika. Für die gute Büroatmosphäre und die sehr effektive Zusammenarbeit, insbesondere im Rahmen der Veröffentlichungen zum RS-Modell. Ohne den ständigen und kritischen Austausch mit Dir wäre eine fehlerfreie numerische Analyse dieses Modells wohl nur schwer möglich gewesen.

Viele meiner Kollegen haben dazu beigetragen, eine gute Arbeitsatmosphäre zu schaffen und so dafür zu sorgen, dass ich gerne nach Garching gekommen bin.
Danke, Michaela. Fürs Zuhören, Motivieren, und für das Korrekturlesen dieser Arbeit.
Danke, Michael. Für das Organisieren nicht nur einer gemeinsamen Reise und den, nennen wir es: freien Gedankenaustausch bei Kaffee und von Dir mitgebrachtem Essen.
Danke, Wolfi. Für Deine freundliche Hilfsbereitschaft, Dein beeindruckend breites physikalisches Wissen und für das schockierend gründliche Korrekturlesen dieser Arbeit.
Danke, David. Durch unsere zuverlässig diametralen Ansichten über jedes x-beliebige Thema habe ich mehr als nur einmal neue, ungeahnte Einsichten gewonnen.
Danke, Christoph. Für so viele wirklich gute Wortspiele. Außerdem sind es immer Dieselben, die bleiben und aufräumen. Und meistens bist Du einer von ihnen.
Danke, Thorsten. Für Neckarzimmern und Deine stetigen Bemühungen, den Laden zusammenzuhalten.
Thank you, Cecila. For agreeing to write my letters of recommendation and for your ever so warm welcome at the SuperB Workshops.
Danke, Alex. Für das Aufzeigen wahrhaft alternativer Lösungsansätze, für Deinen einmaligen Sinn fürs Absurde, dafür, dass Du Dir nicht sofort anmerken lässt, dass Du mehr von Physik verstehst als die Meisten, und für das Korrekturlesen der rohesten aller Rohfassungen.

Besonderer Dank gilt Dir, Stefan, der Du Dich in rührender Art und Weise um die Instandhaltung und Verbesserung des Rechnersystems des Physik Departments kümmerst. Danke, Elke (Krüger). Für Deine Unterstützung in administrativen Angelegenheiten und bei der Beschaffung von Arbeitsmaterial.

I am indebted to the Cornell theoretical elementary particle physics group, in particular Csaba Csaki, Yuval Grossman, Maxim Perelstein and their graduate students, for their warm hospitality during my research visit in March 2009.
I also thank the *Galileo Galilei Institute for Theoretical Physics* in Florence for the hospitality and the INFN for partial support during the completion of this thesis.

Ohne die Hilfe aller bis jetzt Genannten hätte ich diese Arbeit wohl niemals beenden können, aber ohne meine Familie wäre ich niemals so weit gekommen, überhaupt damit anzufangen. Danke, Mama und Papa. Für Eure Unterstützung während der letzten 30 Jahre und für das behütete Umfeld, das Ihr mir geboten habt. Danke, liebe Geschwister Lars und Britta für Euren großen Beitrag hierzu. Und schließlich, völlig zu Unrecht ganz am Schluss danke ich Dir, liebe Simone. Für so viel mehr als ich hier schreiben könnte.

Contents

Chapter 1

Introduction

"Who ordered that?" exclaimed Isidor Rabi upon the discovery of the muon in cosmic rays in 1936. Since then the situation in particle physics has drastically changed. The discovery of any new physics (NP) effect beyond the Standard Model (SM) today would rather be a relief than a nuisance: While the SM is afflicted by a number of conceptual shortcomings that call for its extension, on the other hand it performs remarkably well in accommodating all available data, and no clear indication whatsoever of NP has been observed.

The strongest evidence for the incompleteness of the SM is given by its blindness towards gravity. The electromagnetic, weak and strong forces are an integral part of the SM, while Einstein's theory of general relativity and the SM as a quantum field theory are defined for mutually exclusive physical regimes. However the absence of gravity per se is not the main problem. The strength of the gravitational interactions become comparable to the remaining three forces at the Planck scale, which is roughly $M_{\mathrm{Pl}} \simeq 10^{19}\,\mathrm{GeV}$, while the scale of electroweak (EW) physics is set by the Higgs vacuum expectation value (VEV) $v \simeq 246\,\mathrm{GeV}$. If the SM is assumed to be valid beyond the weak scale and up to the Planck scale where it is replaced by a more fundamental theory, the large separation between the Planck and EW scales is not stable with respect to quantum corrections. Since the Higgs is a scalar particle, its potential is not protected by chiral or gauge symmetries and is thus affected by quantum corrections which are only cut off by the Planck scale. In consequence the generic size of the EW scale is set by the Planck scale unless tremendously fine-tuned cancellations occur. This lack of a plausible mechanism that effectively separates the EW and Planck scales is commonly referred to as the *gauge hierarchy problem*.

A second hierarchy problem of the SM is encountered in its quark sector. The masses of the quarks are measured to be vastly different, ranging over more than five orders of magnitude from the small up quark mass $m_u \sim 0.25\,\mathrm{MeV}$ to the large top quark mass $m_t \sim 170\,\mathrm{GeV}$. A similar observation is made in the mixing of the quarks, where the very hierarchical Cabibbo-Kobayashi-Maskawa (CKM) matrix comprises mixing angles

that differ by almost three orders of magnitude. Unlike the EW scale, these parameters of the SM Lagrangian can be fixed by hand and are protected from excessive quantum corrections by an approximate chiral symmetry. Simply setting the masses and mixing angles to their hierarchic experimental values however contradicts the naturalness principle [1] that requires a physical parameter to be $\mathcal{O}(1)$ unless the degree of symmetry is increased if the parameter is set to zero. The lack of a plausible mechanism that determines the sizes of the SM flavor parameters is referred to as the *flavor hierarchy problem* or *flavor puzzle*.

Numerous attempts to solve the above two problems have been undertaken in the literature. A stabilization of the EW scale is most notably achieved in supersymmetric models [2–5], but also in Technicolor models [6, 7], where electroweak symmetry breaking (EWSB) is induced by the condensate of a strongly coupled sector, or in models of large extra dimensions [8] where the EW scale can be naturally small. Flavor symmetries [9–16] on the other hand are widely employed to address the flavor hierarchy problem. However, while the solution of either problem taken for itself apparently is feasible, a simultaneous treatment of both in a phenomenologically viable theory is an almost unaccomplishable challenge. Supersymmetric flavor models [17–23] are among the most promising efforts in this context, but also these are subject to serious phenomenological tensions [24, 25].

An appealing solution to both problems becomes possible in the framework proposed by Randall and Sundrum (RS) [26]. They suggested to consider a compactified warped extra dimension that is bounded by two 3-branes, referred to as the UV brane and the IR brane. By virtue of the warped metric the effective energy scale depends exponentially on the position along the extra dimension. Thus by localizing gravitational physics on the UV brane and confining the SM fields and the Higgs boson to the IR brane, they were able to address the smallness of the EW scale as compared to the Planck scale in an elegant manner.
Soon however the smallness of the effective energy scale on the IR brane turned out to induce almost unsurmountable tensions with flavor observables and electroweak precision tests (EWPT). This phenomenological problem can be resolved by realizing that the solution of the gauge hierarchy problem only requires the Higgs field to be localized on the IR brane, while all other particles can in principle be allowed to propagate in the five-dimensional (5D) bulk. In fact, promoting the SM gauge bosons and fermions to bulk fields [27–29] and slightly enlarging the bulk gauge group to comprise a custodial symmetry [30] leads to a model that is free from dangerous 4-fermion operators and beyond that is consistent with EWPT, where the most stringent constraints are imposed by the T parameter and the precisely measured $Zb_L\bar{b}_L$ coupling.
Amending the original RS setup in the manner illustrated above turns out to also offer a conceptually novel way of addressing the flavor hierarchy problem: By localizing the bulk quark fields non-uniformly along the extra dimension their hierarchical coupling strength to the Higgs boson can be explained to be of purely geometrical origin. Furthermore, as

the localization properties of the SM quarks are found to depend exponentially on $\mathcal{O}(1)$ parameters, this approach allows to *naturally* generate the large hierarchies in the quark spectrum from a very soft hierarchy in the model parameters. In connection with this geometrical origin of the quark mass hierarchy a so called *RS-GIM mechanism* (named in allusion to the Glashow-Iliopoulos-Maiani mechanism [31] in the SM) arises that keeps flavor changing neutral currents (FCNCs) under control.

In this thesis we will introduce the simplest RS model with custodial protection of the T parameter and the $Zb_L\bar{b}_L$ vertex. This conceptual analysis that partially has been published in [32] is complemented by a full scale phenomenological study of particle-antiparticle oscillations and rare decays in the K and B meson systems. These studies have also been published in [33–36].

The remainder of this work is organized as follows. In chapter 2 we introduce the original RS setup and show in detail how the gauge hierarchy problem is addressed in a 5D space with a warped non-factorizable metric. After detaching the SM fields from the IR brane and developing the formalism that is necessary to describe bulk fields in a warped background we turn towards the phenomenologically motivated RS model with custodial symmetry (RSc) that is characterized by the enlarged gauge group $SU(3)_c \times SU(2)_L \times SU(2)_R \times U(1)_X \times P_{LR}$. We list the full particle content of that model together with the most general bulk action and show how this 5D theory can be reduced to an effective four-dimensional (4D) theory with additional heavy states and modified interaction terms. The flavor structure of the resulting 4D description of the RSc turns out to be very elaborate and will be discussed in great detail in chapter 3. In the course of this analysis we will demonstrate explicitly how the localization properties of bulk fermions can be used to generate the observed hierarchies in the quark masses and mixing angles. Subsequently we will work out the mass matrices and fermion couplings that are present in the RSc. Chapter 4 is devoted to an analysis of the tree level FCNCs mediated by the Z and Higgs bosons as well as the additional Z_H, Z', $A^{(1)}$, $G^{(1)}$ states which are present in the RSc. We will point out how flavor observables related to the oscillations of neutral K and B mesons and to rare K and B decays are affected by these tree level FCNCs and derive expressions for all these observables which are conveniently given in terms of the gauge-fermion and Higgs-fermion couplings worked out in the previous chapter. A global numerical analysis of the most relevant $\Delta F = 2$ and $\Delta F = 1$ observables will be performed in chapter 5. We will show how the severe experimental constraint on the ϵ_K parameter can be satisfied and also impose the other constraints that are available for the $\Delta F = 2$ sector. Our analysis of K and B oscillations will be concluded by a study of CP violation in the B_s system. Subsequently we will turn towards rare K and B decays and give maximal ranges for NP effects in their branching ratios. A considerable part of this study will be devoted to correlations between different rare decay modes as these can be seen as parameter-independent signatures of the model. These characteristic signatures will then be used to contrast the RSc to the Littlest Higgs model with T-parity (LHT) and the SM with a sequential fourth generation of quarks

and leptons (SM4) and to point out how these models could be distinguished by future experiments. Our conclusions will be presented in chapter 6, and a few technical details are relegated to the appendix.

Chapter 2

The Custodially Protected Randall-Sundrum Model

The idea of introducing additional spatial dimensions first arose in Nordstrøm's [37] and shortly afterwards in Kaluza and Klein's [38, 39] attempts to unify Maxwell's theory of electrodynamics and gravity in the first decades of the 20th century. These theories tentatively identified the massless photon with the (55)-component of the metric tensor but eventually turned out to be not quantizable and had to be discarded. Later, in the context of string theory which is only well-defined in 9+1 or 10+1 space-time dimensions [40, 41] extra dimensions re-emerged. In the late 90's they were realized to be a potential solution of the gauge hierarchy problem first in the context of *large extra dimensions*, and most prominently in the Arkani-Hamed-Dimopoulos-Dvali (ADD) model [8] which suggested the presence of two or more compactified large extra dimensions. "Large" in this context refers to sizes of the compactified extra dimensions in the sub-millimeter range, which is barely not excluded by experiments probing gravitational interactions at short distances, for instance the Eötwash gravity balance experiment [42, 43]. In the ADD model the smallness of the weak scale as compared to the observed Planck scale is explained by the fact that the graviton propagates into the large extra dimensions and thus the force of gravity seems to be "diluted" from the standpoint of a four-dimensional observer. The fundamental scale of gravity then can be chosen to be of order of the weak scale since the dilution of the gravitational force is equivalent to a much larger effective suppression scale of gravity in four dimensions. The crucial novelty of this approach is the realization that the Planck scale is not necessarily fundamental—gravity has only been probed directly up to energies corresponding to the millimeter scale [42, 43]—and hence could be of the same size as the weak scale. Explicitly,

$$M_{\mathrm{Pl}}^2 \sim M^{2+n} V_n \,, \tag{2.1}$$

where M_{Pl} is the observed (large) Planck scale, M is the fundamental scale of gravity, n is the number of large extra dimensions and V_n is the volume of the extra-dimensional space. In particular $n = 2$ and compactification radii r_c for the extra dimensions in the

range $100\mu m - 1mm$ can explain the Planck-EW hierarchy while still predicting distinct graviton signatures at near-future collider experiments.
This explanation of the Planck-EW hierarchy however has one conceptual shortcoming: If gravity is to be suppressed by a sufficient amount by introducing only a reasonably small number of extra dimensions, these extra dimensions have to be large in size. But then the typical compactification radius $r_c \sim \mathcal{O}(100\mu m)$ corresponds to an energy scale $\mu_c \sim 1/r_c \sim \mathcal{O}(10^{-3}eV)$ which is much smaller than the EW scale. Thus by explaining the Planck-EW hierarchy, in this way a new unexplained hierarchy between the weak scale and the compactification scale has been introduced.
The RS setup which will be discussed in this chapter approaches the Planck-EW hierarchy problem from a different angle. Also in the RS setup an additional space dimension is introduced with the difference that the 5D space now is warped instead of flat. As a consequence, the fundamental scale of the theory will be Planck-like in contrast to the the ADD model where the EW scale is the only fundamental scale.

2.1 The Original Randall-Sundrum Setup

Inspired by the shortcomings of the ADD approach towards an explanation of the Planck-EW hierarchy, Randall and Sundrum [26] proposed a setup in which this hierarchy is generated by a warped non-factorizable background metric which is defined on the space $M_4 \times S^1/\mathbb{Z}_2$ where M_4 is the ordinary 4D Minkowski space. This metric complies with Poincaré invariance along the ordinary 4D space-time dimensions and is a solution of the 5D Einstein equations for appropriately adjusted cosmological constants on the boundaries and in the bulk of the $S^1/\mathbb{Z}_2$ orbifold. Explicitly, the RS metric is given by

$$ds^2 = e^{-2ky}\eta_{\mu\nu}dx^\mu dx^\nu - dy^2 \equiv g_{MN}dx^M dx^N\,, \tag{2.2}$$

where $y \in [0, L = \pi r_c]$ is the extra-dimensional coordinate, $k \sim M_{\text{Pl}}$ is the curvature scale and $\eta_{\mu\nu} = \text{Diag}(1, -1, -1, -1)$ is the 4D Minkowski metric. In our convention, Greek indices run from 0 to 3, while Latin indices run from 0 to 4.
The boundaries of the extra dimension at $y = 0$ and $y = L$ are referred to as the *ultraviolet* (UV) and *infrared* (IR) brane. The metric for the ordinary 4D space that is induced by (2.2) depends on the position along the extra dimension through the so-called *warp factor* e^{-2ky}. In particular, length and time scales blow up exponentially when moving from the UV brane towards the IR brane[1]. By simple dimensional considerations energy scales are accordingly found to shrink exponentially. Alternatively, the same conclusion is reached if one considers a scalar field that is confined to the IR brane and obtains a VEV [26]. To ensure proper normalization in the 4D theory, a rescaling of this scalar field, and accordingly of its VEV, by a factor of e^{-kL} is necessary. This feature of the metric (2.2) is used to explain the exponential hierarchy between the EW and

[1] This can be seen by considering a fixed proper volume in four dimensions. For larger distances y from the UV brane the warp factor becomes exponentially smaller which has to be balanced by exponentially growing length and time scales.

the Planck scale in the following manner. If the length L of the extra dimension (or equivalently the compactification radius) is chosen to be by a small factor larger than the inverse Planck scale and the Higgs field, whose VEV sets the EW scale, is localized on the IR brane, an exponentially large $v/M_{\rm Pl}$ ratio arises naturally:

$$\frac{v}{M_{\rm Pl}} \simeq e^{-kL} \approx 10^{-16} \quad \text{for } kL \approx 36\,. \tag{2.3}$$

Formally, the compactification radius of the extra dimension arises as the VEV of a modulus field that a priori can take any value [26] and as such needs to be stabilized by some additional mechanism. For instance this can be achieved by introducing additional heavy scalar and fermion fields, as done by Goldberger and Wise [44]. These additional heavy fields radiatively generate an effective potential for the modulus field whose vacuum state then can be adjusted by one's choice of the masses of the heavy fields.

The above setup for our purposes has two parameters: the curvature scale k and the compactification radius r_c or equivalently the length L of the extra-dimensional interval. As the product $kL \simeq 36$ is fixed by the requirement of addressing the Planck-EW hierarchy, it is convenient to swap the parameter L for the mass scale of the lightest excited KK states $f_{\rm RS} = ke^{-kL} \sim \mathcal{O}(\,\text{TeV})$. Beyond these two geometric parameters there are in principle further parameters such as the bulk and brane cosmological constants and the masses of the heavy scalars and fermions introduced to stabilize the compactification radius. We will however not include these additional parameters into our parameter counting since they are fixed once the compactification radius and the metric are specified.

As a final remark on the original geometric setup [26] we want to point out that the warped metric (2.2) corresponds to a slice of 5D anti-de-Sitter space (AdS_5) between the two boundaries at $y = 0$ and $y = L$. This observation has significant implications since a theory in AdS_5 is related to a 4D conformal field theory (CFT) without gravity on the boundary of the AdS_5 space via the AdS/CFT duality. This correspondence is a special case of the Maldacena conjecture [45]. A large number of applications of this correspondence have been discussed in the literature (see for instance [46–51]), among them those in which the extra-dimensional setup is used as a mere tool for making strongly coupled theories, such as Technicolor, calculable by relating them to models with warped extra dimensions.

The RS setup can be used as a basis for realistic models of EWSB [30, 50, 52–55] and gauge coupling unification [56, 57]. We will not discuss these issues in the following but concentrate on the modifications of the original RS setup that lead to the construction of the custodially protected RS model (RSc).

2.2 The Standard Model in the Bulk

In the original RS setup [26] all force and matter fields except for the graviton are localized on the IR brane of the extra dimensional space. In a strict sense this localization is only required for the Higgs field in order to ensure that the EW scale is stabilized by the warped down cut-off $M_{\rm Pl}e^{-kL}$. All remaining fields, the SM fermions and gauge bosons, can in principle be allowed to propagate in the extra dimension. In fact, constraining the SM to the IR brane bears phenomenological problems. The only available effective energy scale on the IR brane is given by the EW scale. Hence non-renormalizable higher dimensional operators involving fermions and gauge bosons are generically only suppressed by powers of the EW scale, according to their individual dimension. Experimentally on the other hand, these non-renormalizable operators are strongly constrained. For instance, EWPT set a lower bound on the effective suppression scale $\Lambda \gtrsim (5-10)\,\text{TeV}$, which is a manifestation of the well known *little hierarchy problem*. Much more severe are the constraints that arise when proton decay or flavor observables, such as the infamous and very precisely measured observable ϵ_K are considered. This observable is strongly affected by left-right operators that are enhanced by renormalization group (RG) effects and chiral factors. To suppress contributions from non-renormalizable operators at a sufficient level, an effective suppression scale far beyond the EW scale [58],

$$\Lambda \gtrsim (10^4 - 10^5)\,\text{TeV}\,, \tag{2.4}$$

is required. Discrete symmetries can in principle forbid the unwanted higher-dimensional operators, but these operators have to be suppressed up to very high orders due to the extreme discrepancy between the EW scale and the required suppression scale (2.4).
In view of these facts it is a natural development to allow all SM fields except for the Higgs field to propagate in the extra-dimensional bulk. In this case the effective suppression scale felt by the light fermions can be much larger than the one cutting off radiative corrections to the Higgs mass and dangerous non-renormalizable operators can be sufficiently suppressed.
We will for this reason from now on consider a RS setup in which the Higgs boson is localized on the IR brane of the 5D space, while all SM fermions and gauge bosons can propagate freely in the extra-dimensional bulk. A comprehensive study analyzing the behavior of fields of different spin in a 5D theory was performed in [59]. Historically, the gauge bosons were the first to be allowed to propagate into the bulk [27,28], to be shortly afterwards followed by the fermion fields. In [29] massless fermion fields were analyzed and it was found that in this case all bulk fermion fields are localized exponentially towards the IR brane. Since however in odd numbers of space-time dimensions any theory of fermions is necessarily non-chiral, bulk mass terms are in general allowed. Their impact was investigated in [60] and it was found that the localization of fermionic zero modes depends exponentially on these mass terms. This property of the localization of fermionic zero modes has far-reaching consequences on the flavor structure of the RSc model and allows to address the flavor puzzle in an utterly novel way as we will discuss in section 3.2.

2.2.1 Bulk Dynamics of Free Fields

The dynamics of the different bulk fields can be obtained from the free 5D action in which all interaction terms have been set to zero. This action is given by

$$S_{\text{free}} = \int_0^L dy \int d^4x \, \sqrt{g} \left[-\frac{1}{4} F_{MN} F^{MN} + \frac{1}{2} \bar{\psi} \left(i \Gamma^M (\partial_M + \omega_M) - m_\psi \right) \psi \right] + h.c. \,, \tag{2.5}$$

where $F_{MN} = \partial_M A_N - \partial_N A_M$ is the field strength tensor, $m_\psi = ck$ is the fermion bulk mass, Γ^M are the Dirac matrices in curved space-time and $\sqrt{g}$ is the Lorentz-invariant measure of integration. The spin-connection ω_M accounts for the dependence of Lorentz transformations on the position along the extra dimension and will drop out in the derivation of the bulk equations of motion (EOMs).

In the above free action we did not bother to include the Higgs kinetic terms and the Higgs potential, since we committed ourselves to the brane Higgs case. For illustration and to be later able to extrapolate from a brane localized Higgs to more general scenarios we however state that

$$S_{\text{free}}^{\text{Higgs}} = \int_0^L dy \int d^4x \, \sqrt{g} \left[(\partial_M H)^\dagger (\partial^M H) - V(H) \right] \,, \tag{2.6}$$

where the $V(H)$ is the Higgs potential.

Applying the variational principle $\delta S_{\text{free}} = 0$ to (2.5), (2.6) and following the discussion in [59] we find[2]

$$\left[-e^{2ky} \eta^{\mu\nu} \partial_\mu \partial_\nu + e^{sky} \partial_5 (e^{-sky} \partial_5) - M_\Phi^2 \right] \Phi(x^\mu, y) = 0 \,. \tag{2.7}$$

This equation summarizes the EOMs of gauge fields, fermions and scalars in a compact form. In the case of gauge fields, $\Phi \equiv A_\mu$, $s = 2$ and $M_\Phi^2 = 0$, while in the case of fermions $\psi_{L,R}$ has to be rescaled by $\Phi = e^{-2ky} \psi_{L,R}$ with $s = 1$ and $M_\Phi^2 = c(c \pm 1)k^2$ for the left- and right-handed modes. For a bulk scalar field one has to set $\Phi = H$, $s = 4$ and the particular form of M_Φ^2 depends on the Higgs potential $V(H)$.

The first step towards solving the differential equation (2.7) is to separate the dependence on the 4D coordinate x^μ and on y. This can be achieved via a *Kaluza-Klein (KK) decomposition* of the bulk fields,

$$\Phi(x^\mu, y) = \frac{1}{\sqrt{L}} \sum_{n=0}^{\infty} \phi^{(n)}(x^\mu) f^{(n)}(y) \,. \tag{2.8}$$

[2]Note that in [59] a different convention for the metric tensor is used, and that therein $\eta_{\mu\nu} = \text{Diag}(-1, +1, +1, +1)$.

Before we proceed, we want to make some comments about the KK decomposition (2.8). It implies that for a 4D observer each bulk field in 5D space manifests itself as an infinite KK tower of particle solutions $\phi^{(n)}(x^\mu)$. The dependence of these particle solutions on the extra-dimensional coordinate is encapsuled in the *bulk profiles* or *shape functions* $f^{(n)}(y)$. In the more intuitive limiting case of a flat extra-dimensional space, that is for $k \to 0$, the y-dependence on the r.h.s. of (2.8) would be described by sine and cosine functions with ever decreasing wavelengths corresponding to heavier and heavier particles.
Inserting the KK-decomposition (2.8) into the EOMs (2.7) we obtain

$$\left[\partial_5^2 - sk\partial_5 - (M_\Phi^2 - e^{2ky} m_n^2)\right] f^{(n)}(y) = 0\,, \tag{2.9}$$

where m_n is the mass of the n-th KK mode,

$$\eta^{\mu\nu}\partial_\mu\partial_\nu \phi^{(n)}(x^\mu) = m_n^2 \phi^{(n)}(x^\mu)\,. \tag{2.10}$$

The EOMs (2.9) are second order differential equations, and as such their solutions $f^{(n)}(y)$ are ambiguous unless two additional conditions are specified. We can choose these to be the boundary conditions (BCs) of the bulk profiles on the UV and IR branes. In principle there are no constraints on how these BCs have to be chosen, but the most applicable ones are referred to as *Dirichlet* and *Neumann* BCs:

Neumann $(+)$ **BC**

$$\partial_5 f^{(n)}(y)\Big|_{\text{brane}} = 0\,, \tag{2.11}$$

Dirichlet $(-)$ **BC**

$$f^{(n)}(y)\Big|_{\text{brane}} = 0\,. \tag{2.12}$$

In the following we will write $(+-)$ for a Neumann BC on the UV brane and Dirichlet BC on the IR brane and accordingly for the remaining combinations of BCs.

The above approach of neglecting all interaction terms, in particular the Higgs interactions, and first working with the action for free fields S_{free} is referred to as the *perturbative approach*. In this approach the non-interacting EOMs are solved and afterwards—as we will do in chapter 3—the various couplings and mass matrices are worked out. The effects of EWSB then are treated as small perturbations to these mass matrices and amount to $\mathcal{O}(v^2/M_{\text{KK}}^2)$ corrections which shift the masses of the heavy KK modes and induce mixing between modes of different KK levels.
The exact approach on the other hand, in which terms proportional to the Higgs VEV v are included into the action, results in modified BCs on the IR brane for the fermions and gauge bosons. The shape functions that are now obtained as solutions of the EOMs are slightly distorted near the IR brane. These distorted modes already encode the effects of EWSB and correspond to mass eigenstates which obey orthonormality relations.
Both approaches have advantages and disadvantages; for instance the perturbative approach is more intuitive but at the same time can only be an approximation as long as

only a finite number of KK modes is taken into account. The exact approach on the other hand automatically includes the effects of the infinite towers of KK modes, but also is less intuitive and obscures interesting features of the model such as cancellations among contributions from different gauge eigenstates to physical observables. We will continue to employ the perturbative approach, and it has been shown in [32, 61] that both approaches lead to equivalent results.

2.2.2 Gauge Fields

To eventually solve the EOMs (2.9) we have to consider gauge bosons and fermions separately. For gauge bosons the KK decomposition reads

$$V_\mu(x^\mu, y) = \frac{1}{\sqrt{L}} \sum_{n=0}^{\infty} V_\mu^{(n)}(x^\mu) f_{\text{gauge}}^{(n)}(y)\,, \tag{2.13}$$

and we obtain for the gauge KK modes [59]

$$f_{\text{gauge}}^{(0)}(y) = 1\,, \tag{2.14}$$

$$f_{\text{gauge}}^{(n)}(y) = \frac{e^{ky}}{N_n}\left[J_1\left(\frac{m_n}{k}e^{ky}\right) + b_1(m_n) Y_1\left(\frac{m_n}{k}e^{ky}\right)\right] \qquad (n = 1, 2, \dots)\,, \tag{2.15}$$

where $J_1(x)$ and $Y_1(x)$ are the Bessel functions of first and second kind. It is important to note that the flat zero mode $f_{\text{gauge}}^{(0)}(y)$ exists only for $(++)$ BCs. An interesting and phenomenologically important feature of the warped geometrical background is that all higher gauge boson modes are strongly peaked towards the IR brane which can be seen from the e^{ky} factor in (2.15). In fig. 2.1 we show the profile functions of the first KK modes with $(++)$ and $(-+)$ BCs.
The bulk profiles $f_{\text{gauge}}^{(n)}(y)$ for given BCs satisfy the orthonormality conditions

$$\frac{1}{L}\int_0^L dy\, f_{\text{gauge}}^{(n)}(y) f_{\text{gauge}}^{(m)}(y) = \delta_{nm}\,. \tag{2.16}$$

The coefficient $b_1(m_n)$ and m_n depend on the boundary conditions on the branes. For $(++)$ fields one obtains [59]

$$b_1(m_n) = -\frac{J_1(m_n/k) + m_n/k\, J_1'(m_n/k)}{Y_1(m_n/k) + m_n/k\, Y_1'(m_n/k)} = b_1(m_n e^{kL})\,, \tag{2.17}$$

which can only be solved numerically for m_n and $b_1(m_n)$. For large values of n, the result can be well approximated by [59]

$$b_1(m_n) = 0\,, \qquad m_n^{\text{gauge}} \simeq \left(n - \frac{1}{4}\right)\pi f_{\text{RS}} \qquad (n = 1, 2, \dots)\,, \tag{2.18}$$

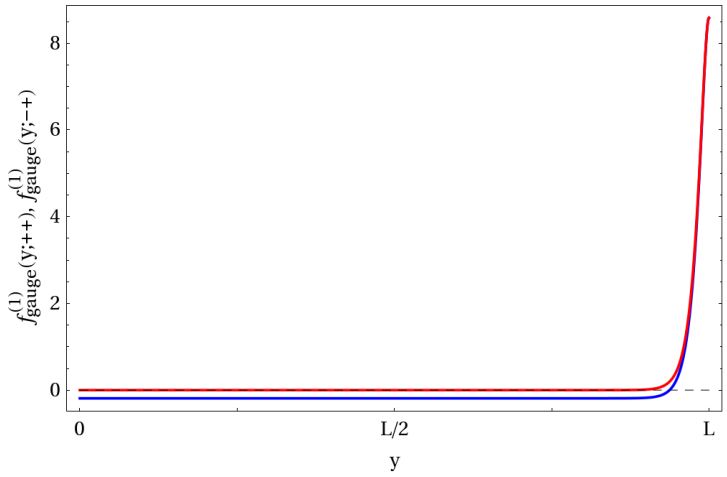

Figure 2.1: The first gauge boson KK modes for $(++)$ (blue, lower curve) and $(-+)$ (red, upper curve) BCs.

however for small values of n it is safer to use the exact numerical result. For the first excited $(++)$ mode for instance we find

$$m_1^{\rm gauge}(++) \simeq 2.45 k e^{-kL} \equiv 2.45 f_{\rm RS} \equiv M_{++}\,, \tag{2.19}$$

where we have introduced the effective new physics scale $f_{\rm RS} \equiv k e^{-kL}$. For $(-+)$ fields m_n and $b_1(m_n)$ have to be determined by solving

$$b_1(m_n) = -\frac{J_1(m_n/k)}{Y_1(m_n/k)} = -\frac{J_1(m_n e^{kL}/k) + m_n e^{kL}/k\, J_1'(m_n e^{kL}/k)}{Y_1(m_n e^{kL}/k) + m_n e^{kL}/k\, Y_1'(m_n e^{kL}/k)}\,. \tag{2.20}$$

In this case we find for the mass of the first excited mode

$$m_1^{\rm gauge}(-+) \simeq 2.40 k e^{-kL} \equiv 2.40 f_{\rm RS} \equiv M_{-+}\,, \tag{2.21}$$

which corresponds to a $\sim 2\%$ suppression of $m_1^{\rm gauge}$ with respect to the $(++)$ case. Finally, the constant N_n in (2.15) has to be determined from the normalization condition (2.16). For fields (also fermions and scalars) with a Neumann BC on the IR brane, N_n is approximately given by [59]

$$N_n \simeq \frac{e^{kL/2}}{\sqrt{\pi L m_n}}\,. \tag{2.22}$$

Note that this approximation is *not* valid in case of a Dirichlet BC on the IR brane.

We conclude the treatment of bulk gauge bosons with some remarks on the fixing of a suitable gauge. The BCs of a gauge field V_μ automatically imply *opposite* BCs for its 5-component. In the RSc model no gauge fields with a Dirichlet BC on the IR brane are present, and hence there is no massless 5-component for any gauge field. This allows us to work in the $V_5 = 0$, $\partial_\mu V^\mu = 0$ gauge for all gauge bosons and entirely disregard their 5-components.

2.2.3 Fermion Fields

For fermions the KK decomposition reads

$$\psi_{L,R}(x^\mu, y) = \frac{e^{2ky}}{\sqrt{L}} \sum_{n=0}^{\infty} \psi_{L,R}^{(n)}(x^\mu) f_{L,R}^{(n)}(y)\,, \tag{2.23}$$

and the fermionic modes are given by [59]

$$f_L^{(0)}(y) = \sqrt{\frac{(1-2c)kL}{e^{(1-2c)kL}-1}} e^{-cky}\,, \tag{2.24}$$

$$f_L^{(n)}(y) = \frac{e^{ky/2}}{N_n}\left[J_\alpha\left(\frac{m_n}{k}e^{ky}\right) + b_\alpha(m_n) Y_\alpha\left(\frac{m_n}{k}e^{ky}\right)\right] \qquad (n = 1, 2, \dots)\,, \tag{2.25}$$

where $\alpha = |c+1/2|$ and again $f_L^{(0)}(y)$ exists only for $(++)$ BCs for the left-handed mode. The right-handed modes automatically obey BCs opposite to those of the left-handed modes and their bulk profiles $f_R^{(n)}(y)$ can be obtained from $f_L^{(n)}(y)$ by replacing $c \to -c$ in the above formulae. The $f_{L,R}^{(n)}(y)$ for given BCs satisfy the orthonormality conditions

$$\frac{1}{L}\int_0^L dy\, e^{ky} f_{L,R}^{(n)}(y) f_{L,R}^{(m)}(y) = \delta_{nm}\,. \tag{2.26}$$

From (2.26) we see that the fermionic profiles with respect to the flat tangent space metric are given by

$$\tilde{f}_L^{(0)} = \sqrt{\frac{(1-2c)kL}{e^{(1-2c)kL}-1}} e^{(\frac{1}{2}-c)ky}\,, \tag{2.27}$$

$$\tilde{f}_L^{(n)} = \frac{e^{ky}}{N_n}\left[J_\alpha\left(\frac{m_n}{k}e^{ky}\right) + b_\alpha(m_n) Y_\alpha\left(\frac{m_n}{k}e^{ky}\right)\right] \qquad (n = 1, 2, \dots)\,, \tag{2.28}$$

where the factor e^{ky} in (2.26) has been absorbed into the the shape functions to make the localization of the zero mode more explicit. In particular we find that the left-handed zero mode $\tilde{f}_L^{(0)}$ is flat for $c = \frac{1}{2}$, peaked towards the UV brane for $c > \frac{1}{2}$ and peaked towards the IR brane for $c < \frac{1}{2}$. In fig. 2.2 we show the fermion zero mode profile for three different bulk mass parameters as well as the first KK mode profile.

As in the gauge boson case, $b_\alpha(m_n)$ and m_n are determined through the BCs on the branes. In the case of left-handed fermions, a $(-)$ BC implies

$$f_L^{(n)}(y)\Big|_{\text{brane}} = 0\,, \tag{2.29}$$

while the $(+)$ BC is modified with respect to the gauge field case and reads

$$(\partial_y + ck) f_L^{(n)}(y)\Big|_{\text{brane}} = 0\,. \tag{2.30}$$

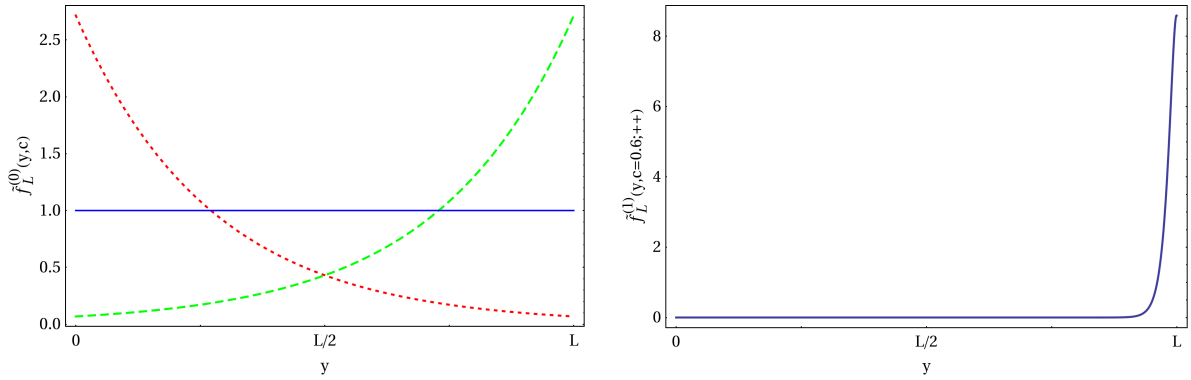

Figure 2.2: Left panel: Fermion zero mode profiles for $c = 0.6$ (red, dotted), $c = 0.5$ (blue, solid) and $c = 0.4$ (green, dashed). Right panel: Fermion KK mode for $(++)$ BCs and $c = 0.6$.

For right-handed fields, again the replacement $c \to -c$ has to be made. $b_\alpha(m_n)$ and m_n are derived completely analogously to the gauge boson case and also here the resulting equations can only be solved numerically. An approximate expression for the fermion masses however is given by

$$m_n^{\text{fermion}} \simeq \left(n + \frac{1}{2}\left(\left| c + \frac{1}{2} \right| - 1 \right) \mp \frac{1}{4} \right) \pi f_{\text{RS}} \,, \tag{2.31}$$

where the $\mp$ sign corresponds to a $(\pm)$ BC for the left-handed fermion mode on the IR brane. As with the analogous expressions for gauge boson masses, the accuracy of this approximation improves with increasing n.

In the discussion above we defined the left- and right-handed fermion modes $f_{L,R}^{(n)}$. However, in any odd number of space-time dimensions, no chiral representations of the Lorentz group exist. We were able to introduce the left- and right-handed fermion modes because just as in four dimensions we can decompose a fermion field ψ into its components ψ_+ and ψ_- that are eigenstates of the γ_5 operator,

$$\gamma_5 \psi_+ = +\psi_+ \,, \quad \gamma_5 \psi_- = -\psi_- \,. \tag{2.32}$$

Unlike however in the 4D case, where ψ_- and ψ_+ sit in the $(2,1)$ and $(1,2)$ representations of the Lorentz group, in 5D they are parts of the same representation. This is a serious problem since in the low energy limit we want to reproduce the SM, which is a genuinely chiral theory in which left- and right-handed fields transform differently under the $SU(2)_L$ gauge symmetry group. A solution to this problem is given by the above observation that the ψ_+ and ψ_- components of a fermion field have to obey opposite boundary conditions. Whenever a ψ_+ mode has $(++)$ BCs and accordingly contains a massless zero mode, its ψ_- counterpart comprises only heavy modes, and vice versa. This allows to introduce a separate multiplet for each chiral component of a SM fermion, such that for each generation of SM quarks three multiplets are needed: $Q_L(++)$, $u_R(--)$, $d_R(--)$, where the BCs are given for the respective ψ_- components. Since in each of these multiplets

either the ψ_+ or the ψ_- mode, but not both, contain a massless zero mode, it is now possible to identify the ψ_- component with a left-handed fermion and the ψ_+ component with a right-handed fermion such that in the end a chiral theory is obtained.
If finally the BCs of the left-handed mode are either $(+-)$ or $(-+)$, both the left- and right-handed fields consist of heavy modes only.

To conclude this discussion of fermion bulk dynamics we want to point out that the fermion bulk mass parameters c are generation dependent, such that for instance they can be different for the up- and top-quark. We have seen above that for each quark generation in the SM three different multiplets are necessary to obtain a chiral 4D theory. Each of these multiplets comes in three distinct copies that correspond to the three quark generations, such that we end up with nine potentially different bulk mass parameters. To unambiguously address the bulk mass parameters c we introduce the notation c^i_k where i is the flavor index and k denotes the particular multiplet. We will return to the issue of assigning the SM quarks to multiplets of the bulk gauge group in section 2.5.3.

2.2.4 Scalar Fields

Although in the framework considered in this thesis we assume that the Higgs field is strictly confined to the IR brane, and therefore no bulk scalars are present, for completeness we also solve the EOMs for this case. Inserting the KK decomposition for bulk scalars

$$H(x^\mu, y) = \frac{1}{\sqrt{L}} \sum_{n=0}^{\infty} H^{(n)}(x) h^{(n)}(y) \tag{2.33}$$

into the EOMs (2.7) with $s = 4$ and $M_\Phi^2 = ak^2$, we find that the general solution yields zero for either choice of BCs. A non-vanishing solution can only be obtained if a boundary mass term $\mp 2\beta k$ with $\beta = 2 \pm \alpha \equiv 2 \pm \sqrt{4+a}$ is introduced on the UV and IR branes. Then, the solution reads

$$h(y) = \sqrt{\frac{2kL(\beta-1)}{e^{2kL(\beta-1)}-1}} e^{\beta k y} \,. \tag{2.34}$$

We can now swap the parameter a for β which controls the localization of the scalar zero mode. For $\beta < 1$ ($\beta > 1$) the mode is localized towards the UV (IR) brane and it is flat for $\beta = 1$. For $\beta \gg 1$, which is a reasonable choice if the scalar mode is to represent a bulk Higgs field, (2.34) simplifies to

$$h(y) = \sqrt{2kL(\beta-1)} e^{kL} e^{\beta k(y-L)} \,. \tag{2.35}$$

In the limit $\beta \to \infty$ the brane Higgs case is recovered. Instead of taking this limit, for calculational purposes it is more convenient to replace the Higgs bulk profile by a δ-function, $h(y) \to \sqrt{L} e^{-ky} \delta(y-L)$.

The scalar KK modes finally are given by

$$h^{(n)}(y) = \frac{e^{2ky}}{N_n}\left[c_1 J_\alpha\left(\frac{m_n}{ke^{-ky}}\right) + c_2 Y_\alpha\left(\frac{m_n}{ke^{-ky}}\right)\right], \tag{2.36}$$

where $c_{1,2}$ are arbitrary constants, the N_n have to be chosen such that the modes are normalized properly,

$$\frac{1}{L}\int_0^L dy\, e^{-2ky} h^{(n)}(y) h^{(m)}(y) = \delta_{nm}\,, \tag{2.37}$$

and the m_n are approximately given by

$$m_n \approx \left(n + \frac{1}{2}\sqrt{4+a} - \frac{3}{4}\right)\pi f_{\mathrm{RS}}\,. \tag{2.38}$$

Typically, the scalar KK modes are significantly heavier than the gauge and fermion KK modes and can be neglected in phenomenological analyses [59].

2.3 The Gauge Group of the RSc

In this section we want to briefly review the phenomenological constraints from EWPT imposed on the RS model with bulk fermions and point out how an enlarged bulk gauge group can contribute to satisfy these constraints. Since a simultaneous fit of oblique and non-oblique corrections is beyond the scope of this thesis (see however [62–71]) we will focus on the three most stringent individual constraints. These are the Peskin-Takeuchi S and T parameters [62] as well as the anomalous $Zb_L\bar{b}_L$ coupling.

The T parameter is sensitive to the breaking of the custodial symmetry and can be seen as a measure for the total isospin breaking of the NP sector. It is easy to see that in the RS model as discussed until now isospin is already broken at the tree level [72]: After EWSB the gauge boson zero modes mix with their heavy KK partners and thereby obtain slightly distorted shape functions. Since these distortions are non-universal for the different gauge bosons, isospin is necessarily broken. It is therefore no surprise that for the RS model with bulk SM fields excessive contributions to the T parameter are found [72–75]. This is in clear contrast to the combined fit [76] of LEP data which yields a rather small value for the T parameter,

$$T = 0.02 \pm 0.09\,, \tag{2.39}$$

where $M_H = 117\,\mathrm{GeV}$ and $U = 0$ have been assumed. To reconcile the RS model in its present form with this small value requires specific fermion localization patterns and even in the most favorable case still imposes a bound on the KK scale of typically 10 TeV which is beyond the reach of the LHC. At first sight this result is surprising, since the

brane localized Higgs sector has a custodial symmetry even after EWSB and one naïvely would expect that corrections to the T parameter therefore are small.
This puzzle has been resolved in [30] where it has been shown that the custodial symmetry needs to be gauged in order to be effective[3] and that enlarging the bulk gauge group by an additional $SU(2)_R$ factor virtually eliminates corrections to the T parameter at tree level. With this additional gauge factor, the bulk gauge group is given by

$$SU(3)_c \times SU(2)_L \times SU(2)_R \times U(1)_X \,, \tag{2.40}$$

where the inclusion of $U(1)_X$ is necessary in order to obtain the correct hypercharges.

The S parameter on the other hand is isospin symmetric and is associated with the (UV finite part of the) momentum dependence of the Z boson self energy. As it is independent of isospin breaking effects it can be thought of as a measure of the total size of the NP sector and it is not protected by the custodial symmetry. In fact, for a RS setup with the above gauge group (2.40) the S parameter is found as

$$S \approx \frac{12\pi v^2}{M_{\mathrm{KK}}^2} \,, \tag{2.41}$$

which in conjunction with the result of the combined EW fit [76],

$$S = 0.04 \pm 0.09 \,, \tag{2.42}$$

yields the lower bound for the mass of the lightest KK gauge boson,

$$M_{\mathrm{KK}} \gtrsim (2-3)\,\mathrm{TeV} \,. \tag{2.43}$$

In addition to the oblique corrections which are parameterized by S, T, U, we also have to consider non-oblique corrections. The phenomenologically most relevant of these are corrections to the $Zb_L\bar{b}_L$ coupling which are experimentally bounded by [76]

$$-2 \cdot 10^{-3} \lesssim \delta g_{Zb_L\bar{b}_L} \lesssim 6 \cdot 10^{-3} \quad (\text{at } 95\% \text{ C.L.}) \,. \tag{2.44}$$

In the RS setup with bulk fermions the corrections to the $Zb_L\bar{b}_L$ coupling are found to have the parameter dependence [30]

$$\delta g_{Zb_L\bar{b}_L} \propto \frac{1-2c}{3-2c}\frac{1}{M_{\mathrm{KK}}^2} \,, \tag{2.45}$$

[3]This becomes evident if the 4D CFT dual [77] of the model is considered. Here the Higgs boson corresponds to a light composite state of the CFT. Since a global symmetry in the CFT corresponds to a gauge symmetry in 5D, the custodial symmetry needs to be gauged in order to protect the Higgs sector.

where c is the localization parameter of the (t_L, b_L) quark doublet. The closer the b_L is localized towards the IR brane the larger the correction, the closer it is localized towards the conformal point ($c = 1/2$) the smaller the correction. The obvious choice for satisfying the experimental constraint (2.44) for not too large $M_{\rm KK}$, that is to simply localize the b_L very close to the conformal point, does not work since in this case the large top mass cannot be reproduced anymore. Fortunately, the gauged custodial symmetry that was introduced to protect the T parameter can also be used to keep corrections to the $Zb_L\bar{b}_L$ coupling under control [78]. For the custodial symmetry to unfold its protective effect also in this case, we need to impose the additional discrete $\mathbb{Z}_2$ symmetry that relates the two $SU(2)$ gauge factors to each other[4],

$$P_{LR}: \; SU(2)_L \leftrightarrow SU(2)_R \,. \tag{2.46}$$

This requires that the $SU(2)_{L,R}$ coupling constants are equal, $g_L = g_R \equiv g$, and that all fermions are embedded into P_{LR} symmetric representations of the bulk gauge group. Finally, the b_L needs to be embedded in a multiplet such that it is a P_{LR} eigenstate, or in other words, $T_R^3 = T_L^3$. If this is the case, the $Zb_L\bar{b}_L$ coupling is protected by the P_{LR} symmetry to all orders, and so are the couplings of all other quarks for which $T_R^3 = T_L^3$ holds. In the following we will see that this is in particular the case for the $Zd_L^i\bar{d}_L^j$ and $Zu_R^i\bar{u}_R^j$ couplings ($i, j = 1, 2, 3$).

The final gauge group, which we will consider in the remainder of this thesis, is the following:

$$SU(3)_c \times SU(2)_L \times SU(2)_R \times U(1)_X \times P_{LR} \,. \tag{2.47}$$

With this gauge group, the multiplet assignment of the b_L quark and the other SM quarks discussed above and a KK scale satisfying the bound $M_{\rm KK} \gtrsim (2-3)\,\text{TeV}$ all constraints from EWPT are satisfied at the tree level[5].

2.4 Projection to Four Dimensions

Through the KK decomposition (2.8) the road towards "condensing" the 5D theory to a 4D theory with additional heavy states and modified SM couplings has been opened. By separating the dependence of the fields on ordinary 4D space coordinates x^μ and the extra-dimensional coordinate y we can effectively perform the integration over the fifth dimension,

$$S = \int_0^L dy \int d^4x\, \mathcal{L} \;\rightarrow\; \int d^4x\, \mathcal{L}' \,. \tag{2.48}$$

[4]The imposition of this discrete symmetry can in fact be motivated by considering a custodial $O(4)$ symmetry which decomposes as $O(4) \sim SU(2)_L \times SU(2)_R \times P_{LR}$.

[5]In particular the T parameter receives loop corrections that are due to the breaking of the custodial symmetry by BCs on the UV brane, as was pointed out in [55], and we will return to this issue in section 3.2.2.

The interaction terms in the effective 4D Lagrangian density $\mathcal{L}'$ comprise *overlap integrals* of the shape functions.
The most important role in our analysis will be played by the gauge-fermion couplings obtained in the procedure of integrating over the extra dimension. The SM gauge-fermion couplings, which involve fermionic zero modes and gauge boson zero modes, at leading order are not modified as the gauge zero modes (2.14) are distributed flatly along the extra dimension and hence the normalization condition (2.26) for the fermionic zero modes applies. On the other hand there now also are interactions between KK gauge bosons and SM fermions. To discuss these couplings we introduce the shorthand

$$g(y) = f^{(1)}_{\text{gauge}}(y, (++)) \tag{2.49}$$

for the bulk profiles of $Z^{(1)}$ and $W_L^{(1)}$ (as well as for the KK gluons $G^{(1)a}$ and KK photon $A^{(1)}$), and

$$\tilde{g}(y) = f^{(1)}_{\text{gauge}}(y, (-+)) \tag{2.50}$$

for the bulk profiles of $Z_X^{(1)}$ and $W_R^{(1)}$. The overlap integrals for KK gluonic and photonic currents and for the ones for the KK modes $Z^{(1)}$ and $W_L^{(1)}$ then are given by

$$\underset{nm}{\mathcal{R}^i_k}(BC)_{L,R} = \frac{1}{L}\int_0^L dy\, e^{ky} f^{(n)}_{L,R}(y, c^i_k, BC) f^{(m)}_{L,R}(y, c^i_k, BC)\, g(y)\,, \tag{2.51}$$

while for $Z_X^{(1)}$ we have

$$\underset{nm}{\mathcal{P}^i_k}(BC)_{L,R} = \frac{1}{L}\int_0^L dy\, e^{ky} f^{(n)}_{L,R}(y, c^i_k, BC) f^{(m)}_{L,R}(y, c^i_k, BC)\, \tilde{g}(y) \tag{2.52}$$

with $\tilde{g}(y) \neq g(y)$ as the shape functions depend weakly on BCs. For charged currents mediated by $W_R^{(1)}$ we also have

$$\underset{nm}{\mathcal{S}^i_k}(BC)(BC')_{L,R} = \frac{1}{L}\int_0^L dy\, e^{ky} f^{(n)}_{L,R}(y, c^i_k, BC) f^{(m)}_{L,R}(y, c^i_k, BC')\, \tilde{g}(y)\,. \tag{2.53}$$

To clarify the discussion in the following chapters we define the intuitive shorthands

$$\begin{aligned}
\underset{nm}{\mathcal{R}_k}(BC)_{L,R} &\equiv \text{Diag}\left(\underset{nm}{\mathcal{R}^1_k}(BC)_{L,R}, \underset{nm}{\mathcal{R}^2_k}(BC)_{L,R}, \underset{nm}{\mathcal{R}^3_k}(BC)_{L,R}\right)\,,\\
\underset{nm}{\mathcal{P}_k}(BC)_{L,R} &\equiv \text{Diag}\left(\underset{nm}{\mathcal{P}^1_k}(BC)_{L,R}, \underset{nm}{\mathcal{P}^2_k}(BC)_{L,R}, \underset{nm}{\mathcal{P}^3_k}(BC)_{L,R}\right)\,,\\
\underset{nm}{\mathcal{S}_k}(BC)(BC')_{L,R} &\equiv \text{Diag}\left(\underset{nm}{\mathcal{S}^1_k}(BC)(BC')_{L,R}, \underset{nm}{\mathcal{S}^2_k}(BC)(BC')_{L,R}, \underset{nm}{\mathcal{S}^3_k}(BC)(BC')_{L,R}\right)\,.
\end{aligned} \tag{2.54}$$

The overlap integrals $\mathcal{R}^i_{k\,nm}(BC)_{L,R}$ and $\mathcal{P}^i_{k\,nm}(BC)_{L,R}$ will be of great importance for our analysis of tree level exchanges of KK gluons and EW gauge bosons in the following chapters. Examples for both as functions of the fermion bulk mass parameter c are shown in fig. 2.3. From this we can see that the breaking of the custodial symmetry

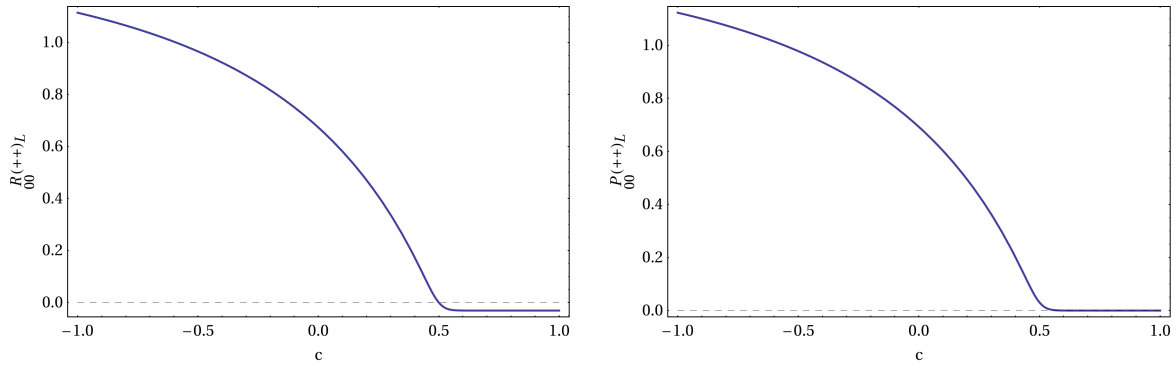

Figure 2.3: Overlap integrals $\mathcal{R}$ (left) of the $(++)$ and $\mathcal{P}$ (right) of the $(-+)$ gauge boson KK modes with fermion zero modes.

by BCs on the UV brane has virtually no impact on the overlap integrals for fermions localized towards the IR brane ($c \lesssim 0.5$) but that for UV localized fermions ($c \gtrsim 0.5$) this breaking effect is more relevant.

2.5 Particle Content

2.5.1 Gauge Sector

The gauge group of the RSc given in (2.47) is larger than the SM gauge group which is broken to the electromagnetic gauge group by the Higgs VEV,

$$SU(3)_c \times SU(2)_L \times U(1)_Y \xrightarrow{\langle H \rangle} SU(3)_c \times U(1)_Q \,. \tag{2.55}$$

Hence it needs to be broken explicitly in a way that does not spoil the desired features of the custodial isospin and parity discussed in section 2.3. Such a breaking pattern can be achieved by assigning different BCs to the gauge fields on the UV brane which will have little impact on physics close to the IR brane. In particular we need to break the $SU(2)_R \times U(1)_X \times P_{LR}$ subgroup of the bulk gauge group and accordingly the gauge fields of the RSc with their appropriate BCs[6] are given by

$$\begin{aligned} &W^a_{L\mu}(++)\,, \qquad B_\mu(++)\,, \\ &W^b_{R\mu}(-+)\,, \qquad Z_{X\mu}(-+)\,, \end{aligned} \tag{2.56}$$

[6]These BCs can be naturally achieved by adding a scalar $SU(2)_R$ doublet with $Q_X = 1/2$ charge on the UV brane, that develops a VEV $v_{\rm UV} \to \infty$ (see [79, 80] for details).

where $a = 1, 2, 3$ and[7] $b = 1, 2$. This assignment of BCs explicitly breaks both $SU(2)_R$ and $U(1)_X$ on the UV brane,

$$SU(2)_R \times U(1)_X \to U(1)_Y \,. \tag{2.57}$$

In fig. 2.4 we summarize the resulting symmetry breaking pattern. The fields B_μ and $Z_{X\mu}$ in (2.56) are related to the original fields $W^3_{R\mu}$ and X_μ via

$$\begin{aligned} Z_{X\mu} &= \cos\phi\, W^3_{R\mu} - \sin\phi\, X_\mu \,, \\ B_\mu &= \sin\phi\, W^3_{R\mu} + \cos\phi\, X_\mu \,, \end{aligned} \tag{2.58}$$

where

$$\cos\phi = \frac{g}{\sqrt{g^2 + g_X^2}} \,, \qquad \sin\phi = \frac{g_X}{\sqrt{g^2 + g_X^2}} \,. \tag{2.59}$$

Of the above gauge bosons those with $(++)$ BCs, $W^a_{L\mu}$ and B_μ, have a zero mode in their KK decomposition which is flat along the extra dimension and massless before EWSB. The lightest mode in the KK tower of the remaining gauge bosons with $(-+)$ BCs on the other hand is strongly peaked towards the IR brane and has a TeV-scale mass $m_1^{\text{gauge}}(-+) \simeq 2.40 f$ as discussed in section 2.2.2.

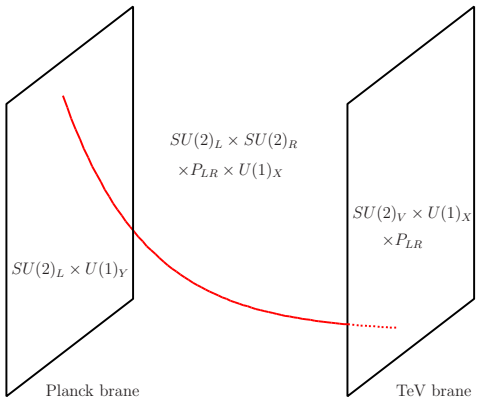

Figure 2.4: The symmetry breaking pattern of the RSc.

Anticipating EWSB it will be useful to follow [81] and define

$$W^\pm_{L\mu} = \frac{W^1_{L\mu} \mp i W^2_{L\mu}}{\sqrt{2}} \,, \qquad W^\pm_{R\mu} = \frac{W^1_{R\mu} \mp i W^2_{R\mu}}{\sqrt{2}} \,, \tag{2.60}$$

as well as

$$\begin{aligned} Z_\mu &= \cos\psi\, W^3_{L\mu} - \sin\psi\, B_\mu \,, \\ A_\mu &= \sin\psi\, W^3_{L\mu} + \cos\psi\, B_\mu \,, \end{aligned} \tag{2.61}$$

[7] Note that one of the W_R states has merged into the B, Z_X system.

where the mixing angle ψ is given in terms of gauge couplings by

$$\cos\psi = \frac{1}{\sqrt{1+\sin^2\phi}}\,, \qquad \sin\psi = \frac{\sin\phi}{\sqrt{1+\sin^2\phi}}\,. \tag{2.62}$$

Note that in the SM the mixing angle in the analog of (2.61) would be given by the Weinberg angle θ_W. Because of mixing between the gauge boson zero modes and heavy KK modes in the RSc, ψ and θ_W are different from each other at order $\mathcal{O}(v^2/f^2)$.

2.5.2 Electroweak Symmetry Breaking

We already anticipated the breaking of the EW symmetry by the VEV of the Higgs boson in the previous subsection. For the derivation of the gauge boson mass eigenstates after EWSB we will now properly introduce the Higgs field. In the spirit of the custodial symmetry the Higgs field needs to transform as a self-dual bi-doublet of the $SU(2)_L \times SU(2)_R$ bulk symmetry and be neutral under the $U(1)_X$,

$$H = \begin{pmatrix} \pi^+/\sqrt{2} & -(h^0 - i\pi^0)/2 \\ (h^0 + i\pi^0)/2 & \pi^-/\sqrt{2} \end{pmatrix}_0 . \tag{2.63}$$

Self-duality in this context implies that

$$\tilde{H} = \epsilon^\dagger H^* \epsilon = H\,, \tag{2.64}$$

where ϵ is the *Levi-Civita-tensor*, the totally antisymmetric tensor of rank two. When the neutral component h^0 of the Higgs bi-doublet develops a 4D effective VEV, the bulk symmetry group is broken according to

$$SU(2)_L \times SU(2)_R \times P_{LR} \to SU(2)_V \times P_{LR}\,. \tag{2.65}$$

We see explicitly that not only in the Higgs sector but also in the gauge sector of the theory an unbroken custodial symmetry $SU(2)_V$ remains intact, which is responsible for the protection of the T parameter. Similarly the P_{LR} symmetry, protecting the $Z d^i_L \bar{d}^j_L$ coupling, remains unbroken.
Combining the symmetry breakings by BCs on the UV brane and by the Higgs VEV on the IR brane, we see that the low energy effective theory is described by the spontaneous breaking pattern

$$SU(2)_L \times U(1)_Y \to U(1)_Q\,, \tag{2.66}$$

as anticipated in section 2.5.1 and required by phenomenology.
Now due to the unbroken gauge invariance of QED and QCD, the gluon and photon fields including their KK modes do not couple to the Higgs boson at leading order in perturbation theory and hence do not mix with each other or with $Z^{(0)}_\mu$, $Z^{(1)}_\mu$, $Z^{(1)}_{X\mu}$ and the higher KK modes of Z and Z_X. Therefore, even after EWSB we have

$$\begin{aligned} M_{A^{(0)}} &= 0\,, \qquad & M_{A^{(1)}} &= M_{++}\,, \\ M_{G^{(0)}} &= 0\,, \qquad & M_{G^{(1)}} &= M_{++}\,, \end{aligned} \tag{2.67}$$

and the corresponding states remain mass eigenstates. On the other hand the kinetic terms for the Higgs field (see 2.5.4)

$$S_{\text{Higgs}} = \int_0^L dy \int d^4x \, \sqrt{g} \, \text{Tr}\big[(D_M H(x^\mu, y))^\dagger (D^M H(x^\mu, y))\big] \tag{2.68}$$

lead to $\mathcal{O}(v^4/M_{\text{KK}}^2)$ corrections to the masses of $W_{L\mu}^{(0)\pm}$, $W_{L\mu}^{(1)\pm}$ and $W_{R\mu}^{(1)\pm}$ as well as of $Z_\mu^{(0)}$, $Z_\mu^{(1)}$ and $Z_{X\mu}^{(1)}$, and mixing between states of the same electric charge is induced. Here $v = 246\,\text{GeV}$ denotes the effective 4D VEV of the h^0 component in (2.63), and

$$\langle H \rangle = \begin{pmatrix} 0 & -v/2 \\ v/2 & 0 \end{pmatrix} . \tag{2.69}$$

If we restrict our discussion to the $n = 0, 1$ gauge boson modes, the gauge-Higgs interactions in (2.68) after EWSB lead to the two mass matrices $\mathcal{M}^2_{\text{charged}}$ and $\mathcal{M}^2_{\text{neutral}}$,

$$\begin{aligned} \mathcal{L} \supset & - \begin{pmatrix} W_L^{(0)+} & W_L^{(1)+} & W_R^{(1)+} \end{pmatrix} \mathcal{M}^2_{\text{charged}} \begin{pmatrix} W_L^{(0)-} \\ W_L^{(1)-} \\ W_R^{(1)-} \end{pmatrix} \\ & - \frac{1}{2} \begin{pmatrix} Z^{(0)} & Z^{(1)} & Z_X^{(1)} \end{pmatrix} \mathcal{M}^2_{\text{neutral}} \begin{pmatrix} Z^{(0)} \\ Z^{(1)} \\ Z_X^{(1)} \end{pmatrix} , \end{aligned} \tag{2.70}$$

which are explicitly given by[8]

$$\mathcal{M}^2_{\text{charged}} = \begin{pmatrix} \frac{g^2v^2}{4L} & \frac{g^2v^2}{4L}\mathcal{I}_1^+ & -\frac{g^2v^2}{4L}\mathcal{I}_1^- \\ \frac{g^2v^2}{4L}\mathcal{I}_1^+ & M_{++}^2 + \frac{g^2v^2}{4L}\mathcal{I}_2^{++} & -\frac{g^2v^2}{4L}\mathcal{I}_2^{-+} \\ -\frac{g^2v^2}{4L}\mathcal{I}_1^- & -\frac{g^2v^2}{4L}\mathcal{I}_2^{-+} & M_{--}^2 + \frac{g^2v^2}{4L}\mathcal{I}_2^{--} \end{pmatrix} , \tag{2.71}$$

and

$$\mathcal{M}^2_{\text{neutral}} = \begin{pmatrix} \frac{g^2v^2}{4L\cos^2\psi} & \frac{g^2v^2\mathcal{I}_1^+}{4L\cos^2\psi} & -\frac{g^2v^2\cos\phi\mathcal{I}_1^-}{4L\cos\psi} \\ \frac{g^2v^2\mathcal{I}_1^+}{4L\cos^2\psi} & M_{++}^2 + \frac{g^2v^2\mathcal{I}_2^{++}}{4L\cos^2\psi} & -\frac{g^2v^2\cos\phi\mathcal{I}_2^{-+}}{4L\cos\psi} \\ -\frac{g^2v^2\cos\phi\mathcal{I}_1^+}{4L\cos\psi} & -\frac{g^2v^2\cos\phi\mathcal{I}_2^{-+}}{4L\cos\psi} & M_{--}^2 + \frac{g^2v^2\cos^2\phi\mathcal{I}_2^{--}}{4L} \end{pmatrix} , \tag{2.72}$$

where the angles ϕ and ψ have been defined in (2.59) and (2.62). The overlap integrals $\mathcal{I}_1^\pm$, $\mathcal{I}_2^{\pm\pm}$ and $\mathcal{I}_2^{\pm\mp}$ for a brane Higgs are given by

$$\begin{aligned} \mathcal{I}_1^+ = g(L) \,, \quad \mathcal{I}_1^- = \tilde{g}(L) \,, \\ \mathcal{I}_2^{++} = g(L)^2 \,, \quad \mathcal{I}_2^{--} = g(L)^2 \,, \quad \mathcal{I}_2^{-+} = g(L)\tilde{g}(L) \,, \end{aligned} \tag{2.73}$$

[8]Note that the coupling constant g is the fundamental 5D coupling constant that is related to the 4D coupling constant by $g = \sqrt{L} g^{4\text{D}}$.

where $g(y)$ and $\tilde{g}(y)$ are the KK-1 bulk profiles of gauge bosons with $(++)$ and $(-+)$ BCs, as defined in (2.49), (2.50).

The diagonalization of the mass matrices (2.71) and (2.72) can be simplified considerably if the effects of the $SU(2)_R$ breaking by BCs on the UV brane are neglected. These effects will become important in the analysis of observables that are sensitive to the breaking of the custodial symmetry[9], such as the T-parameter, but their inclusion is not crucial for the analysis of flavor observables which will be performed in chapter 5. For this analysis we will need to calculate the $\mathcal{O}(v^2/M_{\rm KK}^2)$ corrections to the couplings of the light gauge bosons Z and $W^\pm$ as well as $\mathcal{O}(1)$ corrections to the couplings of the heavy gauge bosons. Since in Feynman diagrams the contributions of the latter couplings will always be suppressed by large gauge boson masses in the propagators, the $\mathcal{O}(1)$ accuracy aimed for by us is indeed adequate. At this level of accuracy, it turns out that the $\mathcal{O}(v^2/M_{\rm KK}^2)$ splitting in the overlap integrals $\mathcal{I}_2^{\pm\pm}$, $\mathcal{I}_2^{\pm\mp}$ can be safely neglected and we identify $\mathcal{I}_2^{--} = \mathcal{I}_2^{-+} = \mathcal{I}_2^{+-} = \mathcal{I}_2^{++} \equiv \mathcal{I}_2$. As a further simplification we will also neglect the $\sim 2\%$ discrepancy between the masses of the first excited gauge boson modes with $(++)$ and $(-+)$ BCs,

$$M_{++}^2 = M_{--}^2 \equiv M^2 \,. \tag{2.74}$$

The overlap integrals $\mathcal{I}_1^\pm$ finally will be treated in a semi-exact way, as the small discrepancy between $\mathcal{I}_1^+$ and $\mathcal{I}_1^-$ softly breaks the custodial protection of the $Zd_L^i\bar{d}_L^j$ and $Zu_R^i\bar{u}_R^j$ couplings which will be discussed in chapter 3. For this reason we will distinguish between $\mathcal{I}_1^+$ and $\mathcal{I}_1^-$ in the expression for the Z boson mass eigenstate, but in all other expressions set $\mathcal{I}_1^+ = \mathcal{I}_1^- \equiv \mathcal{I}_1$.
With these assumptions the diagonalization of (2.71) and (2.72) yields the charged mass eigenstates

$$\begin{aligned}
W^\pm &= W_L^{(0)\pm} + \frac{g^2v^2\mathcal{I}_1}{4LM^2}\left(W_R^{(1)\pm} - W_L^{(1)\pm}\right) , \\
W_H^\pm &= \frac{1}{\sqrt{2}}\left(W_L^{(1)\pm} - W_R^{(1)\pm}\right) , \\
W'^\pm &= \frac{1}{\sqrt{2}}\left(W_R^{(1)\pm} - W_L^{(1)\pm}\right) - \frac{g^2v^2\mathcal{I}_1}{2\sqrt{2}LM^2}W_L^{(0)\pm} ,
\end{aligned} \tag{2.75}$$

and the neutral ones

$$\begin{aligned}
Z &= Z^{(0)} - \frac{g^2v^2}{4LM^2\cos^2\psi}\left(-\mathcal{I}_1^+ Z^{(1)} + \cos\phi\cos\psi\mathcal{I}_1^- Z_X^{(1)}\right) , \\
Z_H &= \frac{1}{\sqrt{2}}\left(\cos\phi Z^{(1)} + \frac{1}{\cos\psi}Z_X^{(1)}\right) ,
\end{aligned}$$

[9]For a collection of formulae that are necessary for the exact diagonalization of the mass matrices (2.71), (2.72) the reader is referred to [32].

$$Z' = \frac{1}{\sqrt{2}}\left(\cos\phi Z_X^{(1)} - \frac{1}{\cos\psi}Z^{(1)}\right) - \frac{g^2v^2\mathcal{I}_1}{2\sqrt{2}LM^2\cos\psi}Z^{(0)}\,. \tag{2.76}$$

The corresponding masses in the charged sector are found to be

$$\begin{aligned} M_W^2 &= \frac{g^2v^2}{4L}\left(1 - \frac{g^2v^2\mathcal{I}_1^2}{2LM^2}\right)\,, \\ M_{W_H}^2 &= M^2\,, \\ M_{W'}^2 &= M^2\left(1 + \frac{g^2v^2\mathcal{I}_2}{2LM^2}\right)\,, \end{aligned} \tag{2.77}$$

and

$$\begin{aligned} M_Z^2 &= \frac{g^2v^2}{4L\cos^2\psi}\left(1 - \frac{g^2v^2\mathcal{I}_1^2}{2LM^2}\right)\,, \\ M_{Z_H}^2 &= M^2\left(1 + \frac{g^2v^2\mathcal{I}_2}{4LM^2}\left(1 - \frac{1}{\cos\phi}\right)\right)\,, \\ M_{Z'}^2 &= M^2\left(1 + \frac{g^2v^2\mathcal{I}_2}{4LM^2}\left(1 + \frac{1}{\cos\phi}\right)\right)\,, \end{aligned} \tag{2.78}$$

for the neutral mass eigenstates[10]. In all the formulae above, the coupling g is the fundamental 5D weak coupling constant and is related to the 4D coupling by $g = \sqrt{L}g^{4D}$.

2.5.3 Fermion Sector

The gauge bosons we discussed in the previous subsection transformed in the adjoint representation of their respective gauge group. The fermions present in the RSc which we will discuss now are not subject to suchlike constraints. Yet, phenomenology imposes several conditions on the gauge transformation properties of fermions in the framework we are considering. We will briefly discuss these constraints and give the multiplet assignments for the quark fields in the RSc. The fermionic mass matrices that arise after EWSB and that connect fermionic zero modes and higher KK modes are—because of the elaborate multiplet structure—more complicated than those for the gauge bosons. Therefore, we will not discuss them here but devote a whole section to their treatment in chapter 3.

Since QCD and QED are unbroken symmetries in the RSc we can assign each quark field a quantum number of $SU(3)_c \times U(1)_Q$. All quark fields that we will introduce in the following transform as triplets under the $SU(3)_c$ gauge group. Tracing the mixing (2.58),

[10]Note that for $\psi = 0$ the results for the neutral gauge bosons reduce to those given for the charged gauge bosons.

(2.61) of the $SU(2)_L \times SU(2)_R \times U(1)_X$ gauge bosons into the photon mass eigenstate we find for the electric charge of a fermion in terms of its fundamental quantum numbers

$$Q = T_L^3 + T_R^3 + X\,, \tag{2.79}$$

where $T_{L,R}^3$ are the field's 3-components of the $SU(2)_{L,R}$ isospins and X is its charge under the $U(1)_X$ gauge group.

Owing to the solution of the 5D chirality problem which was described in section 2.2.3, we need three distinct multiplets of $SU(2)_L \times SU(2)_R$ for each generation of SM quarks to embed the left-handed doublets q_L^i and the right-handed up-type and down-type singlets u_R^i and d_R^i, where $i = 1, 2, 3$ is the generation index. Fortunately, phenomenology provides guidelines towards which multiplets to choose. To start with, in order for the protection of the $Zb_L\bar{b}_L$ coupling outlined in section 2.3 to be effective, the $SU(2)_L \times SU(2)_R$ quantum numbers of the left-handed bottom quark need to satisfy the condition $T_R^3 = T_L^3$. Since left-handed quarks must transform as doublets of $SU(2)_L$, we have $T_L^3 = -1/2$ for the b_L quark and accordingly $T_R^3 = -1/2$, which implies that the (t_L, b_L) quark doublet must transform as components of a $(\mathbf{2}, \mathbf{2})$ bi-doublet under the $SU(2)_L \times SU(2)_R$ gauge group. As far as the protection of the $Zb_L\bar{b}_L$ vertex is concerned, this is only mandatory for the (t_L, b_L) quark doublet but not for the (u_L, d_L) and (c_L, s_L) quark doublets. In order not to explicitly break the flavor symmetries that are present in the Yukawa-less SM and in order to keep the theory as simple as possible, we also assign the (u_L, d_L) and (c_L, s_L) quark doublets to bi-doublets of the $SU(2)_L \times SU(2)_R$ gauge group. With the quantum numbers $T_{L,R}^3$ of all the left-handed down-type quarks being fixed we can now use (2.79) to determine the $U(1)_X$ quantum number that is required to reproduce the proper electric charge. We find that the three quark bi-doublets need to have charge $Q_X = 2/3$ in order to achieve this.
The requirement of eventually being able to construct Yukawa interactions that yield SM-like mass terms for the quarks now forces also the right-handed quarks to have the $U(1)_X$ charges $Q_X = 2/3$ (since the Higgs bi-doublet is neutral under the $U(1)_X$). This implies that the right-handed up-type quarks u_R^i have $T_R^3 = 0$, while the right-handed down-type quarks d_R^i have $T_R^3 = -1$. The most economic multiplet assignment consistent with these requirement is the u_R^i transforming as singlets and the d_R^i transforming as triplets of the $SU(2)_R$. More precisely, the d_R^i need to transform as components of a $(\mathbf{3}, \mathbf{1}) \oplus (\mathbf{1}, \mathbf{3})$ representation of $SU(2)_L \times SU(2)_R$ which is closed under the P_{LR} parity. While these multiplets are the most economic choice, larger multiplets, such as $(\mathbf{1}, \mathbf{2}j + \mathbf{1})$ for the u_R^i and $(\mathbf{2}\ell + \mathbf{1}, \mathbf{1}) \oplus (\mathbf{1}, \mathbf{2}\ell + \mathbf{1})$ for the d_R^i, $j, \ell = 1, 2, ...$ are also conceivable in principle but tend to introduce phenomenological tensions[11]. In the following we will therefore assume that the SM quarks are embedded into the minimal multiplets introduced above. Finally, both the $(\mathbf{2}, \mathbf{2})$ and the $(\mathbf{3}, \mathbf{1}) \oplus (\mathbf{1}, \mathbf{3})$ representations contain additional states which must be prevented from obtaining light or even massless zero modes. This can be

[11] For instance, if the t_R is embedded into a triplet of $SU(2)_R$, its mass is suppressed by a factor of $1/\sqrt{2}$ relative to the singlet case. This requires an un-naturally large top Yukawa coupling in order to reproduce the observed top mass.

achieved by assigning adequate BCs. Also here artistic freedom is limited and we are in addition tightly bound by the symmetry breaking pattern on the UV brane given in (2.57):

- the SM quarks must have $(++)$ BCs,
- the heavy fields must not have $(--)$ BCs lest their chiral partners contain massless zero modes,
- neither $SU(2)_L$ nor $SU(2)_R$ may be broken by BCs on the IR brane,
- only $SU(2)_R$ may be broken by BCs on the UV brane.

The unique solution that is consistent with all of these constraints is given by the following assignment of SM quarks to multiplets of $SU(2)_L \times SU(2)_R \times U(1)_X$:

$$\begin{aligned}
\xi^i_{1L} &= \begin{pmatrix} \chi^{u_i}_L(-+)_{5/3} & q^{u_i}_L(++)_{2/3} \\ \chi^{d_i}_L(-+)_{2/3} & q^{d_i}_L(++)_{-1/3} \end{pmatrix}_{2/3} , \\
\xi^i_{2R} &= u^i_R(++)_{2/3} , \\
\xi^i_{3R} = T^i_{3R} \oplus T^i_{4R} &= \begin{pmatrix} \psi'^i_R(-+)_{5/3} \\ U'^i_R(-+)_{2/3} \\ D'^i_R(-+)_{-1/3} \end{pmatrix}_{2/3} \oplus \begin{pmatrix} \psi''^i_R(-+)_{5/3} \\ U''^i_R(-+)_{2/3} \\ D^i_R(++)_{-1/3} \end{pmatrix}_{2/3} ,
\end{aligned} \tag{2.80}$$

where the subscript of a multiplet denotes the $U(1)_X$ charge and the subscripts of the individual fields correspond to their electric charges as determinded by (2.79). It should be mentioned that in this multiplet assignment the SM d_R quark corresponds to the zero mode of the D_R field. The corresponding states of opposite chirality[12] can be obtained from (2.80) by changing the chirality and exchanging $(+)$ and $(-)$ BCs. Of these fields those with $(++)$ BCs contain massless zero modes that will obtain $\mathcal{O}(v)$ masses after EWSB and can be (up to $\mathcal{O}(v^2/M^2_{\text{KK}})$ mixing effects with KK quark fields) identified with the SM quarks.
Apart from the SM quarks, even the above minimal embedding into multiplets of the bulk gauge group gives rise to a number of additional, heavy (approximately) vector-like quark fields. Arranged according to their electric charges, these are

$$\begin{aligned}
Q = 5/3 : &\qquad \chi^{u_i(n)}, \psi'^{i(n)}, \psi''^{i(n)} , \\
Q = 2/3 : &\qquad q^{u_i(n)}, u^{i(n)}, U'^{i(n)}, U''^{i(n)}, \chi^{d_i(n)} , \\
Q = -1/3 : &\qquad q^{d_i(n)}, D^{i(n)}, D'^{i(n)} .
\end{aligned} \tag{2.81}$$

Thus we see that the framework of custodial protection, by requiring the left-handed doublets to transform as bi-doublets of the bulk gauge group, invariably introduces additional heavy quark fields with exotic charges of which the lightest can have TeV-scale

[12]The left- and right-handed modes are (see discussion of the 5D chirality problem in section 2.2.3) defined via $\psi_{L,R} = \mp\gamma^5\psi_{L,R}$.

masses. The presence of these states offers interesting experimental signatures and in fact a smoking gun signature for the RSc.

The generalization of the multiplet assignment (2.80) to the lepton sector (with right-handed Dirac neutrinos) is straightforward and requires only two modifications. First, the leptons all are color singlets and second, they all need to be neutral under $U(1)_X$ in order to reproduce the correct electric charges.

2.5.4 Fundamental Bulk Action

In section 2.5.2 we already made use of the 5D action coupling the Higgs to the gauge bosons in order to be able to derive the gauge bosons' mass matrices. The form of this action in fact was determined by Lorentz invariance and the concept of the covariant derivative. Also the fermion couplings are determined by these principles, yet the appearance of non-fundamental fermion representations renders the construction of the corresponding terms in the action more intricate. In this section we will give the total 5D bulk action from which all effective 4D interactions can be derived by integrating out the fifth dimension as indicated in section 2.4. This action can be decomposed as

$$S = \int_0^L dy \int d^4x \, \left(\mathcal{L}_{\text{gauge}} + \mathcal{L}_{\text{fermion}} + \mathcal{L}_{\text{Higgs}} + \mathcal{L}_{\text{Yuk}}\right) , \tag{2.82}$$

with the various contributions being discussed in the following.

Gauge sector The kinetic terms for the gauge fields are given by

$$\mathcal{L}_{\text{gauge}} = \sqrt{g}\left[-\frac{1}{4}G^A_{MN}G^{MN,A} - \frac{1}{4}L^a_{MN}L^{MN,a} - \frac{1}{4}R^\alpha_{MN}R^{MN,\alpha} - \frac{1}{4}X_{MN}X^{MN}\right] , \tag{2.83}$$

where

$$G^A_{MN} = \partial_M G^A_N - \partial_N G^A_M - g_s f^{ABC} G^B_M G^C_N \qquad (A = 1, \ldots, 8) \tag{2.84}$$

corresponds to $SU(3)_c$ and g_s is the 5D strong coupling constant.

$$L^a_{MN} = \partial_M W^a_{L,N} - \partial_N W^a_{L,M} - g\varepsilon^{abc} W^b_{L,M} W^c_{L,N} \qquad (a = 1, 2, 3) , \tag{2.85}$$

$$R^\alpha_{MN} = \partial_M W^\alpha_{R,N} - \partial_N W^\alpha_{R,M} - g\varepsilon^{\alpha\beta\gamma} W^\beta_{R,M} W^\gamma_{R,N} \qquad (\alpha = 1, 2, 3) \tag{2.86}$$

correspond to $SU(2)_L$ and $SU(2)_R$, with equal gauge coupling g, and

$$X_{MN} = \partial_M X_N - \partial_N X_M \tag{2.87}$$

is the field strength tensor of $U(1)_X$, whose coupling constant is given by g_X. Here and in the following the square root of $g = \det g_{MN} = e^{-8ky}$ has to be included in order to obtain an invariant integration measure. We denote $SU(2)_L$ indices by lower-case Latin letters $a, b, \ldots$ and $SU(2)_R$ indices by lower-case Greek letters $\alpha, \beta, \ldots$. $SU(3)_c$ indices are denoted by capital Latin letters $A, B, \ldots$, but are usually not made explicit in order to simplify the notation.

Quark sector The quark sector contains fields with the following transformation properties under $SU(2)_L \times SU(2)_R \times U(1)_X$,

$$(\xi_1^i)_{a\alpha} \sim (\mathbf{2},\mathbf{2})_{2/3}\,, \tag{2.88}$$

$$\xi_2^i \sim (\mathbf{1},\mathbf{1})_{2/3}\,, \tag{2.89}$$

$$\xi_3^i = (T_3^i)_a \oplus (T_4^i)_\alpha \sim (\mathbf{3},\mathbf{1})_{2/3} \oplus (\mathbf{1},\mathbf{3})_{2/3}\,. \tag{2.90}$$

All these multiplets transform as triplets under $SU(3)_c$. The fermionic Lagrangian is then given by

$$\begin{aligned}\mathcal{L}_{\text{fermion}} = \frac{1}{2}\sqrt{g}\sum_{i=1}^{3}\Big[&(\bar{\xi}_1^i)_{a\alpha} i\Gamma^M (D_M^1)_{ab,\alpha\beta}(\xi_1^i)_{b\beta} + (\bar{\xi}_1^i)_{a\alpha}(i\Gamma^M\omega_M - c_1^i k)(\xi_1^i)_{a\alpha} \\ &+ \bar{\xi}_2^i(i\Gamma^M D_M^2 + i\Gamma^M\omega_M - c_2^i k)\xi_2^i \\ &+ (\bar{T}_3^i)_a i\Gamma^M (D_M^3)_{ab}(T_3^i)_b + (\bar{T}_3^i)_a(i\Gamma^M\omega_M - c_3^i k)(T_3^i)_a \\ &+ (\bar{T}_4^i)_\alpha i\Gamma^M (D_M^4)_{\alpha\beta}(T_4^i)_\beta + (\bar{T}_4^i)_\alpha(i\Gamma^M\omega_M - c_3^i k)(T_4^i)_\alpha\Big] + h.c.\,,\end{aligned} \tag{2.91}$$

where summation over repeated indices is understood. Writing out the "$+h.c.$" term explicitly, one finds that the two terms including the spin connection ω_M cancel each other [82]. Here, $\Gamma^M = E_A^M\gamma^A$ with[13] $\gamma^A = \{\gamma^\mu, -i\gamma^5\}$, and E_A^M is the inverse vielbein defined through

$$g^{MN} = E_A^M E_B^N \eta^{AB}\,, \tag{2.92}$$

i.e. it connects the warped space to the flat tangent space. For the case of the RS metric (2.2), we have

$$E_A^M = \begin{cases} 1 & \text{for } A = M = 5\,, \\ e^{ky} & \text{for } A = M = \mu\,, \\ 0 & \text{otherwise}\,, \end{cases} \tag{2.93}$$

and the vielbein e_M^A is given by

$$e_M^A = \begin{cases} 1 & \text{for } A = M = 5\,, \\ e^{-ky} & \text{for } A = M = \mu\,, \\ 0 & \text{otherwise}\,. \end{cases} \tag{2.94}$$

The spin connection ω_M is defined through

$$\omega_M = e_N^A(\partial_M E_B^N + \Gamma_{MK}^N E_B^K)\frac{\sigma_A{}^B}{2}\,, \tag{2.95}$$

[13] Here, $\gamma^5 = i\gamma^0\gamma^1\gamma^2\gamma^3$ is defined in the usual 4D way.

with $\sigma_{AB} = \frac{1}{4}[\gamma_A, \gamma_B]$ and the Christoffel symbols $\Gamma^N_{MK} = \frac{1}{2}g^{NR}(\partial_K g_{MR} + \partial_M g_{KR} - \partial_R g_{MK})$, which yields in case of the RS metric (2.2)

$$\omega_M = \begin{cases} \frac{i}{2}ke^{-ky}\gamma_\mu\gamma^5 & \text{for } M = \mu\,, \\ 0 & \text{for } M = 5\,. \end{cases} \tag{2.96}$$

The covariant derivatives D^i_M are given by

$$\begin{aligned}
(D^1_M)_{ab,\alpha\beta} &= (\partial_M + ig_s t^A G^A_M + ig_X Q_X X_M)\delta_{ab}\delta_{\alpha\beta} \\
&\quad + ig(\tau^c)_{ab}W^c_{L,M}\delta_{\alpha\beta} + ig(\tau^\gamma)_{\alpha\beta}W^\gamma_{R,M}\delta_{ab}\,, \\
D^2_M &= \partial_M + ig_s t^A G^A_M + ig_X Q_X X_M\,, \\
(D^3_M)_{ab} &= (\partial_M + ig_s t^A G^A_M + ig_X Q_X X_M)\delta_{ab} + g\varepsilon^{abc}W^c_{L,M}\,, \\
(D^4_M)_{\alpha\beta} &= (\partial_M + ig_s t^A G^A_M + ig_X Q_X X_M)\delta_{\alpha\beta} + g\varepsilon^{\alpha\beta\gamma}W^\gamma_{R,M}\,.
\end{aligned} \tag{2.97}$$

Here $t^A = \lambda^A/2$ $(A = 1, \ldots, 8)$ are the generators of the fundamental representation of $SU(3)_c$, where λ^A are the Gell-Mann matrices. $\tau^a = \sigma^a/2$ $(\tau^\alpha = \sigma^\alpha/2)$ are the generators of the fundamental $SU(2)_L$ $(SU(2)_R)$ representations, where σ^a, σ^α are the Pauli matrices, and $-i\varepsilon^{abc}$ and $-i\varepsilon^{\alpha\beta\gamma}$ are the generators of the adjoint triplet representations of $SU(2)_L$ and $SU(2)_R$. Recall that despite having the same matrix structure, the $SU(2)_L$ and $SU(2)_R$ generators act on different internal spaces.
In addition, the components of the $T^i_{3,4}$ triplets, as given in (2.80) are not identical to those components associated with $a, \alpha = 1, 2, 3$. Instead,

$$(T^i_3)_a = \begin{pmatrix} \frac{1}{\sqrt{2}}(\psi'^i + D'^i) \\ \frac{i}{\sqrt{2}}(\psi'^i - D'^i) \\ U'^i \end{pmatrix}\,, \qquad (T^i_4)_\alpha = \begin{pmatrix} \frac{1}{\sqrt{2}}(\psi''^i + D^i) \\ \frac{i}{\sqrt{2}}(\psi''^i - D^i) \\ U''^i \end{pmatrix}\,. \tag{2.98}$$

The same structure also appears in the gauge sector, where the $W^{1,2}_{L,R}$ are related to $W^\pm_{L,R}$ via $W^\pm_{L,R} = 1/\sqrt{2}(W^1_{L,R} \mp iW^2_{L,R})$.

The fundamental Lagrangian density for the lepton sector with right-handed Dirac neutrinos can be obtained from the fermion Lagrangian (2.91) by setting $g_s = g_X = 0$ in the covariant derivatives (2.97), which takes care of the fact that all leptons transform as singlets under $SU(3)_c \times U(1)_X$.

Higgs sector The Lagrangian describing the Higgs bi-doublet H, given in (2.63), reads

$$\mathcal{L}_{\text{Higgs}} = \sqrt{g}\left[(D_M H)^\dagger_{a\alpha}(D^M H)_{a\alpha} - V(H)\right]\,, \tag{2.99}$$

with

$$(D_M H)_{a\alpha} = \partial_M H_{a\alpha} + ig(\tau^c)_{ab}W^c_{L,M}H_{b\alpha} + ig(\tau^\gamma)_{\alpha\beta}W^\gamma_{R,M}H_{a\beta} \tag{2.100}$$

and $V(H)$ being the potential that eventually leads to EWSB.
Note that in case of a bulk Higgs field, H contains massive KK modes in addition to the zero mode. Their couplings are, due to a similar bulk profile, roughly the same as the Higgs zero mode couplings. The potential $V(H)$ then has to be constructed in such a way that only the zero mode obtains a VEV, as otherwise the consistency with EWPT would be spoiled. Apart from that, since the scalar KK modes are even heavier than the gauge and fermionic KK modes, they can be safely neglected in most phenomenological applications. Therefore, we will not give an explicit expression for $V(H)$, but merely assume that it leads to a VEV for the zero mode and the particular shape function $h(y)$, as given in (2.34).
The kinetic terms in $\mathcal{L}_{\text{Higgs}}$ are responsible for the effects of EWSB in the gauge sector which were discussed in detail in section 2.5.2.

Yukawa sector Finally, we need to construct the Higgs couplings to fermion fields, which will yield the masses of the SM fermions after EWSB. For simplicity, we restrict ourselves to the quark sector, and the Yukawa couplings for the lepton sector can then be obtained in a completely analogous way.
The most general Yukawa coupling including the Higgs bi-doublet H and the quark fields $\xi^i_{1,2,3}$ is given by

$$\begin{aligned}\mathcal{L}_{\text{Yuk}} = -\sqrt{2}\sqrt{g}\sum_{i,j=1}^{3}\Big[&- \lambda^u_{ij}(\bar{\xi}^i_1)_{a\alpha}H_{a\alpha}\xi^j_2 \\ &+ \sqrt{2}\lambda^d_{ij}\left[(\bar{\xi}^i_1)_{a\alpha}(\tau^c)_{ab}(T^j_3)^c H_{b\alpha} + (\bar{\xi}^i_1)_{a\alpha}(\tau^\gamma)_{\alpha\beta}(T^j_4)^\gamma H_{a\beta}\right] + h.c.\Big], \quad (2.101)\end{aligned}$$

where again summation over repeated indices is understood. The normalization factor $\sqrt{2}$ enters the second term in order to canonically normalize the fermion triplets $T^j_{3,4}$, and the overall signs of the two contributions are chosen such that the (00)-components of the mass matrices $\mathcal{M}(2/3)$ and $\mathcal{M}(-1/3)$ in (3.11), (3.12) carry an overall plus sign.[14] Interestingly, while the first coupling, proportional to λ^u_{ij}, contributes only to the mass matrix of charge $+2/3$ quarks, the second term, proportional to λ^d_{ij}, contributes to all charge $+5/3$, $+2/3$ and $-1/3$ mass matrices.

We conclude this chapter by noting that it is possible to extend the theory by adding contributions to the action that are confined to the UV or IR branes. Indeed any such terms that are consistent with the symmetries of the theory will be generated at the loop level even if they are set to zero at tree level. In order to keep the presentation as clear as possible, we will not consider this most general case, but restrict ourselves to the bulk action given in (2.82). The only exception to this rule will be our treatment of different fundamental QCD coupling constants in our numerical analysis in chapter 5.

[14] Recall that the fermionic mass term possesses an overall minus sign.

Chapter 3

The Flavor Structure of the RSc

In section 3.1 of this chapter we will first analyze the mass matrices which arise after EWSB for the quark fields introduced in section 2.5.3. The structure of these matrices and also that of the quark coupling matrices in the RSc is within a certain margin determined by the specific localization of the quark zero modes which will be discussed in section 3.2. Having worked out the quark spectrum of the RSc we will turn our attention towards flavor non-universalities in the couplings of quarks to gauge bosons and the consequential flavor violating couplings. In the RSc there are two main effects which lead to flavor non-universalities in the couplings of quarks to gauge bosons: The first effect arises in the couplings of quark zero modes (whose localization is flavor dependent) to the non-uniformly localized KK gauge boson modes. This effect will be referred to as *flavor violation from gauge boson mixing* and will be discussed in section 3.4. In the course of this analysis we will work out how the custodial protection which was originally introduced to protect the $Zb_L\bar{b}_L$ coupling also strongly affects the other Z and Z' couplings. The second main, yet usually subdominant, origin of flavor violating couplings lies in the mixing of quark zero modes with heavy KK fermions of the same electric charge. This mechanism will be referred to as *flavor violation from KK fermion mixing* and will be treated in great detail in section 3.5. A quantitative comparison of both effects will be performed in the same section. Finally, in addition to flavor violating gauge couplings, also flavor violating Higgs couplings are present in the RSc. Their sources will be briefly summarized in section 3.6.

While in the present work we will concentrate on the couplings that are relevant for the analysis of tree level corrections to a number of observables, the calculation of loop diagrams in the framework of the RSc would require also the knowledge of vertices that exclusively contain non-SM particles. The derivation of all these couplings is beyond the scope of this work, and the reader is referred to [32] where a complete list of couplings that arise in the RSc has been given.

3.1 Quark Mass Matrices

The transformation to mass eigenstates in the gauge sector has been performed in section 2.5.2. The goal of the present section is to construct and diagonalize the mass matrices for the quark fields comprised by the multiplets that are given in (2.80) and their opposite chirality counterparts. To this end we will only consider zero modes and the lowest ($n = 1$) KK modes. As there are only few quark fields with zero modes, we will assign to them the superscript (0). For the excited KK modes we will just use the notation of (2.80), making the ($n = 1$) index implicit.
We will have to deal with three mass matrices corresponding to the electric charges $+5/3$, $+2/3$ and $-1/3$. To this end we group the fermion modes into the following vectors. For the $+5/3$ charge mass matrix we have

$$\begin{aligned}\Psi_L(5/3) &= \left(\chi_L^{u_i}(-+), \psi_L'^i(+-), \psi_L''^i(+-)\right)^T ,\\ \Psi_R(5/3) &= \left(\chi_R^{u_i}(+-), \psi_R'^i(-+), \psi_R''^i(-+)\right)^T ,\end{aligned} \tag{3.1}$$

where the flavor index $i = 1, 2, 3$ runs over the three quark generations. We thus deal with 9-dimensional vectors. Note that in this sector only massive excited KK states are present. For the charge $+2/3$ mass matrix the corresponding vectors read

$$\begin{aligned}\Psi_L(2/3) &= \left(q_L^{u_i(0)}(++), q_L^{u_i}(++), U_L'^i(+-), U_L''^i(+-), \chi_L^{d_i}(-+), u_L^i(--)\right)^T ,\\ \Psi_R(2/3) &= \left(u_R^{i(0)}(++), q_R^{u_i}(--), U_R'^i(-+), U_R''^i(-+), \chi_R^{d_i}(+-), u_R^i(++)\right)^T .\end{aligned} \tag{3.2}$$

Here the first components are zero modes, and $i = 1, 2, 3$ so that we deal with 18-dimensional vectors. The $-1/3$ charge vectors finally are given by

$$\begin{aligned}\Psi_L(-1/3) &= \left(q_L^{d_i(0)}(++), q_L^{d_i}(++), D_L'^i(+-), D_L^i(--)\right)^T ,\\ \Psi_R(-1/3) &= \left(D_R^{i(0)}(++), q_R^{d_i}(--), D_R'^i(-+), D_R^i(++)\right)^T .\end{aligned} \tag{3.3}$$

Again the first entries are zero modes, the remaining ones massive KK modes, and $i = 1, 2, 3$, so that in this case a 12-dimensional vector is obtained.
In order to establish the notation for the construction of the mass matrices let us briefly recall some basic properties of the fermion multiplets and bulk profiles that have been stated in sections 2.2.3, 2.5.3 and 2.5.4.

1. We have three bulk mass matrices c_1, c_2, c_3 corresponding to the three $O(4) \sim SU(2)_L \times SU(2)_R \times P_{LR}$ representations $\xi_1^i, \xi_2^i, \xi_3^i$ ($i = 1, 2, 3$ is the flavor index). In general, the c_k are arbitrary hermitian 3×3 matrices, where $k = 1, 2, 3$ corresponds to the $O(4)$ multiplet ξ_k. In the following we choose to work in the basis where they are real and diagonal, i.e. each of them is described by three real parameters c_k^i.

This can always be achieved by appropriate field redefinitions of the ξ^i multiplets. Explicitly we then have:

$$c_1 \equiv \text{Diag}(c_1^1, c_1^2, c_1^3)\,, \tag{3.4}$$

and similarly for c_2 and c_3. For a given $O(4)$ multiplet with fixed flavor index all bulk mass parameters for different components of the multiplet are equal to each other.

2. The allowed Yukawa couplings, giving mass to the quark zero modes after EWSB, have to preserve the full $O(4) \sim SU(2)_L \times SU(2)_R \times P_{LR}$ gauge symmetry. The possible gauge invariant terms in the full 5D theory can be found in section 2.5.4.

3. The effective 4D Yukawa matrices will involve the quark and Higgs shape functions. We will denote the fermionic ones by $f^Q_{L,k}(y)$ and $f^Q_{R,l}(y)$, corresponding to the k-th and l-th component of $\Psi_L(Q)$ and $\Psi_R(Q)$ in (3.1)–(3.3), and $h(y)$ is the Higgs shape function as given in (2.34).

Having at hand this information and restricting ourselves to $(n = 0, 1)$ for simplicity, we obtain the following effective 4D Yukawa couplings

$$\begin{aligned}
\left[Y_{ij}^{(5/3)}\right]_{kl} &= \frac{1}{\sqrt{2}L^{3/2}} \int_0^L dy\, \lambda^d_{ij} f^{5/3}_{L,k}(y) f^{5/3}_{R,l}(y) h(y)\,, \\
\left[Y_{ij}^{(2/3)}\right]_{kl} &= \frac{1}{2L^{3/2}} \int_0^L dy\, \lambda^d_{ij} f^{2/3}_{L,k}(y) f^{2/3}_{R,l}(y) h(y)\,, \\
\left[\tilde{Y}_{ij}^{(2/3)}\right]_{kl} &= \frac{1}{\sqrt{2}L^{3/2}} \int_0^L dy\, \lambda^u_{ij} f^{2/3}_{L,k}(y) f^{2/3}_{R,l}(y) h(y)\,, \\
\left[Y_{ij}^{(-1/3)}\right]_{kl} &= \frac{1}{\sqrt{2}L^{3/2}} \int_0^L dy\, \lambda^d_{ij} f^{-1/3}_{L,k}(y) f^{-1/3}_{R,l}(y) h(y)\,.
\end{aligned} \tag{3.5}$$

These effective Yukawa matrices are given for the most general case of Higgs field propagating into the bulk with shape function $h(y)$. In our case of a brane Higgs we have to replace the Higgs shape function by a δ-function, $h(y) \to \sqrt{L} e^{ky} \delta(y - L)$. If we further define the *brane overlaps* of the quark zero modes as

$$\begin{aligned}
F^i_Q &\equiv \frac{e^{kL/2}}{\sqrt{L}} f_L(y = L, c^i_1; ++)\,, \\
F^i_{u,d} &\equiv \frac{e^{kL/2}}{\sqrt{L}} f_R(y = L, c^i_{2,3}; ++)\,,
\end{aligned} \tag{3.6}$$

we obtain for the effective Yukawa matrices $[\tilde{Y}^{(2/3)}_{ij}]_{00}$ and $[Y^{(-1/3)}_{ij}]_{00}$ which are relevant

for the masses of the SM quarks,

$$\left[\tilde{Y}^{(2/3)}_{ij}\right]_{00} = \frac{1}{\sqrt{2}} F^i_Q \lambda^u_{ij} F^j_u \,,$$
$$\left[Y^{(-1/3)}_{ij}\right]_{00} = \frac{1}{\sqrt{2}} F^i_Q \lambda^d_{ij} F^j_d \,. \tag{3.7}$$

Finally, we also mention that for $(n = 1)$ KK modes

$$f^{(1)}(y = L, c^i_{1,2,3}) = \begin{cases} \frac{e^{kL/2}}{\sqrt{L}}\sqrt{2} & \text{for } (++) \text{ and } (-+) \text{ BCs} \\ 0 & \text{for } (+-) \text{ and } (--) \text{ BCs} \end{cases} \tag{3.8}$$

holds to a very good approximation independently of the values of the $c^i_{1,2,3}$.
Interestingly, the Yukawa coupling proportional to λ^d_{ij}, connecting ξ^i_1 with ξ^j_3 and being responsible for the SM down quark Yukawa couplings, leads to mass terms not only for the charge $-1/3$ quarks, but simultaneously also to mass terms for the charge $+5/3$ and $+2/3$ quarks. This is a direct consequence of T^j_3 and T^j_4 being placed in the adjoint representations of $SU(2)_L$ and $SU(2)_R$, as can be seen in (2.80).
On the other hand, the term proportional to λ^u_{ij}, connecting ξ^i_1 with ξ^j_2 and being thus responsible for the SM up quark Yukawa coupling, contributes only to the mass matrix for the charge $+2/3$ quarks.
Finally the fermionic KK masses, which can be obtained from solving the bulk equations of motion, have to be included in the mass matrices. Note that both the fermion shape function and the KK mass depend on the bulk mass parameter c *and* on the BCs.
In what follows we will use the 3×3 KK fermion mass matrices $M^{\rm KK}_k$(BC-L), where $k = 1, 2, 3$ labels the representations in (2.80) and their opposite chirality counterparts, and (BC-L) are the BCs for the left-handed modes.
In terms of the mode vectors (3.1)–(3.3) we can write

$$\begin{aligned} \mathcal{L}_{\rm mass} = & -\bar{\Psi}_L(5/3)\, \mathcal{M}(5/3)\, \Psi_R(5/3) + h.c. \\ & -\bar{\Psi}_L(2/3)\, \mathcal{M}(2/3)\, \Psi_R(2/3) + h.c. \\ & -\bar{\Psi}_L(-1/3)\, \mathcal{M}(-1/3)\, \Psi_R(-1/3) + h.c.\,. \end{aligned} \tag{3.9}$$

In order to distinguish zero modes from the KK fermions we will assign the index (0) to the zero mode components of the vectors (3.1)–(3.3). Then the quark mass matrices read

$$\mathcal{M}(5/3) = \begin{pmatrix} M^{\rm KK}_1(-+) & v\left[Y^{(5/3)}_{ij}\right]_{12} & -v\left[Y^{(5/3)}_{ij}\right]_{13} \\ v\left[Y^{(5/3)}_{ij}\right]^\dagger_{21} & M^{\rm KK}_3(+-) & 0 \\ -v\left[Y^{(5/3)}_{ij}\right]^\dagger_{31} & 0 & M^{\rm KK}_3(+-) \end{pmatrix}, \tag{3.10}$$

$$\mathcal{M}(2/3) = \tag{3.11}$$

$$\begin{pmatrix}
v\left[\tilde{Y}_{ij}^{(2/3)}\right]_{00} & 0 & -v\left[Y_{ij}^{(2/3)}\right]_{02} & v\left[Y_{ij}^{(2/3)}\right]_{03} & 0 & v\left[\tilde{Y}_{ij}^{(2/3)}\right]_{05} \\
v\left[\tilde{Y}_{ij}^{(2/3)}\right]_{10} & M_1^{\mathrm{KK}}(++) & -v\left[Y_{ij}^{(2/3)}\right]_{12} & v\left[Y_{ij}^{(2/3)}\right]_{13} & 0 & v\left[\tilde{Y}_{ij}^{(2/3)}\right]_{15} \\
0 & -v\left[Y_{ij}^{(2/3)}\right]_{21}^{\dagger} & M_3^{\mathrm{KK}}(+-) & 0 & -v\left[Y_{ij}^{(2/3)}\right]_{24}^{\dagger} & 0 \\
0 & v\left[Y_{ij}^{(2/3)}\right]_{31}^{\dagger} & 0 & M_3^{\mathrm{KK}}(+-) & v\left[Y_{ij}^{(2/3)}\right]_{34}^{\dagger} & 0 \\
-v\left[\tilde{Y}_{ij}^{(2/3)}\right]_{40} & 0 & -v\left[Y_{ij}^{(2/3)}\right]_{42} & v\left[Y_{ij}^{(2/3)}\right]_{43} & M_1^{\mathrm{KK}}(-+) & -v\left[\tilde{Y}_{ij}^{(2/3)}\right]_{45} \\
0 & v\left[\tilde{Y}_{ij}^{(2/3)}\right]_{51}^{\dagger} & 0 & 0 & -v\left[\tilde{Y}_{ij}^{(2/3)}\right]_{54}^{\dagger} & M_2^{\mathrm{KK}}(--)
\end{pmatrix},$$

$$\mathcal{M}(-1/3) = \begin{pmatrix}
v\left[Y_{ij}^{(-1/3)}\right]_{00} & 0 & -v\left[Y_{ij}^{(-1/3)}\right]_{02} & v\left[Y_{ij}^{(-1/3)}\right]_{03} \\
v\left[Y_{ij}^{(-1/3)}\right]_{10} & M_1^{\mathrm{KK}}(++) & -v\left[Y_{ij}^{(-1/3)}\right]_{12} & v\left[Y_{ij}^{(-1/3)}\right]_{13} \\
0 & -v\left[Y_{ij}^{(-1/3)}\right]_{21}^{\dagger} & M_3^{\mathrm{KK}}(+-) & 0 \\
0 & v\left[Y_{ij}^{(-1/3)}\right]_{31}^{\dagger} & 0 & M_3^{\mathrm{KK}}(--)
\end{pmatrix}. \tag{3.12}$$

These three matrices have to be diagonalized via bi-unitary transformations to find the quark mass eigenstates. In the case of the Higgs field being confined exactly to the IR brane, only Yukawa couplings to those fermion modes are non-vanishing that obey a (+) BC on the IR brane. In that case some of the entries in the above mass matrices in (3.10)–(3.12) vanish:

$$\begin{aligned}
&\mathcal{M}(5/3)_{21} = \mathcal{M}(5/3)_{31} = 0\,, \\
&\mathcal{M}(2/3)_{21} = \mathcal{M}(2/3)_{31} = \mathcal{M}(2/3)_{51} = 0\,, \\
&\mathcal{M}(2/3)_{24} = \mathcal{M}(2/3)_{34} = \mathcal{M}(2/3)_{54} = 0\,, \\
&\mathcal{M}(-1/3)_{21} = \mathcal{M}(-1/3)_{31} = 0\,.
\end{aligned} \tag{3.13}$$

We can then diagonalize the charge $+5/3$, $+2/3$ and $-1/3$ mass matrices by

$$M_{\mathrm{Diag}}(5/3) = \mathcal{X}_L^{\dagger}\,\mathcal{M}(5/3)\,\mathcal{X}_R\,, \tag{3.14}$$

$$M_{\mathrm{Diag}}(2/3) = \mathcal{U}_L^{\dagger}\,\mathcal{M}(2/3)\,\mathcal{U}_R\,, \tag{3.15}$$

$$M_{\mathrm{Diag}}(-1/3) = \mathcal{D}_L^{\dagger}\,\mathcal{M}(-1/3)\,\mathcal{D}_R\,, \tag{3.16}$$

and the corresponding rotations of the $\Psi_{L,R}$ vectors of fermion modes are

$$\Psi_{L,R}(5/3)_{\mathrm{mass}} = \mathcal{X}_{L,R}^{\dagger}\,\Psi_{L,R}(5/3)\,, \tag{3.17}$$

$$\Psi_{L,R}(2/3)_{\mathrm{mass}} = \mathcal{U}_{L,R}^{\dagger}\,\Psi_{L,R}(2/3)\,, \tag{3.18}$$

$$\Psi_{L,R}(-1/3)_{\mathrm{mass}} = \mathcal{D}_{L,R}^{\dagger}\,\Psi_{L,R}(-1/3)\,. \tag{3.19}$$

Note that $\mathcal{X}_{L,R}$, $\mathcal{U}_{L,R}$ and $\mathcal{D}_{L,R}$ are unitary 9×9, 18×18 and 12×12 matrices.

3.2 Solution to the Flavor Puzzle

The exponential dependence of the quark field zero modes on the bulk mass parameters can be used to advantage in the attempt to reproduce the SM quark masses and CKM mixing angles. In section 3.2.1 we will see how very hierarchical 4D Yukawa matrices can be generated from anarchic $\mathcal{O}(1)$ parameters in the 5D Theory. The constraints on the parameter space, in particular on the bulk mass parameters, that are imposed by this construction will be outlined in section 3.2.2.

3.2.1 The SM Yukawa Sector

As was discussed in the previous section the effective 4D Yukawa matrices are in the case of a brane Higgs (up to a factor of $\sqrt{2}$) given by (3.7),

$$\left(Y^{4D}_{u,d}\right)_{ij} = F^i_Q \lambda^{u,d}_{ij} F^j_{u,d}\,, \tag{3.20}$$

where no sum over repeated indices is implied. We see that in the brane Higgs case the expressions for the effective 4D Yukawa matrices factorize into the brane overlaps of the left-handed quark doublets, the fundamental 5D Yukawa matrices and the brane overlaps of the right-handed quark singlets. Two comments about the natural absolute sizes and structures of the ingredients of (3.20) are in order at this point. First, the brane overlaps $F^i_{Q,u,d}$ generically display a large hierarchy as they depend exponentially on the quarks' bulk mass parameters which are assumed to be of order one. Second, the fundamental 5D Yukawa matrices $\lambda^{u,d}$ are assumed to be anarchic with entries of order one.

With these two facts given—large hierarchies in the brane overlaps and no structure in the fundamental 5D Yukawa matrices—expression (3.20) strongly resembles the proposal by Froggatt and Nielsen [83] on how large hierarchies in the quark sector can be explained. This resemblance is only one of outcome, but not of concept, since the underlying physics in both cases is vastly different. A table identifying several conceptual features in the RSc and in the Froggatt-Nielsen setup can be found in [33] where also the original Froggatt-Nielsen formulae are given. To demonstrate how the large hierarchies are generated it is enough to consider approximate relations (see e.g. [84]) between quark masses and mixing angles that neglect any possible structure in the Yukawa matrices and are valid at the $\mathcal{O}(1)$ level. They are given by

$$m^i_{u,d} \simeq \frac{v}{\sqrt{2}} F^i_Q \left\langle \lambda^{u,d} \right\rangle F^i_{u,d}\,, \quad \theta_{ij} \simeq \frac{F^i_Q}{F^j_Q}\,, \tag{3.21}$$

where $\langle \lambda^{u,d} \rangle$ is the typical size of the entries of $\lambda^{u,d}$ and θ_{ij} are the mixing angles in the CKM matrix $V_{\rm CKM} = U_L^\dagger D_L$ with

$$\begin{aligned} m_u^{\rm Diag} &= U_L^\dagger m_u U_R \,, \\ m_d^{\rm Diag} &= D_L^\dagger m_d D_R \,. \end{aligned} \tag{3.22}$$

To clarify how realistic quark masses and mixing angles can arise, we will now exemplarily determine the quark brane overlaps $F^i_{Q,u,d}$ by using the approximate formulae (3.21). From there the bulk mass parameters $c^i_{Q,u,d}$ can be easily derived via (3.6) and (2.24). For this demonstration we assume that the typical size of Yukawa couplings $\langle \lambda^{u,d} \rangle$ is 3 and that for the third-generation quark doublet $F^3_Q = 0.4$ holds. Both choices will be motivated in section 3.2.2. First, F^1_Q and F^2_Q can be determined from (3.21) to be

$$F^2_Q \simeq \lambda_C^2 F^3_Q \simeq 0.02 \quad \text{and} \quad F^1_Q \simeq \lambda_C^3 F^3_Q \simeq 0.005 \,, \tag{3.23}$$

where $\lambda_C \simeq 0.23$ is the sine of the Cabibbo angle. Now all remaining brane overlaps are fixed by the quark mass spectrum,

$$\begin{aligned} F_u^{1,2,3} &\simeq \frac{\sqrt{2} m_{u,c,t}}{3 v F_Q^{1,2,3}} \simeq (0.0006, 0.04, 0.7) \,, \\ F_d^{1,2,3} &\simeq \frac{\sqrt{2} m_{d,s,b}}{3 v F_Q^{1,2,3}} \simeq (0.001, 0.005, 0.01) \,. \end{aligned} \tag{3.24}$$

These naïve estimates in practice will be modified by $\mathcal{O}(1)$ factors, depending on the particular structure of the Yukawa matrices $\lambda^{u,d}$. From (3.6) and (2.24) we find for the bulk mass parameters

$$\begin{aligned} c^1_Q \simeq 0.63 \,, \; c^2_Q \simeq 0.57 \,, \; c^3_Q \simeq 0.42 \,, \\ -c^1_u \simeq 0.67 \,, \; -c^2_u \simeq 0.53 \,, \; -c^3_u \simeq -0.35 \,, \\ -c^1_d \simeq 0.66 \,, \; -c^2_d \simeq 0.60 \,, \; -c^3_d \simeq 0.57 \,. \end{aligned} \tag{3.25}$$

The bulk mass parameters in (3.25) are $\mathcal{O}(1)$ and display only a very soft hierarchy. We have seen explicitly how this choice together with totally anarchic Yukawa matrices can lead to the large hierarchies in the quark masses and mixing angles. Thus the RS setup addresses the SM flavor puzzle by localizing the quark zero modes in a flavor-dependent manner (for first attempts in that direction see [85]). Still the RS model does not actually solve the flavor puzzle, but merely postpones it. There is no prediction for the actual values of the bulk mass parameters and Yukawa couplings made by the RS model, and a more fundamental theory is required to predict the values of the respective parameters. On the other hand, the achievement of the RS model clearly is to reduce the hierarchies in quark masses and mixing angles from exponential to linear ones in a motivated manner.

This mechanism to generate hierarchies, which works very well for quarks, fails in the case of the lepton sector. The crucial difference is that in the lepton sector the mixing angles of the leptonic mixing matrix are not small but one is even close to maximal [76]. In a setup resembling the one discussed above a localization of the lepton fields that would explain the mass hierarchy in the lepton sector would also imply small mixing angles. In the following we will not deal with flavor mixing in the lepton sector and just state that there are several proposals in the literature on how a realistic lepton sector can be achieved [86–88].

As a final point in this section we want to continue our keeping track of parameters of the RSc and state how the fundamental 5D Yukawa matrices can be parameterized in a non-redundant way. Details and intermediate steps of this procedure can be found in [33]. We start from the singular value decomposition for the up- and down-type fundamental Yukawa matrices

$$\lambda^u = \frac{1}{k} e^{i\phi_u} U_u^\dagger D_u V_u \,, \qquad \lambda^d = \frac{1}{k} e^{i\phi_d} U_d^\dagger D_d V_d \,, \tag{3.26}$$

where $U_{u,d}$, $V_{u,d}$ are $SU(3)$ matrices and $D_{u,d}$ are real and diagonal. The $SU(3)$ matrices can be parameterized through the Euler decomposition for $SU(3)$ matrices [89]

$$U(\alpha, a, \gamma, c, \beta, b, \theta, \phi) = e^{i\lambda_3\alpha} e^{i\lambda_2 a} e^{i\lambda_3\gamma} e^{i\lambda_5 c} e^{i\lambda_3\beta} e^{i\lambda_2 b} e^{i\lambda_3\theta} e^{i\lambda_8\phi} \,, \tag{3.27}$$

where λ_i are the generators of $SU(3)$, a, b, c are mixing angles and α, β, γ, ϕ, θ are phases. We can now use the freedom to rephase the quark fields Q_L, u_R and d_R and arrive at

$$\begin{aligned}
\lambda^u &= \frac{1}{k} U_u^\dagger(0, a_{U_u}, 0, c_{U_u}, \beta_{U_u}, b_{U_u}, \theta_{U_u}, 0)\, D_u\, V_u(\alpha_{V_u}, a_{V_u}, \gamma_{V_u}, c_{V_u}, \beta_{V_u}, b_{V_u}, 0, 0) \,, \\
\lambda^d &= \frac{1}{k} U_d(0, a_{U_d}, \gamma_{U_d}, c_{U_d}, \beta_{U_d}, b_{U_d}, 0, 0)\, D_d\, V_d(\alpha_{V_d}, a_{V_d}, \gamma_{V_d}, c_{V_d}, \beta_{V_d}, b_{V_d}, 0, 0) \,,
\end{aligned} \tag{3.28}$$

with $D_u = \mathrm{Diag}(y_u^1, y_u^2, y_u^3)$ and $D_d = \mathrm{Diag}(y_d^1, y_d^2, y_d^3)$. From this parameterization we find 18 real parameters and ten physical phases in the fundamental 5D Yukawa matrices. This parameterization of the fundamental Yukawa matrices looks rather cumbersome. On this account we want to alert the reader that it is of utmost importance to have an expression for $\lambda^{u,d}$ in terms of fundamental model parameters. Only then it is possible to scan the parameter space in an unprejudiced way and not to introduce artificial correlations. A parameterization based on phenomenological quantities, which however is unsuited for our present purposes, has been given in [32].

3.2.2 A Localization Ambiguity

In the previous section the natural generation of large hierarchies in the quark spectrum and mixing angles via delocalized quark wave functions has been demonstrated. We will show now that this procedure still leaves some freedom of choice for the nine quark bulk mass parameters. As can bee seen from the expression (3.20) for $Y_{u,d}^{4D}$, even for fixed

5D Yukawa matrices λ^u, λ^d the localization parameters are not fixed unambiguously. In fact, in [84] it has been pointed out that the quark spectrum and mixing angles are invariant under simultaneous shifts of F_Q and F_u, F_d,

$$F_Q \to \zeta F_Q\,, \qquad F_{u,d} \to \frac{1}{\zeta} F_{u,d}\,, \tag{3.29}$$

where ζ is some real, positive parameter. This linear shift on $F_{Q,u,d}$ implies a non-linear transformation of the $c_{Q,u,d}$ parameters which can easily be derived from (3.6) and (2.24). It has to be made clear that the shift (3.29) is not a symmetry of the RS since although leaving invariant the Yukawa sector it has physical impact on the KK spectrum and the couplings of the model. However, if it is not a symmetry of the model, the presence of such a shift transformation implies that beyond the six quark masses, three mixing angles and one CP violating phase an additional piece of information is necessary to make one's choice of localization parameters unambiguous and to allow for meaningful predictions for flavor signatures. For instance, localizing the right-handed quark fields very close to the IR brane and the left-handed quark fields very close to the UV brane ($\zeta < 1$) enhances the right-handed couplings while the opposite localization scheme enhances the left-handed couplings. Observables such as ϵ_K that receive the largest contribution from left-right operators (see section 4.1) are rather robust with respect to those variations whereas most branching ratios of rare K and B decays (see section 4.2) can vary by several orders of magnitude. In the following we will see how the requirement of perturbativity, experimental bounds on gauge couplings such as $W\bar{t}_L b_L$ and $Z t_L \bar{t}_L$ (see for instance [90–97]), and constraints from electroweak precision observables as discussed in section 2.3 can be used to narrow down the valid parameter space. In doing so it is sufficient to analyze the constraints on the $\left(c_Q^3, c_u^3\right)$ plane, since for given c_Q^3, c_u^3 all other localization parameters are fixed by the quark spectrum and mixing angles. We will now discuss the three main constraints on the $\left(c_Q^3, c_u^3\right)$ plane.

Perturbativity In order to keep physics perturbative up to reasonably high energy scales, the dimensionfull Yukawa couplings λ^u, λ^d cannot be arbitrarily large (see e.g. [98–100]). In naïve dimensional analysis, the 1-loop contribution to the Yukawa couplings with loop momenta cut off at energy E would be $\sim (\langle\lambda^{u,d}\rangle E)^3/(16\pi^2)$, where $\langle\lambda^{u,d}\rangle$ is the typical size of entries in λ^u, λ^d. If this contribution is required to be smaller than the tree level term for energies as large as the mass of the $N_{\rm KK}$-th KK mode, this requires $\langle\lambda^{u,d}\rangle k \lesssim 2\pi/N_{\rm KK}$. For the minimal requirement of $N_{\rm KK} = 2$ this leads to $\langle\lambda^{u,d}\rangle k \lesssim 3$. This bound on the size of a typical entry of the 5D Yukawa matrices λ^u and λ^d also puts constraints on the quark localization parameters c_Q and $c_{u,d}$. In particular the large top quark mass requires that the product $F_Q^3 F_u^3$ can be no smaller than $(\sqrt{2}m_t)/(3v) \approx 0.27$, forbidding the left-handed quark doublet of the third generation and the right-handed top quark singlet to be localized too far away from the IR brane. The constraint on the $\left(c_Q^3, c_u^3\right)$ plane from perturbativity is shown in fig. 3.1; the 3-contour belonging to $(\sqrt{2}m_t)/(3v) = F_{Q_3} F_{u_3}$ marks the boundary of the allowed parameters space, forbidding all values to its right. The remaining contours correspond to lower typical values for the

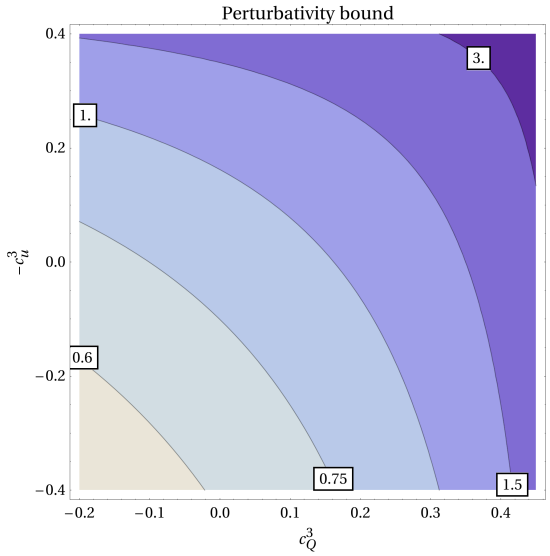

Figure 3.1: The constraint imposed on the $\left(c_Q^3, c_u^3\right)$ plane by the requirement that the theory remains perturbative up to energies $E \simeq M_{\mathrm{KK}}^{(2)}$. Areas to the right of the 3-contour are excluded.

entries of the Yukawa matrices. If we take into account that with the parameterization for the Yukawa matrices λ^u, λ^d chosen in section 3.2.1 the average size of a Yukawa coupling is rather $\langle\lambda^{u,d}\rangle k \approx 3/2$, values of (c_Q^3, c_u^3) close to the 3-contour are very unlikely.

$Zt_L\bar{t}_L$ and $W\bar{t}_Lb_L$ couplings The left-handed coupling of the Z boson to bottom quarks is protected in the RSc [78] and is found to be under control throughout the $\left(c_Q^3, c_u^3\right)$ plane [55]. The same is true for the right-handed couplings of the Z boson to top quarks. Under these circumstances corrections are expected to be most relevant for the left-handed coupling of the Z boson to top quarks. Indeed, we find that for an IR localized left-handed third generation bi-doublet $\xi_{1,L}^3$ these corrections can amount to as much as 20%. Admittedly there are no experimental constraints on this coupling to date [101], which is mainly due to the production mechanism via the strong interaction at the Tevatron, the overwhelming $\gamma \to t\bar{t}$ background and the fact that $t\bar{t}$ pairs at the Tevatron are produced almost at rest which suppresses polarization effects. On the other hand, this coupling is expected to become accessible at the LHC once enough statistics is available.
Sizable corrections are also possible for the $W\bar{t}_Lb_L$ coupling, which is weakly constrained by single top production at the Tevatron, $|V_{tb}| = 0.91(8)$ [102], but very strongly bounded once unitarity of the CKM matrix is assumed [76].
Assuming that both abovementioned couplings will be found to be SM-like in the future, a strong localization of the right-handed top quark towards the IR brane would be preferred. The level of corrections to the $Zt_L\bar{t}_L$ and $W\bar{t}_Lb_L$ couplings in dependence on the localization parameters is shown in fig. 3.2. We will analyze the issue of modified gauge-fermion interactions in more detail in sections 3.4 and 3.5.

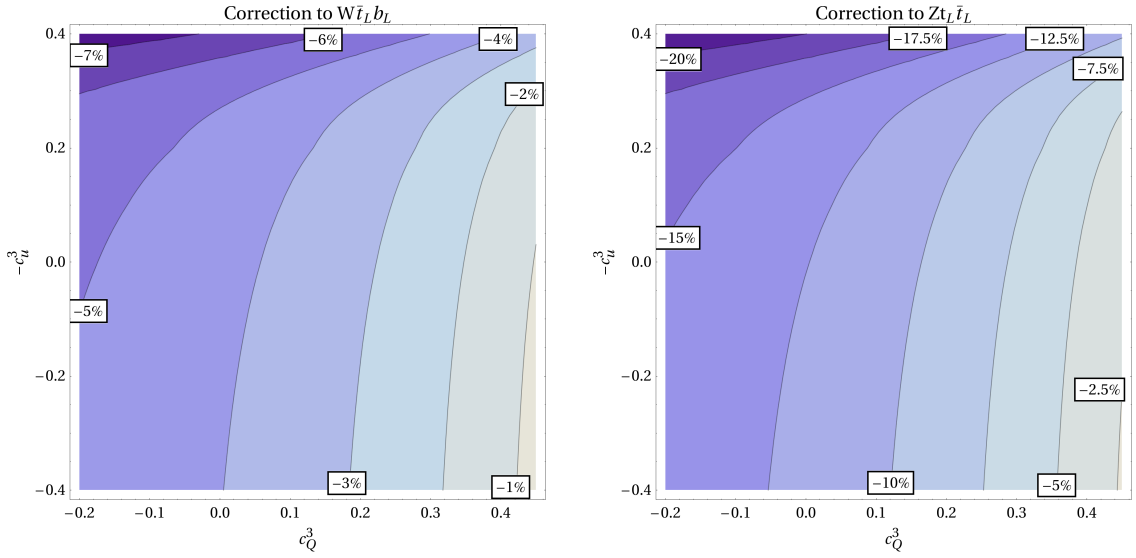

Figure 3.2: Percentaged corrections to the couplings $W\bar{t}_L b_L$ (left panel) and $Zt_L\bar{t}_L$ (right panel).

Electroweak precision observables Ironically, the fermion fields arising from the enlarged multiplets (2.80) introduced in order to protect the $Zb_L\bar{b}_L$ coupling give rise to loop level contributions to the T parameter [55]. This contribution turns out to be negative, unless the left-handed third generation bi-doublet ξ^3_{1L} is localized strongly towards the IR brane which will result in a positive contribution to the T parameter as would be preferred by experimental data [76]. On the other hand, the contributions to T are small but negative for ξ^3_{1L} being localized close to the conformal point $c_{Q_3} \lesssim 0.5$. The dependence of the correction to the T parameter on the relevant localization parameters is shown in fig. 3.3.

From the above discussion we see that the only parameter configuration that is favored by both $Zt_L\bar{t}_L$ and the T parameter violates perturbativity. The remaining portion of parameter space that allows for a positive loop contribution to the T parameter leads to a large negative contribution to the $Zt_L\bar{t}_L$ and $W\bar{t}_L b_L$ couplings. However, due to experimental uncertainties, a small but negative loop contribution to the T parameter is still not excluded depending on the exact value of the S parameter. Following this line of argument, the favored area in the $\left(c^3_Q, c^3_u\right)$ plane then is given by the left-handed bi-doublet ξ^3_{1L} being localized close to the conformal point, $c_{Q_3} \lesssim 0.5$, and the right-handed top quark singlet being strongly localized towards the IR brane, $-c^3_u \lesssim 0$. Throughout the numerical analysis of the present thesis we will therefore assume $0.4 \leqslant c^3_Q \leqslant 0.45$.

It is important to note that this particular corner in the $\left(c^3_Q, c^3_u\right)$ plane is only favored because the custodial symmetry protects the Z couplings to the right-handed up-type quarks from large corrections. A localization of the right-handed top singlet this close to the IR brane would be disastrous in the minimal RS model without custodial protection (which will be denoted RSm from now on). As a result, the RSc tends to favor enhanced

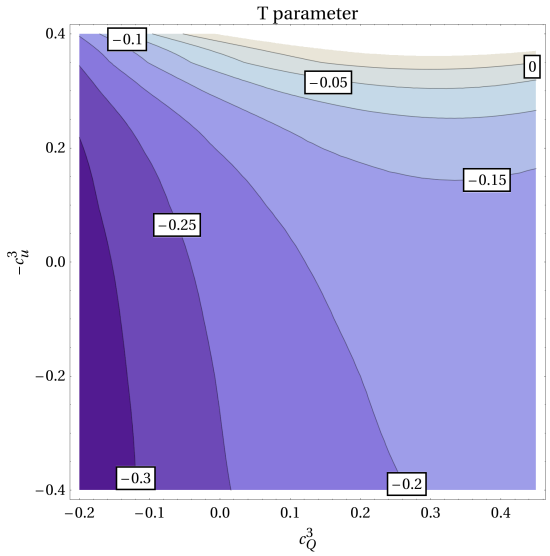

Figure 3.3: The constraint imposed on the $\left(c_Q^3, c_u^3\right)$ plane by the T parameter, based on [55].

right-handed couplings of the EW gauge bosons while the RSm shows no such trend and left- and right-handed couplings are expected to be enhanced or suppressed to roughly the same degree. Already from this insight it becomes clear that the RSc and RSm models should display very different signatures for flavor observables, and in particular rare decays of K and B mesons.

3.3 Flavor Parameters and Total Parameter Count

Before we proceed to calculating the phenomenologically relevant flavor violating vertices, we want to give account of the number of model parameters of the RSc. As already done above, we can without loss of generality choose a basis in which the bulk mass matrices c_1, c_2, c_3 are diagonal. In this case they yield nine real and independent flavor parameters. For the parameterization of the fundamental Yukawa matrices λ^u, λ^d, as can be explicitly seen from the parameterization (3.28), we need the total number of 18 real parameters and ten complex phases. This number is consistent with the fact that two arbitrary unitary 3×3 matrices together have 18 real parameters and 18 complex phases, and that the flavor symmetries of the RSc allow to absorb eight complex phases by field re-definitions. Thus we find 27 real parameters and 10 complex phases in the flavor sector of the RSc, which is 18 real parameters and 9 complex phases in excess of the SM case[1]. These additional parameters can be readily identified as the quark bulk masses which generically are represented by three 3×3 hermitian matrices. Even without further investigation of the flavor structure of the RSc we can conclude at this

[1] An analogous parameter counting also applies to the lepton sector of the RSc.

point that the RSc does not fall into the class of models with Minimal Flavor Violation (MFV) [103–106].

Apart from the parameters in the flavor sector there are two parameters k and L related to the geometrical setup which can be exchanged for the suppression factor e^{-kL} and the mass scale M_{KK}. Of these, the former is fixed by the requirement to address the gauge hierarchy problem[2], while the latter can be chosen arbitrarily in the range $M_{\text{KK}} \gtrsim (2-3)\,\text{TeV}$. Additional parameters in this context, such as the bulk and brane cosmological constants or parameters related to the stabilization of the modulus $r_c = L/\pi$ are assumed to be chosen such that the RS geometrical setup is obtained. Furthermore they are assumed to have no significant impact on the phenomenology of the RSc.
The fundamental gauge couplings g, g_X are related to the 4D couplings via $g_i = \sqrt{L} g_i^{4D}$ and are thus determined by the measured weak and electromagnetic coupling constants. The matching of the fundamental QCD coupling constant g_s to the measured coupling on the other hand is modified in the presence of brane kinetic terms such that at the KK scale, where $g_s^{4D} \simeq 1$, g_s can take values between $\sqrt{L}/2$ and $\sqrt{L}$ and has to be treated as a free parameter (this matching is treated in more detail in section 3.4.2).
In the case of a Higgs boson that is localized on the IR brane, we can assume the Higgs sector to have the minimal set of parameters μ and λ. If the Higgs is detached from the IR brane, the localization parameter β constitutes an additional free parameter.

Finally, for comparison we also give the number of parameters of other NP models, such as the LHT and SM4 that we will contrast against the RSc in section 5.4: Compared to the SM, the LHT has seven additional real parameters and three complex phases [108–111], while the SM4 has five relevant additional real parameters and two complex phases [112].

3.4 Fermion Couplings in the Zero Mode Approximation

In this section we will analyze the flavor violating couplings of quark zero modes to the lightest KK gauge bosons. Apart from directly entering tree level flavor changing processes, the KK gauge bosons after EWSB can also mix into the zero modes with identical quantum numbers. This is relevant for the Z and $W^\pm$ gauge bosons which in this process also receive flavor changing couplings, typically suppressed by mixing angles that are $\mathcal{O}(v^2/M_{\text{KK}}^2)$.

3.4.1 The RS-GIM Mechanism

The KK modes of the gauge bosons—unlike their flat zero modes—are localized non-uniformly along the fifth dimension. More precisely, they are peaked strongly towards

[2]For an alternative approach see however [107].

the IR brane (see fig. 2.1). The couplings of these KK modes to quark zero modes, which are also localized non-uniformly, are described by the overlap integrals $\underset{00}{\mathcal{R}_k}(++)_{L,R}$ and $\underset{00}{\mathcal{P}^i_k}(++)_{L,R}$ defined in (2.51), (2.52) and (2.54), where the first applies to $(++)$ BCs of the KK gauge boson mode and the latter to $(-+)$ BCs. These integrals manifestly depend on the bulk mass parameter c of the fermion that interacts with the KK gauge boson. Hence the 3×3 gauge coupling matrices in the flavor eigenbasis are diagonal, but they are not universal. When transformed to the mass eigenbasis via bi-unitary rotations, these non-universal coupling matrices will obtain off-diagonal entries signaling flavor changing interactions. At first sight such flavor violating couplings of gauge bosons which, although heavy, are exchanged at the tree level seem to be disastrous for the RSc from a phenomenological point of view. Fortunately, these couplings have a particular structure which strongly suppresses their impact on the most relevant flavor observables. This feature of RS models with non-universally localized bulk fermions is referred to as the *RS-GIM mechanism*.

The basis of the RS-GIM mechanism is that the KK gauge boson modes have a localization that is very similar to that of the brane localized Higgs field: both are relevant only close to the IR brane. Hence the couplings of the zero mode fermions to the KK gauge bosons are roughly proportional to their overlaps F_Q, F_u, F_d with the IR brane,

$$\begin{aligned}
\left[\hat{\epsilon}_L^{-1/3,2/3}\right]_{ii} &\sim (F_Q^i)^2\,, \\
\left[\hat{\epsilon}_R^{2/3}\right]_{ii} &\sim (F_u^i)^2\,, \\
\left[\hat{\epsilon}_R^{-1/3}\right]_{ii} &\sim (F_d^i)^2\,,
\end{aligned} \tag{3.30}$$

where the diagonal 3×3 matrices $\hat{\epsilon}^Q_{L,R}$ denote the couplings of fermion zero modes to KK gauge bosons in the flavor eigenbasis. These matrices have to be rotated to the mass eigenbasis via bi-unitary rotations,

$$\begin{aligned}
\hat{\Delta}^{2/3}_{L,R} &= U^\dagger_{L,R}\hat{\epsilon}^{2/3}_{L,R}U_{L,R}\,, \\
\hat{\Delta}^{-1/3}_{L,R} &= D^\dagger_{L,R}\hat{\epsilon}^{-1/3}_{L,R}D_{L,R}\,,
\end{aligned} \tag{3.31}$$

where the 3×3 unitary rotation matrices $U_{L,R}$, $D_{L,R}$ have been defined in (3.22).

We will now investigate the structure of the coupling matrices $\hat{\Delta}^Q_{L,R}$, starting with the case of only two light quark flavors. If the rotation matrices $U_{L,R}$, $D_{L,R}$ are hierarchical, and we have seen in section 3.2.1 that they in fact are, the off-diagonal entries of $\hat{\Delta}^Q_{L,R}$ in the two flavor case for small mixing angle θ are schematically given by

$$\begin{pmatrix} 1 & -\theta \\ \theta & 1 \end{pmatrix}\begin{pmatrix} \epsilon_{11} & 0 \\ 0 & \epsilon_{22} \end{pmatrix}\begin{pmatrix} 1 & \theta \\ -\theta & 1 \end{pmatrix} = \begin{pmatrix} \epsilon_{11} + \mathcal{O}(\theta^2) & \theta(\epsilon_{11} - \epsilon_{22}) \\ \theta(\epsilon_{11} - \epsilon_{22}) & \epsilon_{22} + \mathcal{O}(\theta^2) \end{pmatrix}. \tag{3.32}$$

We see that the flavor changing couplings involving the light quarks (that have small $\epsilon_{ii} \sim (F^i_{Q,u,d})^2$) are not only suppressed by the absolute smallness of their overlaps with the

IR brane, but also by the comparably small difference of these. The situation drastically changes in the three flavor case. Now also terms involving the third generation—with its large IR brane overlap but very small mixing with the first two generations—contribute to the flavor transitions among the two light flavors. Schematically, these contributions are given by $\Delta_{12} \sim \epsilon_{33}\theta_{13}\theta_{23}$ which through $\theta_{i3} \sim F^i_{Q,u,d}/F^3_{Q,u,d}$ is still suppressed by the small IR brane overlaps of the light quarks, although not by the splitting in these overlaps as was the case for two quark flavors. This situation is similar to the SM where loop contributions to flavor changing processes vanish in the limit of universal quark masses due to the unitarity of the CKM matrix [31], hence the naming *RS-GIM mechanism*.

The typical sizes of flavor changing couplings of quark zero modes to KK gauge bosons are governed by the typical IR brane overlaps of the quarks and hence in the end by the quark masses and mixing angles. This allows to define patterns or textures for the coupling matrices $\hat{\Delta}^Q_{L,R}$ that characterize the hierarchies between the averaged entries. We will denote the pattern in the $\hat{\Delta}^Q_L$ coupling matrices by *RS-GIM(Q)* and the ones in $\hat{\Delta}_R^{-1/3,2/3}$ by *RS-GIM(d)*, *RS-GIM(u)*. This characterization will be convenient in our comparison of the impact of KK fermions and of gauge boson mixing on flavor changing couplings in section 3.5.

Finally, we want to point out a further implication of the generation of flavor changing couplings from non-universalities in the gauge couplings of flavor eigenstates. We have seen in the two flavor case how the off-diagonal elements of the coupling matrices $\hat{\Delta}^Q_{L,R}$ are related to the couplings $\hat{\epsilon}^Q_{L,R}$ and to the mixing angle θ. Using the fact that $\mathrm{Det}(\hat{\Delta}^Q_{L,R}) = \mathrm{Det}(\hat{\epsilon}^Q_{L,R})$ and $\mathrm{Tr}(\hat{\Delta}^Q_{L,R}) = \mathrm{Tr}(\hat{\epsilon}^Q_{L,R})$, we can generalize this relation to the three flavor case and find that a condition exists which puts an upper bound on the typical sizes of the sums of the absolute squares of the off-diagonal coupling elements $|[\hat{\Delta}^Q_{L,R}]_{12}|^2 + |[\hat{\Delta}^Q_{L,R}]_{13}|^2 + |[\hat{\Delta}^Q_{L,R}]_{23}|^2$. But this implies that—typically—these off-diagonal coupling elements cannot be simultaneously large. This feature can be seen in fig. 3.4 where we show the absolute squares of the 21 and 32 elements of the $\hat{\Delta}_L^{-1/3}$ coupling matrix (for a (++) KK gauge boson) as a density plot for a random sample of parameter sets. Here light areas correspond to a high density of parameter points while dark areas indicate a low density.

3.4.2 Couplings to KK Gluons and Photons

Since both QCD and QED remain unbroken in the RSc, gluons and photons of different KK level do not mix with each other. The massless gluons and photons therefore couple to the fermion zero modes in a flavor-diagonal and flavor-universal manner. The first gluonic and photonic KK modes $G^{A(1)}$ and $A^{(1)}$ on the other hand have flavor changing couplings to the fermion zero modes, as was discussed in a more general framework in the previous subsection. Here, up to factors of i, Dirac and color matrices, the couplings

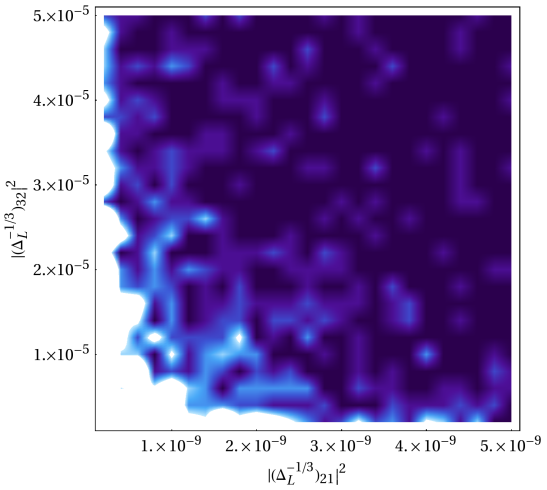

Figure 3.4: Absolute squares of the 21 and 32 elements of the $\hat{\Delta}_L^{-1/3}$ coupling matrix for a (++) KK gauge boson.

in the flavor eigenbasis are given by

$$\begin{aligned}
\hat{\epsilon}_L^{-1/3}(A^{(1)}) &= \hat{\epsilon}_L^{2/3}(A^{(1)}) = \frac{Qe}{\sqrt{L}} \underset{00}{\mathcal{R}_1}(++)_L \,, \\
\hat{\epsilon}_R^{-1/3}(A^{(1)}) &= \frac{Qe}{\sqrt{L}} \underset{00}{\mathcal{R}_3}(++)_R \,, \\
\hat{\epsilon}_R^{2/3}(A^{(1)}) &= \frac{Qe}{\sqrt{L}} \underset{00}{\mathcal{R}_2}(++)_R \,,
\end{aligned} \tag{3.33}$$

and

$$\hat{\epsilon}_{L,R}^{Q}(G^{(1)}) = \frac{g_s}{Qe} \hat{\epsilon}_{L,R}^{Q}(A^{(1)}) \,, \tag{3.34}$$

where g_s and e are the fundamental 5D couplings which at the tree level and in the absence of brane kinetic terms are related to the experimentally determined 4D couplings by $g_s = \sqrt{L} g_s^{4D}$ and $e = \sqrt{L} e^{4D}$. Since the bulk profiles of the left-handed and right-handed fermion zero modes in general are different from each other, we have $\hat{\epsilon}_L^{Q}(G^{(1)}, A^{(1)}) \neq \hat{\epsilon}_R^{Q}(G^{(1)}, A^{(1)})$ which indicates parity violation in the couplings of fermion zero modes to KK gluons and KK photons.
Analogous to the general discussion in the previous subsection, the couplings of quark zero modes to KK gluons and KK photons in the mass eigenbasis are given by

$$\begin{aligned}
\hat{\Delta}_L^{-1/3}(G^{(1)}, A^{(1)}) &= D_L^\dagger \, \hat{\epsilon}_L^{-1/3}(G^{(1)}, A^{(1)}) \, D_L \,, \\
\hat{\Delta}_R^{-1/3}(G^{(1)}, A^{(1)}) &= D_R^\dagger \, \hat{\epsilon}_R^{-1/3}(G^{(1)}, A^{(1)}) \, D_R \,, \\
\hat{\Delta}_L^{2/3}(G^{(1)}, A^{(1)}) &= U_L^\dagger \, \hat{\epsilon}_L^{2/3}(G^{(1)}, A^{(1)}) \, U_L \,, \\
\hat{\Delta}_R^{2/3}(G^{(1)}, A^{(1)}) &= U_R^\dagger \, \hat{\epsilon}_R^{2/3}(G^{(1)}, A^{(1)}) \, U_R \,.
\end{aligned} \tag{3.35}$$

Before we proceed, some comments about the matching condition $g_s = \sqrt{L} g_s^{4D}$ are in order. As mentioned, this relation holds if the coupling constants are matched in the absence of brane kinetic terms for the gluons. However, such brane kinetic terms are not forbidden by symmetry principles and as such will be generated at the loop level even if their bare values are zero. In particular on the UV brane where the momentum cut-off is large these effects are sizeable and induce negative brane kinetic terms. These effectively reduce the 5D coupling by roughly 50% such that we obtain the lowest possible value $g_s\big|_{\text{1-loop}} = \sqrt{L} g_s^{4D}/2$. For an RG evolved QCD coupling $g_s^{4D}(\mu \simeq M_{\text{KK}}) \simeq 1$ and $\sqrt{L} \simeq 6$ we accordingly find[3] $g_s = 6$ for tree level matching and $g_s = 3$ if no bare brane kinetic terms are present and loop effects are taken into account. In the case of positive brane kinetic terms at the tree level, the fundamental QCD coupling is effectively enhanced such that values up to $g_s \simeq 12$ are possible.

On the other hand, in order for the theory to retain perturbative calculability up to energies somewhat beyond the mass of the second KK mode, the fundamental QCD coupling must not be too large. Naïve dimensional analysis suggests $g_s \simeq 6$ as an upper bound for this coupling and the inclusion of helicity and color factors even suggests that $g_s \simeq 3$ marks the maximal value [100]. Since this is an estimate from naïve dimensional analysis we will choose $g_s = 6$ as a reference value in order to be conservative and not to preclude interesting flavor effects right from the start. For completeness we will nevertheless also consider the lowest possible value $g_s = 3$ in our numerical analysis in chapter 5.

3.4.3 Couplings to the Z, Z_H and Z' Gauge Bosons: Custodial Protection

Before EWSB the couplings of $Z^{(0)}$ to quark flavor eigenstates are flavor universal,

$$\begin{aligned}
\hat{\epsilon}_L^{-1/3}(Z^{(0)}) &= g_{Z,L}^{4D}(d)\, \mathbb{1}\,, \\
\hat{\epsilon}_R^{-1/3}(Z^{(0)}) &= g_{Z,R}^{4D}(d)\, \mathbb{1}\,, \\
\hat{\epsilon}_L^{2/3}(Z^{(0)}) &= g_{Z,L}^{4D}(u)\, \mathbb{1}\,, \\
\hat{\epsilon}_R^{2/3}(Z^{(0)}) &= g_{Z,R}^{4D}(u)\, \mathbb{1}\,,
\end{aligned} \tag{3.36}$$

[3] In the following discussion it will be convenient to set $\sqrt{k} \equiv 1$ such that $\sqrt{L} \simeq 6$. This identification is possible since all relevant quantities are sensitive to the product kL only. The only exception to this rule, M_{KK}, is fixed to its value by hand.

while the ones of $Z^{(1)}$ and $Z_X^{(1)}$ are not. The $Z^{(1)}$ couplings are proportional to the KK gluon and KK photon couplings and are given by

$$\begin{aligned}
\hat{\epsilon}_L^{-1/3}(Z^{(1)}) &= g_{Z,L}^{4D}(d)\underset{00}{\mathcal{R}_1}(++)_L\,,\\
\hat{\epsilon}_R^{-1/3}(Z^{(1)}) &= g_{Z,R}^{4D}(d)\underset{00}{\mathcal{R}_3}(++)_R\,,\\
\hat{\epsilon}_L^{2/3}(Z^{(1)}) &= g_{Z,L}^{4D}(u)\underset{00}{\mathcal{R}_1}(++)_L\,,\\
\hat{\epsilon}_R^{2/3}(Z^{(1)}) &= g_{Z,R}^{4D}(u)\underset{00}{\mathcal{R}_2}(++)_R\,.
\end{aligned} \tag{3.37}$$

The $Z_X^{(1)}$ couplings finally are proportional to the $\underset{00}{\mathcal{P}_k}(++)_{L,R}$ integrals defined in (2.52) and (2.54),

$$\begin{aligned}
\hat{\epsilon}_L^{-1/3}(Z_X^{(1)}) &= \kappa_1^{4D}(d)\underset{00}{\mathcal{P}_1}(++)_L\,,\\
\hat{\epsilon}_R^{-1/3}(Z_X^{(1)}) &= \kappa_5^{4D}(d)\underset{00}{\mathcal{P}_3}(++)_R\,,\\
\hat{\epsilon}_L^{2/3}(Z_X^{(1)}) &= \kappa_1^{4D}(u)\underset{00}{\mathcal{P}_1}(++)_L\,,\\
\hat{\epsilon}_R^{2/3}(Z_X^{(1)}) &= \kappa_3^{4D}(u)\underset{00}{\mathcal{P}_2}(++)_R\,.
\end{aligned} \tag{3.38}$$

The couplings $g_{Z,L}^{4D}(u,d)$, $g_{Z,R}^{4D}(u,d)$, $\kappa_1^{4D}(u,d)$, $\kappa_5^{4D}(u,d)$ are collected in appendix A. After EWSB the gauge eigenstates $Z^{(0)}$, $Z^{(1)}$ and $Z_X^{(1)}$ mix among each other to form the mass eigenstates Z, Z_H and Z'. This a priori implies that the couplings of all three mass eigenstates are flavor non-universal. We will now investigate this issue in more detail. With the composition of the neutral mass eigenstates given in (2.76) we find for the Z, Z_H and Z' couplings

$$\begin{aligned}
\hat{\epsilon}_{L,R}^{Q}(Z) &= \hat{\epsilon}_{L,R}^{Q}(Z^{(0)}) + \frac{M_Z^2}{M_{\rm KK}}\left[-\mathcal{I}_1^+\,\hat{\epsilon}_{L,R}^{Q}(Z^{(1)}) + \mathcal{I}_1^-\cos\phi\cos\psi\,\hat{\epsilon}_{L,R}^{Q}(Z_X^{(1)})\right]\,,\\
\hat{\epsilon}_{L,R}^{Q}(Z_H) &= \frac{1}{\sqrt{2}}\left[\cos\phi\,\hat{\epsilon}_{L,R}^{Q}(Z^{(1)}) + \frac{1}{\cos\psi}\,\hat{\epsilon}_{L,R}^{Q}(Z_X^{(1)})\right]\,,\\
\hat{\epsilon}_{L,R}^{Q}(Z') &= \frac{1}{\sqrt{2}}\left[\cos\phi\,\hat{\epsilon}_{L,R}^{Q}(Z_X^{(1)}) - \frac{1}{\cos\psi}\,\hat{\epsilon}_{L,R}^{Q}(Z^{(1)})\right] - \frac{M_Z^2}{M_{\rm KK}^2}\frac{\mathcal{I}_1}{\sqrt{2}}\,\hat{\epsilon}_{L,R}^{Q}(Z^{(0)})\,.
\end{aligned} \tag{3.39}$$

In the limit of exact P_{LR} symmetry and neglecting the symmetry breaking effects by BCs on the UV brane, we have $\mathcal{I}_1^+ = \mathcal{I}_1^-$ and for the overlap integrals

$$\underset{00}{\mathcal{R}_k}(BC)_{L,R} = \underset{00}{\mathcal{P}_k}(BC)_{L,R}\,, \tag{3.40}$$

such that $\hat{\epsilon}^Q_{L,R}(Z^{(1)})$ and $\hat{\epsilon}^Q_{L,R}(Z^{(1)}_X)$ are equal up to the different coupling constants g_Z^{4D} and κ^{4D}. Then,

$$\begin{aligned}
\hat{\epsilon}^Q_{L,R}(Z) &= \hat{\epsilon}^Q_{L,R}(Z^{(0)}) + \frac{M_Z^2}{M_{\mathrm{KK}}}\mathcal{I}_1\left[-g_Z^{4D}(F) + \cos\phi\cos\psi\,\kappa^{4D}(F)\right]\frac{\hat{\epsilon}^Q_{L,R}(Z^{(1)})}{g_Z^{4D}(F)}\,,\\
\hat{\epsilon}^Q_{L,R}(Z_H) &= \frac{1}{\sqrt{2}}\left[\cos\phi\, g_Z^{4D}(F) + \frac{1}{\cos\psi}\,\kappa^{4D}(F)\right]\frac{\hat{\epsilon}^Q_{L,R}(Z^{(1)})}{g_Z^{4D}(F)}\,,\\
\hat{\epsilon}^Q_{L,R}(Z') &= \frac{1}{\sqrt{2}\cos\psi}\left[\cos\phi\cos\psi\,\kappa^{4D}(F) - g_Z^{4D}(F)\right]\frac{\hat{\epsilon}^Q_{L,R}(Z^{(1)})}{g_Z^{4D}(F)} - \frac{M_Z^2}{M_{\mathrm{KK}}^2}\frac{\mathcal{I}_1}{\sqrt{2}}\,\hat{\epsilon}^Q_{L,R}(Z^{(0)})\,,
\end{aligned} \tag{3.41}$$

where $g_Z^{4D}(F)$ and $\kappa^{4D}(F)$ have to be chosen appropriately from $g_{Z,L}^{4D}(u,d)$, $g_{Z,R}^{4D}(u,d)$ and $\kappa_1^{4D}(u,d)$, $\kappa_3^{4D}(u,d)$. To translate the flavor eigenbasis couplings in (3.41) into the mass eigenbasis we simply have to replace the $\hat{\epsilon}$ coupling matrices by $\hat{\Delta}$, which can be obtained from the former by bi-unitary rotations analogous to (3.35).
We see from (3.41) that the Z and Z' couplings are proportional to the same combination of coupling constants,

$$g_Z^{4D}(F) - \cos\phi\cos\psi\,\kappa^{4D}(F)\,, \tag{3.42}$$

and with the explicit expressions for these coupling constants given in appendix A we find that for $F = d_L$ and $F = u_R$ the combination (3.42) vanishes. This is the manifestation of the custodial protection at the technical level. For the Z couplings to left-handed down-type and right-handed up-type quarks the corrections to the leading coupling $g_Z^{4D}(F)\,\mathbb{1}$ are strongly suppressed, so that the flavor conserving couplings are SM-like—among them the $Zb_L\bar{b}_L$ coupling—and the flavor changing couplings vanish in the limit of exact P_{LR} symmetry. It is interesting to note, and this fact was overlooked in the literature for some time, that the construction which was aimed at protecting the $Zb_L\bar{b}_L$ coupling, in the end also suppresses corrections to all other $Zd_L^i\bar{d}_L^j$ couplings and also to the $Zu_R^i\bar{u}_R^j$ couplings. The Z' which is subject to the same protection in the limit of exact P_{LR} symmetry does not couple to the left-handed down-type and right-handed up-type quarks at all. As an example, in fig. 3.5 we contrast the left- and right-handed $Zd\bar{s}$ and $Zs\bar{b}$ couplings using the set of parameter points from our global numerical analysis in chapter 5. We want to point out the following observations:

- With active custodial protection we see that the left-handed couplings are on average suppressed by roughly two orders of magnitude. The slightly stronger suppression in the case of the left-handed (bs) coupling is due to the fact that for heavier quarks the impact of symmetry breaking effects by BCs on the UV brane become less relevant, as can be seen in fig. 2.3.

- As a consequence, $(\hat{\Delta}_R^{-1/3}(Z))_{sd}$ is larger than $(\hat{\Delta}_L^{-1/3}(Z))_{sd}$ for a dominant part of the allowed parameter points and is on average larger than $(\hat{\Delta}_L^{-1/3}(Z))_{sd}$ by two orders of magnitude.

- The dominance of $(\hat{\Delta}_R^{-1/3}(Z))_{bs}$ over $(\hat{\Delta}_L^{-1/3}(Z))_{bs}$ is less pronounced, but still on average $(\hat{\Delta}_R^{-1/3}(Z))_{bs}$ is larger than $(\hat{\Delta}_L^{-1/3}(Z))_{bs}$ by one order of magnitude. The reason for this behavior is independent of the custodial protection and lies in the fact that the left-handed doublet always is localized closer to the IR brane than the right handed down-type singlet and thus couples more strongly to KK gauge bosons. This effect is particularly pronounced for the b quark (cf. the naïve estimate for the fermionic IR brane overlaps in the discussion that led to (3.24)).

- The values of $(\hat{\Delta}_R^{-1/3}(Z))_{bs}$ are on average larger than $(\hat{\Delta}_R^{-1/3}(Z))_{sd}$ by one order of magnitude, as the (b_R, s_R) system is localized closer to the IR brane than the (s_R, d_R) system.

- If the cancellation due to the custodial protection is removed (by setting the κ coupling constants to zero) the left-handed couplings considerably exceed the right-handed couplings, as is to be expected from the ratio of coupling constants $|g^{4D}_{Z,L}(d)/g^{4D}_{Z,R}(d)| \simeq 5.5$ and the fact that the relevant left handed modes are localized closer towards the IR brane than the right handed modes.

For $(\hat{\Delta}_{L,R}^{-1/3}(Z))_{bd}$ we find values between those for the (bs) and (sd) cases.

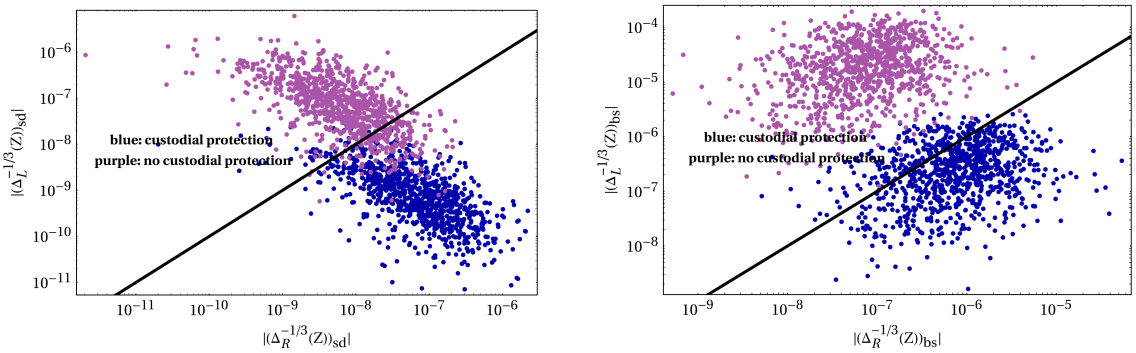

Figure 3.5: $|\hat{\Delta}_L^{-1/3}(Z)|_{ij}$ vs. $|\Delta_R^{-1/3}(Z)|_{ij}$ for $ij = sd$ (left panel) and $ij = bs$ (right panel). The blue points are obtained after imposing all constraints from $\Delta F = 2$ observables (see section 5.2). The purple points show the effect of removing the custodial protection. The solid lines display the equality $|\hat{\Delta}_L^{-1/3}(Z)|_{ij} = |\hat{\Delta}_R^{-1/3}(Z)|_{ij}$.

3.4.4 Couplings to the $W^{\pm}$ Gauge Bosons

In the flavor eigenbasis the couplings of the $W_L^{(0)+}$ and $W_L^{(1)+}$ gauge bosons are given by

$$\hat{\epsilon}_L(W_L^{(0)+}) = \frac{g^{4D}}{\sqrt{2}}\mathbb{1}\,,$$
$$\hat{\epsilon}_L(W_L^{(1)+}) = \frac{g^{4D}}{\sqrt{2}}\underset{00}{R_1}(++)_L\,, \tag{3.43}$$

such that for the mass eigenstates $W^\pm$, $W_H^\pm$, $W'^\pm$ given in (2.75) we find

$$\begin{aligned}
\hat{\epsilon}_L(W^+) &= \frac{g^{4D}}{\sqrt{2}}\left[\mathbb{1} - \mathcal{I}_1 \frac{M_W^2}{M_{\mathrm{KK}}^2} \underset{00}{R_1}(++)_L\right], \\
\hat{\epsilon}_L(W_H^+) &= \frac{g^{4D}}{2} \underset{00}{R_1}(++)_L, \\
\hat{\epsilon}_L(W'^+) &= -\frac{g^{4D}}{2}\left[\underset{00}{R_1}(++)_L + \mathcal{I}_1 \frac{M_W^2}{M_{\mathrm{KK}}^2}\mathbb{1}\right].
\end{aligned} \tag{3.44}$$

The couplings of the $SU(2)_R$ gauge boson $W_R^{(1)\pm}$ do not enter above as it mediates changes of T_R^3 and hence does not couple to pairs of SM quarks. Again, we can transform the couplings to flavor eigenstates to the mass eigenbasis using the unitary matrices U_L, D_L. In contrast to the SM, where the CKM matrix is simply given by $U_L^\dagger D_L$, the CKM matrix in the RSc is given by

$$\begin{aligned}
V_{\mathrm{CKM}} &= U_L^\dagger \left[\mathbb{1} - \mathcal{I}_1 \frac{M_W^2}{M_{\mathrm{KK}}^2} \underset{00}{R_1}(++)_L\right] D_L \\
&\equiv V_{\mathrm{CKM}}^0 + \frac{v^2}{M_{\mathrm{KK}}^2} U_L^\dagger \, \Delta_{\mathrm{gauge}} \, D_L \,.
\end{aligned} \tag{3.45}$$

Since Δ_{gauge} in general is not proportional to the unit matrix, the CKM matrix (3.45) is not unitary. We will return to this issue and investigate typical deviations of the CKM matrix from its SM structure in section 3.5.4.

3.5 Impact of KK Fermions

In this section we will investigate the quantitative impact of heavy vector-like KK fermions on SM fermion couplings. This effect is relevant for the couplings of all massive gauge bosons, but we will concentrate on the couplings of SM quarks to the Z and $W^\pm$ gauge bosons as well as to the first KK excitation of the gluons. A particularly elegant way to proceed is to construct an effective theory by integrating out the heavy modes that mix with the SM fermions at $\mathcal{O}(v^2/M_{\mathrm{KK}}^2)$. The construction of such an effective theory starting from a generic theory with heavy vector-like fermions has been presented in [35], where also a comparison of the exact numerical calculation[4] in the context of the RSc to the results obtained in the effective theory approach has been performed. In section 3.5.1 we will recapitulate the most important aspects of this derivation. In sections 3.5.2–3.5.5 we will give the expressions obtained in the effective theory and calculate the corrections to the affected couplings. A central concern of the presented analysis will

[4]By exact numerical calculation we refer to the explicit construction of the full (multi-dimensional) gauge coupling and mass matrices connecting all considered states and the transformation of the former into the mass eigenbasis by numerical diagonalization of the latter.

be to show that the custodial protection of the $Zd_L^i\bar{d}_L^j$ and $Zu_R^i\bar{u}_R^j$ couplings discussed in section 3.4.3 is *not* spoilt by the presence of mixing of the SM quarks with heavy vector-like KK states.

3.5.1 The Effective Theory Approach

Effective theory approaches treating the impact of heavy vector-like fermions have been presented in [113] in a covariant formulation and more recently in [35] in terms of individual fields. We will follow the latter approach and to this end define the vectors $\Psi_{L,R}(Q)\,,\, Q = 5/3, 2/3, -1/3$ which comprise the SM quarks as well as an arbitrary number of heavy vector-like states[5]. We will assume in the following that also the heavy vector-like states are organized in three distinct generations. Then the $\Psi_{L,R}(2/3)$ states have $3(N+1)$ components and the $\Psi_{L,R}(-1/3)$ states have $3(M+1)$ components each. In the case of the RSc in which the first excited KK states are taken into account, these vectors are given by (3.2)–(3.3), such that $N = 5$ and $M = 3$.

Fundamental Lagrangian Before the heavy states are integrated out and before the EW symmetry is broken, the most general Lagrangian density relevant for our analysis is given by

$$\mathcal{L} = \mathcal{L}_{\text{kin}} + \tilde{\mathcal{L}}_{\text{mass}} + \mathcal{L}_{\text{Yuk}} + \mathcal{L}_Z + \mathcal{L}_W + \mathcal{L}_{\text{KK gluons}}\,, \tag{3.46}$$

and we will discuss its parts in the following. The (canonically normalized) kinetic terms for all quarks in the theory are conventionally given by

$$\begin{aligned}\mathcal{L}_{\text{kin}} = {} & \bar{\Psi}_L(2/3)i\partial\!\!\!/\Psi_L(2/3) + \bar{\Psi}_R(2/3)i\partial\!\!\!/\Psi_R(2/3) \\ & + \bar{\Psi}_L(-1/3)i\partial\!\!\!/\Psi_L(-1/3) + \bar{\Psi}_R(-1/3)i\partial\!\!\!/\Psi_R(-1/3)\,,\end{aligned} \tag{3.47}$$

and their mass terms before EWSB read

$$\tilde{\mathcal{L}}_{\text{mass}} = -\bar{\Psi}_L(2/3)\tilde{\mathcal{M}}(2/3)\Psi_R(2/3) - \bar{\Psi}_L(-1/3)\tilde{\mathcal{M}}(-1/3)\Psi_R(-1/3) + \text{ h.c.}\,. \tag{3.48}$$

Here $\tilde{\mathcal{M}}(2/3)$ and $\tilde{\mathcal{M}}(-1/3)$ are $3(N+1)\times 3(N+1)$ and $3(M+1)\times 3(M+1)$ diagonal matrices. The first three entries on the diagonal corresponding to SM quark masses vanish at this stage, while the remaining entries are $\mathcal{O}(f)$ with f being the mass scale of heavy fermions (in the RSc, this mass scale f is given by the KK scale M_{KK}). The masses of the SM quarks as well as corrections to the masses of the heavy states are as usual generated through Yukawa interactions in the process of EWSB. As far as our analysis of corrections to fermion couplings from mixing with heavy vector-like states is concerned, it will be sufficient to consider the lower component Φ of the Higgs doublet. The Yukawa interactions in terms of the quark vectors $\Psi_{L,R}(Q)$ are given by

$$\begin{aligned}\mathcal{L}_{\text{Y}} = {} & -\Phi\left[\bar{\Psi}_L(2/3)\mathcal{Y}(2/3)\Psi_R(2/3)\right. \\ & \left. + \bar{\Psi}_L(-1/3)\mathcal{Y}(-1/3)\Psi_R(-1/3) + \text{ h.c.}\right]\,,\end{aligned} \tag{3.49}$$

[5] Our discussion will not be affected by the presence of additional quarks with exotic charges, as is in fact the case in the RSc.

where $\mathcal{Y}(2/3)$ and $\mathcal{Y}(-1/3)$ are $3(N+1)\times 3(N+1)$ and $3(M+1)\times 3(M+1)$ complex matrices. For easier reference we will denote the 3×3 matrices in flavor space that build up these matrices by $Y_{\alpha\beta}(2/3)$ and $Y_{\alpha\beta}(-1/3)$, where $\alpha,\beta = 0,1,...,N$ or $0,1,...,M$.
The couplings to the Z and $W^{\pm}$ gauge bosons[6] are conveniently defined by $\mathcal{L}_Z = J_\mu(Z)Z^\mu$ and $\mathcal{L}_W = J_\mu(W^+)W^{+\mu} +$ h.c. where

$$\begin{aligned} J_\mu(Z) = &\ \bar{\Psi}_L(2/3)\gamma_\mu \mathcal{A}_L^{2/3}(Z)\Psi_L(2/3) \\ &+ \bar{\Psi}_R(2/3)\gamma_\mu \mathcal{A}_R^{2/3}(Z)\Psi_R(2/3) \\ &+ \bar{\Psi}_L(-1/3)\gamma_\mu \mathcal{A}_L^{-1/3}(Z)\Psi_L(-1/3) \\ &+ \bar{\Psi}_R(-1/3)\gamma_\mu \mathcal{A}_R^{-1/3}(Z)\Psi_R(-1/3)\,, \end{aligned} \tag{3.50}$$

and

$$\begin{aligned} J_\mu(W^+) = &\ \bar{\Psi}_L(2/3)\gamma_\mu \mathcal{G}_L(W^+)\Psi_L(-1/3) \\ &+ \bar{\Psi}_R(2/3)\gamma_\mu \mathcal{G}_R(W^+)\Psi_R(-1/3)\,. \end{aligned} \tag{3.51}$$

In the above expressions (3.50), (3.51) the matrices $\mathcal{A}_{L,R}^{2/3}(Z)$ and $\mathcal{A}_{L,R}^{-1/3}(Z)$ are $3(N+1)\times 3(N+1)$ and $3(M+1)\times 3(M+1)$ matrices, while $\mathcal{G}_{L,R}(W^+)$ are $3(N+1)\times 3(M+1)$ matrices.
The couplings to KK gluons finally are described by $\mathcal{L}_{\text{KK gluons}} = J_\mu(G^{A(1)})G^{A(1)\mu}$ with

$$\begin{aligned} J_\mu(G^{A(1)}) = &\ \bar{\Psi}_L(2/3)\gamma_\mu \mathcal{A}_L^{2/3}(G^{A(1)})\Psi_L(2/3) \\ &+ \bar{\Psi}_R(2/3)\gamma_\mu \mathcal{A}_R^{2/3}(G^{A(1)})\Psi_R(2/3) \\ &+ \bar{\Psi}_L(-1/3)\gamma_\mu \mathcal{A}_L^{-1/3}(G^{A(1)})\Psi_L(-1/3) \\ &+ \bar{\Psi}_R(-1/3)\gamma_\mu \mathcal{A}_R^{-1/3}(G^{A(1)})\Psi_R(-1/3)\,, \end{aligned} \tag{3.52}$$

where $\mathcal{A}_{L,R}^{2/3}(G^{A(1)})$ and $\mathcal{A}_{L,R}^{-1/3}(G^{A(1)})$ are $3(N+1)\times 3(N+1)$ and $3(M+1)\times 3(M+1)$ matrices.
Also here it will be convenient to decompose these coupling matrices into their 3×3 building blocks $[A_{L,R}(Z)]_{\alpha\beta}$, $[A_{L,R}(G^{A(1)})]_{\alpha\beta}$, $[G_{L,R}(W^+)]_{\alpha\beta}$ which are matrices in flavor space. These building blocks can be shown to have the following model-independent properties [114]:

i) $[A_{L,R}(Z)]_{00}$ and $[A_{L,R}(Z)]_{ii}$ are non-zero diagonal matrices

ii) $[A_{L,R}(Z)]_{ij} = 0$ for $i \neq j$

iii) $[A_{L,R}(Z)]_{i0} = [A_{L,R}(Z)]_{0j} = 0\,,$

[6] More accurately, we are dealing with the couplings to the linear combinations of gauge fields that after EWSB will be identified with the Z and $W^{\pm}$ bosons.

where the $[A_{L,R}(Z)]_{\alpha\beta}$ in this listing also stand for $[G_{L,R}(W^+)]_{\alpha\beta}$. The only statement that can be made about the $[A_{L,R}(G^{A(1)})]_{\alpha\beta}$ matrices at this stage is that they are all diagonal. They are however not proportional to the unit matrix since they couple quark zero modes to a non-flat gauge KK mode and as such their diagonal entries depend on the localization parameters of the individual quark modes. It should also be emphasized that all these coupling matrices discussed above are given before EWSB and hence couplings that were non-vanishing in [32] because of the mixing of Z and $W^\pm$ with other gauge bosons are absent now.

Integrating out of heavy states Having at hand all the relevant terms in the fundamental Lagrangian, we can construct a low-energy theory that involves only SM quark and gauge boson fields and the Higgs field. There are several methods for achieving this goal. In the context of our analysis it is most convenient to integrate out the heavy fermions at tree level by using their EOMs. Inserting the solution for these equations into the fundamental Lagrangian (3.46) and expanding in powers of $1/f$ results in an effective Lagrangian of which the $D = 4$ part is the SM Lagrangian and the $D = 6$ part is the one we are interested in. The corrections to the Z and $W^\pm$ couplings that result from the mixing with heavy vector-like fermions are then obtained by performing EWSB through the replacement

$$\Phi = \frac{1}{\sqrt{2}}\,[v + H]\,, \tag{3.53}$$

where H denotes the physical neutral Higgs boson and $v = 246\,\text{GeV}$ is the conventional vacuum expectation value.
This procedure is well known (see for instance [66, 115]), and instead of presenting the details of this derivation we will give a recipe for finding the corrections to the couplings in question directly from the fundamental Lagrangian (3.46). To this end we introduce

$$\mathcal{L}_{\text{mass}} = -\bar{\Psi}_L(2/3)\mathcal{M}(2/3)\Psi_R(2/3) - \bar{\Psi}_L(-1/3)\mathcal{M}(-1/3)\Psi_R(-1/3) + h.c.\,, \tag{3.54}$$

where $\mathcal{M}(2/3)$ and $\mathcal{M}(-1/3)$ are $3(N+1)\times 3(N+1)$ and $3(M+1)\times 3(M+1)$ matrices. They are constructed by adding $\tilde{\mathcal{L}}_{\text{mass}}$ in (3.48) and the mass terms resulting from the Yukawa Lagrangian in (3.49) after EWSB. As done for the Yukawa and gauge coupling matrices we decompose these mass matrices into their building blocks $M_{\alpha\beta}(2/3)$ and $M_{\alpha\beta}(-1/3)$ which are 3×3 matrices in flavor space. Among the building blocks are the matrices $M_{00}(2/3)$ and $M_{00}(-1/3)$ that represent the mass matrices of the SM quarks in the absence of heavy vector-like states.
The mass matrices $\mathcal{M}(2/3)$ and $\mathcal{M}(-1/3)$ are complex and non-diagonal, and despite their obvious model dependence there are a number of properties that hold model-independently:

1. $M_{kk} = \mathcal{O}(f)$ for $k \neq 0$,
2. $M_{00} = \frac{v}{\sqrt{2}}Y_{00} = \mathcal{O}(v)$,
3. $M_{ij} = \frac{v}{\sqrt{2}}Y_{ij}$ for $i \neq j \neq 0$ are $\mathcal{O}(v)$ (or vanish entirely)

4. $M_{0k} = \frac{v}{\sqrt{2}} Y_{0k}$ and $M_{k0} = \frac{v}{\sqrt{2}} Y_{k0}$ are generally $\mathcal{O}(v)$, but if $M_{0k} \neq 0$ then $M_{k0} = 0$ and vice versa. This property follows from the fact [114] that only one of the chiralities of each vector-like fermion couples to the SM quarks through mass terms.

To simplify expressions we introduce the shorthand $M_{kk}(Q) \equiv M_k(Q)$ for the 3×3 mass matrices with identical indices. With this notation the solutions to the EOMs can be written for the M heavy charge $-1/3$ fermions $D^k_{L,R}$ as[7]

$$D^k_L = -\sum_{\substack{j=1 \\ j\neq k}}^{3} \left[M_k^{-1} M_{0k}^\dagger - M_k^{-1} M_{jk}^\dagger M_j^{-1} M_{0j}^\dagger \right] d_L \,,$$

$$D^k_R = -\sum_{\substack{j=1 \\ j\neq k}}^{3} \left[M_k^{-1} M_{k0} - M_k^{-1} M_{kj} M_j^{-1} M_{j0} \right] d_R \,, \tag{3.55}$$

where terms on the r.h.s. that do not affect the final expressions at $\mathcal{O}(v^2/f^2)$ were dropped. In (3.55) all mass matrices are for the down-type quarks, that is $M_{\alpha\beta} = M_{\alpha\beta}(-1/3)$. Analogous expressions for the up-type quarks can be easily obtained by replacing the quark fields and mass matrices accordingly.
We can now plug (3.55) into the fundamental Lagrangian (3.46) to obtain an effective theory in which no heavy vector-like states are present anymore. Before we can however use this effective theory to calculate corrections to the quark couplings, we need to renormalize the kinetic terms of the light quarks. Indeed, inserting (3.55) into the kinetic terms of the heavy fields in (3.47) we find that the light quark kinetic terms are no longer canonically normalized. Keeping only the leading $\mathcal{O}(v^2/f^2)$ terms, the canonical form of the kinetic terms is recovered through the transformations

$$d_L \to \left(\mathbb{1} - \frac{1}{2} M_{0k} M_k^{-2} M_{0k}^\dagger \right) d_L \,,$$

$$d_R \to \left(\mathbb{1} - \frac{1}{2} M_{k0}^\dagger M_k^{-2} M_{k0} \right) d_R \,, \tag{3.56}$$

where summation over repeated indices is understood.
The resulting effective theory that contains only light quarks allows to derive the corrections to the SM quark-gauge couplings in a straightforward manner. This procedure is in principle also applicable to the Higgs couplings if the full expression (3.53) for Φ is used to obtain the solution to the EOMs of the heavy states instead of just its constant VEV. However, the corrections to the SM quark-Higgs couplings obtained in this framework are negligible (see discussion in [33, 35]) as certain effects that have been shown to affect the Higgs couplings in [116] are not visible in an effective theory approach. We will briefly discuss these effects in section 3.6.
In the following we will discuss the expressions for mass and gauge coupling matrices of the SM quarks that are obtained from the effective theory we have constructed.

[7] In this, $d_{L,R}$ and $D^k_{L,R}$ with $k = 1, ...M$ are vectors in flavor space.

3.5.2 Corrections to SM Mass Matrices

For the mass matrices of up- and down-type quarks, as defined in (3.54) but with all heavy states removed, we find the general expression

$$\begin{aligned} M &= M_{00} + M_{0k} M_k^{-1} M_{kj} M_j^{-1} M_{j0} \\ &\quad - \frac{1}{2}\left[M_{0k} M_k^{-2} M_{0k}^\dagger M_{00} + M_{00} M_{k0}^\dagger M_k^{-2} M_{k0} \right] , \end{aligned} \tag{3.57}$$

where here and in the following summation over repeated indices but with $k \neq j$ is understood, as indicated in (3.55). In (3.57) the correction to M_{00} in the first line originates from pure heavy mass terms and the correction in the second line is introduced by the canonical redefinition of the light quark fields (3.56).
In order to be able to give expressions for gauge couplings in the mass eigenbasis, we need to diagonalize the mass matrices $M(Q)\,,\ Q = -1/3, 2/3$ in (3.57) via bi-unitary transformations. Since this procedure is straightforward, in the following we will only give expressions for the gauge couplings in the flavor eigenbasis. For the numerical comparison in later sections we will of course consider the gauge couplings in the mass eigenbasis.

3.5.3 Corrections to Z Couplings

For the couplings to neutral Z gauge bosons as defined in (3.50) but with heavy vector-like states removed we find

$$\begin{aligned} A_L(Z) &= [A_L(Z)]_{00} + M_{0k} M_k^{-1} [A_L(Z)]_{kk} M_k^{-1} M_{0k}^\dagger \\ &\quad - \frac{1}{2}\left(M_{0k} M_k^{-2} M_{0k}^\dagger [A_L(Z)]_{00} + [A_L(Z)]_{00} M_{0k} M_k^{-2} M_{0k}^\dagger \right) , \end{aligned} \tag{3.58}$$

and

$$\begin{aligned} A_R(Z) &= [A_R(Z)]_{00} + M_{k0}^\dagger M_k^{-1} [A_R(Z)]_{kk} M_k^{-1} M_{k0} \\ &\quad - \frac{1}{2}\left(M_{k0}^\dagger M_k^{-2} M_{k0} [A_R(Z)]_{00} + [A_R(Z)]_{00} M_{k0}^\dagger M_k^{-2} M_{k0} \right) . \end{aligned} \tag{3.59}$$

These formulae apply to both charge $+2/3$ and $-1/3$ quarks with appropriate use of $[A_{L,R}^{2/3}(Z)]_{\alpha\alpha}$ or $[A_{L,R}^{-1/3}(Z)]_{\alpha\alpha}$ couplings, and similarly for the mass matrices. The corrections in (3.58) and (3.59) which modify the tree level value are of different origin: The corrections in the respective first lines are due to interactions of heavy states with the SM Z gauge boson while the remaining corrections stem from the canonical redefinition of the SM quarks.
We will now adapt these model-independent expressions to the RSc. The coupling matrices $[A_{L,R}^Q]_{\alpha\alpha}$ in this case are proportional to 3×3 unit matrices with the proportionality

	(0,0)	(1,1)	(2,2)	(3,3)
$A_L^{-1/3}$	$g_{Z,L}^{4D}(d)$	$g_{Z,L}^{4D}(d)$	$g_Z^{4D}(D')$	$g_{Z,R}^{4D}(d)$
$A_R^{-1/3}$	$g_{Z,R}^{4D}(d)$	$g_{Z,L}^{4D}(d)$	$g_Z^{4D}(D')$	$g_{Z,R}^{4D}(d)$

Table 3.1: Weak charges in the coupling matrices of down-type quarks to the Z gauge boson.

	(0,0)	(1,1)	(2,2)	(3,3)	(4,4)	(5,5)
$A_L^{2/3}$	$g_{Z,L}^{4D}(u)$	$g_{Z,L}^{4D}(u)$	$g_Z^{4D}(U')$	$g_Z^{4D}(U'')$	$g_Z^{4D}(\chi^d)$	$g_{Z,R}^{4D}(u)$
$A_R^{2/3}$	$g_{Z,R}^{4D}(u)$	$g_{Z,L}^{4D}(u)$	$g_Z^{4D}(U')$	$g_Z^{4D}(U'')$	$g_Z^{4D}(\chi^d)$	$g_{Z,R}^{4D}(u)$

Table 3.2: Weak charges in the coupling matrices of up-type quarks to the Z gauge boson.

constants given by the weak charges[8] collected in tables 3.1 and 3.2. The explicit structure of the mass matrices for the charge $2/3$ and $-1/3$ quarks is given in (3.11) and (3.12). In the following we give the final expressions for the $Zd_{L,R}^i\bar{d}_{L,R}^j$ and $Zu_{L,R}^i\bar{u}_{L,R}^j$ couplings in the RSc taking advantage of model specific cancellations wherever possible.

$\mathbf{Zd_L^i\bar{d}_L^j}$ couplings Adapting (3.58) to the RSc and considering first the charge $-1/3$ quarks we find

$$\begin{aligned} A_L^{-1/3}(Z) = {} & g_{Z,L}^{4D}(d)\mathbb{1} \\ & + \left(g_Z^{4D}(D') - g_{Z,L}^{4D}(d)\right) M_{02}\frac{1}{M_2^2}M_{02}^\dagger \\ & + \left(g_{Z,R}^{4D}(d) - g_{Z,L}^{4D}(d)\right) M_{03}\frac{1}{M_3^2}M_{03}^\dagger\,, \end{aligned} \tag{3.60}$$

where for the mass matrix elements $M_{\alpha\beta} = M_{\alpha\beta}(-1/3)$ can be obtained from (3.12). Evidently, the terms involving M_1 have cancelled against each other as a consequence of $[A_L^{-1/3}]_{00} = [A_L^{-1/3}]_{11}$. With the expressions for the coupling constants given in appendix A we finally find

$$A_L^{-1/3}(Z) = g_{Z,L}^{4D}(d)\mathbb{1} + \frac{1}{2}\frac{g^{4D}}{\cos\psi}\left(M_{03}\frac{1}{M_3^2}M_{03}^\dagger - M_{02}\frac{1}{M_2^2}M_{02}^\dagger\right). \tag{3.61}$$

In the limit of exact P_{LR} symmetry $P_{LR}(D) = D'$ holds and as a consequence we have $|M_{03}| = |M_{02}|$, $M_3 = M_2$ which guarantees that the $\mathcal{O}(v^2/M_{\text{KK}}^2)$ correction to the coupling $A_L^{2/3}(Z)$ vanishes. This result again expresses the protection of the $Zd_L^i\bar{d}_L^j$ couplings which is a consequence of the choice $T_R^3 = T_L^3$ for the quantum numbers of the left-handed down-type SM quarks. We also see that the assignment of the right-handed down-type

[8] Note that tables 3.1 and 3.2 explicitly show the vector-like couplings of the KK fermions in the RSc.

SM quark to the P_{LR} symmetric $(\mathbf{3},\mathbf{1})\oplus(\mathbf{1},\mathbf{3})$ multiplet is a vital condition for the protection of the $Zd_L^i\bar{d}_L^j$ coupling in the presence of mixing with heavy vector-like KK states.

$\mathbf{Zd_R^i\bar{d}_R^j}$ couplings For the right-handed down-type SM quarks, (3.59) in the RSc takes the following form:

$$\begin{aligned} A_R^{-1/3}(Z) = {} & g_{Z,R}^{4D}(d)\mathbb{1} \\ & + \left(g_{Z,L}^{4D}(d) - g_{Z,R}^{4D}(d)\right) M_{10}^\dagger \frac{1}{M_1^2} M_{10} \\ & + \left(g_Z^{4D}(D') - g_{Z,R}^{4D}(d)\right) M_{20}^\dagger \frac{1}{M_2^2} M_{20}\,. \end{aligned} \tag{3.62}$$

This time the terms involving M_3 have cancelled each other as a consequence of $[A_R^{-1/3}]_{00} = [A_R^{-1/3}]_{33}$. Using the expressions for the Z couplings collected in appendix A we find

$$A_R^{-1/3}(Z) = g_{Z,R}^{4D}(d)\mathbb{1} - \frac{g^{4D}}{\cos\psi}\left(\frac{1}{2}M_{10}^\dagger\frac{1}{M_1^2}M_{10} + M_{20}^\dagger\frac{1}{M_2^2}M_{20}\right). \tag{3.63}$$

Now the terms $\mathcal{O}(v^2/M_{\rm KK}^2)$ do not cancel each other and the mixing of SM quarks with KK fermions has an impact on right-handed down-type quark couplings to the Z boson. We will investigate the relative size of this effect compared to the result obtained in the zero mode approximation (ZMA) at the end of this section.

$\mathbf{Zu_L^i\bar{u}_L^j}$ couplings For the left-handed up-type SM quarks we find from (3.58)

$$\begin{aligned} A_L^{2/3}(Z) = {} & g_{Z,L}^{4D}(u)\mathbb{1} \\ & + \left(g_Z^{4D}(U') - g_{Z,L}^{4D}(u)\right) M_{02}\frac{1}{M_2^2}M_{02}^\dagger \\ & + \left(g_Z^{4D}(U'') - g_{Z,L}^{4D}(u)\right) M_{03}\frac{1}{M_3^2}M_{03}^\dagger \\ & + \left(g_{Z,R}^{4D}(u) - g_{Z,L}^{4D}(u)\right) M_{05}\frac{1}{M_5^2}M_{05}^\dagger\,, \end{aligned} \tag{3.64}$$

where this time the mass matrix elements $M_{\alpha\beta} = M_{\alpha\beta}(2/3)$ can be obtained from (3.11). The terms in (3.64) are not related by the custodial parity P_{LR}. Using the explicit charge factors given in appendix A we find in this case

$$A_L^{2/3}(Z) = g_{Z,L}^{4D}(u)\mathbb{1} - \frac{1}{2}\frac{g^{4D}}{\cos\psi}\left(M_{02}\frac{1}{M_2^2}M_{02}^\dagger + M_{03}\frac{1}{M_3^2}M_{03}^\dagger + M_{05}\frac{1}{M_5^2}M_{05}^\dagger\right). \tag{3.65}$$

We see that the terms $\mathcal{O}(v^2/M_{\rm KK}^2)$ do not cancel each other and the mixing of SM quarks with KK fermions has an impact on the left-handed up-quark couplings to the Z boson. We will return to this issue and investigate the relative size of this effect compared to the ZMA result at the end of this section.

$Zu^i_R\bar{u}^j_R$ couplings Finally, using (3.59) we find

$$\begin{aligned} A_R^{2/3}(Z) = {} & g_{Z,R}^{4D}(u)\mathbb{1} \\ & + \left(g_{Z,L}^{4D}(u) - g_{Z,R}^{4D}(u)\right) M_{10}^\dagger \frac{1}{M_1^2} M_{10} \\ & + \left(g_Z^{4D}(\chi^d) - g_{Z,R}^{4D}(u)\right) M_{40}^\dagger \frac{1}{M_4^2} M_{40}\,. \end{aligned} \tag{3.66}$$

As in the case of the $Zd^i_L\bar{d}^j_L$ couplings we note that the terms in the above expression are related by the custodial parity P_{LR}, which acts on the quark fields as $P_{LR}(q^u) = \chi^d$, $P_{LR}(u) = u$, and also ensures that $|M_{10}| = |M_{40}|$ and $M_1 = M_4$, up to small symmetry breaking effects by the BCs on the UV brane. With the explicit charge factors given in appendix A we find

$$A_R^{2/3}(Z) = g_{Z,R}^{4D}(u)\mathbb{1} + \frac{1}{2}\frac{g^{4D}}{\cos\psi}\left(M_{10}^\dagger \frac{1}{M_1^2} M_{10} - M_{40}^\dagger \frac{1}{M_4^2} M_{40}\right)\,. \tag{3.67}$$

Evidently, in the limit $|M_{10}| = |M_{40}|$, $M_1 = M_4$, the $\mathcal{O}(v^2/M_{\rm KK}^2)$ correction to the coupling $A_R^{2/3}(Z)$ vanishes, expressing the protection of the $Zu^i_R\bar{u}^j_R$ couplings even in the presence of mixing with KK fermions. Also here the cancellation hinges on the fact that the right-handed up-type SM quark is assigned to the P_{LR} symmetric $(\mathbf{1},\mathbf{1})$ multiplet of the bulk gauge group.

Having worked out the explicit expressions (3.61), (3.63), (3.65), (3.67) for the Z couplings in the effective theory we now want to compare the impact of KK fermions on these couplings to the one arising from the mixing of SM gauge bosons with heavy KK gauge modes. To this end we denote the KK fermion contribution to a given Z coupling by $[A^Q_{L,R}(Z)]^{ij}_{\rm KK}$ while the contribution from gauge boson mixing to a given Z coupling is denoted by $[A^Q_{L,R}(Z)]^{ij}_{\rm gauge}$. These quantities then are calculated for the set of parameter points that will be used for the analysis of rare K and B decays in chapter 5 and that are found to reproduce the quark masses and mixings as well as the measured observables in $K^0 - \bar{K}^0$ and $B^0 - \bar{B}^0$ oscillations.
For the $Zd^i_L\bar{d}^j_L$ and $Zu^i_R\bar{u}^j_R$ couplings which are protected by the custodial symmetry, the relative impact of KK fermion mixing turns out to be very small. This is due to the fact that the effects of $SU(2)_R \times P_{LR}$ breaking by BCs on the UV brane are much smaller for fermionic KK modes than they are for the gauge boson KK modes. As an example, in fig. 3.6 we compare the contributions from KK fermion mixing and gauge boson mixing that enter the $Zs_L\bar{d}_L$ and $Zc_R\bar{u}_R$ couplings. In these density plots, light-colored areas correspond to a high density of parameter points while darker areas correspond to lower densities. We see that for all points in parameter space the KK fermion mixing contribution is by several orders of magnitude smaller than the contribution from gauge boson mixing.

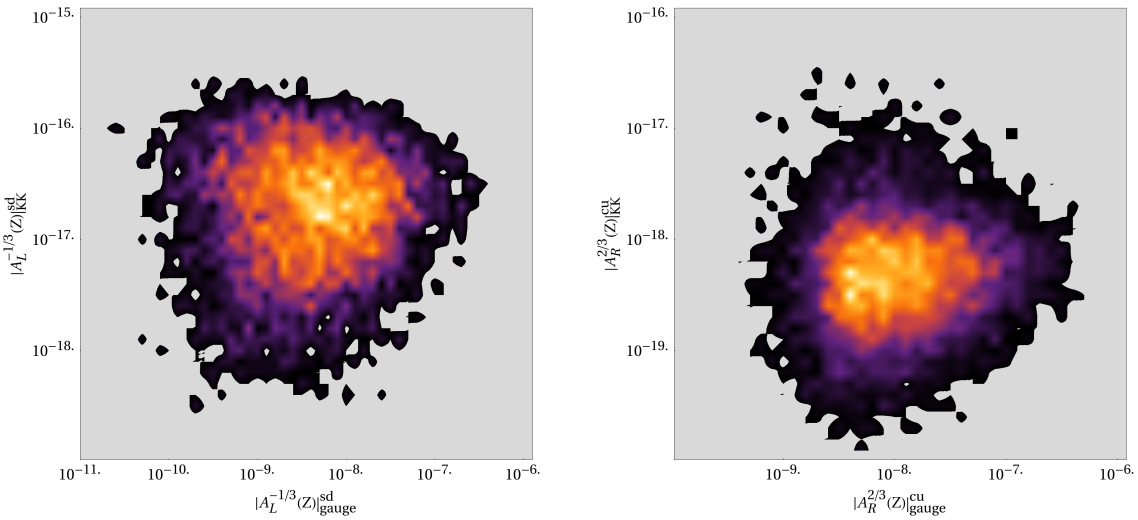

Figure 3.6: Comparison of contributions from KK fermion mixing and gauge boson mixing to the custodially protected $Zs_L\bar{d}_L$ coupling (left panel) an to the custodially protected $Zc_R\bar{u}_R$ coupling (right panel). These results have been obtained by using the effective theory expressions.

In the case of couplings that are not protected by the custodial symmetry, the corrections from KK fermion mixing are still subdominant but can in principle be of the same order of magnitude as the contribution from gauge boson mixing. To get a feeling for in which elements of the $Zd_R^i\bar{d}_R^j$, $Zu_L^i\bar{u}_L^j$ couplings these corrections can potentially become important, it is instructive to investigate the patterns of hierarchy in the KK fermion and gauge boson mixing contributions separately and eventually compare them to each other.
We find that the hierarchies in the gauge boson mixing contributions $[A^Q_{L,R}(Z)]_{\text{gauge}}$ which enter the couplings of the Z boson are constrained by the presence of the RS-GIM mechanism (cf. section 3.4.1). This should be compared to the flavor hierarchies in the corrections $[A^Q_{L,R}]_{\text{KK}}$ stemming from KK fermion mixing. From the state vectors (3.2), (3.3) and from the mass matrices of up- and down-quarks in (3.11), (3.12) we find that here the patterns are dictated by the hierarchies in the fermion zero mode shape functions on the IR brane, F^Q, F^u, F^d, which are vectors in flavor space and have been defined in (3.6). More precisely, the contributions from KK fermion mixing to gauge couplings should typically be proportional to outer products of these quantities, given by e.g. $\left(F^u \circ F^d\right)_{ij} \equiv F^u_i F^d_j$. In table 3.3 we summarize the expected hierarchies between flavor transitions for couplings that are not protected by the custodial symmetry.
As indicated above these hierarchies allow to predict for which flavor transition $j \to i$ the effects of KK fermion mixing can potentially become important compared to the gauge boson mixing contributions. We list the entries that receive the largest relative contributions from KK fermion mixing in the fourth row of table 3.3. In the case of $A_L^{2/3}(Z)$, the flavor hierarchies in gauge boson mixing and KK fermion mixing contributions are roughly equal, such that the relative importance of KK fermion mixing is roughly equal for all flavor transitions of this coupling. We compare the gauge boson mixing and KK

	Zd_Rd_R	Zu_Lu_L
$[A(Z)]_{\text{gauge}}$ -pattern	RS-GIM (d)	RS-GIM (Q)
$[A(Z)]_{\text{KK}}$ -pattern	$F_d \circ F_d$	$F_Q \circ F_Q$
$\lvert[A(Z)]_{\text{KK}}/[A(Z)]_{\text{gauge}}\rvert$ maximal in	sd	tc, tu, cu

Table 3.3: Hierarchies in the gauge boson mixing and KK fermion mixing contributions to the Z boson couplings that are not protected by the custodial symmetry. In the last line we give the elements of the coupling matrices which is on average affected most by KK fermion mixing.

fermion mixing contributions for the flavor transitions that are expected to be affected most by the latter contribution in fig. 3.7. Also here we find that the contributions from gauge boson mixing typically are dominant.

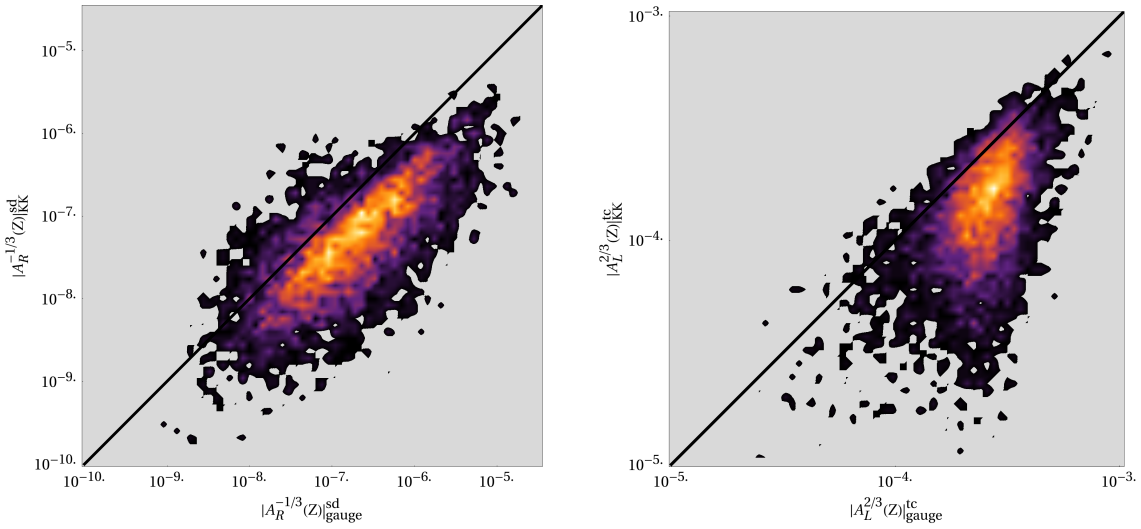

Figure 3.7: Comparison of contributions from KK fermion mixing and gauge boson mixing to the unprotected $Zs_R\bar{d}_R$ coupling (left panel) and to the unprotected $Zt_L\bar{c}_L$ coupling (right panel).

In summary we find that for all Z couplings the KK fermion contribution is significantly smaller than the contribution from gauge boson mixing for a majority of points in parameter space, and in particular for those points that produce the largest effects in the respective coupling. This result is fortunate for several reasons. First, the contributions from the mixing with KK fermions are highly model-dependent, inasmuch as they depend critically on the multiplets of the bulk gauge group that are chosen to accommodate the SM quarks. Second, and even more important, the calculation of these contributions requires detailed knowledge of the bulk profiles of the KK fermion modes and of the full fermionic mass matrices which is not required for the calculation of the gauge mixing contribution.

	(0,0)	(1,1)	(2,2)
G_L	$g^{4D}/\sqrt{2}$	$g^{4D}/\sqrt{2}$	g^{4D}
G_R	0	$g^{4D}/\sqrt{2}$	g^{4D}

Table 3.4: Weak charges in the coupling matrices of the W^+ gauge boson.

3.5.4 Corrections to Charged Couplings

For the couplings to charged gauge bosons as defined in (3.51) but with heavy vector-like states removed we find

$$\begin{aligned} G_L(W^+) &= \left[G_L(W^+)\right]_{00} + M_{0k}(2/3)M_k^{-1}(2/3)\left[G_L(W^+)\right]_{kk} M_k^{-1}(-1/3)M_{0k}^\dagger(-1/3) \\ &\quad - \frac{1}{2}M_{0k}(2/3)M_k^{-2}(2/3)M_{0k}^\dagger(2/3)\left[G_L(W^+)\right]_{00} \\ &\quad - \frac{1}{2}\left[G_L(W^+)\right]_{00} M_{0k}(-1/3)M_k^{-2}(-1/3)M_{0k}^\dagger(-1/3)\,, \end{aligned} \tag{3.68}$$

$$G_R(W^+) = M_{k0}^\dagger(2/3)M_k^{-1}(2/3)\left[G_R(W^+)\right]_{kk} M_k^{-1}(-1/3)M_{k0}(-1/3)\,, \tag{3.69}$$

where the non-vanishing coupling matrices $[G_{L,R}(W^+)]_{\alpha\alpha}$ with $\alpha = 0, i$ are proportional to 3×3 unit matrices and the proportionality constants in the RSc are collected in table 3.4. We note that the first of these equations (3.68) has the same structure as the Z couplings in (3.58) and (3.59). The first correction on the r.h.s. originates from the interactions of the heavy fermion fields with SM gauge bosons and the remaining terms in (3.68) are the consequence of the redefinitions of the light fields given in (3.56). An exception in this sense is the coupling $G_R(W^+)$ which vanishes at leading order so that the redefinitions of the light fields do not matter at order v^2/f^2.
Two consequences of (3.68) and (3.69) are of particular interest: an additional contribution to the violation of unitarity of the CKM matrix and the appearance of right-handed W couplings. We will discuss both effects quantitatively in the following.

Violation of unitarity of the CKM matrix Rotating (3.68) to the mass eigenbasis we find that also KK fermion mixing modifies the CKM matrix:

$$V_{\rm CKM} \,=\, U_L^\dagger\, G_L(W^+)\, D_L \,\equiv\, U_L^\dagger\, \left[G_L(W^+)\right]_{00}\, D_L + \frac{v^2}{M_{\rm KK}^2} U_L^\dagger\, \Delta_{\rm KK}\, D_L\,. \tag{3.70}$$

We will now compare this correction to the CKM matrix to the one arising from gauge boson mixing, $\frac{v^2}{M_{\rm KK}^2} U_L^\dagger\, \Delta_{\rm gauge}\, D_L$, given in (3.45). As it turns out, the contribution from KK fermion mixing for most elements of the CKM matrix is numerically smaller than the gauge boson mixing contribution. Analogous to our approach in the case of the Z couplings we can work out the textures of the matrices $\Delta V_{\rm CKM}^{\rm KK}$ and $\Delta V_{\rm CKM}^{\rm gauge}$ to identify the entries in which the relative impact of the KK fermion mixing is typically maximal.

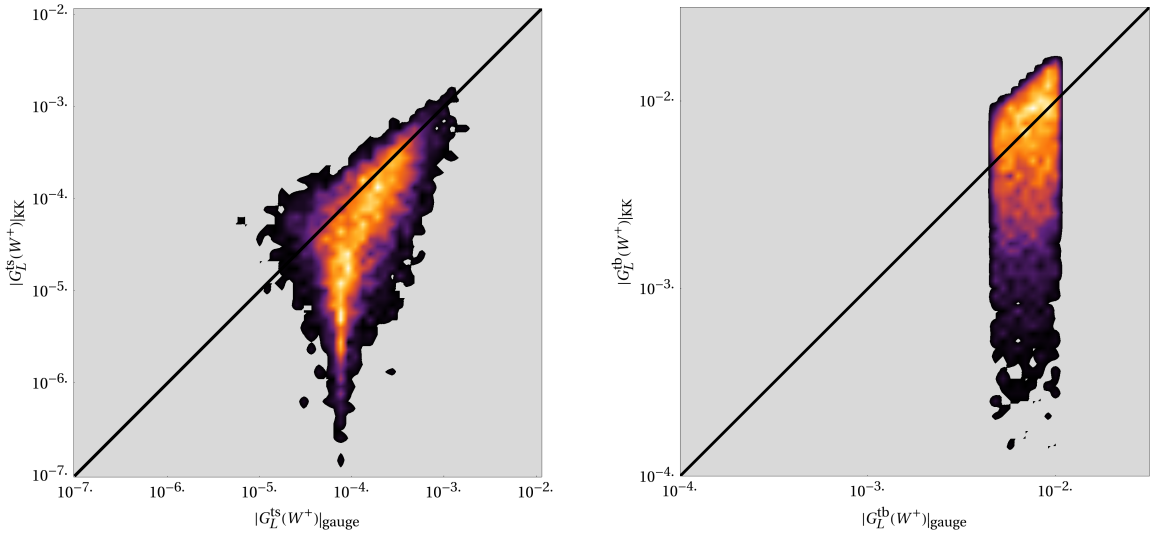

Figure 3.8: Comparison of contributions from KK fermion mixing and gauge boson mixing to the $W^+\bar{t}_L s_L$ (left panel) and $W^+\bar{t}_L b_L$ coupling (right panel).

We find that $\Delta V_{\text{CKM}}^{\text{gauge}}$ roughly has the same structure as the CKM matrix itself, while the structure of $\Delta V_{\text{CKM}}^{\text{KK}}$ is dictated by the outer product $F_Q \circ F_Q$. Accordingly, the largest relative impact of KK fermion mixing typically occurs in the tb, ts and cb elements of the CKM matrix. In fig. 3.8 we compare the corrections from gauge boson and KK fermion mixing to the CKM matrix for the data sets also used in our global numerical analysis in chapter 5. We observe that only in the case of the tb element the impact of KK fermions is typically larger than the impact of gauge boson mixing.

Finally, in table 3.5 we list the typical and maximal deviations of the CKM unitarity relations that are found in the RSc. The quantities K^u and K^d listed in that table are defined as

$$\begin{aligned} K^u &\equiv V_{\text{CKM}} V_{\text{CKM}}^\dagger = \mathbb{1} + \frac{v^2}{M_{\text{KK}}^2} U_L^\dagger \left(\Delta_r + \Delta_r^\dagger\right) U_L \,, \\ K^d &\equiv V_{\text{CKM}}^\dagger V_{\text{CKM}} = \mathbb{1} + \frac{v^2}{M_{\text{KK}}^2} D_L^\dagger \left(\Delta_r^\dagger + \Delta_r\right) D_L \,, \end{aligned} \tag{3.71}$$

where "r" can stand for either "gauge" or "KK". This table shows that the impact from both KK fermion and gauge boson to the violation of CKM unitarity is small; still, for the first column and first row unitarity relations, the deviation from the SM is of the same order as the current experimental uncertainty [76], such that with improved data one could in principle put constraints on the RSc parameter space. In doing so one would also have to study effects that modify the definition of the weak gauge coupling, such as corrections to the muon decay amplitude, and preferably also electroweak precision observables.

		$\langle K_{\text{gauge}} - \mathbb{1} \rangle$	$\lvert K_{\text{gauge}} - \mathbb{1} \rvert_{\max}$	$\langle K_{\text{KK}} - \mathbb{1} \rangle$	$\lvert K_{\text{KK}} - \mathbb{1} \rvert_{\max}$
$\lvert V_{ud}\rvert^2 + \lvert V_{cd}\rvert^2 + \lvert V_{td}\rvert^2 =$	K^d_{11}	$3.5{\cdot}10^{-3}$	$3.5{\cdot}10^{-3}$	$6.8{\cdot}10^{-7}$	$1.9{\cdot}10^{-5}$
$0.95 \quad 5{\cdot}10^{-2} \quad 8{\cdot}10^{-5}$					
$\lvert V_{us}\rvert^2 + \lvert V_{cs}\rvert^2 + \lvert V_{ts}\rvert^2 =$	K^d_{22}	$3.3{\cdot}10^{-3}$	$3.5{\cdot}10^{-3}$	$2.4{\cdot}10^{-5}$	$5.1{\cdot}10^{-4}$
$5{\cdot}10^{-2} \quad 0.95 \quad 2{\cdot}10^{-3}$					
$\lvert V_{ub}\rvert^2 + \lvert V_{cb}\rvert^2 + \lvert V_{tb}\rvert^2 =$	K^d_{33}	$1.4{\cdot}10^{-2}$	$1.9{\cdot}10^{-2}$	$8.4{\cdot}10^{-3}$	$2.1{\cdot}10^{-2}$
$1{\cdot}10^{-5} \quad 2{\cdot}10^{-3} \quad 1$					
$\lvert V_{ud}\rvert^2 + \lvert V_{us}\rvert^2 + \lvert V_{ub}\rvert^2 =$	K^u_{11}	$3.5{\cdot}10^{-3}$	$3.5{\cdot}10^{-3}$	$1.8{\cdot}10^{-6}$	$3.3{\cdot}10^{-5}$
$0.95 \quad 5{\cdot}10^{-2} \quad 1{\cdot}10^{-5}$					
$\lvert V_{cd}\rvert^2 + \lvert V_{cs}\rvert^2 + \lvert V_{cb}\rvert^2 =$	K^u_{22}	$3.3{\cdot}10^{-3}$	$3.5{\cdot}10^{-3}$	$3.9{\cdot}10^{-5}$	$4.8{\cdot}10^{-4}$
$0.95 \quad 5{\cdot}10^{-2} \quad 2{\cdot}10^{-3}$					
$\lvert V_{td}\rvert^2 + \lvert V_{ts}\rvert^2 + \lvert V_{tb}\rvert^2 =$	K^u_{33}	$1.4{\cdot}10^{-2}$	$1.9{\cdot}10^{-2}$	$8.4{\cdot}10^{-3}$	$2.1{\cdot}10^{-2}$
$8{\cdot}10^{-5} \quad 2{\cdot}10^{-3} \quad 1$					
$V_{ud}V^*_{us} + V_{cd}V^*_{cs} + V_{td}V^*_{ts} =$	K^d_{12}	$1.4{\cdot}10^{-6}$	$5.4{\cdot}10^{-5}$	$9.1{\cdot}10^{-7}$	$2.5{\cdot}10^{-5}$
$0.22 \quad 0.22 \quad 4{\cdot}10^{-4}$					
$V_{ud}V^*_{ub} + V_{cd}V^*_{cb} + V_{td}V^*_{tb} =$	K^d_{13}	$3.7{\cdot}10^{-5}$	$3.0{\cdot}10^{-4}$	$2.0{\cdot}10^{-5}$	$1.8{\cdot}10^{-4}$
$4{\cdot}10^{-3} \quad 9{\cdot}10^{-3} \quad 9{\cdot}10^{-3}$					
$V_{us}V^*_{ub} + V_{cs}V^*_{cb} + V_{ts}V^*_{tb} =$	K^d_{23}	$1.6{\cdot}10^{-4}$	$1.6{\cdot}10^{-3}$	$9.4{\cdot}10^{-5}$	$8.7{\cdot}10^{-4}$
$9{\cdot}10^{-4} \quad 4{\cdot}10^{-2} \quad 4{\cdot}10^{-2}$					
$V_{ud}V^*_{cd} + V_{us}V^*_{cs} + V_{ub}V^*_{cb} =$	K^u_{12}	$1.1{\cdot}10^{-5}$	$2.7{\cdot}10^{-4}$	$4.5{\cdot}10^{-6}$	$1.1{\cdot}10^{-4}$
$0.22 \quad 0.22 \quad 2{\cdot}10^{-4}$					
$V_{ud}V^*_{td} + V_{us}V^*_{ts} + V_{ub}V^*_{tb} =$	K^u_{13}	$7.2{\cdot}10^{-5}$	$4.2{\cdot}10^{-4}$	$3.2{\cdot}10^{-5}$	$2.2{\cdot}10^{-4}$
$9{\cdot}10^{-3} \quad 9{\cdot}10^{-3} \quad 4{\cdot}10^{-3}$					
$V_{cd}V^*_{td} + V_{cs}V^*_{ts} + V_{cb}V^*_{tb} =$	K^u_{23}	$5.9{\cdot}10^{-4}$	$1.7{\cdot}10^{-3}$	$3.0{\cdot}10^{-4}$	$1.1{\cdot}10^{-3}$
$2{\cdot}10^{-3} \quad 4{\cdot}10^{-2} \quad 4{\cdot}10^{-2}$					

Table 3.5: CKM unitarity relations and the amount by which they are broken in the RSc. For comparison in the first column we also give numerical values for the absolute values of the three terms on the l.h.s. of the relations separately.

Right-handed W$^\pm$ couplings From (3.69) we see that in the RSc the $W^\pm$ gauge boson not only couples to left-handed quarks, but also to the right-handed ones. Analogous to the CKM matrix we can define a coupling matrix $V_{\rm R}$ that describes the transitions of mass eigenstates mediated by $W^\pm$ such that the interaction vertices are given by

$$\bar{u}^i_R W^+ d^j_R \sim \frac{g^{4D}}{\sqrt{2}} \left(V_{\rm R}\right)_{ij} . \tag{3.72}$$

Following the line of argument in section 3.5.3, where we deduced the pattern of the KK fermion mixing contribution to the Z couplings, we find that the $V_{\rm R}$ coupling matrix has a hierarchy among its elements that is very different from that of the CKM matrix. Being characterized by the pattern described by $F^u \circ F^d$, the elements of $V_{\rm R}$ increase mildly along its rows, e.g. $V_{\rm R}^{ud} < V_{\rm R}^{us} < V_{\rm R}^{ub}$ and more strongly along its columns, e.g. $V_{\rm R}^{ud} < V_{\rm R}^{cd} < V_{\rm R}^{td}$. This implies that $V_{\rm R}$ is neither approximately diagonal nor symmetric. Numerically, using the same sets of parameter points also used for the analysis of rare decays in chapter 5, we find the entries of $V_{\rm R}$ to have the typical values

$$V_{\rm R} \approx \begin{pmatrix} 1\cdot 10^{-7} & 1\cdot 10^{-7} & 3\cdot 10^{-7} \\ 9\cdot 10^{-6} & 3\cdot 10^{-5} & 3\cdot 10^{-5} \\ 8\cdot 10^{-5} & 2\cdot 10^{-4} & 9\cdot 10^{-4} \end{pmatrix} . \tag{3.73}$$

For comparison, we mention that indirect bounds on right-handed W couplings from the measurement of the $b \to s\gamma$ decay branching ratio and LEP precision data have been derived in [90–97]. There it is found that the most severe constraints apply to the $W\bar{t}_R b_R$ coupling which is constrained at the 4‰ level, and we conclude that right-handed W couplings at present impose no significant constraint on the RSc parameter space.

3.5.5 Corrections to KK Gluon Couplings

The expressions for the KK gluon couplings after the heavy vector-like states have been integrated out are in fact analogous to those for the Z couplings with two differences: In the RSc the occurring 3×3 coupling matrices are not proportional to the unit matrix and hence do not commute with the 3×3 mass matrices, and further also coupling matrices $[A_{L,R}(G^{A(1)})]_{\alpha\beta}$ with $\alpha \neq \beta$ can be non-vanishing[9]. Taking this into account we can adapt (3.58), (3.59) to the KK gluon couplings and find

$$\begin{aligned} A_L(G^{A(1)}) = {} & \left[A_L(G^{A(1)})\right]_{00} + M_{0k} M_k^{-1} \left[A_L(G^{A(1)})\right]_{k\ell} M_\ell^{-1} M_{0\ell}^\dagger \\ & - \frac{1}{2} M_{0k} M_k^{-2} M_{0k}^\dagger \left[A_L(G^{A(1)})\right]_{00} \\ & - \frac{1}{2} \left[A_L(G^{A(1)})\right]_{00} M_{0k} M_k^{-2} M_{0k}^\dagger , \end{aligned} \tag{3.74}$$

[9]The reason for the second difference lies in the fact that unlike for the Z and $W^\pm$ coupling matrices now also gauge couplings involving different KK levels of quarks are present. In the former cases such couplings were vanishing by virtue of the flat gauge boson bulk profiles and orthonormality conditions for the fermion profiles.

	(0,0)	(1,1)	(2,2)	(3,3)	(0,1)&(1,0)	(0,3)&(3,0)
$A_L^{-1/3}$	$\underset{00}{\mathcal{R}_1(++)_L}$	$\underset{11}{\mathcal{R}_1(++)_L}$	$\underset{11}{\mathcal{R}_3(+-)_L}$	$\underset{11}{\mathcal{R}_3(--)_L}$	$\underset{01}{\mathcal{R}_1(++)_L}$	-
$A_R^{-1/3}$	$\underset{00}{\mathcal{R}_3(++)_R}$	$\underset{11}{\mathcal{R}_1(--)_R}$	$\underset{11}{\mathcal{R}_3(-+)_R}$	$\underset{11}{\mathcal{R}_3(++)_R}$	-	$\underset{01}{\mathcal{R}_3(++)_R}$

Table 3.6: Overlap integrals in the coupling matrices of down-type quarks to the KK gluon $G^{a(1)}$.

	(0,0)	(1,1)	(2,2)&(3,3)	(4,4)	(5,5)	(0,1)&(1,0)	(0,5)&(5,0)
$A_L^{2/3}$	$\underset{00}{\mathcal{R}_1(++)_L}$	$\underset{11}{\mathcal{R}_1(++)_L}$	$\underset{11}{\mathcal{R}_3(+-)_L}$	$\underset{11}{\mathcal{R}_1(-+)_L}$	$\underset{11}{\mathcal{R}_2(--)_L}$	$\underset{01}{\mathcal{R}_1(++)_L}$	-
$A_R^{2/3}$	$\underset{00}{\mathcal{R}_2(++)_R}$	$\underset{11}{\mathcal{R}_1(--)_R}$	$\underset{11}{\mathcal{R}_3(-+)_R}$	$\underset{11}{\mathcal{R}_1(+-)_R}$	$\underset{11}{\mathcal{R}_2(++)_R}$	-	$\underset{01}{\mathcal{R}_2(++)_R}$

Table 3.7: Overlap integrals in the coupling matrices of up-type quarks to the KK gluon $G^{a(1)}$.

and

$$\begin{aligned} A_R(G^{A(1)}) = &\left[A_R(G^{A(1)})\right]_{00} + M_{k0}^\dagger M_k^{-1}\left[A_R(G^{A(1)})\right]_{k\ell} M_\ell^{-1} M_{\ell 0} \\ &- \frac{1}{2} M_{k0}^\dagger M_k^{-2} M_{k0}\left[A_R(G^{A(1)})\right]_{00} \\ &- \frac{1}{2}\left[A_R(G^{A(1)})\right]_{00} M_{k0}^\dagger M_k^{-2} M_{k0}\,. \end{aligned} \tag{3.75}$$

As was the case for the Z coupling these formulae apply to both charge $+2/3$ and $-1/3$ quarks with appropriate use of couplings and mass matrices. Also the statements about the origin of the different corrections made subsequent to (3.58) (3.59) apply here.
The coupling matrices $[A_{L,R}(G^{A(1)})]_{\alpha\beta}$ are all proportional to the strong coupling constant g_s^{4D}, but also involve overlap integrals of the profiles of the KK gluon and the fermions participating in the interaction. Explicit expressions for the coupling matrices in terms of the overlap integrals $\underset{nm}{\mathcal{R}_k(BC)_{L,R}}$ defined in (2.51), (2.54) are given in tables 3.6 and 3.7. Evaluating the corrections to the KK gluon couplings numerically, we find that they amount to at most 10% of the ZMA results and hence can be safely neglected.

3.6 Flavor Violating Higgs Couplings from Profile Discontinuities

Flavor off-diagonal Higgs couplings in the mass eigenbasis can arise whenever the RS contributions to quark masses and to the Yukawa couplings are not aligned. In the mass insertion approximation the RS contributions up to $\mathcal{O}(v^2/M_{\rm KK}^2)$ are represented by the two diagrams in fig. 3.9. The first diagram contributes equally to the quarks'

masses after EWSB and their Yukawa couplings. The second diagram however affects masses and Yukawa couplings in a different manner since its contribution to the Yukawa couplings comes with a combinatorial factor of three that is due to the three different choices of which two external Higgs lines are set to their VEVs. This shift between quark masses and Yukawa couplings results in flavor off-diagonal Higgs couplings once we go to the mass eigenstate basis.

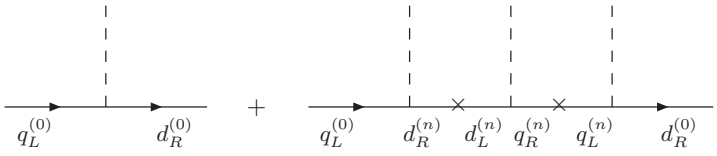

Figure 3.9: RS contributions to quark masses and Yukawa couplings.

At first glance the overall contribution from the second diagram in fig. 3.9 seems to be negligible since both the $q_R^{(n)}$ and $d_L^{(n)}$ modes obey Dirichlet boundary conditions on the IR brane. This is the reason why we did not discuss the Higgs couplings in the effective theory approach employed in the previous section. In [116] however the point has been made that the profiles of $q_R^{(n)}$ and $d_L^{(n)}$ do not exactly vanish on the IR brane but display a small discontinuity that is proportional to the Higgs VEV. After regularization of this discontinuity and summing over the infinite tower of KK modes it is found that a non-vanishing misalignment between quark masses and Yukawa couplings is generated by this diagram. In the following we will briefly summarize the main results of [116] and set the notation for the discussion of the phenomenological impact of tree level Higgs exchanges in chapter 4.
The relevant Lagrangian is given by

$$\mathcal{L}_{\text{Yuk}} = \sum_{n_1=0}^{\infty} \bar{q}_L^{i(n_1)} \lambda_{ij}^d \sum_{n_2=0}^{\infty} d_R^{j(n_2)} H + \sum_{m_1=1}^{\infty} \bar{d}_L^{i(m_1)} \bar{\lambda}_{ij}^d \sum_{m_2=1}^{\infty} q_R^{j(m_2)} H + h.c.\,, \tag{3.76}$$

where λ^d and $\bar{\lambda}^d$ are fundamental 5D Yukawa matrices. It is important to note that the Yukawa matrix $\bar{\lambda}^d$ which couples the scalar currents $d_L^{i(m_1)} q_R^{j(m_2)}$ to the Higgs field is not required for the generation of quark masses and hence could be set to zero, which would eliminate the second diagram's contribution to flavor off-diagonal Higgs couplings. However, since this choice for $\bar{\lambda}^d$ without profound physical reason contradicts naturalness, in the following we will set $\bar{\lambda}^d$ to be equal[10] to λ^d.
An additional source of misalignment between quark masses and Yukawa couplings is the modification of the kinetic terms by the mixing of SM quarks and KK quarks after EWSB as described in section 3.5.1 and first discussed in this context in [84] (see also [117]). These flavor-dependent corrections to the kinetic terms make redefinitions of the quark fields necessary which in turn give rise to an additional shift between quark masses and Yukawa couplings. For the first two generations of quarks this contribution

[10]Note that the choice $\bar{\lambda}^d = \lambda^d$ is mandatory in the bulk Higgs scenario.

is found to be negligible, but for the third generation this effect can be of the same size as the one outlined above.

After this rather qualitative description we now summarize the main results of [116] for the case of a brane-localized Higgs field. The total misalignment between quark masses and Yukawa couplings comprises two contributions, $\hat{\Delta}^d = \hat{\Delta}^d_1 + \hat{\Delta}^d_2$, where $\hat{\Delta}^d_1$ is the contribution represented by the diagrams in fig. 3.9 and $\hat{\Delta}^d_2$ is due to rescaling of the quark fields as to canonize their kinetic terms. Explicitly, the authors of [116] find

$$\hat{\Delta}^d_1 = \frac{2}{3} F_Q \lambda^d \left(\bar{\lambda}^d\right)^\dagger \lambda^d F_d \frac{v^3}{f^2_{RS}}\,, \tag{3.77}$$

and

$$\hat{\Delta}^d_2 = m^d \left(m^{d\dagger} K(c_Q) + K(-c_d) m^{d\dagger}\right) m^d \frac{1}{f^2_{\rm RS}}\,, \tag{3.78}$$

where $f_{\rm RS} = k e^{-kL} \approx M_{\rm KK}/2.45$ is the warped-down curvature of the extra dimension which sets the scale of mass of the lightest KK states. The matrices $K(c) = {\rm Diag}(K(c^i))$ and $F_{Q,d} = {\rm Diag}(f(c^i_{Q,d}))$ are functions that depend on the quark localization and are defined via

$$f(c) \equiv \sqrt{\frac{1-2c}{1-e^{-(1-2c)kL}}}\,, \tag{3.79}$$

$$K(c) \equiv \frac{1}{1-2c}\frac{1}{e^{(1-2c)kL}-1}\left(-1 + \frac{e^{(1-2c)kL}-e^{-2kL}}{3-2c} + \frac{e^{(2c-1)kL}-e^{-2kL}}{1+2c}\right). \tag{3.80}$$

The flavor off-diagonal components of the Yukawa couplings in the mass eigenbasis are obtained from $\hat{\Delta}^d$ via the bi-unitary transformation

$$\hat{Y}_{\text{off-diag.}} = D^\dagger_L \hat{\Delta}^d D_R\,, \tag{3.81}$$

where D_L and D_R are the unitary rotations that diagonalize the down-type quark mass matrix.

Chapter 4

Impact on Flavor Observables

With the spectrum and couplings of the RSc at hand there are now two different approaches, direct and indirect, to test its implications experimentally. Following the former approach, additional particle states are analyzed in high energy collisions where they manifest themselves as resonances or in their decay products. The indirect approach on the other hand is based on the fact that processes which are very rare in the SM can receive detectable corrections from the exchange of virtual heavy states. Of particular interest in this context are processes that connect states with different flavor content and that in the SM can only take place at loop level. In the following we will adhere to the indirect approach and investigate the impact of the RSc on flavor observables.

In chapter 3 the appearance of flavor violating couplings of fermions to neutral gauge bosons and the Higgs has been pointed out and their origin has been discussed. Given these couplings it is obvious that the RSc contains FCNCs at the tree level mediated by particles with masses which are—if the original RS solution of the Planck-EW hierarchy problem [26] is taken at face value—not very much larger than the EW scale. Fortunately, there is a built-in protection of observables related to light quarks in the initial and final states, the so-called RS-GIM mechanism which was introduced in section 3.4.1. Nevertheless it is mandatory to determine the quantitative impact of these tree level FCNCs on flavor observables and investigate whether the RS-GIM mechanism sufficiently suppresses flavor violation in the RSc. To answer this question we will discuss in detail the contributions of tree level KK gluon, EW gauge boson and Higgs exchanges to the amplitudes M_{12}^K, M_{12}^d and M_{12}^s in the RSc and give formulae for ΔM_K, ΔM_d, ΔM_s, ϵ_K, $S_{\psi K_S}$, $S_{\psi\phi}$, $\Delta\Gamma_q/\Gamma_q$ and $A_{\rm SL}^q$ in a form suitable for the study of the size of the new contributions. Parts of this analysis have already been published in [33].

To extend our analysis to rare decays of K and B mesons we will subsequently generalize the gauge invariant SM functions X, Y, Z to the RSc taking into account the tree level contributions of EW gauge bosons. The generalized flavor dependent functions X_i, Y_i, Z_i, $(i = K, d, s)$ then will be used to derive expressions for the branching ratios of the exclusive decays $K^+ \to \pi^+\nu\bar{\nu}$, $K_L \to \pi^0\nu\bar{\nu}$, $B_{d,s} \to \mu^+\mu^-$, $K_L \to \mu^+\mu^-$ and $K_L \to \pi^0\ell^+\ell^-$, as well as for the two inclusive modes $B \to X_{d,s}\nu\bar{\nu}$ in a compact form.

While the first comprehensive study of rare decays was performed by us in [34], partial studies have been presented in [98, 118, 119].
Our presentation includes the contributions from all operators originating exclusively from tree level exchanges of electroweak gauge bosons. Consequently we do not discuss the dipole operators that enter the respective effective Hamiltonians first at the one-loop level. This implies that the effective Hamiltonians for $b \to d\ell^+\ell^-$ and $b \to s\ell^+\ell^-$ transitions given below are incomplete and we cannot yet perform the phenomenology of decays such as $B \to K^*\ell^+\ell^-$, $B \to X_{s,d}\ell^+\ell^-$ and $B \to X_{s,d}\gamma$.

4.1 Particle-Antiparticle Oscillations

4.1.1 $\Delta F = 2$ Processes in the SM

In the present section we will use conventions and notation of [120] so that an easy comparison with the SM predictions and with the results obtained in the LHT and SM4 models in section 5.4 will be possible.
The SM Hamiltonians for $K^0 - \bar{K}^0$ and $B^0_{s,d} - \bar{B}^0_{s,d}$ oscillations can be found in (3.1) and (3.2) of [120]. The SM contribution to the off-diagonal element M_{12} in the neutral K and B_d meson mass matrices is given as

$$\left(M_{12}^K\right)_{\rm SM} = \frac{G_F^2}{12\pi^2} F_K^2 \hat{B}_K m_K M_W^2 \left[\lambda_c^{*2}\eta_1 S_c + \lambda_t^{*2}\eta_2 S_t + 2\lambda_c^*\lambda_t^*\eta_3 S_{ct}\right] , \tag{4.1}$$

$$\left(M_{12}^d\right)_{\rm SM} = \frac{G_F^2}{12\pi^2} F_{B_d}^2 \hat{B}_{B_d} m_{B_d} M_W^2 \left[\left(\lambda_t^{(d)*}\right)^2 \eta_B S_t\right] , \tag{4.2}$$

where $\lambda_i = V_{is}^* V_{id}$ and $\lambda_t^{(q)} = V_{tb}^* V_{tq}$ with V_{ij} the elements of the CKM matrix. S_c, S_t and S_{ct} are the one-loop box functions for which explicit expressions are given e. g. in [120]. The factors η_i are QCD corrections evaluated at the next-to-leading order (NLO) level in [121–125]. Finally $\hat{B}_K$ and $\hat{B}_{B_d}$ are the well-known non-perturbative factors. The amplitude $(M_{12}^s)_{\rm SM}$ can be obtained from (4.2) by simply replacing d by s.
It should be emphasized that in the SM only a single operator

$$(\bar{s}d)_{V-A}(\bar{s}d)_{V-A} = [\bar{s}\gamma_\mu(1-\gamma_5)d] \otimes [\bar{s}\gamma^\mu(1-\gamma_5)d] \tag{4.3}$$

and accordingly

$$(\bar{b}q)_{V-A}(\bar{b}q)_{V-A} = \left[\bar{b}\gamma_\mu(1-\gamma_5)q\right] \otimes \left[\bar{b}\gamma^\mu(1-\gamma_5)q\right] \tag{4.4}$$

contributes to M_{12}^K and M_{12}^q $(q = d, s)$. Moreover, complex phases only enter through the CKM factors λ_i and $\lambda_t^{(q)}$.

4.1.2 $\Delta F = 2$ Processes in the RSc

Tree Level KK Gluon Contributions The expressions (4.1) and (4.2) for $(M_{12})_{\rm SM}$ can be generalized to include the new tree level contributions from neutral KK gauge

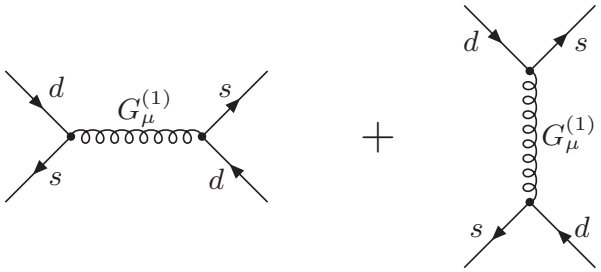

Figure 4.1: Tree level contribution of the lightest KK gluon to $K^0 - \bar{K}^0$ oscillations.

bosons and the Higgs boson. We begin our discussion with the tree level exchanges of the lightest KK gluons $G_\mu^{(1)}$ which are shown in fig. 4.1. With the flavor off-diagonal couplings of SM quark mass eigenstates to the lightest KK gluon, $\Delta_{L,R}^{ij}(G^{(1)}) \equiv (\hat{\Delta}_{L,R}^{-1/3}(G^{(1)}))_{ij}$ defined in (3.35) the effective Hamiltonian for $\Delta S = 2$ transitions is given by

$$\begin{aligned}\left[\mathcal{H}_{\text{eff}}^{\Delta S=2}\right]_{\text{KK}}^{\text{QCD}} = \frac{{p_{\text{UV}}}^2}{2M_{\text{KK}}^2}\Big[&\left(\Delta_L^{sd}(G^{(1)})\right)^2\left(\bar{s}_L\gamma_\mu t^A d_L\right)\left(\bar{s}_L\gamma^\mu t^A d_L\right)\\ &+\left(\Delta_R^{sd}(G^{(1)})\right)^2\left(\bar{s}_R\gamma_\mu t^A d_R\right)\left(\bar{s}_R\gamma^\mu t^A d_R\right)\\ &+2\Delta_L^{sd}(G^{(1)})\Delta_R^{sd}(G^{(1)})\left(\bar{s}_L\gamma_\mu t^A d_L\right)\left(\bar{s}_R\gamma^\mu t^A d_R\right)\Big],\end{aligned} \tag{4.5}$$

where p_{UV} takes into account the potential impact of brane kinetic terms on the matching of the 5D to the 4D QCD coupling constant. We observe that the tree level contributions have a flavor structure that is different from the CKM pattern and that new operators enter the effective Hamiltonians for K oscillations. Diagrams analogous to those in fig. 4.1 contribute to $B_{d,s}^0 - \bar{B}_{d,s}^0$ mixing and the relevant effective Hamiltonians can be obtained by replacing sd in (4.5) by bd and bs.

The effective Hamiltonian in (4.5) is valid at scales $\mu \sim \mathcal{O}(M_{\text{KK}})$ and has to be evolved to low energy scales $\mu \sim \mathcal{O}(2\,\text{GeV})$, $\mu \sim \mathcal{O}(m_b)$ at which the hadronic matrix elements of the operators in question can be calculated by means of lattice methods. The relevant anomalous dimension matrices necessary for this RG evolution have been calculated at two-loop level in [126,127] and analytic formulae for the relevant QCD factors analogous to η_i in (4.1) and (4.2) can be found in [128].

Since the gluon induced operators in (4.5) have a non-trivial color structure it will be convenient in view of the RG evolution to transform them to the operator basis used in [128],

$$\begin{aligned}\mathcal{Q}_1^{VLL} &= \left(\bar{s}\gamma_\mu P_L d\right)\left(\bar{s}\gamma^\mu P_L d\right),\\ \mathcal{Q}_1^{VRR} &= \left(\bar{s}\gamma_\mu P_R d\right)\left(\bar{s}\gamma^\mu P_R d\right),\\ \mathcal{Q}_1^{LR} &= \left(\bar{s}\gamma_\mu P_L d\right)\left(\bar{s}\gamma^\mu P_R d\right),\\ \mathcal{Q}_2^{LR} &= \left(\bar{s}P_L d\right)\left(\bar{s}P_R d\right),\end{aligned} \tag{4.6}$$

where we suppressed color indices as they are summed over within each bracket.
A straightforward application of the so-called *Fierz identities* (see e.g. [129]) yields the effective Hamiltonian for KK gluon mediated $\Delta S = 2$ transitions in the basis (4.6) with the Wilson coefficients corresponding to $\mu \sim \mathcal{O}(M_{\rm KK})$,

$$\left[\mathcal{H}_{\rm eff}^{\Delta S=2}\right]_{\rm KK}^{\rm QCD} = \left[C_1^{VLL}\mathcal{Q}_1^{VLL} + C_1^{VRR}\mathcal{Q}_1^{VRR} + C_1^{LR}\mathcal{Q}_1^{LR} + C_2^{LR}\mathcal{Q}_2^{LR}\right] , \tag{4.7}$$

where

$$\begin{aligned}
\left[C_1^{VLL}(M_{\rm KK})\right]^{\rm QCD} &= \frac{2}{3}\frac{p_{\rm UV}^2}{4M_{\rm KK}^2}\left(\Delta_L^{sd}(G^{(1)})\right)^2 , \\
\left[C_1^{VRR}(M_{\rm KK})\right]^{\rm QCD} &= \frac{2}{3}\frac{p_{\rm UV}^2}{4M_{\rm KK}^2}\left(\Delta_R^{sd}(G^{(1)})\right)^2 , \\
\left[C_1^{LR}(M_{\rm KK})\right]^{\rm QCD} &= -\frac{2}{3}\frac{p_{\rm UV}^2}{4M_{\rm KK}^2}\Delta_L^{sd}(G^{(1)})\Delta_R^{sd}(G^{(1)}) , \\
\left[C_2^{LR}(M_{\rm KK})\right]^{\rm QCD} &= -4\frac{p_{\rm UV}^2}{4M_{\rm KK}^2}\Delta_L^{sd}(G^{(1)})\Delta_R^{sd}(G^{(1)}) .
\end{aligned} \tag{4.8}$$

Analogous expressions exist for the $B_d^0 - \bar{B}_d^0$ and $B_s^0 - \bar{B}_s^0$ systems, with sd replaced by bd and bs.

Tree Level Electroweak Contributions The KK gluon tree level contributions in fig. 4.1 discussed until now are believed to dominate the NP contributions to $\Delta F = 2$ processes in the RSc. However we will demonstrate now that while this assumption is justified in the case of ϵ_K and ΔM_K, in the case of $B_{d,s}$ observables it is mandatory to include also tree level EW gauge boson contributions. The dominant EW contributions in the RSc do not come from the Z boson but from tree level exchanges of the two new heavy gauge bosons Z_H and Z'. They also turn out to be much larger than the KK photon contribution.
Let us begin with the KK photon contribution $A^{(1)}$. The contributing diagrams are analogous to those shown in fig. 4.1 with $G^{(1)}$ replaced by $A^{(1)}$. The calculation on the other hand is simplified relative to the KK gluon case by the fact that in the absence of the color matrices t^A one immediately obtains the result in the operator basis (4.6). We find the following corrections to the Wilson coefficients $C_i(M_{\rm KK})$ in (4.8):

$$\begin{aligned}
\left[C_1^{VLL}(M_{\rm KK})\right]^{\rm QED} &= \frac{1}{2M_{\rm KK}^2}\left[\Delta_L^{sd}(A^{(1)})\right]^2 , \\
\left[C_1^{VRR}(M_{\rm KK})\right]^{\rm QED} &= \frac{1}{2M_{\rm KK}^2}\left[\Delta_R^{sd}(A^{(1)})\right]^2 , \\
\left[C_1^{LR}(M_{\rm KK})\right]^{\rm QED} &= \frac{1}{M_{\rm KK}^2}\left[\Delta_L^{sd}(A^{(1)})\right]\left[\Delta_R^{sd}(A^{(1)})\right] ,
\end{aligned}$$

$$\left[C_2^{LR}(M_{\rm KK})\right]^{\rm QED} = 0\,, \tag{4.9}$$

with the couplings $\Delta^{ij}_{L,R}(A^{(1)}) \equiv (\hat{\Delta}^{-1/3}_{L,R}(A^{(1)}))_{ij}$ defined in (3.35). We observe that in contrast to KK gluon exchange this time no contribution to the C_2^{LR} operator is induced.
Next we consider the contributions of the Z, Z_H and Z' gauge bosons to the effective Hamiltonian of particle-antiparticle mixing. While the KK gluon and photon contributions are universal to all RS models with bulk fermions, the contributions discussed in the following depend sensitively on the EW gauge group and the choice of fermion representations. In particular they will be very different in the RSc and RSm models (for flavor analyses in the RSm see for instance [84, 117]).
The calculation of $\mathcal{O}(v^2/M_{\rm KK}^2)$ tree level contributions from the Z, Z_H and Z' gauge bosons proceeds similarly to the calculation of the KK photon contribution and we find

$$\begin{aligned}
\left[C_1^{VLL}(M_{\rm KK})\right]^{\rm EW} &= \frac{1}{2M_{\rm KK}^2}\left[\left(\Delta_L^{sd}(Z^{(1)})\right)^2 + \left(\Delta_L^{sd}(Z_X^{(1)})\right)^2\right]\,,\\
\left[C_1^{VRR}(M_{\rm KK})\right]^{\rm EW} &= \frac{1}{2M_{\rm KK}^2}\left[\left(\Delta_R^{sd}(Z^{(1)})\right)^2 + \left(\Delta_R^{sd}(Z_X^{(1)})\right)^2\right]\,,\\
\left[C_1^{LR}(M_{\rm KK})\right]^{\rm EW} &= \frac{1}{M_{\rm KK}^2}\left[\Delta_L^{sd}(Z^{(1)})\Delta_R^{sd}(Z^{(1)}) + \Delta_L^{sd}(Z_X^{(1)})\Delta_R^{sd}(Z_X^{(1)})\right]\,,\\
\left[C_2^{LR}(M_{\rm KK})\right]^{\rm EW} &= 0\,,
\end{aligned} \tag{4.10}$$

where the couplings $\Delta^{ij}_{L,R}(Z^{(1)}) \equiv (\hat{\Delta}^{-1/3}_{L,R}(Z^{(1)}))_{ij}$ and $\Delta^{ij}_{L,R}(Z_X^{(1)}) \equiv (\hat{\Delta}^{-1/3}_{L,R}(Z_X^{(1)}))_{ij}$ can be obtained from (3.37), (3.38) and already include the relevant weak couplings and charges.

At this point it is not necessary to transform the gauge bosons to the mass eigenbasis. We still want to point out that the mass eigenstate Z contributes negligibly and that the Z' contribution is suppressed with respect to the one of Z_H. In the case of the Z boson, flavor violating couplings are suppressed by $M_Z^2/M_{\rm KK}^2$ with respect to those of Z_H and in addition by the custodial protection. The light Z mass entering the propagator can only partly compensate for this.
In order to estimate the size of EW contributions when compared to the KK gluon exchanges we factor out all the couplings and charge factors from the different $\Delta^{sd}_{L,R}$ matrices. The remaining $\tilde{\Delta}^{sd}_{L,R}$ then are universal for the gauge bosons considered here up to small deviations due to the different boundary condition of $Z_X^{(1)}$ on the UV brane, whose inclusion amounts to only a percent effect on $\Delta^{sd}_{L,R}(Z_X^{(1)})$.
Adding the contributions (4.8), (4.9), (4.10) and evaluating the various couplings we find

$$\begin{aligned}
C_1^{VLL}(M_{\rm KK}) &= \frac{1}{4M_{\rm KK}^2}(0.67p_{\rm UV}^2 + 0.02 + 0.56)(\tilde{\Delta}_L^{sd})^2\,,\\
C_1^{VRR}(M_{\rm KK}) &= \frac{1}{4M_{\rm KK}^2}(0.67p_{\rm UV}^2 + 0.02 + 0.98)(\tilde{\Delta}_R^{sd})^2\,,
\end{aligned}$$

$$C_1^{LR}(M_{\rm KK}) = \frac{1}{4M_{\rm KK}^2}(-0.67p_{\rm UV}^2 + 0.04 + 1.13)(\tilde{\Delta}_L^{sd}\tilde{\Delta}_R^{sd})\,, \tag{4.11}$$

where the three contributions correspond to tree level exchanges of the KK gluon, KK photon and combined (Z, Z_H, Z') exchanges[1]. The Wilson coefficient $C_2^{LR}(M_{\rm KK})$ receives only KK gluon contributions at $\mu \sim \mathcal{O}(M_{\rm KK})$ and, as we will see below, also a contribution from tree level Higgs exchanges, but is not modified by EW interactions.

The EW contributions are dominated by Z_H exchanges and in the case of C_1^{VLL}, C_1^{VRR} and C_1^{LR} amount to +87% (+350%), +150% (+600%) and −175% (−700%) corrections for $g_s = 6$ ($g_s = 3$). In particular the sign of $C_1^{LR}(M_{\rm KK})$ is reversed by the inclusion of the EW contributions.

We conclude that the EW gauge boson contributions to the Wilson coefficients C_1^{VLL}, C_1^{VRR} and C_1^{LR} at $\mu \sim \mathcal{O}(M_{\rm KK})$ are of the same order as the KK gluon contributions and have to be taken into account. In the case of ϵ_K and ΔM_K the strong enhancement of the coefficient C_2^{LR} through QCD renormalization group effects and the chiral enhancement of the hadronic matrix element of $\mathcal{Q}_2^{LR}$ assure that KK gluon contributions still dominate over EW contributions, although the reversal of the sign of C_1^{LR} slightly intensifies the constraints from ϵ_K and ΔM_K. However, in the case of $B_{d,s}$ physics observables the QCD renormalization group enhancement in the LR sector is smaller than in the K sector and the chiral enhancement of $\langle\mathcal{Q}_2^{LR}\rangle$ and $\langle\mathcal{Q}_1^{LR}\rangle$ is absent. Therefore the $\mathcal{Q}_1^{VLL}$ operator becomes important even without the EW contributions and it is further enhanced when these contributions are taken into account.

At first sight our finding that EW contributions can compete with QCD contributions or even exceed them is surprising. On the other hand one should remember that KK gluon contributions similarly to EW contributions are suppressed by their large masses and the main difference between these contributions results from gauge couplings, color factors, weak charges and RG effects. Our analysis shows that with the exception of C_2^{LR} all these effects conspire to make EW heavy gauge boson contributions as important as the KK gluon contributions in $\Delta B = 2$ observables.

Tree Level Higgs Contributions The Lagrangian relevant for Higgs contributions to $\Delta S = 2$ transitions is given by

$$\mathcal{L}_{\rm NC}^{\rm Higgs} = -\hat{Y}_{21}\bar{s}_L d_R H - \hat{Y}_{12}^*\bar{s}_R d_L H\,, \tag{4.12}$$

where $\hat{Y}$ is the down-type 3×3 Yukawa matrix for quarks in the mass eigenbasis at energy scale $\mu \sim \mathcal{O}(M_H)$ as given in (3.81). If we define $\Delta_R^H \equiv \hat{Y}_{21}$, $\Delta_L^H \equiv \hat{Y}_{12}^*$, the effective Hamiltonian for $\Delta S = 2$ transitions induced by tree level Higgs exchanges is

[1]These results are obtained neglecting the running of the EW gauge couplings between the EW scale M_Z and the KK scale $M_{\rm KK}$. Taking into account also these contributions, we would have corrections to the gauge couplings at the 5% level, so that we can easily neglect them.

found to be

$$\left[\mathcal{H}_{\text{eff}}^{\Delta S=2}\right]^{\text{Higgs}} = \frac{1}{2M_H^2}\left[\left(\Delta_L^H\right)^2(\bar{s}P_Ld)(\bar{s}P_Ld) + \left(\Delta_R^H\right)^2(\bar{s}P_Rd)(\bar{s}P_Rd) + 2\Delta_L^H\Delta_R^H(\bar{s}P_Ld)(\bar{s}P_Rd)\right], \tag{4.13}$$

which in the operator basis of [128] is equivalent to the effective Hamiltonian

$$\left[\mathcal{H}_{eff}^{\Delta S=2}\right]^{\text{Higgs}} = \frac{1}{2M_H^2}\left[\left(\Delta_L^H\right)^2 Q_1^{SLL} + \left(\Delta_R^H\right)^2 Q_1^{SRR} + 2\Delta_L^H\Delta_R^H Q_2^{LR}\right]. \tag{4.14}$$

Relative to the operator basis (4.6), tree level Higgs exchanges induce the additional operators Q_1^{SLL}, Q_1^{SRR} and the operators Q_2^{SLL}, Q_2^{SRR} that these mix with under renormalization, such that the full operator basis is given by

$$\begin{aligned}
\mathcal{Q}_1^{VLL} &= (\bar{s}\gamma_\mu P_Ld)\,(\bar{s}\gamma^\mu P_Ld)\,, & \mathcal{Q}_1^{SLL} &= (\bar{s}P_Ld)(\bar{s}P_Ld)\,,\\
\mathcal{Q}_1^{VRR} &= (\bar{s}\gamma_\mu P_Rd)\,(\bar{s}\gamma^\mu P_Rd)\,, & \mathcal{Q}_1^{SRR} &= (\bar{s}P_Rd)(\bar{s}P_Rd)\,,\\
\mathcal{Q}_1^{LR} &= (\bar{s}\gamma_\mu P_Ld)\,(\bar{s}\gamma^\mu P_Rd)\,, & \mathcal{Q}_2^{SLL} &= (\bar{s}\sigma_{\mu\nu}P_Ld)(\bar{s}\sigma^{\mu\nu}P_Ld)\,,\\
\mathcal{Q}_2^{LR} &= (\bar{s}P_Ld)\,(\bar{s}P_Rd)\,, & \mathcal{Q}_2^{SRR} &= (\bar{s}\sigma_{\mu\nu}P_Rd)(\bar{s}\sigma^{\mu\nu}P_Rd)\,.
\end{aligned} \tag{4.15}$$

The Wilson coefficients at energy scale $\mu \sim \mathcal{O}(M_H)$ are given by

$$\begin{aligned}
\left[C_1^{SLL}(M_H)\right]^{\text{Higgs}} &= \frac{1}{2M_H^2}\left(\Delta_L^H\right)^2,\\
\left[C_1^{SRR}(M_H)\right]^{\text{Higgs}} &= \frac{1}{2M_H^2}\left(\Delta_R^H\right)^2,\\
\left[C_2^{LR}(M_H)\right]^{\text{Higgs}} &= \frac{1}{M_H^2}\Delta_L^H\Delta_R^H\,.
\end{aligned} \tag{4.16}$$

Analogous expressions for the $B_{d,s}$ systems can be obtained by replacing $\Delta_L^H = \hat{Y}_{12}^*$, $\Delta_R^H = \hat{Y}_{21}$ by $\hat{Y}_{13}^*$, $\hat{Y}_{31}$ and $\hat{Y}_{23}^*$, $\hat{Y}_{32}$.

4.1.3 Combined Contributions to M_{12} at the Physical Scale

With the various contributions given in (4.8)–(4.10) we obtain the total Wilson coefficients induced by tree level exchange of gauge bosons,

$$[C_i(M_{\text{KK}})]^{\text{gauge}} = [C_i(M_{\text{KK}})]^{\text{QCD}} + [C_i(M_{\text{KK}})]^{\text{QED}} + [C_i(M_{\text{KK}})]^{\text{EW}}\,. \tag{4.17}$$

The RG evolution of the gauge boson contribution from $\mu \sim \mathcal{O}(M_{\text{KK}})$ to a low energy scale μ_0 can be performed separately from the additive SM contribution, even if $\mathcal{Q}_1^{VLL}$ is equal up to a factor of 1/4 to the SM operator $(\bar{s}d)_{V-A}\,(\bar{s}d)_{V-A}$. We recall that $\mathcal{Q}_1^{VLL}$

and $\mathcal{Q}_1^{VRR}$ renormalize without mixing with other operators and their evolution being the same as QCD is insensitive to the sign of γ_5. But as $C_1^{VLL}(M_{\rm KK}) \neq C_1^{VRR}(M_{\rm KK})$, their Wilson coefficients at μ_0 will differ from each other. On the other hand $\mathcal{Q}_1^{LR}$ and $\mathcal{Q}_2^{LR}$ mix under renormalization so that the RG evolution operator is a 2×2 matrix.
The tree level Higgs contribution is generated at a different scale and displays a different behavior under RG evolution such that is has to be dealt with separately. The flavor off-diagonal Yukawa couplings entering (4.12) are generated at or beyond the KK mass scale. In the following, we will take this scale to be $\mu = M_{\rm KK}$. From this high energy scale the Yukawa couplings have to be evolved down to the scale $\mu = M_H$ of the Higgs mass where new effective interactions are generated by tree level exchanges of the Higgs boson. The RG evolution of these couplings is in fact identical to that of quark masses and is well known at the NLO level. From this scale in turn the Wilson coefficients of the new operators have to be evolved down to the physically relevant scale μ_0 according to their anomalous dimensions as was done in the case of the gauge boson contribution. As $\mathcal{Q}_1^{SLL,SRR}$ and $\mathcal{Q}_2^{SLL,SRR}$ mix under renormalization, also their RG evolution operators are given by 2×2 matrices.
At the physically relevant scale μ_0 the contributions $[C_i(\mu_0)]^{\rm gauge}$ and $[C_i(\mu_0)]^{\rm Higgs}$ stemming from tree level gauge boson and Higgs exchanges, can be added up to form the total NP contribution. The outcome of this analysis is an effective Hamiltonian relevant at the low energy scale μ_0,

$$\begin{aligned}\left[\mathcal{H}_{\rm eff}^{\Delta S=2}\right]_{\rm KK} = \big[&C_1^{VLL}(\mu_0)\mathcal{Q}_1^{VLL} + C_1^{VRR}(\mu_0)\mathcal{Q}_1^{VRR} \\ &+ C_1^{LR}(\mu_0)\mathcal{Q}_1^{LR} + C_2^{LR}(\mu_0)\mathcal{Q}_2^{LR} \\ &+ C_1^{SLL}(\mu_0)\mathcal{Q}_1^{SLL} + C_2^{SLL}(\mu_0)\mathcal{Q}_2^{SLL} \\ &+ C_1^{SRR}(\mu_0)\mathcal{Q}_1^{SRR} + C_2^{SRR}(\mu_0)\mathcal{Q}_2^{SRR}\big]\,, \end{aligned} \tag{4.18}$$

with analogous expressions for the $\Delta B = 2$ Hamiltonians.
The contribution of the KK gauge bosons $G^{(1)}, A^{(1)}, Z_H, Z'$ and the Higgs boson to the off-diagonal element M_{12}^K is then obtained from

$$2m_K \left(M_{12}^K\right)^*_{\rm KK} = \langle \bar{K}^0 | \left[\mathcal{H}_{\rm eff}^{\Delta S=2}\right]_{\rm KK} | K^0 \rangle \,. \tag{4.19}$$

To this end one has to evaluate the hadronic matrix elements

$$\langle \bar{K}^0 | \mathcal{Q}_i(\mu) | K^0 \rangle \equiv \langle \mathcal{Q}_i(\mu) \rangle \tag{4.20}$$

which can be parameterized as follows

$$\langle \mathcal{Q}_1^{VLL}(\mu) \rangle = \langle \mathcal{Q}_1^{VRR}(\mu) \rangle = \frac{2}{3} m_K^2 F_K^2 B_1^{VLL}(\mu)\,, \tag{4.21}$$

$$\langle \mathcal{Q}_1^{LR}(\mu) \rangle = -\frac{1}{3} R(\mu) m_K^2 F_K^2 B_1^{LR}(\mu)\,, \tag{4.22}$$

$$\langle \mathcal{Q}_2^{LR}(\mu) \rangle = \frac{1}{2} R(\mu) m_K^2 F_K^2 B_2^{LR}(\mu)\,, \tag{4.23}$$

$$\langle \mathcal{Q}_1^{SLL}(\mu)\rangle = \langle \mathcal{Q}_1^{SRR}(\mu)\rangle = -\frac{5}{12}R(\mu)m_K^2F_K^2B_1^{SLL}(\mu)\,, \tag{4.24}$$

$$\langle \mathcal{Q}_2^{SLL}(\mu)\rangle = \langle \mathcal{Q}_2^{SRR}(\mu)\rangle = -R(\mu)m_K^2F_K^2B_2^{SLL}(\mu)\,, \tag{4.25}$$

where the chiral enhancement factor $R(\mu)$ is given by

$$R(\mu) = \left(\frac{m_K}{m_s(\mu)+m_d(\mu)}\right)^2. \tag{4.26}$$

The scale-dependent B_i parameters are known from lattice calculations and are related to the parameters B_1, B_2, B_3, B_4 and B_5 calculated in [130, 131] by

$$B_1^{VLL} \equiv B_1\,,\ B_1^{LR} \equiv B_5\,,\ B_2^{LR} \equiv B_4\,,\ B_1^{SLL} \equiv B_2\,,\ B_2^{SLL} \equiv \frac{5}{3}B_2 - \frac{2}{3}B_3\,. \tag{4.27}$$

It should be stressed that the $B_i(\mu)$ are not RG invariant parameters in contrast to $\hat{B}_K$ in (4.1), but in view of the results in [128, 130, 131] it is easier to use them in this way. Collecting all these results we find ($\mu_L = 2\,\mathrm{GeV}$)

$$\begin{aligned}\left(M_{12}^K\right)_{\mathrm{KK}} = \frac{1}{3}m_KF_K^2\cdot\Big[&\left(C_1^{VLL}(\mu_L)+C_1^{VRR}(\mu_L)\right)B_1^K\\ &-\frac{1}{2}R(\mu_L)C_1^{LR}(\mu_L)B_5^K+\frac{3}{4}R(\mu_L)C_2^{LR}(\mu_L)B_4^K\\ &-\frac{5}{8}R(\mu_L)\left(C_1^{SLL}(\mu_L)+C_1^{SRR}(\mu_L)\right)B_2^K\\ &-\frac{3}{2}R(\mu_L)\left(C_2^{SLL}(\mu_L)+C_2^{SRR}(\mu_L)\right)\left(\frac{5}{3}B_2^K-\frac{2}{3}B_3^K\right)\Big]^*.\end{aligned} \tag{4.28}$$

Analogous expressions can be derived for $\left(M_{12}^d\right)_{\mathrm{KK}}$ and $(M_{12}^s)_{\mathrm{KK}}$ relevant for $B_d^0-\bar{B}_d^0$ and $B_s^0-\bar{B}_s^0$ oscillations. For these, $\mu_b = 4.6\,\mathrm{GeV}$ has to be used, and

$$R^q(\mu) = \left(\frac{m_{B_q}}{m_b(\mu)+m_q(\mu)}\right)^2. \tag{4.29}$$

The values for B_i in the $\overline{\mathrm{MS}}$-Naïve Dimensional Regularization (NDR) scheme that we will use in our analysis have been extracted from [130] and [131] for the $K^0-\bar{K}^0$ and $B_{s,d}^0-\bar{B}_{s,d}^0$ systems. They are collected in table 4.1, together with the relevant values of μ_0. The final results for M_{12}^K, M_{12}^d and M_{12}^s, which govern the analysis of $\Delta F=2$ transitions in the RSc, are then given by

$$M_{12}^i = \left(M_{12}^i\right)_{\mathrm{SM}} + \left(M_{12}^i\right)_{\mathrm{KK}} \qquad (i = K,d,s)\,. \tag{4.30}$$

	B_1	B_2	B_3	B_4	B_5	μ_0
K^0-$\bar{K}^0$	0.57	0.68	1.06	0.81	0.56	2.0 GeV
B^0-$\bar{B}^0$	0.87	0.79	0.92	1.15	1.73	4.6 GeV

Table 4.1: Values of the parameters B_i in the $\overline{\text{MS}}$-NDR scheme obtained in [130] (K^0-$\bar{K}^0$) and [131] (B^0-$\bar{B}^0$). The scale μ_0 at which C_i are evaluated is given in the last column. For $\hat{B}_K$ in (4.1) we use $\hat{B}_K = 0.725 \pm 0.026$ [132].

4.1.4 Basic Formulae for $\Delta F = 2$ Observables

We now collect the formulae that we will use in our numerical analysis. We would like to emphasize that, although physical observables are phase convention independent, some of the formulae collected in this section depend on the phase convention chosen for the CKM matrix and yield correct results only if the standard phase convention [133] is used consistently.
The $K_L - K_S$ mass difference is given by

$$\Delta M_K = 2\left[\text{Re}\left(M_{12}^K\right)_{\text{SM}} + \text{Re}\left(M_{12}^K\right)_{\text{KK}}\right] \tag{4.31}$$

and the CP-violating parameter ϵ_K by

$$\epsilon_K = \frac{\kappa_\epsilon e^{i\varphi_\epsilon}}{\sqrt{2}(\Delta M_K)_{\text{exp}}}\left[\text{Im}\left(M_{12}^K\right)_{\text{SM}} + \text{Im}\left(M_{12}^K\right)_{\text{KK}}\right] , \tag{4.32}$$

where we use $\varphi_\epsilon = (43.51 \pm 0.05)^\circ$ and $\kappa_\epsilon = 0.92 \pm 0.02$ [134] thus taking into account that $\varphi_\epsilon \neq \pi/4$ and including an additional effect from $\text{Im}A_0$, the imaginary part of the 0-isospin amplitude in $K \to \pi\pi$.
For the mass differences in the $B_{d,s}^0 - \bar{B}_{d,s}^0$ systems we have

$$\Delta M_q = 2\left|(M_{12}^q)_{\text{SM}} + (M_{12}^q)_{\text{KK}}\right| \qquad (q = d, s) . \tag{4.33}$$

Let us then write [135]

$$M_{12}^q = (M_{12}^q)_{\text{SM}} + (M_{12}^q)_{\text{KK}} = (M_{12}^q)_{\text{SM}}\, C_{B_q} e^{2i\varphi_{B_q}} \tag{4.34}$$

where

$$\begin{aligned} \left(M_{12}^d\right)_{\text{SM}} &= \left|\left(M_{12}^d\right)_{\text{SM}}\right| e^{2i\beta} , \qquad \beta \approx 22^\circ , \\ (M_{12}^s)_{\text{SM}} &= |(M_{12}^s)_{\text{SM}}|\, e^{2i\beta_s} , \qquad \beta_s \simeq -1^\circ , \end{aligned} \tag{4.35}$$

with the phases β and β_s are defined through

$$V_{td} = |V_{td}|e^{-i\beta} \quad \text{and} \quad V_{ts} = -|V_{ts}|e^{-i\beta_s} . \tag{4.36}$$

We find then

$$\Delta M_q = (\Delta M_q)_{\rm SM} C_{B_q} \tag{4.37}$$

and[2]

$$\begin{aligned} S_{\psi K_S} &= \sin(2\beta + 2\varphi_{B_d})\,, \\ S_{\psi\phi} &= \sin(2|\beta_s| - 2\varphi_{B_s})\,, \end{aligned} \tag{4.38}$$

with the latter two observables being the coefficients of $\sin(\Delta M_d t)$ and $\sin(\Delta M_s t)$ in the time dependent CP asymmetries in the $B_d^0 \to \psi K_S$ and $B_s^0 \to \psi\phi$ decays. Thus in the presence of non-vanishing NP phases φ_{B_d} and φ_{B_s} these two asymmetries do not measure β and β_s but $(\beta + \varphi_{B_d})$ and $(|\beta_s| - \varphi_{B_s})$.
Finally, we give the expressions for the width differences $\Delta\Gamma_q$ and the semileptonic CP-asymmetries $A_{\rm SL}^q$,

$$\frac{\Delta\Gamma_q}{\Gamma_q} = -\left(\frac{\Delta M_q}{\Gamma_q}\right)^{\rm exp} \left[{\rm Re}\left(\frac{\Gamma_{12}^q}{M_{12}^q}\right)^{\rm SM} \frac{\cos 2\varphi_{B_q}}{C_{B_q}} - {\rm Im}\left(\frac{\Gamma_{12}^q}{M_{12}^q}\right)^{\rm SM} \frac{\sin 2\varphi_{B_q}}{C_{B_q}}\right], \tag{4.39}$$

$$A_{\rm SL}^q = {\rm Im}\left(\frac{\Gamma_{12}^q}{M_{12}^q}\right)^{\rm SM} \frac{\cos 2\varphi_{B_q}}{C_{B_q}} - {\rm Re}\left(\frac{\Gamma_{12}^q}{M_{12}^q}\right)^{\rm SM} \frac{\sin 2\varphi_{B_q}}{C_{B_q}}\,. \tag{4.40}$$

Theoretical predictions of both $\Delta\Gamma_q$ and $A_{\rm SL}^q$ require the non-perturbative calculation of the off-diagonal matrix element Γ_{12}^q, the absorptive part of the $B_q^0 - \bar{B}_q^0$ amplitude. For further details the reader is referred to section 3.8 of [120] and we here just give [136]

$${\rm Re}\left(\frac{\Gamma_{12}^d}{M_{12}^d}\right)^{\rm SM} = -(3.0 \pm 1.0)\cdot 10^{-3}\,, \qquad {\rm Re}\left(\frac{\Gamma_{12}^s}{M_{12}^s}\right)^{\rm SM} = -(2.6 \pm 1.0)\cdot 10^{-3}\,, \tag{4.41}$$

$${\rm Im}\left(\frac{\Gamma_{12}^d}{M_{12}^d}\right)^{\rm SM} = -(6.4 \pm 1.4)\cdot 10^{-4}\,, \qquad {\rm Im}\left(\frac{\Gamma_{12}^s}{M_{12}^s}\right)^{\rm SM} = (2.6 \pm 0.5)\cdot 10^{-5}\,. \tag{4.42}$$

Finally, we notice that ${\rm Re}\left(\frac{\Gamma_{12}^s}{M_{12}^s}\right)^{\rm SM} \gg {\rm Im}\left(\frac{\Gamma_{12}^s}{M_{12}^s}\right)^{\rm SM}$ and that hence for SM-like ΔM_s a correlation between $A_{\rm SL}^s$ and $S_{\psi\phi}$ exists. This correlation has been pointed out in [137] and has been investigated model-independently in [138] and in the context of the LHT and SM4 models in [120] and [139]. We will see in chapter 5 that such a correlation also exists in the RSc.

[2]These simple formulae follow only if there are no additional weak phases in the decay amplitudes for $B_d^0 \to \psi K_S$ and $B_s^0 \to \psi\phi$. In the RSc there are tree level charged current contributions with non-vanishing weak phases; however, these are suppressed by $M_W^2/M_{\rm KK}^2$ with respect to the SM and therefore can be neglected.

4.2 Rare K and B Decays

4.2.1 The $K \to \pi\nu\bar{\nu}$ System

We will start our discussion of exclusive rare decays with the famous $K \to \pi\nu\bar{\nu}$ system. Both the charged and the neutral mode are theoretically very clean, but also extremely difficult to measure due to the neutrinos in the final state. While $Br(K^+ \to \pi^+\nu\bar{\nu})$ has been observed at the E949 experiment in Brookhaven [140],

$$Br(K^+ \to \pi^+\nu\bar{\nu})_{\text{exp}} = (17.3^{+11.5}_{-10.5}) \cdot 10^{-11}\,, \tag{4.43}$$

which is to be compared to the most recent SM prediction [141]

$$Br(K^+ \to \pi^+\nu\bar{\nu})_{\text{SM}} = (8.5 \pm 0.7) \cdot 10^{-11}\,, \tag{4.44}$$

the $K_L \to \pi^0\nu\bar{\nu}$ decay still awaits discovery. Here the experimental upper bound [142]

$$Br(K_L \to \pi^0\nu\bar{\nu}) \leq 6.7 \cdot 10^{-8} \tag{4.45}$$

exceeds the SM prediction [143]

$$Br(K_L \to \pi^0\nu\bar{\nu})_{\text{SM}} = (2.8 \pm 0.6) \cdot 10^{-11} \tag{4.46}$$

by more than three orders of magnitude. A more stringent model-independent theoretical bound on $Br(K_L \to \pi^0\nu\bar{\nu})$ can be deduced from the Grossman-Nir (GN) bound [144],

$$Br(K_L \to \pi^0\nu\bar{\nu}) \leq 4.3 Br(K^+ \to \pi^+\nu\bar{\nu})\,, \tag{4.47}$$

in connection with the measurement of $Br(K^+ \to \pi^+\nu\bar{\nu})$. The experimental situation described above will improve significantly within the next decade when the NA62 experiment at CERN ($K^+ \to \pi^+\nu\bar{\nu}$) and the E14 experiment at KEK ($K_L \to \pi^0\nu\bar{\nu}$) will start their operation.

Apart from favorable experimental prospects, the great importance of the $K \to \pi\nu\bar{\nu}$ system is added to by its discriminating power between different models of NP. For instance, it has been shown in [145] that in models in which NP enters dominantly through left-handed couplings and the NP phase in ϵ_K and the $K \to \pi\nu\bar{\nu}$ system is universal, points in the $(Br(K^+ \to \pi^+\nu\bar{\nu}), Br(K_L \to \pi^0\nu\bar{\nu}))$ plane are forced to lie on two distinct branches. This behavior for instance has been observed in the LHT [111] and the SM4 [139]. In this sense a precise measurement of both modes in the $K \to \pi\nu\bar{\nu}$ system could shed light on elementary properties of physics beyond the SM and help to distinguish between different models of NP. We will return to this issue in chapter 5.

The effective Hamiltonian for $s \to d\nu\bar{\nu}$ transitions in the SM is given as

$$[\mathcal{H}^{\nu\bar{\nu}}_{\text{eff}}]^K_{\text{SM}} = g^2_{\text{SM}} \sum_{\ell=e,\mu,\tau} \left[\lambda_c^{(K)} X^{\ell}_{\text{NNL}}(x_c) + \lambda_t^{(K)} X(x_t)\right] (\bar{s}d)_{V-A} (\bar{\nu}_\ell \nu_\ell)_{V-A} + h.c.\,, \tag{4.48}$$

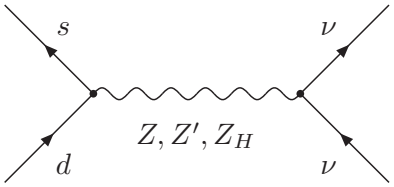

Figure 4.2: Tree level contributions of Z, Z' and Z_H to the $s \to d\nu\bar{\nu}$ effective Hamiltonian.

where $x_i = m_i^2/M_W^2$ and $\lambda_i^{(K)} = V_{is}^* V_{id}$. The functions $X_{\rm NNL}^{\ell}(x_c)$, $X(x_t)$ comprise internal charm and top quark contributions and are known to high accuracy including QCD corrections [141, 146, 147]. For convenience we have introduced the notation for the effective SM coupling

$$g_{\rm SM}^2 = \frac{G_F}{\sqrt{2}} \frac{\alpha}{2\pi \sin^2\theta_W} \,. \tag{4.49}$$

As we have seen in section 3.4, in the RSc the Z boson and the additional heavy neutral gauge bosons Z_H and Z' have flavor violating couplings. Accordingly the effective Hamiltonian receives contributions from the tree level exchange of these particles. The diagrams corresponding to the Z contribution are shown in fig. 4.2, and a straightforward calculation of these diagrams yields the new contribution to $[\mathcal{H}_{\rm eff}^{\nu\bar{\nu}}]^K$,

$$[\mathcal{H}_{\rm eff}^{\nu\bar{\nu}}]_Z^K = \frac{\Delta_L^{\nu\nu}(Z)}{M_Z^2} \left[\Delta_L^{sd}(Z)(\bar{s}_L\gamma^\mu d_L) + \Delta_R^{sd}(Z)(\bar{s}_R\gamma^\mu d_R)\right](\bar{\nu}_L\gamma_\mu\nu_L) + h.c.\,. \tag{4.50}$$

The contributions of Z' and Z_H to $[\mathcal{H}_{\rm eff}^{\nu\bar{\nu}}]^K$ can be obtained from (4.50) by replacing Z by Z' and Z_H. Explicit expressions for the quark couplings $\Delta_{L,R}^{sd}(Z)$, $\Delta_{L,R}^{sd}(Z')$ and $\Delta_{L,R}^{sd}(Z_H)$ can be obtained from (3.39), while the flavor universal neutrino couplings $\Delta_L^{\nu\nu}(Z)$, $\Delta_L^{\nu\nu}(Z')$ and $\Delta_L^{\nu\nu}(Z_H)$ are given in appendix A.
Combining the contributions of Z, Z' and Z_H in (4.50) with the SM contribution in (4.48),

$$[\mathcal{H}_{\rm eff}^{\nu\bar{\nu}}]^K = [\mathcal{H}_{\rm eff}^{\nu\bar{\nu}}]_{\rm SM}^K + [\mathcal{H}_{\rm eff}^{\nu\bar{\nu}}]_Z^K + [\mathcal{H}_{\rm eff}^{\nu\bar{\nu}}]_{Z'}^K + [\mathcal{H}_{\rm eff}^{\nu\bar{\nu}}]_{Z_H}^K \,, \tag{4.51}$$

we find the total effective Hamiltonian for $s \to d\nu\bar{\nu}$ transitions,

$$\begin{aligned}[\mathcal{H}_{\rm eff}^{\nu\bar{\nu}}]^K = {} & g_{\rm SM}^2 \sum_{\ell=e,\mu,\tau} \left[\lambda_c^{(K)} X_{\rm NNL}^{\ell}(x_c) + \lambda_t^{(K)} X_K^{V-A}\right](\bar{s}d)_{V-A}(\bar{\nu}_\ell\nu_\ell)_{V-A} \\ & + g_{\rm SM}^2 \sum_{\ell=e,\mu,\tau} \left[\lambda_t^{(K)} X_K^{V}\right](\bar{s}d)_{V}(\bar{\nu}_\ell\nu_\ell)_{V-A} + h.c.\,. \end{aligned} \tag{4.52}$$

In this we have introduced the generalized loop functions X_K^{V-A} and X_K^V,

$$X_K^{V-A} = X(x_t) + \sum_{i=Z,Z',Z_H} (X_i^K)^{V-A} \,, \qquad X_K^V = \sum_{i=Z,Z',Z_H} (X_i^K)^V \,, \tag{4.53}$$

which will turn out to be useful later on. The individual contributions to these are given by

$$(X_i^K)^{V-A} = \frac{1}{\lambda_t^{(K)}} \frac{\Delta_L^{\nu\nu}(i)}{4M_i^2 g_{\rm SM}^2} \left[\Delta_L^{sd}(i) - \Delta_R^{sd}(i)\right] , \tag{4.54}$$

$$(X_i^K)^{V} = \frac{1}{\lambda_t^{(K)}} \frac{\Delta_L^{\nu\nu}(i)}{2M_i^2 g_{\rm SM}^2} \Delta_R^{sd}(i) , \tag{4.55}$$

where $i = Z,\, Z_H,\, Z'$.
Having at hand the effective Hamiltonian for $s \to d\nu\bar{\nu}$ transitions it is straightforward to obtain explicit expressions for the branching ratios $Br(K^+ \to \pi^+\nu\bar{\nu})$ and $Br(K_L \to \pi^0\nu\bar{\nu})$. Due to the tree level exchanges of EW gauge bosons in the RSc the operator $(\bar{s}d)_V(\bar{\nu}\nu)_{V-A}$ is present in addition to the usual SM operator $(\bar{s}d)_{V-A}(\bar{\nu}\nu)_{V-A}$. Therefore both matrix elements $\langle\pi^+|(\bar{s}d)_{V-A}|K^+\rangle$ and $\langle\pi^+|(\bar{s}d)_V|K^+\rangle$ have to be evaluated. Fortunately, as both K^+ and π^+ are pseudoscalar mesons, only the vector current part contributes and we simply have

$$\left\langle\pi^+|(\bar{s}d)_{V-A}|K^+\right\rangle = \left\langle\pi^+|(\bar{s}d)_V|K^+\right\rangle . \tag{4.56}$$

This means that the effects of NP contributions can be effectively collected in a single function that generalizes the SM loop function $X(x_t)$. Denoting this function by

$$X_K \equiv X_K^{V-A} + X_K^V \equiv |X_K| e^{i\,\theta_X^K} , \tag{4.57}$$

we can make use of the formulae of section 3.3 in [111]. In particular we have

$$\begin{aligned} Br(K^+ \to \pi^+\nu\bar{\nu}) &= \kappa_+ \left[\tilde{r}^2 A^4 \left|X_K\right|^2 + 2\tilde{r}\bar{P}_c(X) A^2 R_t \left|X_K\right| \cos\beta_X^K + \bar{P}_c(X)^2\right] , \\ Br(K_L \to \pi^0\nu\bar{\nu}) &= \kappa_L \left[\frac{V_{ts}V_{td}}{\lambda^5}\right]^2 (\sin\beta_X^K)^2 |X_K|^2 , \end{aligned} \tag{4.58}$$

with [141, 143, 147–149]

$$\begin{aligned} \kappa_+ &= (5.36 \pm 0.026) \cdot 10^{-11} , \qquad \kappa_L = (2.31 \pm 0.01) \cdot 10^{-10} , \\ \tilde{r} &= \left|\frac{V_{ts}}{V_{cb}}\right| \simeq 0.98 , \quad A = 0.822(16) , \quad R_t = \frac{1}{\lambda}\left|\frac{V_{td}}{V_{cb}}\right| = 0.97 , \\ \bar{P}_c(X) &= \left(1 - \frac{\lambda^2}{2}\right) P_c(x) , \quad P_c(X) = 0.42 \pm 0.05 , \end{aligned} \tag{4.59}$$

where $P_c(X)$ is calculated in the SM and includes next-to-next-to-leading order (NNLO) QCD corrections [141], electroweak corrections [143] and long distance contributions [149]. The angle β_X^K finally is defined as

$$\beta_X^K = \beta - \beta_s - \theta_X^K , \tag{4.60}$$

with β and β_s introduced in (4.36).
Note that, in contrast to the real function $X(x_t)$, the new function X_K is complex which implies new CP-violating effects that can be best tested in the very clean decay $K_L \to \pi^0\nu\bar{\nu}$.

4.2.2 Inclusive Decays $B \to X_d \nu\bar{\nu}$ and $B \to X_s \nu\bar{\nu}$

B decays with neutrinos in the final state provide a very good probe of modified Z penguin contributions [150,151]. Unfortunately, their measurement appears to be even more challenging than that of the rare K decays discussed in section 4.2.1 (for a summary of experimental prospects at future Super-B machines see however [152]). Recent analyses of these decays within the SM and several NP scenarios can be found in [153, 154].
From the analysis of rare B decays in [34] we know that the effects in the two exclusive modes $B \to K\nu\bar{\nu}$ and $B \to K^*\nu\bar{\nu}$ are small, and we will therefore in the following concentrate on the theoretically clean decays $B \to X_{s,d}\nu\bar{\nu}$.
The result for $s \to d\nu\bar{\nu}$ transitions obtained in the previous section can be generalized to the case of $b \to d\nu\bar{\nu}$ and $b \to s\nu\bar{\nu}$ transitions by properly adjusting the flavor indices and neglecting the internal charm contributions. The effective Hamiltonian for $b \to q\nu\bar{\nu}$ ($q = d, s$) is then found as

$$\begin{aligned}[\mathcal{H}_{\rm eff}^{\nu\bar{\nu}}]^{B_q} = g_{\rm SM}^2 \sum_{\ell=e,\mu,\tau} \left[\lambda_t^{(q)} X_q^{V-A}\right](\bar{b}q)_{V-A}(\bar{\nu}_\ell\nu_\ell)_{V-A} \\ + g_{\rm SM}^2 \sum_{\ell=e,\mu,\tau} \left[\lambda_t^{(q)} X_q^{V}\right](\bar{b}q)_{V}(\bar{\nu}_\ell\nu_\ell)_{V-A} + h.c.\,, \end{aligned} \tag{4.61}$$

with

$$X_q^{V-A} = X(x_t) + \sum_{i=Z,Z',Z_H} (X_i^q)^{V-A}\,, \qquad X_q^V = \sum_{i=Z,Z',Z_H} (X_i^q)^V\,. \tag{4.62}$$

The individual contributions to this are given by

$$(X_i^q)^{V-A} = \frac{1}{\lambda_t^{(q)}} \frac{\Delta_L^{\nu\nu}(i)}{4M_i^2 g_{\rm SM}^2} \left[\Delta_L^{bq}(i) - \Delta_R^{bq}(i)\right]\,, \tag{4.63}$$

$$(X_i^q)^{V} = \frac{1}{\lambda_t^{(q)}} \frac{\Delta_L^{\nu\nu}(i)}{2M_i^2 g_{\rm SM}^2} \Delta_R^{bq}(i)\,, \tag{4.64}$$

where $i = Z$, Z_H, Z' and again all relevant $\Delta_{L,R}^{bq}$ entries can be obtained from (3.39).
From this effective Hamiltonian we can now derive expressions for the branching ratios $Br(B \to X_{d,s}\nu\bar{\nu})$. Generalizing the corresponding formulae in [111] to also incorporate right-handed currents, we find

$$\frac{Br(B \to X_s\nu\bar{\nu})}{Br(B \to X_s\nu\bar{\nu})_{\rm SM}} = \frac{\left|X_s^{V-A} + \frac{X_s^V}{2}\right|^2 + \left|\frac{X_s^V}{2}\right|^2}{X(x_t)^2}\,. \tag{4.65}$$

We started our derivation of these branching ratios from the effective Hamiltonian for $s \to d\nu\bar{\nu}$ transitions. In fact, in the SM and models with Constrained Minimal Flavor Violation (CMFV) [105, 106, 138], in which all flavor violation is governed by the CKM matrix and only SM operators are relevant[3] we find the decay modes $K \to \pi\nu\bar{\nu}$ and

[3] See [7, 103, 104] for a more general definition of MFV, in which new operators are allowed.

$B \to X_{d,s}\nu\bar{\nu}$ to depend on a single real function X, which implies a strong correlation between these modes. In contrast to this in the RSc the generalized functions X_i ($i = K, d, s$) are flavor non-universal and complex and accordingly we expect the universality in NP effects in the mentioned decay modes to be strongly violated. We will investigate this breakdown of universality in chapter 5 in more detail.

4.2.3 $K_L \to \pi^0 \ell^+ \ell^-$

Until now we have been discussing decay processes with neutrinos in the final state. We will now extend our discussion to decays into systems containing also charged leptons. We start with the rare decays $K_L \to \pi^0 e^+ e^-$ and $K_L \to \pi^0 \mu^+ \mu^-$ which are dominated by CP-violating contributions. In the SM the main contribution comes from the mixing induced CP violation and its interference with the direct CP violating contribution [155–158]. The direct CP violating contribution to the branching ratio is $\sim 4 \cdot 10^{-12}$, while the CP conserving contribution is at most $3 \cdot 10^{-12}$. Among the rare K meson decays the decays in question belong to the theoretically cleanest, although second to the $K \to \pi\nu\bar{\nu}$ decays. Furthermore, the $K_L \to \pi^0 \ell^+ \ell^-$ modes are not as sensitive to NP contributions as $K_L \to \pi^0 \nu\bar{\nu}$, as the dominant CP violating contributions are practically determined by the measurement of the parameter ϵ_K and the $K_S \to \pi^0 \ell^+ \ell^-$ decay branching ratios and NP can only affect the subleading direct CP violating contribution. As was however pointed out in [159], in the presence of large new CP violating phases the direct CP violating contribution can become the dominant contribution and the branching ratios for $K_L \to \pi^0 \ell^+ \ell^-$ can be significantly enhanced.

In the SM, neglecting QCD corrections, the top quark contribution to the effective Hamiltonian for $s \to d\ell^+\ell^-$ reads

$$\begin{aligned}\left[\mathcal{H}_{\text{eff}}^{\ell\bar{\ell}}\right]_{\text{SM}}^{K} = &-g_{\text{SM}}^2 \left[\lambda_t^{(K)} Y(x_t)\right] (\bar{s}d)_{V-A} (\bar{\ell}\ell)_{V-A} \\ &+4 g_{\text{SM}}^2 \sin^2\theta_W \left[\lambda_t^{(K)} Z(x_t)\right] (\bar{s}d)_{V-A} (\bar{\ell}\ell)_{V} + h.c.\,. \end{aligned} \tag{4.66}$$

Here $Y(x_t)$ and $Z(x_t)$ are one-loop functions, analogous to $X(x_t)$, which result from penguin and box diagrams. The charm contributions and QCD corrections are irrelevant for the discussion presented here but will be included in our numerical analysis. We also remark that in principle also dipole operators could be included here, but that in K decays, as discussed in [160], they can be fully neglected.

Also in this case, $[\mathcal{H}_{\text{eff}}^{\ell\bar{\ell}}]^K$ receives tree level contributions of the gauge bosons Z, Z' and Z_H, and as now charged leptons appear in the final state, also the KK photon $A^{(1)}$ contributes. The quark couplings on the left hand side of the diagram shown in fig. 4.3 are the same as those already encountered in the case of the $s \to d\nu\bar{\nu}$ transition. The couplings on the right hand side, which involve charged leptons are parameterized by the matrices $\Delta_{L,R}^{\ell\ell}(Z)$ listed in appendix A. Evaluating the Z exchange in fig. 4.3 results

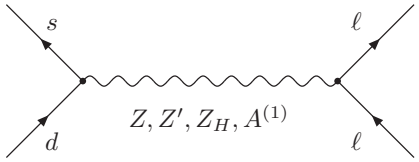

Figure 4.3: Tree level contributions of Z, Z', Z_H and $A^{(1)}$ to the $s \to d\ell^+\ell^-$ effective Hamiltonian.

in

$$\left[\mathcal{H}_{\text{eff}}^{\ell\bar{\ell}}\right]_Z^K = \frac{1}{M_Z^2}\left[\Delta_L^{bs}(Z)(\bar{s}_L\gamma^\mu d_L) + \Delta_R^{bs}(Z)(\bar{s}_R\gamma^\mu d_R)\right] \times \left[\Delta_L^{\ell\ell}(Z)(\bar{\ell}_L\gamma_\mu\ell_L) + \Delta_R^{\ell\ell}(Z)(\bar{\ell}_R\gamma_\mu\ell_R)\right] + h.c.\,, \tag{4.67}$$

which contains additional operators relative to (4.66). The exchange of Z', Z_H and $A^{(1)}$ gauge bosons yields analogous contributions which can simply be obtained from (4.67) by consecutively replacing Z by Z', Z_H and $A^{(1)}$.
Following along the lines of discussion in section 4.2.1, we find that the effective Hamiltonian governing $s \to d\ell^+\ell^-$ transitions can be written in the compact form

$$\begin{aligned}\left[\mathcal{H}_{\text{eff}}^{\ell\bar{\ell}}\right]^K = &-g_{\text{SM}}^2\left[\lambda_t^{(K)}Y_K^{V-A}\right](\bar{s}d)_{V-A}(\bar{\ell}\ell)_{V-A}\\ &+4g_{\text{SM}}^2\sin^2\theta_W\left[\lambda_t^{(K)}Z_K^{V-A}\right](\bar{s}d)_{V-A}(\bar{\ell}\ell)_V\\ &-g_{\text{SM}}^2\left[\lambda_t^{(K)}Y_K^{V}\right](\bar{s}d)_{V}(\bar{\ell}\ell)_{V-A}\\ &+4g_{\text{SM}}^2\sin^2\theta_W\left[\lambda_t^{(K)}Z_K^{V}\right](\bar{s}d)_{V}(\bar{\ell}\ell)_V + h.c.\,,\end{aligned} \tag{4.68}$$

where we have introduced the functions $Y_K^{V-A,V}$ and $Z_K^{V-A,V}$ defined as

$$\begin{aligned}Y_K^{V-A} &= Y(x_t) + \sum_{i=Z,Z',Z_H,A^{(1)}}(Y_i^K)^{V-A}\,, \qquad Y_K^V = \sum_{i=Z,Z',Z_H,A^{(1)}}(Y_i^K)^V\,,\\ Z_K^{V-A} &= Z(x_t) + \sum_{i=Z,Z',Z_H,A^{(1)}}(Z_i^K)^{V-A}\,, \qquad Z_K^V = \sum_{i=Z,Z',Z_H,A^{(1)}}(Z_i^K)^V\,.\end{aligned} \tag{4.69}$$

The individual gauge bosons' contributions entering (4.69) are given by

$$\begin{aligned}(Y_i^K)^{V-A} &= -\frac{1}{\lambda_t^{(K)}}\frac{\left[\Delta_L^{\ell\ell}(i) - \Delta_R^{\ell\ell}(i)\right]}{4M_i^2 g_{\text{SM}}^2}\left[\Delta_L^{sd}(i) - \Delta_R^{sd}(i)\right]\,,\\ (Z_i^K)^{V-A} &= \frac{1}{\lambda_t^{(K)}}\frac{\Delta_R^{\ell\ell}(i)}{8M_i^2 g_{\text{SM}}^2\sin^2\theta_W}\left[\Delta_L^{sd}(i) - \Delta_R^{sd}(i)\right]\,,\end{aligned}$$

$$(Y_i^K)^V = -\frac{1}{\lambda_t^{(K)}}\frac{\left[\Delta_L^{\ell\ell}(i) - \Delta_R^{\ell\ell}(i)\right]}{2M_i^2 g_{\rm SM}^2}\Delta_R^{sd}(i)\,,$$
$$(Z_i^K)^V = \frac{1}{\lambda_t^{(K)}}\frac{\Delta_R^{\ell\ell}(i)}{4M_i^2 g_{\rm SM}^2 \sin^2\theta_W}\Delta_R^{sd}(i)\,, \tag{4.70}$$

where $i = Z,\, Z_H,\, Z',\, A^{(1)}$.
The effective Hamiltonian (4.68) now allows to conveniently derive the branching ratios for the $K_L \to \pi^0\ell^+\ell^-$ decay modes. As in the case of the $K \to \pi\nu\bar{\nu}$ system only the vector current part of Y_K^{V-A}, Z_K^{V-A} contributes to the final branching ratios and we can therefore define the functions

$$Y_K = Y_K^{V-A} + Y_K^V = |Y_K|\, e^{i\theta_Y^K}\,,$$
$$Z_K = Z_K^{V-A} + Z_K^V = |Z_K|\, e^{i\theta_Z^K}\,, \tag{4.71}$$

which are sufficient to jointly describe the SM and RSc contributions. Using [159] we can adapt the formulae in [156–158, 161] to the RSc and find

$$Br(K_L \to \pi^0\ell^+\ell^-) = \left(C_{\rm dir}^\ell \pm C_{\rm int}^\ell\,|a_s| + C_{\rm mix}^\ell\,|a_s|^2 + C_{\rm CPC}^\ell\right)\cdot 10^{-12}\,, \tag{4.72}$$

where

$$\begin{aligned}
C_{\rm dir}^e &= (4.62 \pm 0.24)(\omega_{7V}^2 + \omega_{7A}^2)\,, & C_{\rm dir}^\mu &= (1.09 \pm 0.05)(\omega_{7V}^2 + 2.32\omega_{7A}^2)\,,\\
C_{\rm int}^e &= (11.3 \pm 0.3)\omega_{7V}\,, & C_{\rm int}^\mu &= (2.63 \pm 0.06)\omega_{7V}\,,\\
C_{\rm mix}^e &= 14.5 \pm 0.05\,, & C_{\rm mix}^\mu &= 3.36 \pm 0.20\,,\\
C_{\rm CPC}^e &\simeq 0\,, & C_{\rm CPC}^\mu &= 5.2 \pm 1.6\,,\\
& & |a_s| &= 1.2 \pm 0.2\,,
\end{aligned} \tag{4.73}$$

with

$$\omega_{7V} = \frac{1}{2\pi}\left[P_0 + \frac{|Y_K|}{\sin^2\theta_W}\frac{\sin\beta_Y^K}{\sin(\bar{\beta}-\bar{\beta}_s)} - 4|Z_K|\frac{\sin\beta_Z^K}{\sin(\bar{\beta}-\bar{\beta}_s)}\right]\left[\frac{{\rm Im}\,\lambda_t^{(K)}}{1.4\cdot 10^{-4}}\right]\,,$$
$$\omega_{7A} = -\frac{1}{2\pi}\frac{|Y_K|}{\sin^2\theta_W}\frac{\sin\beta_Y^K}{\sin(\bar{\beta}-\bar{\beta}_s)}\left[\frac{{\rm Im}\,\lambda_t^{(K)}}{1.4\cdot 10^{-4}}\right]\,. \tag{4.74}$$

Here $P_0 = 2.88 \pm 0.06$ [160] includes NLO QCD corrections and

$$\beta_Y^K = \bar{\beta} - \bar{\beta}_s - \theta_Y^K\,, \qquad \beta_Z^K = \bar{\beta} - \bar{\beta}_s - \theta_Z^K\,, \tag{4.75}$$

with $\theta_{Y,Z}^K$ defined in (4.71). The effect of the NP contributions is mainly observable in ω_{7A}, as the corresponding contributions to ω_{7V} cancel to a large extend.

The present experimental bounds [162, 163],

$$Br(K_L \to \pi^0 e^+ e^-) < 28 \cdot 10^{-11}\,, \qquad Br(K_L \to \pi^0 \mu^+ \mu^-) < 38 \cdot 10^{-11}\,, \tag{4.76}$$

are still by one order of magnitude larger than the SM predictions [161],

$$\begin{aligned} Br(K_L \to \pi^0 e^+ e^-)_{\rm SM} &= 3.54^{+0.98}_{-0.85}\left(1.56^{+0.62}_{-0.49}\right) \cdot 10^{-11}\,, \\ Br(K_L \to \pi^0 \mu^+ \mu^-)_{\rm SM} &= 1.41^{+0.28}_{-0.26}\left(0.95^{+0.22}_{-0.21}\right) \cdot 10^{-11}\,, \end{aligned} \tag{4.77}$$

with the values in parentheses corresponding to the "−" sign in (4.72), that is to destructive interference between contributions of direct and indirect CP violation. A recent discussion of the current theoretical status of this interference sign can be found in [164] where the results of [157,158,165] are critically analyzed. From this discussion, constructive interference seems to be favored although as yet no final assessment of this issue is possible.

4.2.4 The Short Distance Contribution to $K_L \to \mu^+\mu^-$

The short distance (SD) contribution to $Br(K_L \to \mu^+\mu^-)$ is governed by the same effective Hamiltonian that is also responsible for the $K_L \to \pi^0\ell^+\ell^-$ decays. Despite this analogy, in contrast to the decays discussed until now the SD contribution calculated here is only a part of a dispersive contribution to $K_L \to \mu^+\mu^-$ which is by far dominated by the absorptive contribution with two internal photon exchanges. Consequently the SD contribution constitutes only a small fraction of the branching ratio. Moreover, because of long distance (LD) contributions to the dispersive part of $K_L \to \mu^+\mu^-$, the extraction of the SD part from the data is subject to considerable uncertainties. The most recent (conservative) estimate gives [166]

$$Br(K_L \to \mu^+\mu^-)_{\rm SD} \le 2.5 \cdot 10^{-9}\,, \tag{4.78}$$

to be compared with the SM prediction $(0.8 \pm 0.1) \cdot 10^{-9}$ [167].
When evaluating the SD contribution to $Br(K_L \to \mu^+\mu^-)$ two simplifications occur with respect to the $K_L \to \pi^0\ell^+\ell^-$ modes. Since K_L is a pseudoscalar, we have

$$\langle 0|(\bar{s}d)_V|K_L\rangle = 0\,, \tag{4.79}$$

so that only the axial part of the quark vertex contributes. Due to the conserved vector current then also the vector component of the $\bar{\mu}\mu$-vertex drops out and as in the SM only the axial part is relevant. In consequence only the $(V-A)\otimes(V-A)$ operator contributes and following [159] we thus obtain for the RSc

$$Br(K_L \to \mu^+\mu^-)_{\rm SD} = 2.08 \cdot 10^{-9}\left[\bar{P}_c\,(Y_K) + A^2 R_t \left|Y_K^{V-A}\right| \cos\bar{\beta}_Y^K\right]^2\,, \tag{4.80}$$

where we have defined

$$\bar{\beta}_Y^K \equiv \beta - \beta_s - \bar{\theta}_Y^K\,, \tag{4.81}$$

and

$$\bar{P}_c\,(Y_K) \equiv \left(1 - \frac{\lambda^2}{2}\right) P_c\,(Y_K)\,, \tag{4.82}$$

with $P_c\,(Y_K) = 0.113 \pm 0.017$ [167].

4.2.5 $B_{d,s} \to \mu^+\mu^-$

Of particular interest are the branching ratios of the decay modes $B_{d,s} \to \mu^+\mu^-$, of which at least the $B_s \to \mu^+\mu^-$ decay is hoped to be measured in the coming years. Up to today there are only experimental upper bounds on these two modes by the CDF [168] and DØ [169] (in parentheses) experiments,

$$Br(B_s \to \mu^+\mu^-) \leq 5.8\ (12) \cdot 10^{-8}\,, \quad Br(B_d \to \mu^+\mu^-) \leq 1.8 \cdot 10^{-8}\,, \tag{4.83}$$

which are still larger than the respective SM predictions [139, 170]

$$Br(B_s \to \mu^+\mu^-)_{\rm SM} = (3.2\pm0.2)\cdot10^{-9}\,, \quad Br(B_d \to \mu^+\mu^-)_{\rm SM} = (1.1\pm0.1)\cdot10^{-10}\,, \tag{4.84}$$

by one order (two orders) of magnitude for $B_s \to \mu^+\mu^-$ ($B_d \to \mu^+\mu^-$).
As in the SM and in models of CMFV, both these modes experience a strong chiral suppression in the RSc. This suppression cannot be removed through the exchanges of the gauge bosons that are present in the RSc, but in principle could be removed through tree level exchanges of the Higgs boson. However, the flavor changing quark-Higgs couplings in the RSc are found to be small [33, 36, 116] and beyond that Higgs contributions to $B_{d,s} \to \mu^+\mu^-$ are suppressed by the tiny $H\bar{\mu}\mu$ vertex. Consequently we can restrict our attention to the contributions of the SM Z boson and the heavy KK gauge bosons Z_H, Z' and $A^{(1)}$.
The $B_{d,s} \to \mu^+\mu^-$ decays are governed by the effective Hamiltonian for $b \to s\ell^+\ell^-$ transitions which can be obtained from (4.67)–(4.70) by properly adjusting the flavor indices and neglecting the charm contribution. We note that in this case also the operators $\mathcal{Q}_{7\gamma}$ and $\mathcal{O}_{8G}$ which are responsible for the $b \to s\gamma$ decay would enter the effective Hamiltonian. These operators arise at the loop level and their calculation in the RSc is beyond the scope of the present work. Fortunately, following the line of argument in section 4.2.4 we find that also here only the $(V-A)\otimes(V-A)$ operator contributes to the branching ratio and we find ($q = d, s$)

$$\frac{Br(B_q \to \mu^+\mu^-)}{Br(B_q \to \mu^+\mu^-)_{\rm SM}} = \frac{|Y_q^{V-A}|^2}{Y(x_t)^2}\,. \tag{4.85}$$

This concludes our analysis of flavor observables in the down quark sector, which is the foundation for our numerical analysis in the following chapter.

Chapter 5

Global Numerical Analysis

Having carefully calculated the flavor dependent corrections to the gauge and Higgs couplings and the resulting modifications of flavor observables, we are now in the situation to perform a global analysis of particle-antiparticle oscillations and rare decays in the K and B meson systems. The main focus and aims of our analysis will be presented in section 5.1 where also the numerical procedure is described in a manner as to keep our approach fully traceable. Section 5.2 is devoted to a study of NP effects in particle-antiparticle oscillations in the K and B meson systems, and rare K and B decays will be discussed in section 5.3. We will conclude our global analysis by a comparison of the results found in the RSc to two other models of NP, the LHT and SM4 models, in section 5.4.

5.1 Preliminaries

In the following numerical analysis we will not so much try to include the numerous sub-leading flavor effects that are present in the RSc, but rather perform a theoretically sound and complete calculation taking into account the main flavor violating effects and give a survey of the main phenomenological features of the model. The most pressing issues in the author's view that concern flavor observables and that have to be clarified are listed in the following.

We have seen that there are various contributions to $\Delta F = 2$ observables. The natural question in this context then is which of these contributions is the dominant one, and which implications about the pattern of flavor violation result from its dominance. Furthermore, is it possible to reproduce all $\Delta F = 2$ observables, and in particular ϵ_K, in the presence of comparably light KK modes without having to rely on strong accidental cancellations among different parameters? If so, how much potential for large effects in CP violating observables in the B_s system is left?

In our subsequent analysis of $\Delta F = 1$ observables we will again have to investigate which of the particles that can be exchanged at tree level yields the dominant contribution and which pattern of flavor violation results from this fact. Since in this context

we are talking mainly about EW gauge bosons[1], the question naturally arises whether this pattern is model-independent or relies on the presence of the custodial symmetry. After we have addressed these rather technical issues we will work out by how much the various decay rates of K and B mesons can deviate from their SM values and whether there are—preferably parameter independent—correlations between different rare decay rates. In conjunction with this issue it is also interesting to investigate whether significant enhancements beyond the SM in different observables are possible *simultaneously*. In particular the answers to the latter two questions will yield important input to the comparison of the RSc to the LHT and SM4 models.

The strategy for the following global numerical analysis was first developed in [33] in the framework of $\Delta F = 2$ observables and afterwards extended to the analysis of $\Delta F = 1$ observables in [34]. Final refinements that allow to include the NP effects of tree level Higgs exchanges were implemented in [36]. For details beyond those given in this section the reader is referred to these papers.
First we note that the custodial symmetry of the RSc allows consistence with EWPT for masses of the lightest KK states as low as[2] $M_{\rm KK} \geq (2-3)\,\text{TeV}$ and we accordingly fix the new physics scale $f_{\rm RS} = ke^{-kL} = 1\,\text{TeV}$, which corresponds to

$$M_{\rm KK} \simeq 2.45\,\text{TeV}\,. \tag{5.1}$$

In order to be able to predict the size of NP effects in a sensible manner we need to constrain the parameter space to those regions that reproduce the SM quark masses and mixing angles, as well as the Jarlskog invariant [171], all within 2σ of their measured value. Concretely, we proceed as follows. In the flavor sector the 28 parameters comprising the absolute values, angles and phases entering the parameterization (3.28) of the fundamental Yukawa matrices $\lambda^{u,d}$ are randomly chosen in their respective ranges $[1/3, 3]$, $[0, \pi/2]$ and $[0, 2\pi]$. Of these, the range for the absolute values is determined by the requirement that the theory remains perturbative somewhat beyond the mass of the second KK excitation [98–100], and by the fact that we want to avoid extreme (IR) localizations for the right-handed top quark. Subsequently, the nine bulk mass parameters are determined in a manner such that the resulting 4D Yukawa matrices reproduce the quark spectrum of the SM. This procedure is considerably simplified by employing the Froggatt-Nielsen formulae [83] which can also be found in [33]. In this, it is important that the fit is performed to the quark masses at the high scale $\mu_s \sim \mathcal{O}(M_{\rm KK})$ which have to be determined from the $\overline{MS}$ masses using NLO RG evolution. The quark masses and mixing angles relevant for our analysis are given in tables 5.1 and 5.2. Since however the quark spectrum does not unambiguously fix the nine bulk mass parameters we can choose c_Q^3 randomly in the range

$$0.4 \leq c_Q^3 \leq 0.45\,, \tag{5.2}$$

[1] The Higgs contributions are negligible here since its couplings to leptons are mass suppressed.

[2] EWPT also impose constraints on the bulk mass parameters of the fermions [55], which are taken into account by our choice of c_Q^3 (cf. section 3.2.2).

which is motivated by our analysis in section 3.2.2. In this context we want to point out that the impact of the choice of this range on NP effects in flavor observables is small as long as $c_Q^3 < 0.5$.

	$\mu = 2\,\text{GeV}$	$\mu = 4.6\,\text{GeV}$	$\mu = 172\,\text{GeV}$	$\mu = 3\,\text{TeV}$
$m_u(\mu)$	3.0(10) MeV	2.5(8) MeV	1.6(5) MeV	1.4(5) MeV
$m_d(\mu)$	6.0(15) MeV	4.9(12) MeV	3.2(8) MeV	2.7(7) MeV
$m_s(\mu)$	110(15) MeV	90(12) MeV	60(8) MeV	50(7) MeV
$m_c(\mu)$	1.04(8) GeV	0.85(7) GeV	0.55(4) GeV	0.45(4) GeV
$m_b(\mu)$	—	4.2(1) GeV	2.7(1) GeV	2.2(1) GeV
$m_t(\mu)$	—	—	162(2) GeV	135(2) GeV

Table 5.1: Renormalized quark masses at various scales, evaluated using NLO RG running. The 1σ uncertainties are given in parentheses.

For each parameter point that is found to reproduce the SM quark masses and mixing angles we subsequently evaluate the $\Delta F = 2$ observables discussed in section 4.1 for two different values of the fundamental QCD coupling constant, $g_s = 6$ as the reference value and also the smallest possible value $g_s = 3$. The input parameters that are necessary for this task are given in table 5.2. In addition to the observables themselves we determine the amount of fine tuning in each observable according to the measure introduced by Barbieri and Giudice (BG) [172],

$$\Delta_{\text{BG}}(O)\Big|_x = \underset{i}{\text{Max}} \left| \frac{d \log O}{d \log x_i} \right| = \underset{i}{\text{Max}} \left| \frac{O}{x_i} \frac{dO}{dx_i} \right| , \tag{5.3}$$

where O is an observable and $x = (x_1, x_2, ...)$ is a point in parameter space. Since we are interested in *typical* or generic values of observables and the associated BG fine tuning in the RSc, we will present our results in the form of density plots rather than ordinary scatter plots. Having at hand predictions for all $\Delta F = 2$ observables we will then impose the available experimental constraints from ϵ_K, ΔM_K, ΔM_d, ΔM_s and $S_{\psi K_S}$ on the parameter space[3]. In applying these constraints we impose rather conservative bounds in order not to overlook interesting signatures in the not yet measured observables. To also keep track of the BG fine tuning $\Delta_{\text{BG}}(\epsilon_K)$, we will distinguish between points in parameter space with $\Delta_{\text{BG}}(\epsilon_K) \leq 20$ and $\Delta_{\text{BG}}(\epsilon_K) > 20$. With the suchlike prepared parameter sets we will finally investigate the impact of NP contributions on the CP violating observables in B_s mixing, $S_{\psi\phi}$, A_{SL}^s and $\Delta\Gamma_s/\Gamma_s$.
For our analysis of rare K and B decays we will again only take into account those parameter points that simultaneously satisfy all experimental constraints from $\Delta F = 2$ observables. We will calculate the decay branching ratios for the $K \to \pi\nu\bar{\nu}$, $K_L \to \pi^0\ell^+\ell^-$,

[3] As a result we obtain two sets of parameter points, one of them being consistent with the data for the choice of $g_s = 6$ and the other for $g_s = 3$. To be able to compare the phenomenological predictions for the different values of g_s we ensure that both sets have roughly the same size.

$K_L \to \mu^+\mu^-$, $B_{d,s} \to \mu^+\mu^-$ and $B \to X_{d,s}\nu\bar{\nu}$ modes and show the most interesting correlations between those—since it turns out that the results are distributed around the SM predictions—in the form of ordinary scatter plots. In these scatter plots, *light blue* points correspond to the choice $g_s = 3$, *dark blue* points correspond to $g_s = 6$ and *orange points* imply that in addition to $g_s = 6$ also the fine tuning constraint $\Delta_{\mathrm{BG}}(\epsilon_K) \leq 20$ has been imposed. On occasion we will remove the custodial protection for the purpose of illustration. In this case, *light-red* points correspond to $g_s = 3$, *dark-red* points correspond to $g_s = 6$ and *green* points imply that in addition to $g_s = 6$ also the fine tuning constraint has been imposed.

Some of the discovered correlations turn out to be different in the RSc than in other models of NP, such as the LHT and SM4 models. Since correlations between observables allow to make statements about parameter independent phenomenological model features, we will compare these correlations in the RSc to those in the two aforementioned NP models.

$\lambda = \lvert V_{us}\rvert = 0.2255 \pm 0.0019$	$G_F = 1.16637 \cdot 10^{-5}\,\mathrm{GeV}^{-2}$
$\lvert V_{ub}\rvert = (3.93 \pm 0.36) \cdot 10^{-3}$	$M_W = 80.403(29)\,\mathrm{GeV}$
$\lvert V_{cb}\rvert = (41.2 \pm 1.1) \cdot 10^{-2}$ [76]	$\alpha(M_Z) = 1/127.9$
$\gamma = 78(20)^\circ$	$\sin^2\theta_W = 0.23122$
$J_{\mathrm{SM}} = \left(3.08^{+0.16}_{-0.18}\right) \cdot 10^{-5}$ [76]	$m_K^0 = 497.614\,\mathrm{MeV}$
$\Delta M_K = 0.5292(9) \cdot 10^{-2}\,\mathrm{ps}^{-1}$	$m_{B_d} = 5279.5\,\mathrm{MeV}$ [76]
$\lvert\varepsilon_K\rvert = (2.229 \pm 0.012) \cdot 10^{-3}$ [132]	$m_{B_s} = 5366.4\,\mathrm{MeV}$ [133]
$\Delta M_d = (0.507 \pm 0.005)\,\mathrm{ps}^{-1}$	$\eta_1 = 1.32(32)$ [121]
$\Delta M_s = (17.77 \pm 0.12)\,\mathrm{ps}^{-1}$ [173]	$\eta_3 = 0.47 \pm 0.04$ [122, 123]
$S_{\psi K_S} = 0.672 \pm 0.024$ [132]	$\eta_2 = 0.5765 \pm 0.0065$ [124]
$\bar{m}_c = (1.268 \pm 0.009)\,\mathrm{GeV}$ [132, 174, 175]	$\eta_B = 0.551 \pm 0.007$ [124, 176]
$\bar{m}_t = (163.5 \pm 1.7)\,\mathrm{GeV}$ [177]	$F_{B_s} = (238.8 \pm 9.5)\,\mathrm{MeV}$
$F_K = (155.8 \pm 1.7)\,\mathrm{MeV}$	$F_{B_d} = (192.9 \pm 9.9)\,\mathrm{MeV}$
$\hat{B}_K = 0.725 \pm 0.026$	$F_{B_s}\sqrt{\hat{B}_{B_s}} = (275 \pm 13)\,\mathrm{MeV}$
$\hat{B}_{B_d} = 1.26 \pm 0.11$	$F_{B_d}\sqrt{\hat{B}_{B_d}} = (216 \pm 15)\,\mathrm{MeV}$ [132]
$\hat{B}_{B_s} = 1.26 \pm 0.11$ [132]	$\xi = 1.21(4)$ [178]
$\hat{B}_{B_s}/\hat{B}_{B_d} = 1.00(3)$ [178]	$\alpha_s(M_Z) = 0.118(2)$ [76]

Table 5.2: Values of the experimental and theoretical quantities used as input parameters.

5.2 K and B Meson Oscillations

5.2.1 Anatomy of RSc Contributions

We will start our numerical analysis with a look at the off-diagonal mixing amplitudes M_{12}^i, $(i = K, d, s)$ which are the basic quantities from which all $\Delta F = 2$ observables can be calculated. Hence the pattern of NP contributions can be inferred from these objects in the most transparent manner. The M_{12}^i receive contributions from tree level exchanges of KK gluons, the Z_H and Z' gauge bosons, as well as from the Higgs boson, while the contributions from the KK photon and the Z gauge boson are subleading. The first question we want to address is which of the individual contributions, the one from gauge bosons or the one from the Higgs boson, typically is dominant. To this end in the left panel of fig. 5.1 we show the imaginary and real parts of the Higgs contributions $(M_{12}^K)_{\text{Higgs}}$ divided by the gauge boson contribution $(M_{12}^K)_{\text{gauge}}$ for a fundamental QCD coupling constant $g_s = 3$ and a Higgs mass $M_H = 115\,\text{GeV}$. The same is shown for the B_s system in the right panel of that figure. Since we are interested in typical effects, we chose to present our results in the form of density plots in which light areas correspond to a high density of points and darker areas correspond to lower densities. For the plots

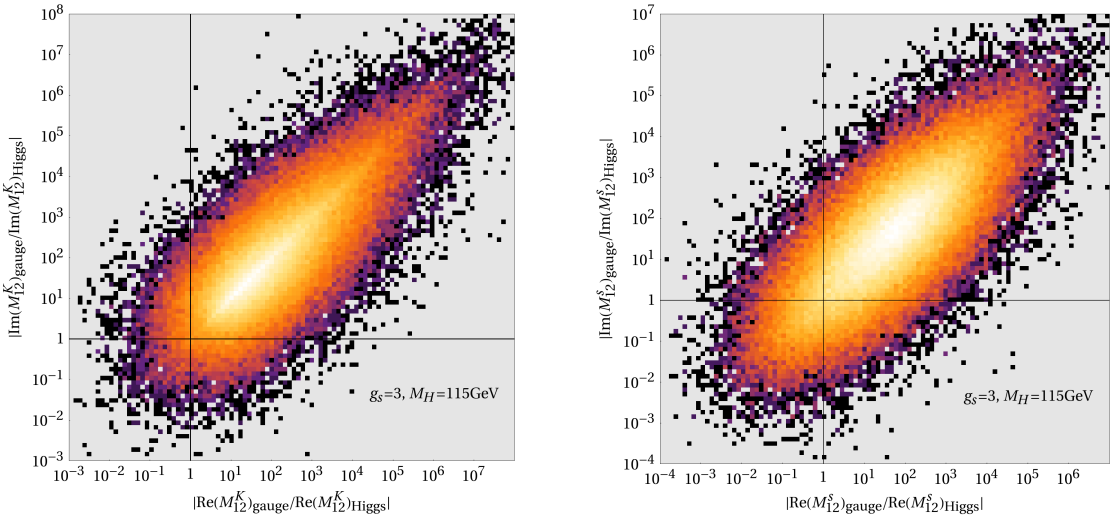

Figure 5.1: $|\text{Im}(M_{12}^K)_{\text{gauge}}/\text{Im}(M_{12}^K)_{\text{Higgs}}|$ vs. $|\text{Re}(M_{12}^K)_{\text{gauge}}/\text{Re}(M_{12}^K)_{\text{Higgs}}|$ (left panel) and $|\text{Im}(M_{12}^s)_{\text{gauge}}/\text{Im}(M_{12}^s)_{\text{Higgs}}|$ vs. $|\text{Re}(M_{12}^s)_{\text{gauge}}/\text{Re}(M_{12}^s)_{\text{Higgs}}|$ (right panel), all plotted on logarithmic axes.

in fig. 5.1 we have chosen the lowest possible value for the fundamental QCD coupling, $g_s = 3$ to be conservative. We see that even for this choice the gauge boson contribution dominates the Higgs contribution by one to two orders of magnitude[4] in both the K

[4]Here we have forestalled the fact that despite the partial cancellation in C_1^{LR} larger values of g_s do lead to larger total gauge boson contributions even in the $B_{d,s}$ systems where C_2^{LR} is not clearly dominant.

and B_s systems. From the dominance of the gauge boson contribution in the B_s system we deduce that the larger Higgs couplings to heavy quarks are compensated by larger KK gauge boson couplings in this case (cf. the discussion of the RS-GIM mechanism). We therefore conclude that the Higgs contribution to $\Delta F = 2$ observables can be safely neglected in the remainder of our analysis and we therefore will employ the notation $(M_{12})_{\mathrm{RSc}}$ instead of $(M_{12})_{\mathrm{gauge}}$ et cetera from now on.

Higgs contributions beyond the brane Higgs scenario As a short digression from the main line of our analysis we want to investigate under which circumstances the Higgs contributions can actually exceed the gauge boson contributions. For simplicity we will only consider the gluonic part of the latter contribution, but for fixed value of g_s the following results also apply to the remaining contributions. To extrapolate our hitherto acquired results to the bulk Higgs case we use [100]

$$(\delta\epsilon_K)^{\mathrm{gluon}} \propto \frac{(g_s)^2}{Y_{\mathrm{KK}}^2}\frac{1}{a^2(\beta)}\frac{1}{M_{\mathrm{KK}}^2}\,, \tag{5.4}$$

where $a(\beta)$ depends on the localization of the Higgs field and Y_{KK} is the typical coupling of the Higgs field to the lightest fermionic KK excitations. For a brane localized Higgs we find that $Y_{\mathrm{KK}} = 2\langle\lambda^d\rangle$. Furthermore, from (3.77) we see that the Higgs contribution to ϵ_K scales like

$$(\delta\epsilon_K)^{\mathrm{Higgs}} \propto \frac{Y_{\mathrm{KK}}^2}{M_{\mathrm{KK}}^2}\,, \tag{5.5}$$

with nearly no dependence on the localization of the Higgs field [116].
Using (5.4), (5.5) we can infer an estimate for the ratio $R \equiv \left\langle (\delta\epsilon_K)^{\mathrm{gluon}}/(\delta\epsilon_K)^{\mathrm{Higgs}}\right\rangle$ for arbitrary values of $(g_s, Y_{\mathrm{KK}}, \beta)$ from the value R_0 that is determined for $(g_s = 3, Y_{\mathrm{KK}} \simeq 3, \beta = \infty)$. Explicitly,

$$R(g_s, Y_{\mathrm{KK}}, \beta) \simeq \left(\frac{g_s}{3}\right)^2 \left(\frac{0.5}{a(\beta)}\right)^2 \left(\frac{3}{Y_{\mathrm{KK}}}\right)^4 R_0\,, \tag{5.6}$$

where the ratio R_0 is found to be $R_0 \sim 33$ and $a(\beta)$ is given for several values of β in [100]: $a(\infty) = 0.5$, $a(2) = 0.75$, $a(1) = 1$, $a(0) = 1.5$.
In fig. 5.2 we show the ratio $R(g_s = 3, Y_{\mathrm{KK}}, \beta)$ as a function of β for two different values of Y_{KK}. The lower curve corresponds to the maximal value consistent with the perturbativity estimate, $Y_{\mathrm{KK}} = 6\sqrt{2}$ (where an additional factor $\sqrt{2}$ is due to the localization of the Higgs in the bulk [100]), and the upper one to the value $Y_{\mathrm{KK}} = 6/\sqrt{2}$, which corresponds to the average if values are randomly chosen between 0 and the maximal value. We observe that as soon as the Higgs field is detached from the IR brane the Higgs contribution to ϵ_K can in principle exceed the KK gluon contribution, although depending on the typical size of Yukawa couplings this outcome is not imperative. The possible dominance of the Higgs contributions is largely due to the increase of the maximally allowed value for Y_{KK} by a factor of $\sqrt{2}$, but also by the shift of the quark zero modes towards the UV

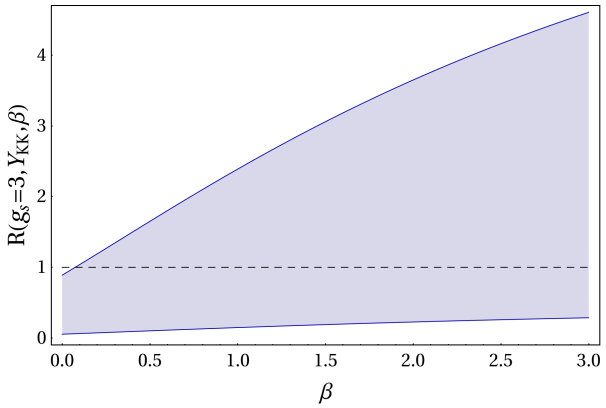

Figure 5.2: The ratio R for $g_s = 3$ as a function of β for $Y_{\rm KK} = 6\sqrt{2}$ (lower curve) and $Y_{\rm KK} = 6/\sqrt{2}$ (upper curve).

brane that becomes possible for a bulk Higgs[5] and is parameterized by the function $a(\beta)$.

Next, we want to investigate the absolute size of the RSc contribution to $\Delta F = 2$ observables. In fig. 5.3 we show the complex plane of KK gluon and EW contributions

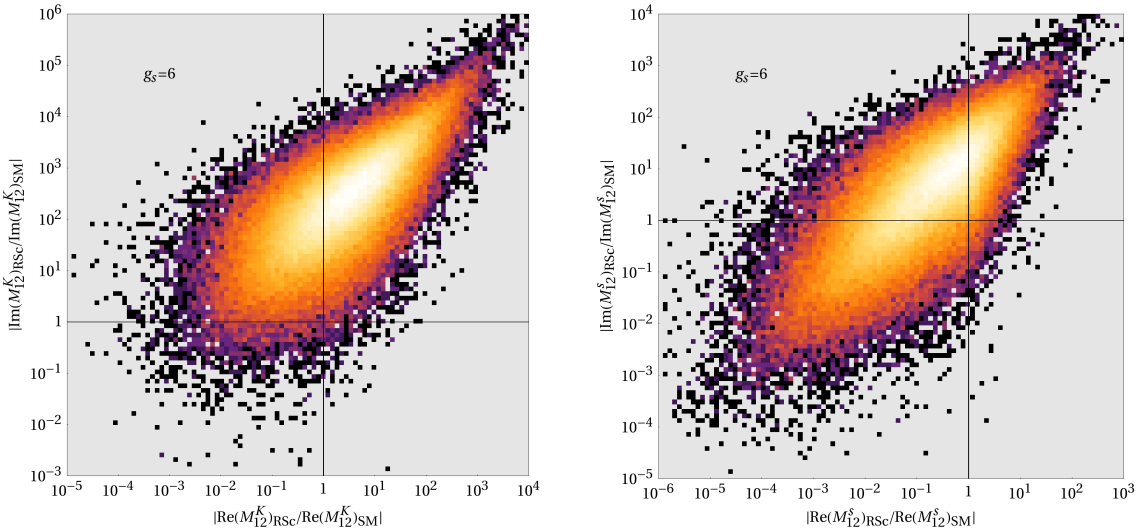

Figure 5.3: $|\mathrm{Re}(M_{12}^i)_{\rm RSc}/\mathrm{Re}(M_{12}^i)_{\rm SM}|$ and $|\mathrm{Im}(M_{12}^i)_{\rm RSc}/\mathrm{Im}(M_{12}^i)_{\rm SM}|$ plotted on logarithmic axes for the K system ($i = K$, left panel) and the B_s system ($i = s$, right panel).

to $M_{12}^{K,s}$ normalized to the SM short distance contribution $(M_{12}^{K,s})_{\rm SM}$ for the reference value $g_s = 6$. In the left panel, where the K system is shown, we see that while the

[5] At this point it is important to keep in mind that observables that depend on positive powers of $Y_{\rm KK} \propto \lambda^d$, such as the neutron EDM d_n [98], $Br(B \to X_s\gamma)$ [100] and ϵ'/ϵ [179] for fixed $M_{\rm KK}$ constrain the size of the Yukawa couplings such that configurations for which the Higgs contribution is found to be dominant may already be excluded.

real part of the RSc contribution can be enhanced over $\mathrm{Re}(M_{12}^{K,s})_{\mathrm{SM}}$ by several orders of magnitude—which clearly is in contradiction to the ΔM_K measurement even in the presence of sizeable LD contributions to that observable—typical values are roughly comparable to the SM value. Thus, due to the large uncertainty in the non-perturbative LD contributions to ΔM_K, this observable does not impose a stringent constraint on the RSc parameter space and agreement with experimental data is naturally obtained. In the case of the imaginary part the situation is vastly different. Since the RSc contribution to M_{12}^K is expected to have an $\mathcal{O}(1)$ phase, its imaginary part typically exceeds the λ_t-suppressed imaginary part of $(M_{12}^K)_{\mathrm{SM}}$ by more than two orders of magnitude. Thus, unlike ΔM_K, $\epsilon_K \propto \mathrm{Im}(M_{12}^K)$ is expected to impose a stringent bound on the model's parameter space. This large disparity in the imaginary parts is a manifestation of the *flavor coincidence problem* which is common to most models of physics beyond the SM. It also illustrates the impact and failure of the RS-GIM mechanism: Despite tree level contributions of TeV-scale particles that are enhanced chirally and by RG running effects (by more than two orders of magnitude), the real part of M_{12}^K is on average adequately protected from too large corrections. Only in the case of the imaginary part which is strongly suppressed in the SM (by roughly two orders of magnitude) the RS-GIM mechanism is overcome and corrections are typically too large.
The analogous situation in the case of the B_s system is shown in the right panel of fig. 5.3. Again we observe that enhancements of both real and imaginary parts of M_{12}^s by several orders of magnitude are possible. Typical values for the real part of the RSc contribution on the other hand are even smaller than the SM value, while typical values for the imaginary part exceed the SM by a mere order of magnitude. Also here the latter fact is due to a suppression of $\mathrm{Im}(M_{12}^s)_{\mathrm{SM}}$ with respect to $\mathrm{Re}(M_{12}^s)_{\mathrm{SM}}$, although the suppression is weaker than in the K system. We conclude that while in this case the experimental data on ΔM_s can be naturally reproduced, the $\mathcal{O}(1)$ phase of (M_{12}^s) implies significant effects in CP violating observables such as $S_{\psi\phi}$.
In the B_d system which is not shown we find that again both the real and imaginary parts of $(M_{12}^d)_{\mathrm{RSc}}$ can exceed the SM by several orders of magnitude while the typical values roughly have the same size as the SM contribution. Agreement for both ΔM_d and $S_{\psi K_S}$ with the experimental data therefore can be naturally obtained and no stringent bound on the parameter space is imposed by these observables.

After we have obtained an overview of the absolute size of RSc effects in the K and $B_{d,s}$ systems, we now will investigate the underlying operator structure. In fig. 5.4 we have calculated the isolated contributions of the $\mathcal{Q}_1^{VLL}$ and $\mathcal{Q}_2^{LR}$ operators[6] for $g_s = 6$ in the K and B_s systems. In the left panel of that figure we see that the impact of the scalar left-right operator $\mathcal{Q}_2^{LR}$ typically exceeds the impact of the left-left operator $\mathcal{Q}_1^{VLL}$ by two orders of magnitude. From this we can conclude that the exchange of KK gluons dominates the RSc contribution to $K^0 - \bar{K}^0$ oscillations for a fundamental QCD

[6]We choose to consider $\mathcal{Q}_2^{LR}$ alone as it is the only operator that at leading order is not generated by the exchange of EW gauge bosons. The contribution of the other left-right operator $\mathcal{Q}_1^{LR}$ is subleading and proportional to the one from Q_2^{LR}.

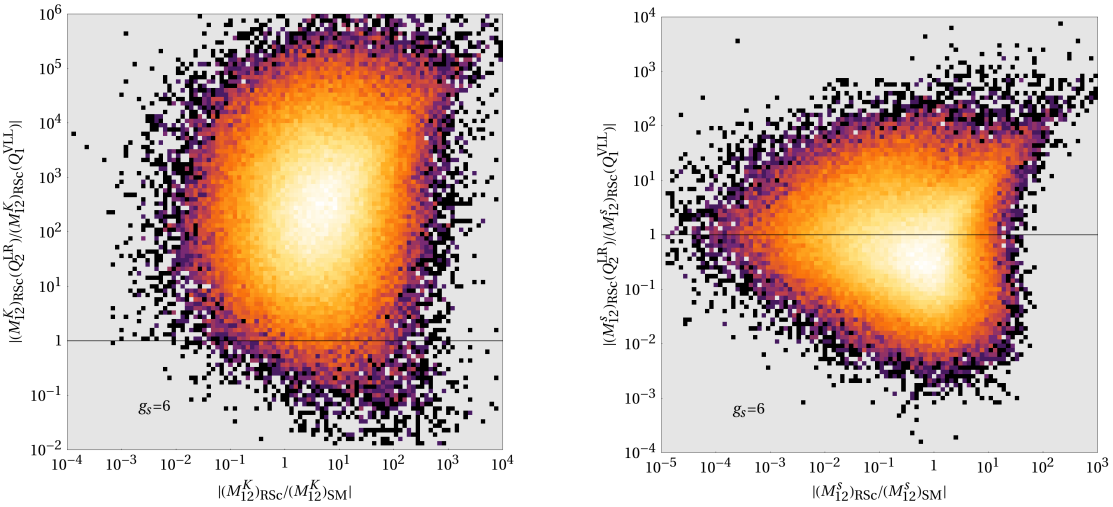

Figure 5.4: The ratio of the contributions of only $\mathcal{Q}_2^{LR}$ and$\mathcal{Q}_1^{VLL}$ to $(M_{12}^K)_{\rm RSc}$ (left panel) and $(M_{12}^s)_{\rm RSc}$ (right panel) as functions of $(M_{12}^i)_{\rm RSc}/(M_{12}^i)_{\rm SM}$ $(i = K, s)$.

coupling $g_s = 6$. This dominance still prevails if we take $g_s = 3$ for the fundamental QCD coupling even if we assume that the $\mathcal{Q}_1^{VLL}$ operator is of purely EW origin.

In the right panel of fig. 5.4 the ratio of the $\mathcal{Q}_2^{LR}$ and $\mathcal{Q}_1^{VLL}$ operator contributions to $B_s^0 - \bar{B}_s^0$ oscillations is shown. This time the scalar left-right operator typically contributes less than the left-left operator albeit still at a comparable level for $g_s = 6$. For lower values of the fundamental QCD coupling however it is clear that the contribution from the $\mathcal{Q}_2^{LR}$ operator becomes less important. We recall that the $\mathcal{Q}_1^{VLL}$ operator receives sizeable (for $g_s = 3$ even dominant) contributions from tree level exchanges of EW gauge bosons. Thus, in contrast to the K system, EW contributions have a significant impact in the B_s and also B_d systems—a fact that has been overlooked in the literature for some time.

We will conclude this survey of the anatomy of the RSc contributions to $\Delta F = 2$ observables by briefly explaining the dominance of the different operators in the K and $B_{d,s}$ systems. First, in the K system the impact of both left-right operators, $\mathcal{Q}_{1,2}^{LR}$ is chirally enhanced by a factor $R(\mu) \approx 20$, whereas the same factor in the $B_{d,s}$ system only amounts to $R^q(\mu) \approx 1$. Second, in particular the operator $\mathcal{Q}_2^{LR}$ is enhanced in the RG evolution from the high scale $\mu_s \simeq 3\,\text{TeV}$ down to the physically relevant scales $\mu_L \simeq 2\,\text{GeV}$ for the K system and $\mu_b \simeq 4.6\,\text{GeV}$ for the $B_{d,s}$ systems. Accordingly, the enhancement is stronger in the former case. Finally, the flavor violating effect in the $B_{d,s}$ systems are stronger for left-handed quarks than for right handed ones. The reason for this behavior is that in order to reproduce the large top mass the left-handed (t_L, b_L) doublet and the right-handed top singlet t_R need to be localized in the IR, while all other quark fields are UV localized. In consequence the b_L couples stronger to the IR localized KK gluons than the b_R does. This effect is in fact also present in the K system—the (c_L, s_L) doublet is localized closer to the conformal point than the s_R singlet is—but

it is much weaker here[7]. For the same reason also the impact of the $\mathcal{Q}_1^{VRR}$ operator is sub-leading in the $B_{d,s}$ systems. Finally we mention that we did not need to discuss the contribution from the $\mathcal{Q}_1^{LR}$ operator as it is proportional to the $\mathcal{Q}_2^{LR}$ contribution but significantly smaller for all viable values of g_s.

5.2.2 The ϵ_K Constraint

Our discussion of the RSc contributions to M_{12}^K in the previous section already raised the issue of reconcilability of ϵ_K with the experimental data which within uncertainties agrees with the SM value. From the left panel of fig. 5.3 we can in fact conclude that generically ϵ_K in the RSc is by more than two orders of magnitude too large. In [99] this observation has been used to derive a lower bound $M_{\rm KK} \geq 20\,\text{TeV}$ on the KK scale. In a more detailed analysis [33] which determined the average BG fine tuning that is necessary to obtain a viable prediction for ϵ_K, we confirmed this bound by requiring that the average fine tuning is smaller than $\mathcal{O}(20)$. While a number of model building attempts to soften this bound can be found in the literature [180–183], we will follow a different approach here.

The estimate in [99] for the bound on the KK scale assumes that the fundamental Yukawa matrices $\lambda^{u,d}$ are completely anarchic—but what happens if this assumption is relaxed? To answer this question we will resort to the parameterization for the Yukawa matrices given in section 3.2.1 and the ranges for the parameters stated in section 5.1, but keep the KK scale fixed at $M_{\rm KK} \simeq 2.45\,\text{TeV}$. The Yukawa matrices obtained in this manner are clearly not anarchic, as their various entries can differ by as much as an order of magnitude. To ensure that the predictions for flavor observables that are obtained in this approach do not depend on extremely unlikely cancellations between model parameters, we also calculate the BG fine tuning. In fig. 5.5 we show the BG fine tuning in ϵ_K as a function of that observable normalized to its experimental value for two different values of the fundamental QCD coupling g_s. From the left panel of this figure we immediately see that typically $\epsilon_K \sim \mathcal{O}(10^2)(\epsilon_K)_{\rm exp}$ and that in this case the fine tuning is small, typically below 20. For lower and more realistic values of ϵ_K the average fine tuning steeply increases so that for values that are consistent with the experimental data we find an average tuning of $\mathcal{O}(700)$. Despite this generic trend there obviously are areas in parameter space for which $(\epsilon_K)_{\rm exp}$ is roughly reproduced and the required tuning is moderate or even small. In the right panel of fig. 5.5 the same situation is shown for the minimal QCD coupling $g_s = 3$. In this case, the typical value for ϵ_K is roughly by a factor of four smaller, while the fine tuning is more or less independent of the size of this coupling.

To conclude the treatment of ϵ_K we repeat that there are indeed areas in parameter space for which ϵ_K can be *naturally* consistent with experiment. While it is obviously true that for these areas in parameter space the NP contributions are small and therefore higher order effects such as loop corrections become important, a case can be made that

[7] This can be seen from the approximate values of the brane overlaps F_Q^i, F_d^i given in (3.23) and (3.24).

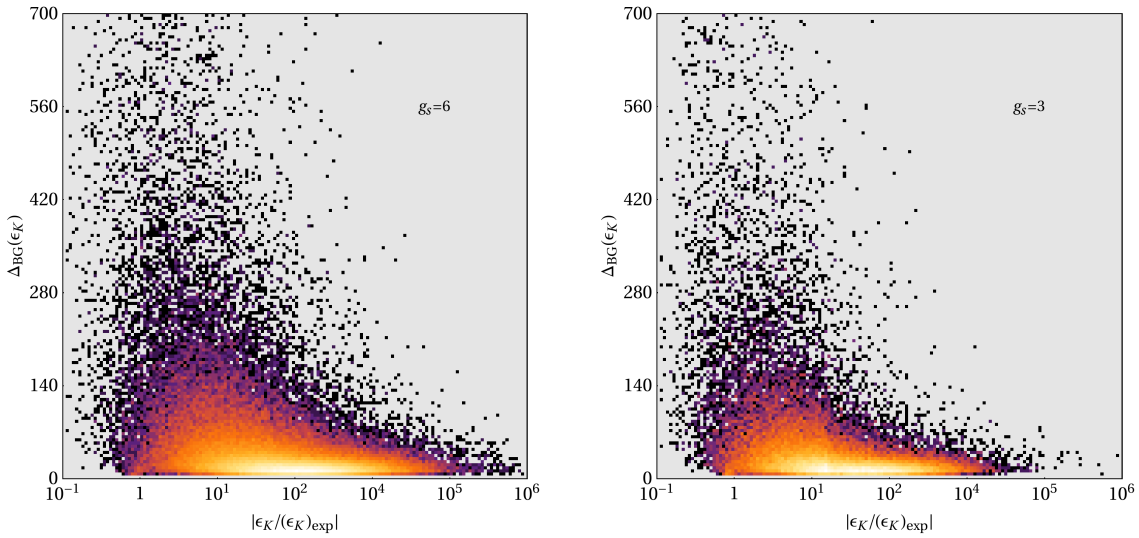

Figure 5.5: The BG fine tuning in ϵ_K as a function of $|\epsilon_K/(\epsilon_K)_{\rm exp}|$ plotted on a logarithmic scale for $g_s = 6$ (left panel) and $g_s = 3$ (right panel).

these corrections leave the global picture unchanged. In the case of the impact of KK fermions on the gauge couplings this statement has been checked numerically.

5.2.3 Experimentally Measured $\Delta F = 2$ Observables

In the previous section we have seen that the strong constraint imposed on the RSc by ϵ_K can be satisfied in a natural way. In the present section we will extend our fine tuning analysis to the remaining $\Delta F = 2$ observables that have been measured experimentally. In particular we will consider the CP conserving mass differences ΔM_K, ΔM_d and ΔM_s as well as the CP asymmetry in the B_d system, $S_{\psi K_S}$.

We will first look at ΔM_K which is sensitive to the real part of M_{12}^K. Although this observable depends on the same fundamental quantity as ϵ_K, we see in the left panel of fig. 5.6, where we show the fine tuning in ΔM_K as a function of that observable normalized to its experimental value, that typical values in the RSc are SM-like and thus slightly short of the experimental measurement. In view of the large theoretical uncertainties in the non-perturbative LD contributions to ΔM_K we find that the RSc prediction agrees well with the data if we assume that the SD contribution amounts to $(70 \pm 10)\%$ of the measured value. The average fine tuning turns out to be smaller than 20 for the phenomenologically relevant region, which is clearly much smaller than in the case of ϵ_K. This fact comes as no surprise if we recall the generic features of $(M_{12}^K)_{\rm RSc}$ shown in fig. 5.3 where we found its real part to be roughly comparable to the SM value.

The CP asymmetry $S_{\psi K_S}$ which is sensitive to the CP violating phase in B_d mixing is measured to very high accuracy and is very clean on the theoretical side. Also here we

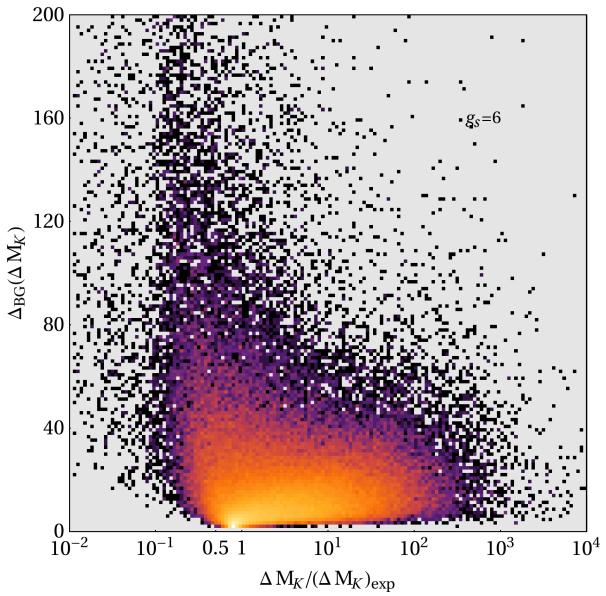

Figure 5.6: The BG fine tuning in ΔM_K as a function of $|\Delta M_K/(\Delta M_K)_{\text{exp}}|$ plotted on a logarithmic scale for $g_s = 6$.

are interested in whether the RSc can naturally reproduce the experimental data. As done for the $\Delta S = 2$ observables, we calculate the BG fine tuning in $S_{\psi K_S}$ and show our results in fig. 5.7. Typical values for $S_{\psi K_S}$ are SM-like and slightly larger than the experimental result, while the average fine tuning is found to be very small, roughly $\lesssim 5$. Taken together, figs. 5.5–5.7 indicate that beyond naturally satisfying individual constraints from $\Delta F = 2$ observables, the RSc is able to resolve certain tensions that occur in the unitarity triangle fits of the SM. The observables ΔM_d and ΔM_s display a behavior that is very similar to the case of $S_{\psi K_S}$ and we therefore do not show the corresponding plots.

In our discussion of all observables for which experimental results exist we have seen that all individual constraints can be satisfied naturally. Among those the ϵ_K constraint is the most severe and its imposition drastically reduces the available parameter space. Our initial question however was whether it is possible to satisfy *all* experimental constraints on $\Delta F = 2$ observables *simultaneously*. We find that this is indeed possible. Even more we find that ϵ_K and the other $\Delta F = 2$ observables are only weakly correlated, such that filtering for those points that yield a valid (untypically small) ϵ_K does not preclude the possibility of satisfying the remaining constraints, which are typically met. As an example for this fact we show the correlation between $S_{\psi K_S}$ and ϵ_K in fig. 5.8.

For the remainder of this analysis we will only consider those points in parameter space that in addition to the SM quark masses, mixing angles and CP invariant also satisfy all available constaints from $\Delta F = 2$ processes in the K, B_d and B_s systems.

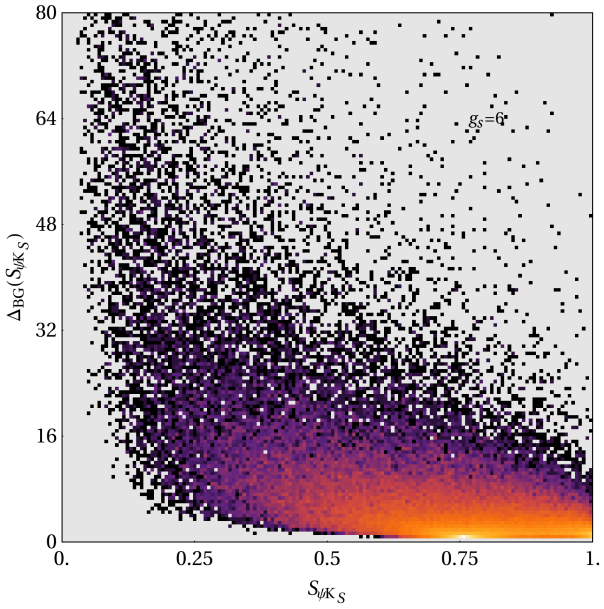

Figure 5.7: The BG fine tuning in $S_{\psi K_S}$ as a function of $S_{\psi K_S}$ for $g_s = 6$.

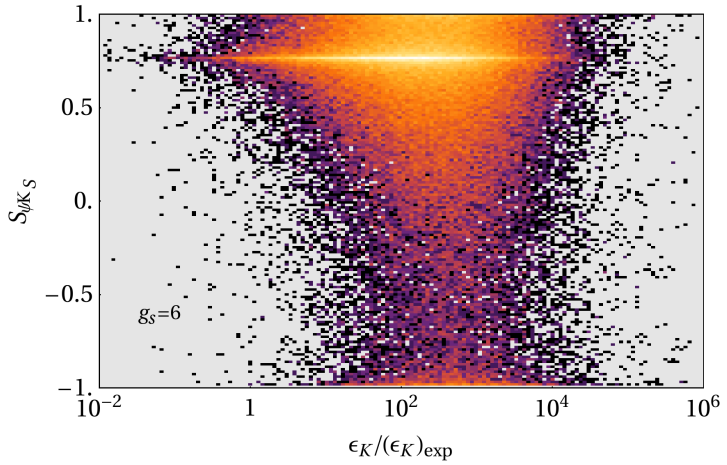

Figure 5.8: $S_{\psi K_S}$ as a function of $|\epsilon_K/(\epsilon_K)_{\rm exp}|$ plotted on a logarithmic scale for $g_s = 6$.

5.2.4 CP Violation in the B_s System

With the constrained parameter sets constructed in the previous section we are now able to investigate the possible size of effects in the not yet (precisely) measured CP violating observables in the B_s system, namely the time-dependent CP asymmetry $S_{\psi\phi}$ in the decay $B_s \to \psi\phi$, the semileptonic CP asymmetry A^s_{SL} and the normalized width difference $\Delta\Gamma_s/\Gamma_s$. These three quantities constitute a particularly interesting system of observables: If the decay $B_s \to \psi\phi$ is not affected by non-perturbative contributions, a measurement of $S_{\psi\phi}$ beyond its tiny SM value would be a clear-cut signal for CP violation in B_s mixing. Furthermore, in this case there are strong model-independent correlations between $S_{\psi\phi}$, A^s_{SL} and $\Delta\Gamma_s/\Gamma_s$ such that a deviation in either of these observables from its SM value entails deviations from the SM also in the other two observables. These considerations have gained in importance with the recent data from Tevatron [184–186], hinting at an enhancement in $S_{\psi\phi}$ by more than an order of magnitude over the SM value $(S_{\psi\phi})_{\rm SM} \simeq 0.04$.

In the left panel of fig. 5.9 we show the semileptonic CP asymmetry A^s_{SL} as a function of $S_{\psi\phi}$. The model-independent correlation between these two observables advertised above is immediately noticeable. Due to this correlation, both observables can be enhanced or suppressed only simultaneously. While values of these asymmetries close to the SM seem to be most likely, we find that the whole range of NP phases is possible so that $-1 < S_{\psi\phi} < 1$ and the value $S_{\psi\phi} \simeq 0.7$ recently reported by the CDF and DØ collaborations [184–186] can be reached. Accordingly, also A^s_{SL} can be enhanced by two orders of magnitude beyond its SM value. In the right panel of fig. 5.9 we show the same plot but this time for the minimal fundamental QCD coupling $g_s = 3$. We observe that while the model-independent correlation is even more pronounced, the lower value of g_s does not derogate the possible enhancement in the CP asymmetries beyond the SM. Large effects, although they seem to occur slightly less frequently, are possible also in this case. We therefore conclude that the—by roughly a factor four—smaller total RSc contributions for $g_s = 3$ are balanced by a greater number of parameter points that pass the phenomenological constraints. Finally, we are interested in the dependence of CP violation in the B_s system on the degree naturalness of our choice of parameter space. To this end we impose an additional constraint on the amount of fine tuning in ϵ_K, $\Delta_{\rm BG}(\epsilon_K) \leq 20$. We find that this constraint does not qualitatively modify the situation shown in fig. 5.9 beyond obvious statistical effects.

In the left panel of fig. 5.10 finally we show the normalized width difference $\Delta\Gamma_s/\Gamma_s$ as a function of $S_{\psi\phi}$. Also here the correlation between these two observables is a striking feature of the plot and could become particularly useful if in the future a precise measurement of $\Delta\Gamma_s/\Gamma_s$ will be available and in this manner large values for $S_{\psi\phi}$ could in principle be excluded. Unfortunately the converse, that is the exclusion of small $S_{\psi\phi}$, is not feasible in this framework. In the right panel of fig. 5.10 we show the same plot but for the minimal fundamental QCD coupling $g_s = 3$. As was the case for A^s_{SL}, the impact of this change is small. Also an imposition of the fine tuning constraint $\Delta_{\rm BG}(\epsilon_K) \leq 20$ has no specific effect apart from reducing the total number of parameter points.

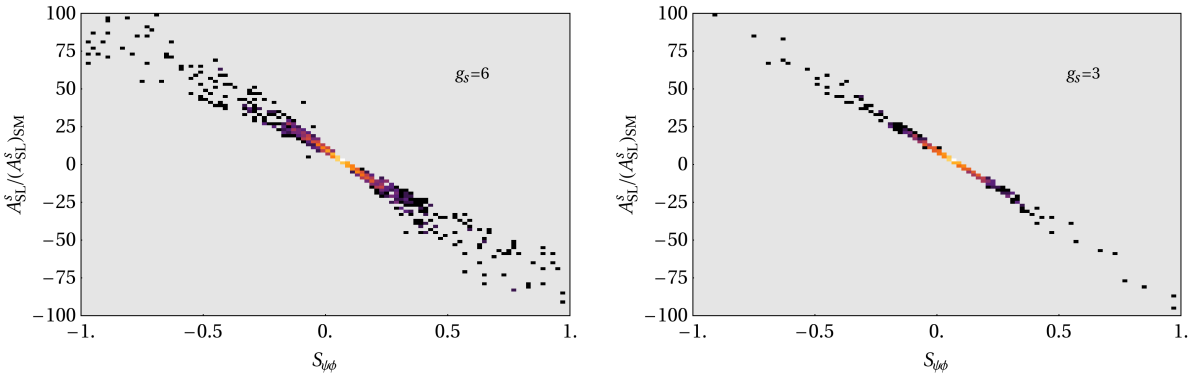

Figure 5.9: A^s_{SL} normalized to its SM value as a function of $S_{\psi\phi}$ for $g_s = 6$ (left panel) and $g_s = 3$ (right panel).

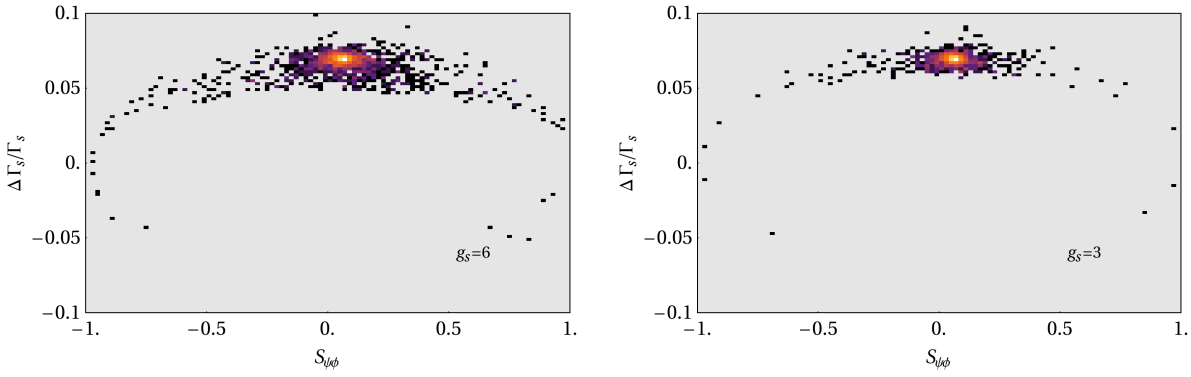

Figure 5.10: $\Delta\Gamma_s/\Gamma_s$ as a function of $S_{\psi\phi}$ for $g_s = 6$ (left panel) and $g_s = 3$ (right panel).

5.3 Rare K and B Decays

5.3.1 Anatomy of Z, Z_H and Z' Contributions

The key to understanding the relative sizes of different decay branching ratios and correlations between them in the RSc lies in the knowledge of the proportions of the various NP contributions. We will therefore begin our analysis of rare K and B decays with an investigation of the anatomy of the Z, Z_H and Z' contributions.
The NP contributions to the functions X, Y and Z given in section 4.2 are a product of three main components: the coupling of the respective gauge boson to the down-type quarks, its propagator in the low energy limit, and finally the gauge boson's coupling to leptons. For a given meson system characterized by the flavor indices (ij) there are six distinct contributions from the three gauge bosons Z, Z_H and Z' coupling to left- and right-handed down-type quarks, $\Delta^{ij}_{L,R}(Z)\,, \Delta^{ij}_{L,R}(Z_H)\,, \Delta^{ij}_{L,R}(Z')$. Two of them, the couplings of Z and Z' to the left-handed quarks are suppressed by the custodial symmetry. To understand the relative sizes of these six contributions, it is necessary to investigate the hierarchies in the above mentioned building blocks as we will do in the following.
We note that in case of the Y and Z functions also the KK photon $A^{(1)}$ contributes. However its couplings to fermions are suppressed by the smallness of the electromagnetic coupling $e^{4\mathrm{D}}$ and the electric quark charge, so that its contributions turn out to be small (if not absent) in all cases.

Couplings to quarks For the gauge couplings to left-handed quarks the hierarchy is given by the mixing of gauge bosons into mass eigenstates, cf. (2.76), and by the suppression induced by the custodial protection. Numerically, we find

$$\Delta^{ij}_L(Z_H) : \Delta^{ij}_L(Z') : \Delta^{ij}_L(Z) \sim \mathcal{O}(10^4) : \mathcal{O}(10^3) : 1\,. \tag{5.7}$$

For the couplings to the right-handed quarks, the hierarchy is solely determined by the mixing of gauge bosons into mass eigenstates, and is given by

$$\Delta^{ij}_R(Z_H) : \Delta^{ij}_R(Z') : \Delta^{ij}_R(Z) \sim \mathcal{O}(10^2) : \mathcal{O}(10^2) : 1\,, \tag{5.8}$$

where these hierarchies hold for the K, B_d and B_s systems likewise, that is for $ij = sd$, $ij = bd$ and $ij = bs$.
We note that in the presence of an exact protective P_{LR} symmetry the flavor violating couplings $\Delta^{ij}_L(Z)$ and $\Delta^{ij}_L(Z')$ would vanish identically. In this limit the same linear combination of $Z^{(1)}$ and $Z^{(1)}_X$ enters the Z and Z' mass eigenstates, so that the same cancellation of contributions is effective. Taking into account the P_{LR}-symmetry breaking effects on the UV brane, the custodial protection mechanism is not exact anymore, but still powerful enough to suppress $\Delta^{ij}_L(Z)$ by two orders of magnitude. In the case of Z', the mixing angles for $Z^{(1)}$ and $Z^{(1)}_X$ are modified by roughly 10% when including the violation of the P_{LR} symmetry. Accordingly, the protection is weaker in the case of Z'

and $\Delta_L^{ij}(Z')$ is suppressed only by one order of magnitude compared to the case without protection.
As the right-handed down-type quarks are no P_{LR}-eigenstates, the custodial protection mechanism is not effective in the case of $\Delta_R^{ij}(Z)$ and $\Delta_R^{ij}(Z')$, which explains the different pattern of hierarchies in the right-handed sector. This general picture is unaffected by the inclusion of the effects of KK fermion mixing as has been shown in section 3.5.

Gauge boson propagators If we assume the additional neutral gauge bosons Z_H and Z' to be degenerate in mass, their contribution to the functions X, Y and Z is suppressed by a factor $M_Z^2/M_{\rm KK}^2 \sim \mathcal{O}(10^{-3})$ with respect to the Z contribution.

Couplings to leptons For this comparison, we assume the lepton zero mode localization to be flavor independent, that is we assume degenerate bulk masses in the lepton sector. Since leptons are significantly lighter than the quarks of the same generation, we choose them to be localized towards the UV brane and set the bulk mass parameters to $c = \pm 0.7$ for left- and right-handed leptons. This assumption is well motivated by the observation that the flavor conserving couplings depend only very weakly on the actual value of c, provided $c > 0.5$ for left-handed leptons ($c < -0.5$ for right-handed leptons). Since the couplings of gauge boson mass eigenstates are dominated by the $Z^{(0)}$ and $Z^{(1)}$ contributions[8], their hierarchy does not depend on the particular handedness or charge of the involved leptons. In contrast to the Z_H and Z' coupling, the Z coupling to the lepton sector is not suppressed by an overlap integral of shape functions and hence is expected to be dominant. Numerically,

$$\Delta_{L,R}^{\nu\nu,\ell\ell}(Z_H) : \Delta_{L,R}^{\nu\nu,\ell\ell}(Z') : \Delta_{L,R}^{\nu\nu,\ell\ell}(Z) \sim \mathcal{O}(10^{-1}) : \mathcal{O}(10^{-1}) : 1\,. \tag{5.9}$$

This hierarchy is obviously the same in the K, B_d and B_s systems.

The above considerations now can be used to weight the contributions of Z, Z_H and Z' coupling to left- and right-handed quarks. Combining the ratios obtained in the previous three paragraphs we find that the contributions from the Z_H and Z coupling to left-handed quarks are comparable in size, while the corresponding contribution from Z' is clearly negligible. The contribution from couplings to right-handed quarks is strictly dominated by the Z gauge boson. To finally determine the dominant overall contribution, we note that due to the custodial protection and the particular structure of the model the Z boson couples much more strongly to right-handed quarks than to left-handed quarks, $\Delta_R^{ij}(Z) \gg \Delta_L^{ij}(Z)$, which is even more the case if we concentrate on parameter sets that can produce significant modifications to the functions X, Y and Z. Hence the main message from our semi-analytic analysis is the following: If the effects in rare K and B decays are significant, they are dominantly caused by the Z boson coupling

[8]This is due to the fact that the absolute value of the overlap integral of a $(++)$ gauge boson with UV localized fermions is much larger than the corresponding absolute value of the overlap integral for a $(-+)$ gauge boson, as can be seen in fig. 2.3.

to *right-handed* down-type quarks. This is in contrast to other models of NP, where left-handed couplings yield the dominant contribution to rare decays—such as the LHT or SM4 models—and we can expect a very specific pattern of flavor violation for rare decays in the RSc.

5.3.2 Violation of Universality

As the tree level contributions from the Z boson turned out to be dominant, we restrict our qualitative discussion to these contributions, and from this try to predict the relative sizes of possible NP effects in the K and $B_{d,s}$ systems. In our quantitative analysis we will however consider the full NP contribution. We will first determine the typical sizes of the generalized loop functions $X_i^{V,V-A}$, $Y_i^{V,V-A}$ and $Z_i^{V,V-A}$ $(i = K, d, s)$ in the RSc. To do so we have to take into account that NP contributions are enhanced non-universally by factors $1/\lambda_t^{(i)}$ relative to the SM. As these factors have largely disparate sizes, $\lambda_t^{(K)} \simeq 4 \cdot 10^{-4}$, $\lambda_t^{(d)} \simeq 1 \cdot 10^{-2}$ and $\lambda_t^{(s)} \simeq 4 \cdot 10^{-2}$, such that

$$\frac{1}{\lambda_t^{(K)}} : \frac{1}{\lambda_t^{(d)}} : \frac{1}{\lambda_t^{(s)}} \sim 100 : 4 : 1\,, \tag{5.10}$$

we would naïvely expect the deviation from the SM functions in the K system to be by more than an order of magnitude larger than in the B_d system, and those in turn by a factor of four larger than in the B_s system. Having at hand numerical results for a large number of parameter sets, we find that the strong hierarchy in the factors $1/\lambda_t^{(i)}$ is only partially compensated by the opposite hierarchy in the Z couplings $\Delta_R^{ij}(Z)$,

$$\Delta_R^{bs}(Z) : \Delta_R^{bd}(Z) : \Delta_R^{sd}(Z) \sim 9 : 6 : 1\,, \tag{5.11}$$

so that still larger effects are expected in K physics than in $B_{d,s}$ physics. In any case the universality of the functions X, Y and Z in the K and B systems that is present in the SM is necessarily broken in the RSc.
Combining (5.10) and (5.11) we find that the size of the NP contributions on average drops by a factor of four when going from the K to the B_d system and by another factor of two when going from the B_d to the B_s system.
How would this situation change in the absence of the custodial symmetry? In this case the left-handed Z couplings would yield the dominant contribution to tree level rare decays. Based on our parameter sets[9] we find for the left-handed couplings

$$\Delta_L^{bs}(Z) : \Delta_L^{bd}(Z) : \Delta_L^{sd}(Z) \sim 130 : 30 : 1\,, \tag{5.12}$$

[9]To be exact, apart from checking consistence with EWPT, one would have to repeat the analysis of $\Delta F = 2$ observables in the absence of custodial symmetry. Since however the most stringent constraint in the $\Delta F = 2$ sector comes from ϵ_K which is KK gluon dominated and since the remaining observables turn out to be roughly in agreement with experiment, taking the same parameter sets should not drastically modify the following result.

and we see that the hierarchy in the $1/\lambda_t^{(i)}$ is roughly compensated[10]. Hence we expect the relative NP effects in the K and B systems to be roughly of the same size. This very different pattern compared to the RSc could one day allow to distinguish experimentally between the RSc and RSm models if several decay branching ratios are observed above the SM expectation.
After this brief digression we return to our initial objective of determining the deviations of the generalized loop functions $X_i^{V,V-A}$, $Y_i^{V,V-A}$ and $Z_i^{V,V-A}$ $(i = K, d, s)$ from the SM values $X_0(x_t)$, $Y_0(x_t)$ and $Z_0(x_t)$. First we determine the possible ranges for X_i $(i = K, d, s)$. The 5σ ranges for these quantities are numerically found to be

$$0.60 \leq \frac{|X_K|}{X(x_t)} \leq 1.30\,, \qquad 0.90 \leq \frac{|X_d|}{X(x_t)} \leq 1.12\,, \qquad 0.95 \leq \frac{|X_s|}{X(x_t)} \leq 1.08\,, \tag{5.13}$$

where we have imposed the fine tuning constraint $\Delta_{\rm BG}(\epsilon_K) \leq 20$ and taken into account that theses distributions can be asymmetric around the SM value. As predicted, the relative size of NP effects in the K system is by approximately a factor of four larger than that in the B_d system which in turn is by a factor of two larger than in the B_s system. This implies that CP conserving effects in the K system are much larger than in the B systems, where they in fact are found to be disappointingly small. We do not state the ranges for the Y and Z functions (see however [34]) as these scale inversely to the SM values

$$X(x_t) = 1.48\,, \qquad Y(x_t) = 0.94\,, \qquad Z(x_t) = 0.65\,, \tag{5.14}$$

and hence can be inferred from (5.13).
In the left panel of fig. 5.11 we show the breakdown of universality in the absolute values of X_K and X_s. The black line in this plot indicates the CMFV limit in which the X, Y, Z functions are universal for the K and B systems. In the RSc this universality is strongly broken, mainly by the large effects in the K system.
A similar picture is obtained for the ranges of the phases of X_i $(i = K, d, s)$,

$$-45^\circ \leq \theta_X^K \leq 25^\circ\,, \qquad -9^\circ \leq \theta_X^d \leq 8^\circ\,, \qquad -2^\circ \leq \theta_X^s \leq 7^\circ\,. \tag{5.15}$$

These different ranges imply that the in any case experimentally inaccessible CP violating effects in $b \to d\nu\bar{\nu}$ and $b \to s\nu\bar{\nu}$ transitions are very small, but also that those in K_L decays can be significant. An analogous pattern is found for the phases of the Y_i and Z_i functions which can be found in [34]. In the right panel of fig. 5.11 we illustrate the breakdown of universality in the phases θ_X^K and θ_X^s.
Apart from the obvious breakdown of universality, fig. 5.11 displays a second interesting feature. Especially in the right panel of that figure we see that extremal effects in both phases do not tend to show up simultaneously. If we assume anarchic phases in the elements of the coupling matrix $\Delta_R^{ij}(Z)$, which dominantly enters the X_i functions—and

[10]This is a subtle consequence of the fact that it is the hierarchy in the IR brane overlaps of the left-handed doublets which is responsible for the smallness of the CKM mixing angles.

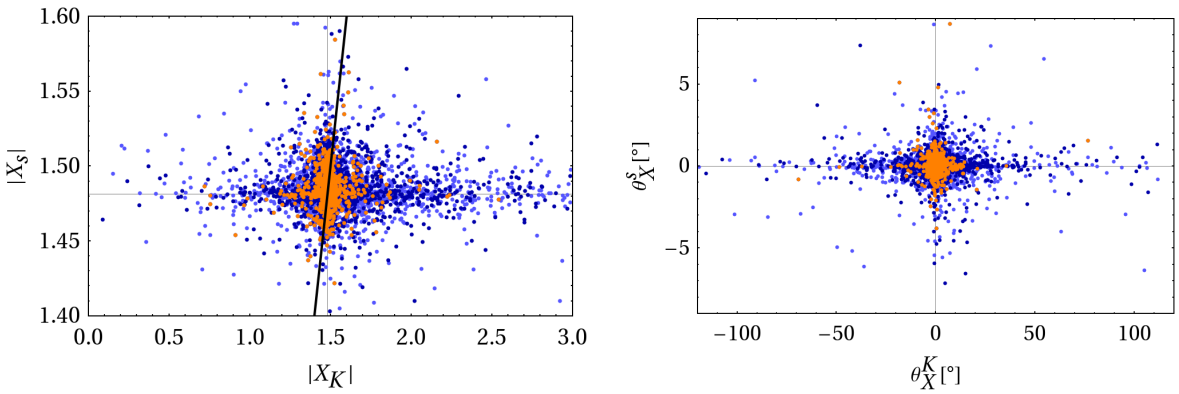

Figure 5.11: Breakdown of universality between $|X_K|$, $|X_s|$ (left panel) and $\mathrm{Arg}(X_K)$, $\mathrm{Arg}(X_s)$ (right panel). The light blue points represent data sets obtained for $g_s = 3$, dark blue points correspond to $g_s = 6$ and orange points indicate the imposition of the fine tuning constraint $\Delta_{\mathrm{BG}}(\epsilon_K) \leq 20$ for $g_s = 6$. The solid black line indicates the flavor universal CMFV limit.

there is no indication why this should not be the case—this finding can be explained in the light of the discussion that led to fig. 3.4: For a given point in parameter space, the couplings of the Z boson to different meson systems do not tend to be simultaneously large.

5.3.3 Rare K Decays

From our analysis of the X, Y, Z functions in the previous section we know that the most spectacular effects can be expected in the K system. In this section we will consider the theoretically cleanest and most prominent modes of rare K decays, $Br(K^+ \to \pi^+\nu\bar{\nu})$, $Br(K_L \to \pi^0\nu\bar{\nu})$, $Br(K_L \to \pi^0\ell^+\ell^-)$ and the short distance contribution to $Br(K_L \to \mu^+\mu^-)$.

Of the above decays the $K \to \pi\nu\bar{\nu}$ modes are highly sensitive to NP and beyond that offer the possibility of distinguishing between different models of NP once both branching ratios are accurately measured. In fig. 5.12 we show $Br(K_L \to \pi^0\nu\bar{\nu})$ as a function of $Br(K^+ \to \pi^+\nu\bar{\nu})$. We find that $Br(K^+ \to \pi^+\nu\bar{\nu})$ can be enhanced by roughly a factor of two, which would allow to reach the central experimental value of $\sim 17 \cdot 10^{-11}$. For $Br(K_L \to \pi^0\nu\bar{\nu})$ the enhancement is typically even larger and can reach up to values of four such that the model-independent Grossman-Nir bound [144], which puts an upper bound on $Br(K_L \to \pi^0\nu\bar{\nu})$ for given $Br(K^+ \to \pi^+\nu\bar{\nu})$ can be saturated in the RSc. So after all the $K_L \to \pi^0\nu\bar{\nu}$ mode is more sensitive to the impact of the RSc than the $K^+ \to \pi^+\nu\bar{\nu}$ mode. Apart from the possible enhancements it is noteworthy that in the RSc the two branching ratios are virtually uncorrelated. Unlike in the LHT or SM4 models, where a strict branch structure was found [111, 139], here fixing the value of either branching ratio does not preclude or favor a particular value for the second branching ratio. The reason for this different behavior has been pointed out in [145]. In

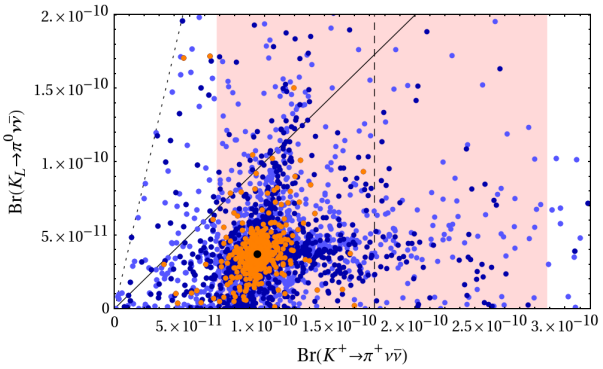

Figure 5.12: $Br(K_L \to \pi^0\nu\bar{\nu})$ as a function of $Br(K^+ \to \pi^+\nu\bar{\nu})$. The shaded area represents the experimental 1σ-range for $Br(K^+ \to \pi^+\nu\bar{\nu})$ with the central value indicated by the dashed vertical line. The GN bound is displayed by the dotted line, while the solid line indicates equality of both branching ratios. The black point represents the SM prediction.

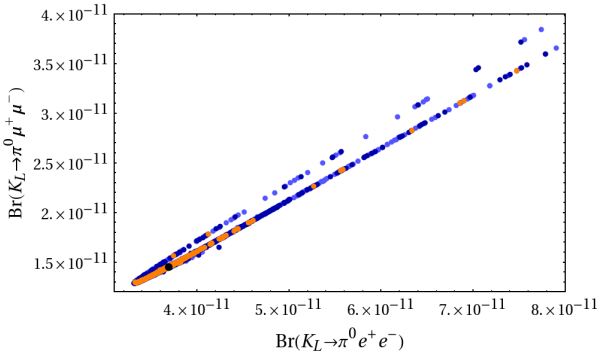

Figure 5.13: $Br(K_L \to \pi^0\mu^+\mu^-)$ as a function of $Br(K_L \to \pi^0 e^+ e^-)$ assuming constructive interference. The black point represents the SM prediction.

summary, in the two other NP models the strong correlation in the $Br(K \to \pi\nu\bar{\nu})$ plane is caused by the ϵ_K constraint which, due to the presence of right-handed currents and non-universal phases in ϵ_K and $K \to \pi\nu\bar{\nu}$ loses its constraining power in the RSc. We will briefly return to the non-correlation in the $K \to \pi\nu\bar{\nu}$ system in section 5.4 where we compare the global features of the RSc to those of the LHT and SM4 models.

The second pair of branching ratios we want to have a closer look at is the $K_L \to \pi^0\ell^+\ell^-$ system. In fig. 5.13 we show $Br(K_L \to \pi^0\mu^+\mu^-)$ as a function of $Br(K_L \to \pi^0 e^+ e^-)$. Both branching ratios can be typically enhanced by 40%, staying still far below their experimental upper bounds (4.76). We also observe that the two branching ratios are strongly correlated, as was also found in the LHT and SM4 models. Such a correlation in fact is common to all models in which no scalar operators are present [157, 158, 161]. So while on the one hand the correlation shown in fig. 5.13 gives no handle on distinguishing between the RSc, LHT and SM4 models, detecting its violation by experiment would

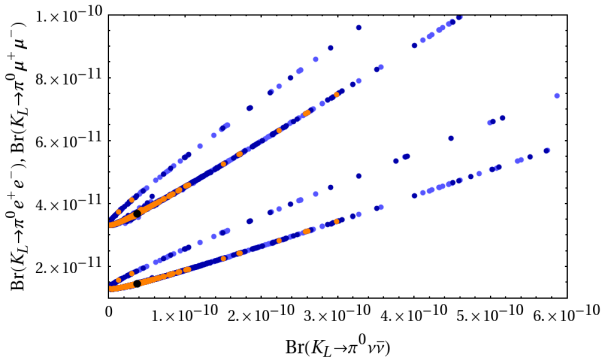

Figure 5.14: $Br(K_L \to \pi^0 e^+ e^-)$ (upper curve) and $Br(K_L \to \pi^0 \mu^+ \mu^-)$ (lower curve) as a function of $Br(K_L \to \pi^0 \nu\bar{\nu})$ assuming constructive interference in $Br(K_L \to \pi^0 \ell^+ \ell^-)$. The black points represent the SM predictions.

shed light on the operator structure of new physics.

In fig. 5.14 we show $Br(K_L \to \pi^0 e^+ e^-)$ and $Br(K_L \to \pi^0 \mu^+ \mu^-)$ as functions of $Br(K_L \to \pi^0 \nu\bar{\nu})$. Again we observe a strong correlation between these modes, implying that a strong enhancement of $Br(K_L \to \pi^0 \nu\bar{\nu})$ entails a significant enhancement of $Br(K_L \to \pi^0 \ell^+ \ell^-)$. Since both branching ratios receive dominantly or exclusively CP violating contributions, the strong correlation between both implies that the CP phase that enters these modes is universal. Finally we note that the gradient of the correlation is smaller than one, so that the typical enhancement in $Br(K_L \to \pi^0 \ell^+ \ell^-)$ is smaller than in $Br(K_L \to \pi^0 \nu\bar{\nu})$. This is related to the fact that the NP effects in the former modes are dominated by indirect CP violating contributions which are basically fixed by ϵ_K and $K_S \to \pi^0 \ell^+ \ell^-$, as discussed in section 4.2.3.

The last observable that we want to analyze in this section is related to the $K_L \to \mu^+ \mu^-$ decay. While it is known that the SD contribution constitutes only a small fraction of the whole dispersive contribution to the branching ratio, the LD contributions are afflicted with large uncertainties. Therefore the perturbative part of the branching ratio $Br(K_L \to \mu^+ \mu^-)$ cannot be directly related to the measured branching ratio. A conservative upper bound on $Br(K_L \to \mu^+ \mu^-)_{\mathrm{SD}}$ however has been derived in [166] and is given in (4.78). In the left panel of fig. 5.15 we show $Br(K_L \to \mu^+ \mu^-)_{\mathrm{SD}}$ as a function of $Br(K^+ \to \pi^+ \nu\bar{\nu})$. Clearly, $Br(K_L \to \mu^+ \mu^-)_{\mathrm{SD}}$ can be enhanced beyond the indirect bound (4.78), although this is typically not the case. Even more striking is the strong inverse correlation between the two CP conserving branching ratios $Br(K_L \to \mu^+ \mu^-)_{\mathrm{SD}}$ and $Br(K^+ \to \pi^+ \nu\bar{\nu})$: Large enhancements of the former mode up to or beyond its indirect bound require SM-like values for the latter mode and vice versa, and it is interesting to note that a confirmation of the central value of the $K^+ \to \pi^+ \nu\bar{\nu}$ branching ratio in the RSc would imply a vanishing SD contribution to $Br(K_L \to \mu^+ \mu^-)$. The reason for this correlation can be traced back to the dominance of the right-handed Z coupling in

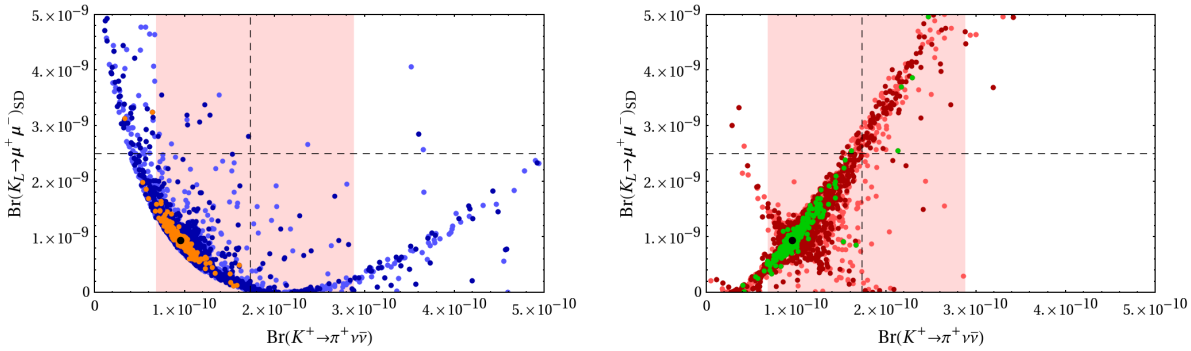

Figure 5.15: Left panel: The SD contribution to $Br(K_L \to \mu^+\mu^-)$ as a function of $Br(K^+ \to \pi^+\nu\bar{\nu})$. Right panel: The same, but with removed custodial symmetry. The shaded area represents the experimental 1σ-range for $Br(K^+ \to \pi^+\nu\bar{\nu})$ with the central value indicated by the dashed vertical line. The dashed horizontal line corresponds to the indirect bound (4.78) on $Br(K_L \to \mu^+\mu^-)_{\rm SD}$ and the black point represents the SM prediction.

the framework of the RSc. Since π^+, K^+ and K_L are pseudo-scalar mesons, we find for the matrix elements

$$\begin{aligned} \langle \pi^+|(\bar{s}d)_{V-A}|K^+\rangle &= +\langle \pi^+|(\bar{s}d)_{V+A}|K^+\rangle\,, \\ \langle 0|(\bar{s}d)_{V-A}|K_L\rangle &= -\langle 0|(\bar{s}d)_{V+A}|K_L\rangle\,, \end{aligned} \tag{5.16}$$

so that the $(V+A)$ RSc contribution faces the $(V-A)$ SM contribution with an opposite sign in the two branching ratios considered here. The correctness of these considerations can be easily checked: by removing the custodial protection. This is shown in the right panel of fig. 5.15. Without custodial protection the left-handed Z couplings are no longer suppressed and in fact constitute the dominant source of NP effects, which results in a simultaneous suppression or enhancement of $Br(K_L \to \mu^+\mu^-)_{\rm SD}$ and $Br(K^+ \to \pi^+\nu\bar{\nu})$. Thus the correlation between the two modes considered here represents a very good probe of the operator structure of NP and has the potential to exclude the RSc. In view of this, theoretical progress on the determination of the LD contribution to $Br(K_L \to \mu^+\mu^-)$ would be of vital importance.

5.3.4 Rare B Decays

In the following we want to give an overview over the exclusive decays $Br(B_{d,s} \to \mu^+\mu^-)$ and the two inclusive modes $Br(B \to X_{d,s}\nu\bar{\nu})$. From our general analysis in section 5.3.2 we already know that NP effects in the B systems are much less spectacular than in the K system. On the other hand these modes are highly sensitive to the effects of the custodial symmetry and offer an interesting experimental ground for studying its impact. Decay modes that do not suffer from the suppression of the left-handed couplings and that can potentially be strongly enhanced, such as $B \to X_s\gamma$ and $B \to X_s\ell^+\ell^-$ require the inclusion of loop-induced dipole operators and are beyond the scope of this thesis.

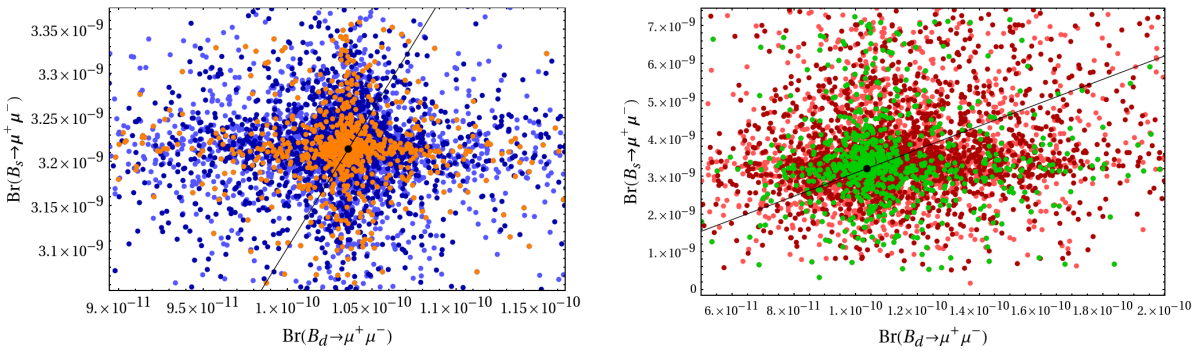

Figure 5.16: Left panel: $Br(B_s \to \mu^+\mu^-)$ as a function of $Br(B_d \to \mu^+\mu^-)$. Right panel: The same, but with removed custodial symmetry. The black line corresponds to the CMFV correlation and the black point represents the SM prediction.

Estimates for the branching ratios of these modes in the RSc have however been obtained in [98, 100].

In the left panel of fig. 5.16 we show the purely leptonic modes $B_{d,s} \to \mu^+\mu^-$. As indicated above, we find the possible enhancements of both branching ratios to be very small, roughly 10% for $B_d \to \mu^+\mu^-$ and 5% for $B_s \to \mu^+\mu^-$. These small effects are caused by the absence of scalar operators which could in principle lift the strong chiral suppression of these modes, and by the custodial protection which suppresses the left-handed Z couplings below the level of the right-handed couplings. If the suppression from the custodial protection is lifted[11], as we show in the right panel of fig. 5.16, the possible effects in both modes are considerably larger and amount to typically 50% for $B_d \to \mu^+\mu^-$ and 80% for $B_s \to \mu^+\mu^-$. Let us now return to the left panel of fig. 5.16 which displays another interesting feature. As was the case for the X_K and X_s functions in section 5.3.2 (see fig. 5.11), also here (though less pronounced) we observe that simultaneous effects in the two branching ratios seem to be disfavored[12]. This observation again can be traced back to our discussion of the relation between different flavor violating quark couplings of a given gauge boson in the context of fig. 3.4. We finally mention that the black line corresponds to the CMFV limit in which the ratio of both branching ratios is equal to their ratio in the SM. This CMFV correlation is obviously strongly broken in the RSc, regardless of the presence or absence of the custodial protection.

The situation in the case of the inclusive modes $B \to X_{d,s}\nu\bar{\nu}$ shown in fig. 5.17 is very

[11] Note that the removal of the custodial protection as done here in general leads to tensions with EWPT such that for a more detailed analysis one would have to take these constraints into account as well. So while we are certainly in no position to make predictions for the RSm model, the procedure employed by us allows to investigate the impact of the custodial protection.

[12] This effect is even less pronounced (if present at all) in the case of removed custodial protection. The difference here is that in the absence of custodial protection, there is no single coupling that is clearly dominant.

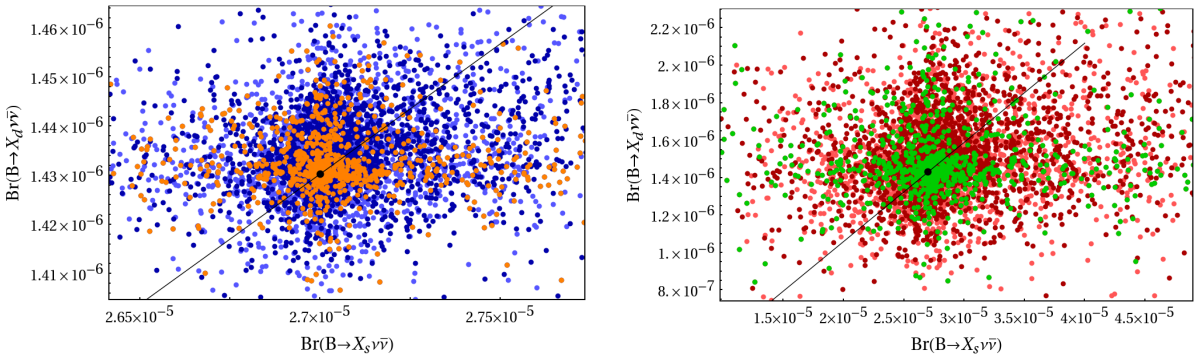

Figure 5.17: Left panel: $Br(B \to X_d \nu\bar{\nu})$ as a function of $Br(B \to X_s \nu\bar{\nu})$. Right panel: The same, but with removed custodial symmetry. The black line corresponds to the universal CMFV result given by the ratio $|V_{td}|^2/|V_{ts}|^2$ and the black point represents the SM prediction.

similar to the one discussed above. The enhancement of these modes in the RSc is small, typically below 5% and as for the purely leptonic modes strong enhancements are possible if the custodial protection is removed. Also here the CMFV correlation between the branching ratios is strongly violated.

5.3.5 Correlations Between Observables in K and B Physics

Until now we have only considered K and B observables separately. What we have seen in this analysis so far is that the most significant NP effects can show up in rare K decays, in particular in the $K \to \pi\nu\bar{\nu}$ system, and in the observables that are related to CP violation in B_s mixing, in particular in the time dependent CP asymmetry $S_{\psi\phi}$. In the present section we want to address the question whether these effects are independent of each other or in fact correlated.

We commence our analysis by contrasting the two single most spectacular observables in the RSc from the viewpoint of possible enhancements, $Br(K_L \to \pi^0\nu\bar{\nu})$ and $S_{\psi\phi}$, which are shown in fig. 5.18. The most striking feature of this plot is that large enhancements in $Br(K_L \to \pi^0\nu\bar{\nu})$ and $S_{\psi\phi}$ are mutually exclusive. Large values in either observable strongly favor a SM-like value in the second observable. Thus a confirmation of the recent combined analysis [184] of the CDF [185] and DØ [186] collaborations which suggest a value for $S_{\psi\phi}$ as high as $\simeq 0.7$ would preclude almost any visible effect in $K_L \to \pi^0\nu\bar{\nu}$ in the context of the RSc. If on the other hand a SM-like time dependent CP asymmetry $S_{\psi\phi}$ is found in future experiments, the road would be open for large effects in $K_L \to \pi^0\nu\bar{\nu}$. The correlation between the CP conserving decay branching ratio $Br(K^+ \to \pi^+\nu\bar{\nu})$ and $S_{\psi\phi}$ turns out to be very similar and we do not show it here. Although beyond doubt it is too soon to speculate we take the liberty of mentioning that in this context a confirmation of the central values of both the $Br(K^+ \to \pi^+\nu\bar{\nu})$ and $S_{\psi\phi}$ measurements would put the RSc under pressure. In this sense the upcoming experiments NA62, E14 and LHCb really have the potential to seriously challenge or

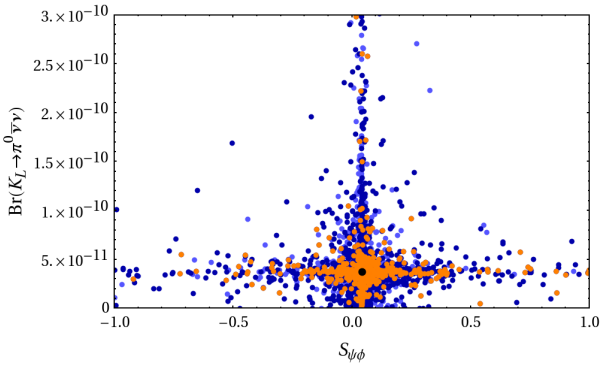

Figure 5.18: $Br(K_L \to \pi^0 \nu\bar{\nu})$ as a function of the CP asymmetry $S_{\psi\phi}$. The black point represents the SM prediction.

even exclude the RSc.
On account of the significance of the correlation discussed above we will try to give an explanation for its emergence. We have seen earlier in the discussion of the RS-GIM mechanism in section 3.4.1 that for a given chirality the entries of the gauge coupling matrices are related and have the tendency not to be large simultaneously. The rare K decay modes are dominated by the right-handed Z coupling, so a large K branching ratio favors small $Vb_R\bar{s}_R$ couplings, where $V = Z, Z_H, Z', A^{(1)}, G^{(1)}$. As $S_{\psi\phi}$ also receives contributions from the $\mathcal{Q}_1^{VLL}$ operator (see fig. 5.4) which is insensitive to right-handed couplings this effect alone does not explain the observed correlation. A second effect that is of relevance here was pointed out in [187]. In those cases where the $\mathcal{Q}_1^{VLL}$ operator yields a significant contribution to $S_{\psi\phi}$, the left-handed quarks are slightly more localized towards the IR brane than on average. By virtue of the transformation given in (3.29) this implies that for fixed Yukawa couplings the right-handed quarks are slightly farther away from the IR brane. This entails smaller right-handed couplings and hence smaller rare decay branching ratios. We have however checked that in this context the former effect is the dominant one[13].

In fig. 5.19 we show the ratio $Br(B_s \to \mu^+\mu^-)/Br(B_s \to \mu^+\mu^-)_{\rm SM}$ as a function of $Br(K^+ \to \pi^+\nu\bar{\nu})$ both with and without custodial symmetry. Also here we identify a correlation between both observables that disfavors simultaneous large effects. Since this time the correlation is due to the structure of the right-handed couplings alone, it is weaker than the one between $K \to \pi\nu\bar{\nu}$ and $S_{\psi\phi}$. Still, for values of $Br(K^+ \to \pi^+\nu\bar{\nu})$ close to the experimental central value, $Br(B_s \to \mu^+\mu^-)$ is essentially SM-like.
To conclude our discussion of correlations between K and B decays in fig. 5.20 we show the branching ratios $Br(K_L \to \mu^+\mu^-)_{\rm SD}$ and $Br(B_s \to \mu^+\mu^-)$. As before, effects are larger in the K than in the B_s mode, and also here significant effects are favored to be mutually exclusive. The CMFV correlation which is represented by the black line also

[13]This can be done e.g. by considering also the correlations between $S_{\psi\phi}$ and $Br(B_s \to \mu^+\mu^-)$ which should also be mutually exclusive if the second effect was the dominant one.

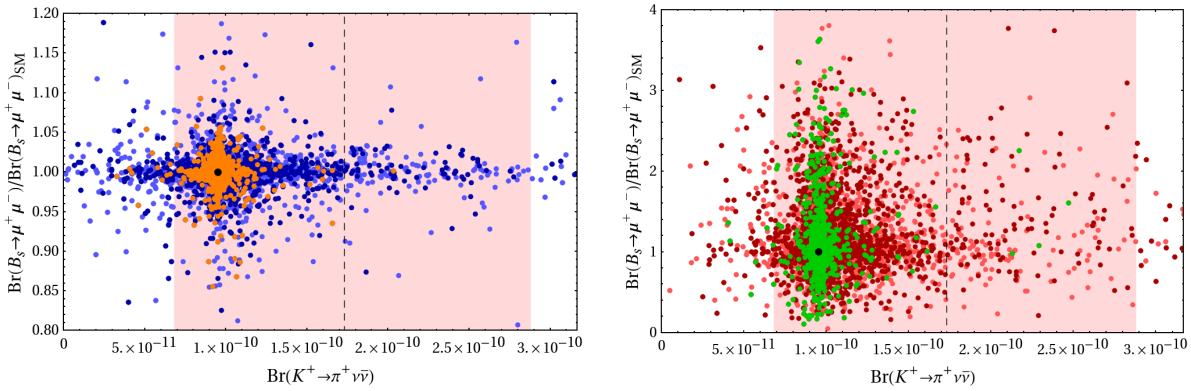

Figure 5.19: Left panel: The ratio $Br(B_s \to \mu^+\mu^-)/Br(B_s \to \mu^+\mu^-)_{\rm SM}$ as a function of $Br(K^+ \to \pi^+\nu\bar{\nu})$. Right panel: The same, but with removed custodial symmetry. The shaded area represents the experimental 1σ-range for $Br(K^+ \to \pi^+\nu\bar{\nu})$ with the central value indicated by the dashed vertical line. The black point represents the SM prediction.

here is strongly violated.
If the custodial protection is removed, as is shown in the right panels of figs. 5.19 and 5.20, the left-handed Z couplings are no longer suppressed and the possible NP effects in the K and B decay modes become comparable in size. This behavior can be quantitatively understood based on the hierarchy in the SM contributions, which is determined by (5.10) and on the hierarchy of the left-handed Z couplings given in (5.12).

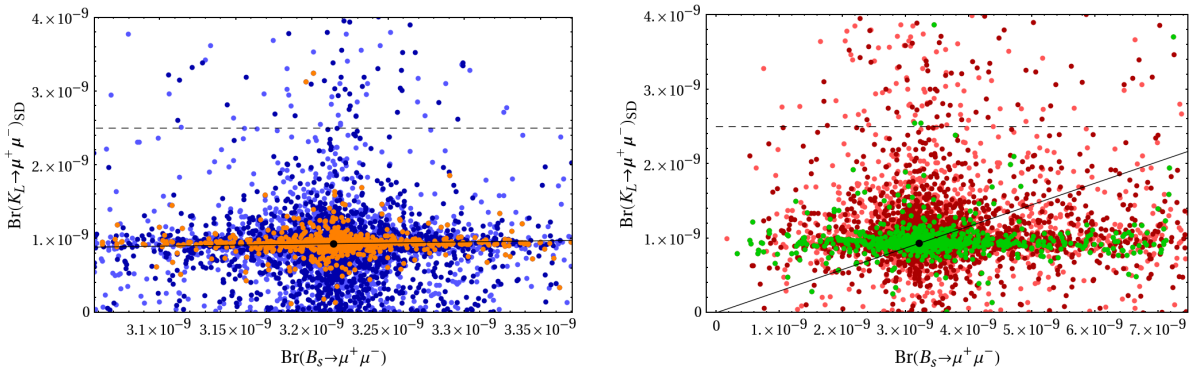

Figure 5.20: Left panel: $Br(K_L \to \mu^+\mu^-)_{\rm SD}$ as a function of $Br(B_s \to \mu^+\mu^-)$. Right panel: The same, but with removed custodial symmetry. The dashed horizontal line corresponds to the indirect bound (4.78) on $Br(K_L \to \mu^+\mu^-)_{\rm SD}$ while the solid line indicates the CMFV correlation. The black point represents the SM prediction.

5.4 Comparison to Other Models of New Physics

In the previous sections 5.2 and 5.3 we have identified a number of parameter independent phenomenological correlations and properties of the RSc. These features are

characteristic for the RSc and can be used to distinguish it from other models of NP. To demonstrate how and under which circumstances this can be achieved we will in the following perform an explicit comparison with two selected NP models: the Littlest Higgs model with T-parity and the SM with a sequential fourth generation of quarks.

5.4.1 The Littlest Higgs Model with T-Parity

One way to protect the Higgs mass from large corrections and thereby resolve the little hierarchy problem is to let the Higgs arise as a pseudo Goldstone boson of a spontaneously broken (approximate) global symmetry [188, 189]. The characteristic features of *little Higgs* models [190, 191] is that the symmetry breaking of the global symmetry occurs *collectively* such that corrections to the Higgs potential at the 1-loop level diverge at most logarithmically. The most economic implementation of collective symmetry breaking is achieved in the case of the *Littlest Higgs* model [192] (LH), which is based on the symmetry breaking pattern $SU(5) \to SO(5)$ and in which the additional gauge bosons A_H, Z_H, $W_H^\pm$, as well as a heavy partner to the top quark and a phenomenologically irrelevant scalar triplet Φ are present. By construction, the LH model is an effective theory with a cut-off $\Lambda \simeq 4\pi f_{\rm LH}$, where $f_{\rm LH}$ is the scale at which the global symmetry is spontaneously broken. To prevent tree level exchanges of the additional gauge bosons, in which case EWPT would imply a strong bound on the NP scale $f_{\rm LH}$, a discrete $\mathbb{Z}_2$ symmetry denoted *T-parity* [193, 194] is introduced which then allows a symmetry breaking scale as low as $f_{\rm LH} \simeq 500\,\text{GeV}$. Phenomenological consistency of the resulting *Littlest Higgs model with T-parity* (LHT) requires the additional introduction of a second, T-odd, top partner and of three generations of *mirror quarks and leptons* [195]. The masses of the additional particles depend on the symmetry breaking scale and are typically $\sim (300 - 1500)\,\text{GeV}$. While the LH model belonged to the class of MFV models and NP effects were found to be small [196, 197], the interactions of the mirror quarks with SM quarks and heavy gauge bosons effectively introduce an additional mixing matrix V_{Hd} [198] with $3 + 3$ additional flavor parameters [110], such that the LHT model is beyond MFV. On the other hand, NP in the LHT enters exclusively through left-handed couplings and accordingly no non-SM operators are induced. From this pattern we can expect that there are significant effects in flavor violating observables, but also that there are distinct correlations between different observables. A number of flavor analyses have been performed in [120, 199–205], and a recent numerical update can be found in [206]. In the following we will highlight the observables that allow for the most definite distinction from the RSc.

In fig. 5.21 we show the semileptonic CP asymmetry A_{SL}^s as a function of $S_{\psi\phi}$ in the LHT. Also here the decay amplitude for $B \to \psi\phi$ receives no additional weak phase and hence there is a strong correlation between A_{SL}^s and $S_{\psi\phi}$. In contrast to the RSc (cf. fig. 5.9), $S_{\psi\phi}$ can hardly be enhanced beyond ~ 0.2 which would seriously challenge the LHT model if the recent data suggesting $S_{\psi\phi} \simeq 0.7$ is confirmed.

In CP violation in the B_s system the difference between the LHT and RSc models is

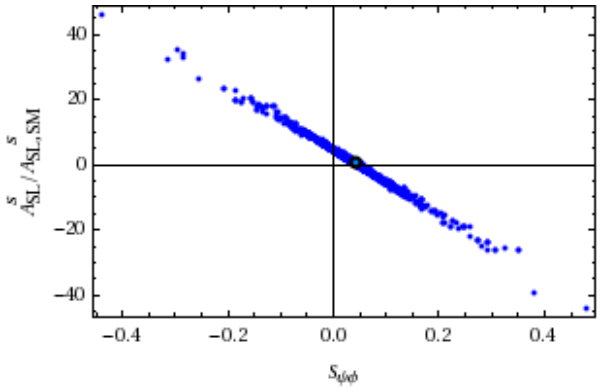

Figure 5.21: A^s_{SL} as a function of $S_{\psi\phi}$ in the LHT (figure taken from [120]). The black circle represents the SM prediction.

found to be only gradual, but due to the different coupling structure in both models we expect a more drastic discrepancy in the correlations between rare K decays. In fig. 5.22 we show the correlations between $Br(K^+ \to \pi^+\nu\bar{\nu})$ and $Br(K_L \to \pi^0\nu\bar{\nu})$ (left panel) and $Br(K_L \to \mu^+\mu^-)_{\text{SD}}$ (right panel). We note that while the overall amount of possible NP effects is roughly comparable in both models, in the $K \to \pi\nu\bar{\nu}$ system (cf. fig. 5.12) there now is a strong correlation between both branching ratios which results in two distinct branches in the $Br(K \to \pi\nu\bar{\nu})$ plane. This correlation implies that if the measurement of $Br(K^+ \to \pi^+\nu\bar{\nu})$ is confirmed, $Br(K_L \to \pi^0\nu\bar{\nu})$ in the LHT is predicted to be essentially SM-like. In the RSc no such prediction for the latter branching ratio can be given. The reason for this different behavior is that due to the absence of new operators in the LHT and due to the universality of CP phases, $\Delta S = 2$ and $\Delta S = 1$ observables are strongly related and thus the constraint on the ϵ_K parameter excludes large areas in the $Br(K \to \pi\nu\bar{\nu})$ plane. In the RSc on the other hand, left-right operators contribute significantly to the ϵ_K parameter, thus spoiling the relation between the $\Delta S = 2$ and $\Delta S = 1$ sectors. For a more detailed explanation in a model-independent framework the reader is referred to [145]. As already mentioned, the $K \to \pi\nu\bar{\nu}$ system thus can be seen as a sensitive probe of the operator structure of NP models.

Also in the case of $Br(K_L \to \mu^+\mu^-)$ and $Br(K^+ \to \pi^+\nu\bar{\nu})$ we observe a correlation in the LHT that is very different from the one that was found in the context of the RSc (cf. fig. 5.15). In fact, the correlation in the LHT strongly resembles the one obtained for the case of removed custodial protection in the RSc. This once more emphasizes that in the LHT left-handed couplings play the dominant role while in the RSc this part is taken by the right-handed couplings unless the custodial protection is absent. If we further assume that the central experimental value for $Br(K^+ \to \pi^+\nu\bar{\nu})$ will continue to stay above the SM value, this would imply an almost vanishing value for $Br(K_L \to \mu^+\mu^-)_{\text{SD}}$ in the RSc, while the LHT predicts a SD contribution to the branching ratio that is very close to the indirect bound (4.78).

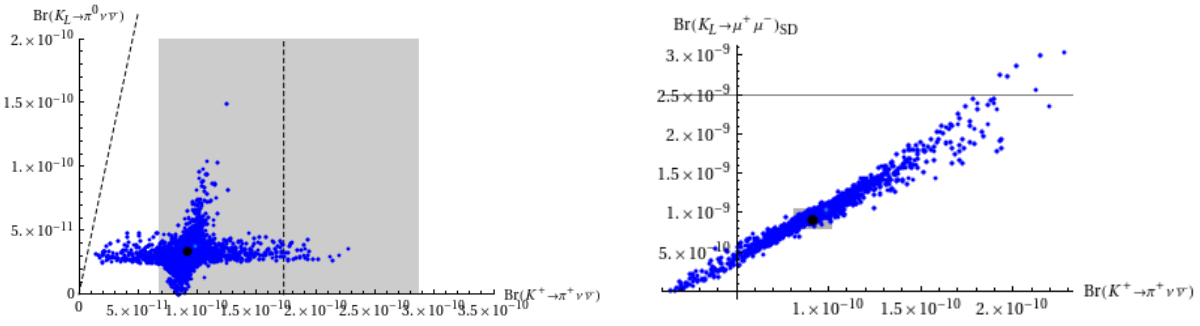

Figure 5.22: Correlations between rare K decay branching ratios in the LHT. Left panel: $Br(K_L \to \pi^0\nu\bar{\nu})$ as a function of $Br(K^+ \to \pi^+\nu\bar{\nu})$. The shaded area represents the experimental 1σ-range for $Br(K^+ \to \pi^+\nu\bar{\nu})$ with the central value indicated by the dashed vertical line. Right panel: $Br(K_L \to \mu^+\mu^-)_{\rm SD}$ as a function of $Br(K^+ \to \pi^+\nu\bar{\nu})$. The dashed horizontal line corresponds to the indirect bound (4.78) on $Br(K_L \to \mu^+\mu^-)_{\rm SD}$ and the black points represent the respective SM predictions. Both figures were taken from [206].

To summarize, we have seen that in particular the time-dependent CP asymmetry $S_{\psi\phi}$, the branching ratios in the $K \to \pi\nu\bar{\nu}$ system and the SD contribution to $Br(K_L \to \mu^+\mu^-)$ would, if measured with sufficient accuracy, provide an excellent chance to distinguish between the RSc and LHT models or even to strongly disfavor both of them. On the other hand, a number of qualitative features are shared by both models. Among them are the comparably small effects in rare B decays, a mutual exclusiveness of large effects in rare K decays and $S_{\psi\phi}$[14] as well as the strictly linear correlations between $Br(K_L \to \pi^0\ell^+\ell^-)$ and $Br(K_L \to \pi^0\nu\bar{\nu})$ which signal the universality of the CP phase in these modes and the absence of scalar operators.

5.4.2 The Standard Model with a Fourth Generation

The SM with a sequential fourth generation of quarks and leptons is one of the simplest extensions of the SM. While it does not solve any of the conceptual problems that afflict the SM, the SM4 is likely to have a number of profound implications. For instance, while being consistent with EWPT [207–212], the presence of a fourth generation could allow to reconcile the lower bound on the Higgs mass from LEPII with the SM fit [208, 210, 213]. Furthermore, $SU(5)$ gauge coupling unification [214], EW baryogenesis [215–217] and dynamical EWSB [218–223] could be viable in the context of the SM4.
The mass of the additional top quark t' which is relevant for additional flavor violation in the down-sector has to lie in the range $300\,\text{GeV} \leq m_{t'} \leq 600\,\text{GeV}$ (with the lower bound given by non-observation and EWPT and the upper bound being imposed by the Landau pole of the t' Yukawa coupling) and thus is lighter than the additional particles in both the LHT and RSc models. Apart from that the chief features of the SM4 can be

[14] It should be noted that the deeper reason for this feature is different in both models. In the case of the LHT it is given by the severe constraint on the ϵ_K parameter which excludes simultaneous large effects [111].

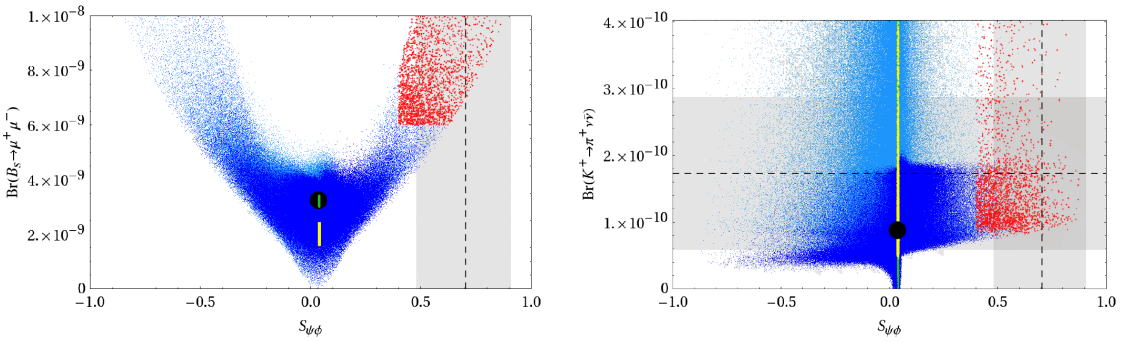

Figure 5.23: Left Panel: $Br(B_s \to \mu^+\mu^-)$ as a function of $S_{\psi\phi}$ in the SM4. Right panel: $Br(K^+ \to \pi^+\nu\bar{\nu})$ as a function of $S_{\psi\phi}$ in the SM4. The shaded areas represent the experimental 1σ-ranges with the central values indicated by dashed lines and the black points represent the respective SM predictions. Both figures were taken from [139].

summarized by stating that the effects of the t' do not decouple, in contrast to the LHT and RSc models, and that also in the SM4 no new operators are generated besides those that are present in the SM. In the flavor sector the generalization to four generations introduces three additional mixing angles θ_{i4} $(i = 1, 2, 3)$, and two additional phases δ_{14}, δ_{24}.

In a recent analysis [139] we investigated the possible flavor effects in the SM4 and found spectacular deviations from the SM in various observables. While the following discussion is based on that paper, numerous additional analyses have been performed in [209–212, 224–230]. In the following we will highlight the phenomenological features of the SM4 that most spectacularly deviate from those identified in the RSc.

We start with the correlation between $Br(B_s \to \mu^+\mu^-)$ and $S_{\psi\phi}$ which is shown in the left panel of fig. 5.23. In the RSc the former observable was found to be potentially enhanced by at most 5% beyond its SM value. In the SM4 on the other hand, $Br(B_s \to \mu^+\mu^-)$ not only can be enhanced by more than a factor of three, but is also subject to a strong positive correlation with $S_{\psi\phi}$. Thus if the large measured value for $S_{\psi\phi}$ prevails, a SM-like value for $Br(B_s \to \mu^+\mu^-)$ would put the SM4 under pressure while an enhanced branching ratio clearly would disfavor the RSc.

In the right panel of fig. 5.23 we have plotted $Br(K^+ \to \pi^+\nu\bar{\nu})$ as a function of $S_{\psi\phi}$. By itself this plot shows the large possible enhancements in both observables that are possible in the SM4 whereas no clear correlation is visible. Additionally we notice that in contrast to the RSc large simultaneous enhancements in $S_{\psi\phi}$ and $Br(K^+ \to \pi^+\nu\bar{\nu})$ are possible. So while a confirmation of the current central values of these observables would certainly rule out the RSc, the SM4 could easily accommodate that.

The correlations between rare K decays were identified as a powerful probe of a model's operator structure. In the left panel of fig. 5.24 we show $Br(K_L \to \pi^0\nu\bar{\nu})$ as a function of $Br(K^+ \to \pi^+\nu\bar{\nu})$ in the SM4. The possible enhancement in the $K^+ \to \pi^+\nu\bar{\nu}$ mode is found to be roughly a factor of four, while $K_L \to \pi^0\nu\bar{\nu}$ can be enhanced by more than a

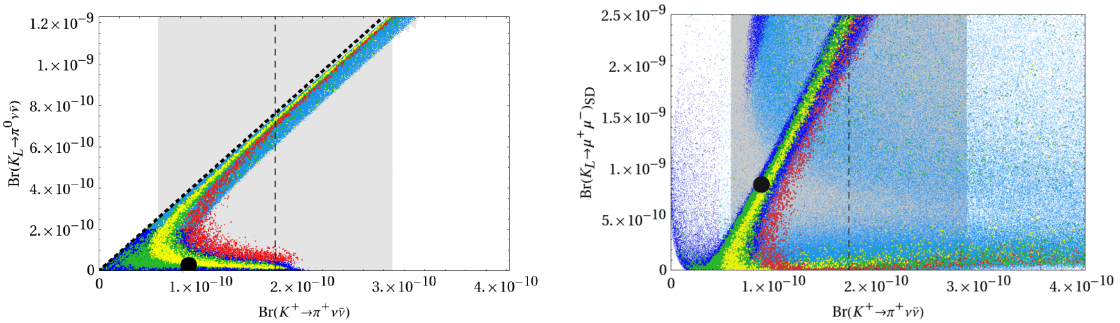

Figure 5.24: Correlations between rare K decay branching ratios in the SM4. Left panel: $Br(K_L \to \pi^0\nu\bar{\nu})$ as a function of $Br(K^+ \to \pi^+\nu\bar{\nu})$. Right panel: $Br(K_L \to \mu^+\mu^-)_{\rm SD}$ as a function of $Br(K^+ \to \pi^+\nu\bar{\nu})$. The shaded areas represent the experimental 1σ-ranges with the central values indicated by dashed lines and the black points represent the respective SM predictions. Both figures were taken from [139].

factor of 40. Similar to the LHT there is a clear branch structure in the $Br(K \to \pi\nu\bar{\nu})$ plane that arises because of the purely left-handed NP couplings and the universality of the CP phase in the $K \to \pi\nu\bar{\nu}$ system and $K^0 - \bar{K}^0$ mixing [145]. In the SM4 the upper branch saturates the GN bound, and on the lower branch $Br(K^+ \to \pi^+\nu\bar{\nu})$ is bounded from above such that branching ratios cannot exceed the central experimental value by more than 10%. Thus, finding the two branching ratios in the $K \to \pi\nu\bar{\nu}$ system to lie in between the two branches in the left panel of fig. 5.24 or finding $Br(K^+ \to \pi^+\nu\bar{\nu})$ significantly beyond the current experimental value for SM-like $Br(K_L \to \pi^0\nu\bar{\nu})$ would put the SM4 under pressure while such an outcome is clearly possible within the RSc. On the other hand, if in the future $Br(K^+ \to \pi\nu\bar{\nu})$ is found at or beyond its current experimental central value and $Br(K_L \to \pi^0\nu\bar{\nu})$ is found close to the GN bound, the RSc would be disfavored although such a result could in principle be obtained in fine tuned scenarios.
A further possibility to distinguish between the different NP models under consideration is through $Br(K_L \to \mu^+\mu^-)_{\rm SD}$ and $Br(K^+ \to \pi^+\nu\bar{\nu})$ which are shown for the SM4 in the right panel of fig. 5.24. Here the correlation is less clear-cut than in the RSc and LHT models: While there is a pronounced branch on which both branching ratios are either simultaneously enhanced or suppressed, a number of additional structures can be identified such that basically every outcome for the branching ratios is possible[15]. Hence future experimental and theoretical results that strongly disfavor the RSc, such as $Br(K^+ \to \pi^+\nu\bar{\nu})$ being measured close to the current experimental central value and $Br(K_L \to \mu^+\mu^-)_{\rm SD}$ being determined to be SM-like or larger, can be easily reproduced within the SM4 framework.

In conclusion, the most characteristic features of the SM4 that allow to tell it apart from

[15] In [139] it has been shown that the different structures in the right panel of fig. 5.24 can be related to different classes of parameter sets that are characterized by the scaling (n_1, n_2, n_3) of the mixing angles $(\theta_{14}, \theta_{24}, \theta_{34})$ as (approximate) powers of $\lambda_C = |V_{us}|$.

both the LHT and RSc models are the following:

- The SM4 has the potential to generate branching ratios for $B_s \to \mu^+\mu^-$ that exceed 10^{-8} which clearly is impossible in the RSc and LHT models,
- there is a positive correlation between $Br(B_s \to \mu^+\mu^-)$ and $S_{\psi\phi}$,
- simultaneous enhancements in $Br(K \to \pi\nu\bar{\nu})$ and $S_{\psi\phi}$ are possible,
- the correlation between $Br(K^+ \to \pi^+\nu\bar{\nu})$ and $Br(K_L \to \mu^+\mu^-)_{\rm SD}$ allows for values that are off the main linear branch,
- and finally the $Br(K \to \pi\nu\bar{\nu})$ system displays a clear branch structure as is expected from the operator structure of the SM4, with the upper branch saturating the GN bound and the lower branch being cut off not far beyond the experimental central value for $Br(K^+ \to \pi^+\nu\bar{\nu})$.

On the other hand since also in the SM4 no scalar operators are present and the CP phase entering CP violating K decays is universal, the linear correlations between $Br(K_L \to \pi^0\ell^+\ell^-)$ and $Br(K_L \to \pi^0\nu\bar{\nu})$ in the SM4 are very similar to those in the LHT and RSc models although the absolute size of enhancements is larger. In particular we find that the former modes can be enhanced by as much as an order of magnitude while in the latter mode an enhancement by a factor of 40 is possible.

Chapter 6

Conclusions

From the model building point of view, the RS model with custodial symmetry and bulk fermions offers an interesting solution to two of the main problems of the SM: While the gauge hierarchy problem is solved by virtue of the warped background metric, the generation of a hierarchical quark spectrum is achieved by the non-uniform localization of quark fields along the fifth dimension. Since the localization of bulk fermions depends exponentially on their $\mathcal{O}(1)$ bulk mass parameters, large hierarchies in masses and mixing angles can be obtained in a natural manner, as we have demonstrated explicitly. As a side effect, the non-uniform localization of quark fields also induces tree level FCNCs. We have carefully studied the two main origins hereof, namely the flavor dependent couplings of KK gauge bosons to SM quarks and the mixing of SM quarks with heavy KK states. We have shown explicitly that the first contribution is dominant and that a pattern of flavor violation arises which implies smaller effects for light quarks and larger effects for heavy quarks. This fact, which is commonly referred to as the RS-GIM mechanism, is responsible for the comparably small corrections to the particularly well measured K physics observables and thus significantly ameliorates the flavor coincidence problem. While this is a rather qualitative statement, we set out to perform a quantitative analysis of the impact on flavor observables in the RSc. Based on our results for the flavor violating couplings, we derived analytic expressions for their impact on particle-antiparticle oscillations and rare decays and subsequently performed a global numerical analysis of flavor observables in the RSc.
The first part of this analysis was devoted to the implications of the RSc for the observables in the $\Delta F = 2$ sector. Here we concentrated on the the mass differences ΔM_K, ΔM_d and ΔM_s in the neutral K and B meson systems as well as on the measure of indirect CP violation in $K^0 - \bar{K}^0$ mixing, ϵ_K, on the CP asymmetries $S_{\psi K_S}$ and $S_{\psi\phi}$, the semileptonic CP asymmetry A_{SL}^s and the width difference $\Delta\Gamma_s$. To be able to make an assessment of how naturally the available experimental constraints can be satisfied in the RSc, we also considered the fine tuning in each observable. The results of our analysis of $\Delta F = 2$ observables can be summarized as follow:

- $K^0 - \bar{K}^0$ oscillations are found to be dominantly affected by the contributions of the $\mathcal{Q}_2^{LR}$ operator which receives strong chiral and QCD enhancements. As this

operator cannot be induced by EW gauge bosons, tree level exchanges of KK gluons yield the most important contributions to $\Delta S = 2$ observables for all viable values of the fundamental QCD coupling constant $3 \leq g_s \leq 6$.

- The strong chiral and QCD enhancement encountered in the K system is absent in the case of $B^0 - \bar{B}^0$ oscillations and other operators, most notably $\mathcal{Q}_1^{VLL}$, become relevant. Consequently, tree level exchanges of the EW gauge bosons Z_H and Z' have a considerable impact on $\Delta B = 2$ observables and need to be taken into account.

- The contributions of the Higgs boson, the KK photon $A^{(1)}$ and the Z boson to $\Delta F = 2$ observables on the other hand are found to be negligible, where the suppression of the latter is a consequence of the custodial protection of the $Zb_L\bar{b}_L$ coupling.

- Although the generic bound $M_{\rm KK} \gtrsim 20\,\text{TeV}$ [99] which is induced by the ϵ_K constraint is roughly confirmed by our analysis, the RSc can accommodate this constraint for considerably lower values $M_{\rm KK} \simeq (2-3)\,\text{TeV}$ with only small or moderate fine tuning, if the assumption of strictly anarchic Yukawa couplings is relaxed. On top of this, the remaining experimental constraints in the $\Delta F = 2$ sector, namely ΔM_K, $\Delta M_{d,s}$ and $S_{\psi K_S}$ can be simultaneously satisfied almost without any necessary fine tuning.

- After imposing all available $\Delta F = 2$ constraints, the time-dependent CP asymmetry $S_{\psi\phi}$ can still be strongly enhanced beyond its small SM prediction such that the full range $-1 \leq S_{\psi\phi} \leq 1$ can be populated. Due to the model independent correlation [137] between the semileptonic CP asymmetry A_{SL}^s and $S_{\psi\phi}$ also the former observable can be enhanced by roughly two orders of magnitude beyond its SM value. These possible enhancements are to a good approximation independent of the choice of the fundamental QCD coupling constant $3 \leq g_s \leq 6$.

The second part of our numerical analysis addressed the quantitative effects in rare K and B decays which are still possible after all available constraints from the $\Delta F = 2$ sector have been imposed. Here we considered the branching ratios for the decay modes $K^+ \to \pi^+\nu\bar{\nu}$, $K_L \to \pi^0\nu\bar{\nu}$, $K_L \to \pi^0\ell^+\ell^-$ ($\ell = e, \mu$), $K_L \to \mu^+\mu^-$, $B_{d,s} \to \mu^+\mu^-$ and $B \to X_{d,s}\nu\bar{\nu}$. Apart from giving the mere possible enhancements in these branching ratios we also analyzed in detail the emerging parameter independent correlations between different branching ratios and also between $\Delta F = 2$ and $\Delta F = 1$ observables. The results of this part of our analysis are summarized by the following statements:

- Taking into consideration the different masses and coupling strengths to quarks and leptons of the EW gauge bosons, the right-handed Z couplings are found to yield the dominant contribution to rare K and B decays. This fact is due to the custodial suppression of the left-handed Z couplings and is responsible for a very specific pattern of flavor effects and the emergence of a number of interesting correlations between different branching ratios.

- In particular, enhancements in rare K decay branching ratios are potentially large, but only very much smaller effects are observed in the $B_{d,s}$ systems. This hierarchical pattern is unique to the RS model with custodial symmetry and is absent in the minimal RS model.

- Quantitatively, $Br(K_L \to \pi^0\nu\bar{\nu})$, $Br(K^+ \to \pi^+\nu\bar{\nu})$, $Br(K_L \to \mu^+\mu^-)_{\rm SD}$ can be enhanced by factors of two to three and $Br(K_L \to \pi^0\ell^+\ell^-)$ by roughly 40%, while the enhancements in B decay modes are typically below 10%. As was the case for the CP asymmetries $S_{\psi\phi}$ and A_{SL}^s, we find that also here the ranges for possible enhancements are independent of the fundamental QCD coupling constant $3 \leq g_s \leq 6$.

- Connected to this pattern of flavor violation we observe that the flavor universality in the generalized loop functions X, Y, Z is strongly broken. This breakdown of universality can also be observed at the level of branching ratios where the relevant CMFV relations are strongly violated.

- We identify a number of interesting correlations between different rare K decay modes but also between the latter and the CP asymmetry $S_{\psi\phi}$.

  In contrast to models with dominant left-handed currents, where the $K \to \pi\nu\bar{\nu}$ modes are strongly correlated, there is no visible correlation in the RSc.

  The short distance contribution to $Br(K_L \to \mu^+\mu^-)$ is inversely correlated to the branching ratio of the $K^+ \to \pi^+\nu\bar{\nu}$ decay mode such that an enhancement in either branching ratio is accompanied by a suppression in the other mode. This behavior can be traced back to the dominance of the right-handed Z couplings.

  Finally, the CP asymmetry $S_{\psi\phi}$ is strongly correlated with rare K decay branching ratios. This correlation implies that simultaneous enhancements in both systems beyond the respective SM predictions are disfavored in the RSc. Unlike the previous correlations, this result is independent of the EW gauge group and hence is present in both the RSc and RSm models.

These results, and in particular the specific correlations between various different observables that we have identified, allow in principle for an experimental test of the RSc and a clear distinction from other models of NP. We have indicated how such a distinction can be performed for different future experimental outcomes in the particular case of the LHT and SM4 models. Results for key observables in this context will hopefully be supplied within the next years by the upcoming flavor experiments NA62 ($K^+ \to \pi^+\nu\bar{\nu}$) and LHCb ($S_{\psi\phi}$, $B_s \to \mu^+\mu^-$) at CERN as well as E14 at KEK ($K_L \to \pi^0\nu\bar{\nu}$). In this sense flavor physics really is complementary to direct NP searches in high energy collisions, as will be performed at the ATLAS and CMS experiments, and could even lead to the discovery of the first real evidence for physics beyond the Standard Model.

Appendix A

Couplings and Charge Factors

In this appendix we list all the couplings and the charge factors that were used throughout this thesis, and that can be easily computed using

$$g_Z^{4D}(F) = \frac{g^{4D}}{\cos\psi}\left[T_L^3 - (\sin\psi)^2 Q\right] ,$$
$$\kappa^{4D}(F) = \frac{g^{4D}}{\cos\phi}\left[T_R^3 - (Q - T_L^3)\sin^2\phi\right] , \tag{A.1}$$

together with tables A.1 and A.2. First, we give the charge factors in the couplings of SM down-type quarks (both left- and right-handed) to the Z, Z_X gauge bosons,

$$g_{Z,L}^{4D}(d) = \frac{g^{4D}}{\cos\psi}\left[-\frac{1}{2} + \frac{1}{3}\sin^2\psi\right] , \qquad g_{Z,R}^{4D}(d) = \frac{g^{4D}}{\cos\psi}\left[\frac{1}{3}\sin^2\psi\right] ,$$
$$\kappa_1^{4D}(d) = \frac{g^{4D}}{\cos\phi}\left[-\frac{1}{2} - \frac{1}{6}\sin^2\phi\right] , \qquad \kappa_5^{4D}(d) = \frac{g^{4D}}{\cos\phi}\left[-1 + \frac{1}{3}\sin^2\phi\right] . \tag{A.2}$$

Analogously, the charge factors in the couplings of SM up-type quarks (both left- and

Field	Charge Q	Isospin T_L^3	Isospin T_R^3
$q_L^{u_i(0)}(++)$	$\frac{2}{3}$	$\frac{1}{2}$	$-\frac{1}{2}$
$q_L^{d_i(0)}(++)$	$-\frac{1}{3}$	$-\frac{1}{2}$	$-\frac{1}{2}$
$u_R^i(++)$	$\frac{2}{3}$	0	0
$D_R^i(++)$	$-\frac{1}{3}$	0	-1

Table A.1: SM quark content of the RSc.

right-handed) to the Z, Z_X gauge bosons read:

$$g_{Z,L}^{4D}(u) = \frac{g^{4D}}{\cos\psi}\left[\frac{1}{2} - \frac{2}{3}\sin^2\psi\right], \qquad g_{Z,R}^{4D}(u) = \frac{g^{4D}}{\cos\psi}\left[-\frac{2}{3}\sin^2\psi\right],$$
$$\kappa_1^{4D}(u) = \frac{g^{4D}}{\cos\phi}\left[-\frac{1}{2} - \frac{1}{6}\sin^2\phi\right], \qquad \kappa_3^{4D}(u) = \frac{g^{4D}}{\cos\phi}\left[-\frac{2}{3}\sin^2\phi\right], \tag{A.3}$$

and the charge factors in the couplings of the additional (vector-like) fermion fields (χ^{u^i}, χ^{d^i}, U'^i, U''^i and D'^i) to the Z, Z_X gauge bosons are given by

$$g_Z^{4D}\left(\chi^u\right) = \frac{g^{4D}}{\cos\psi}\left[\frac{1}{2} - \frac{5}{3}\sin^2\psi\right], \qquad \kappa^{4D}\left(\chi^u\right) = \frac{g^{4D}}{\cos\phi}\left[\frac{1}{2} - \frac{7}{6}\sin^2\phi\right],$$
$$g_Z^{4D}\left(\chi^d\right) = \frac{g^{4D}}{\cos\psi}\left[-\frac{1}{2} - \frac{2}{3}\sin^2\psi\right], \qquad \kappa^{4D}\left(\chi^d\right) = \frac{g^{4D}}{\cos\phi}\left[-\frac{1}{2} + \frac{5}{6}\sin^2\phi\right],$$
$$g_Z^{4D}\left(U'\right) = g_Z(U'') = \frac{g^{4D}}{\cos\psi}\left[-\frac{2}{3}\sin^2\psi\right], \qquad \kappa^{4D}\left(U'\right) = \kappa\left(U''\right) = \frac{g^{4D}}{\cos\phi}\left[-\frac{2}{3}\sin^2\phi\right],$$
$$g_Z^{4D}\left(D'\right) = \frac{g^{4D}}{\cos\psi}\left[-1 + \frac{1}{3}\sin^2\psi\right], \qquad \kappa^{4D}\left(D'\right) = \frac{g^{4D}}{\cos\psi}\left[\frac{4}{3}\sin^2\phi\right]. \tag{A.4}$$

The lepton couplings of Z, Z_H and $A^{(1)}$ that were used in the present work can be obtained from the corresponding quark couplings by

- replacing the c's in all $\underset{00}{\mathcal{R}}(++)_{L,R}$ by ± 0.7 for left- and right-handed lepton modes,
- adjusting the couplings and charge factors properly.

The relevant couplings can be determined through (A.1) and for the charged leptons are given by

$$g_{Z,L}^{4\mathrm{D}}(\ell) = \frac{g^{4\mathrm{D}}}{\cos\psi}\left(-\frac{1}{2} + \sin^2\psi\right), \qquad g_{Z,R}^{4\mathrm{D}}(\ell) = \frac{g^{4\mathrm{D}}}{\cos\psi}\sin^2\psi\,,$$
$$\kappa_1^{4\mathrm{D}}(\ell) = -\frac{1}{2}g^{4\mathrm{D}}\cos\phi\,, \qquad \kappa_5^{4\mathrm{D}}(\ell) = -g^{4\mathrm{D}}\cos\phi\,, \tag{A.5}$$

while for the case of neutrinos we find

$$g_{Z,L}^{4\mathrm{D}}(\nu) = \frac{1}{2}\frac{g^{4\mathrm{D}}}{\cos\psi}\,, \qquad g_{Z,R}^{4\mathrm{D}}(\nu) = 0\,, \tag{A.6}$$

$$\kappa_1^{4\mathrm{D}}(\nu) = -\frac{1}{2}g^{4\mathrm{D}}\cos\phi\,, \qquad \kappa_5^{4\mathrm{D}}(\nu) = 0\,. \tag{A.7}$$

The lepton couplings that are most relevant for our analysis are those of the Z boson. These couplings are dominated by the $Z^{(0)}$ admixture of the Z mass eigenstate and accordingly are given by

$$\Delta_{L,R}^{\ell\ell}(Z) = g_{Z,L,R}^{4D}(\ell)\,, \qquad \Delta_L^{\nu\nu}(Z) = g_{Z,L}^{4D}(\nu)\,. \tag{A.8}$$

For the lepton couplings of Z_H and Z' we finally obtain the explicit expressions

$$\Delta_L^{\ell\ell,\nu\nu}(Z_H) = \frac{1}{\sqrt{2}L}\int_0^L dy\, e^{ky}\,[f_L(y,c=0.7)]^2\left(g_{Z,L}^{4D}(\ell,\nu)\cos\phi\, g(y) + \frac{\kappa_1^{4D}(\ell,\nu)}{\cos\psi}\,\tilde{g}(y)\right),$$

$$\Delta_R^{\ell\ell,\nu\nu}(Z_H) = \frac{1}{\sqrt{2}L}\int_0^L dy\, e^{ky}\,[f_R(y,c=0.7)]^2\left(g_{Z,R}^{4D}(\ell,\nu)\cos\phi\, g(y) + \frac{\kappa_5^{4D}(\ell,\nu)}{\cos\psi}\,\tilde{g}(y)\right),$$

$$\begin{aligned}\Delta_L^{\ell\ell,\nu\nu}(Z') &= -\frac{g^2v^2\mathcal{I}_1}{2\sqrt{2}LM^2\cos\psi}g_{Z,L}(\ell,\nu)\\ &\quad+\frac{1}{\sqrt{2}L}\int_0^L dy\, e^{ky}\,[f_L(y,c=0.7)]^2\left(\cos\phi\kappa_1^{4D}(\ell,\nu)\,\tilde{g}(y) - \frac{g_{Z,L}}{\cos\psi}\,g(y)\right),\\ \Delta_R^{\ell\ell,\nu\nu}(Z') &= -\frac{g^2v^2\mathcal{I}_1}{2\sqrt{2}LM^2\cos\psi}g_{Z,R}(\ell,\nu)\\ &\quad+\frac{1}{\sqrt{2}L}\int_0^L dy\, e^{ky}\,[f_R(y,c=0.7)]^2\left(\cos\phi\kappa_5^{4D}(\ell,\nu)\,\tilde{g}(y) - \frac{g_{Z,R}}{\cos\psi}\,g(y)\right).\end{aligned} \quad \text{(A.9)}$$

Field	Charge Q	Isospin T_L^3	Isospin T_R^3
$\chi_L^{u_i}(-+)$	$\frac{5}{3}$	$\frac{1}{2}$	$\frac{1}{2}$
$\chi_L^{d_i}(-+)$	$\frac{2}{3}$	$-\frac{1}{2}$	$\frac{1}{2}$
$q_L^{u_i}(++)$	$\frac{2}{3}$	$\frac{1}{2}$	$-\frac{1}{2}$
$q_L^{d_i}(++)$	$-\frac{1}{3}$	$-\frac{1}{2}$	$-\frac{1}{2}$
$u_L^i(--)$	$\frac{2}{3}$	0	0
$\psi_L'^i(+-)$	$\frac{5}{3}$	1	0
$\psi_L''^i(+-)$	$\frac{5}{3}$	0	1
$U_L'^i(+-)$	$\frac{2}{3}$	0	0
$U_L''^i(+-)$	$\frac{2}{3}$	0	0
$D_L'^i(+-)$	$-\frac{1}{3}$	-1	0
$D_L^i(--)$	$-\frac{1}{3}$	0	-1

Table A.2: Heavy quark content of the RSc. The quantum numbers of the the right-handed heavy quarks are the same and only their parities on the boundaries have to be reversed.

Bibliography

[1] G. 't Hooft, *Naturalness, chiral symmetry, and spontaneous chiral symmetry breaking*, *NATO Adv. Study Inst. Ser. B Phys.* **59** (1980) 135.

[2] J. Wess and J. Bagger, *Supersymmetry and supergravity*, . Princeton, USA: Univ. Pr. (1992) 259 p.

[3] S. P. Martin, *A supersymmetry primer*, `hep-ph/9709356`.

[4] M. E. Peskin, *Supersymmetry in Elementary Particle Physics*, `arXiv:0801.1928`.

[5] M. M. Nojiri *et al.*, *Physics Beyond the Standard Model: Supersymmetry*, `arXiv:0802.3672`.

[6] E. Farhi and L. Susskind, *Technicolor*, *Phys. Rept.* **74** (1981) 277.

[7] R. S. Chivukula and H. Georgi, *Composite Technicolor Standard Model*, *Phys. Lett.* **B188** (1987) 99.

[8] N. Arkani-Hamed, S. Dimopoulos, and G. R. Dvali, *The hierarchy problem and new dimensions at a millimeter*, *Phys. Lett.* **B429** (1998) 263–272, [`hep-ph/9803315`].

[9] E. Dudas, S. Pokorski, and C. A. Savoy, *Soft scalar masses in supergravity with horizontal $U(1)_X$ gauge symmetry*, *Phys. Lett.* **B369** (1996) 255–261, [`hep-ph/9509410`].

[10] L. J. Hall and H. Murayama, *A Geometry of the generations*, *Phys. Rev. Lett.* **75** (1995) 3985–3988, [`hep-ph/9508296`].

[11] R. Barbieri, L. J. Hall, S. Raby, and A. Romanino, *Unified theories with $U(2)$ flavor symmetry*, *Nucl. Phys.* **B493** (1997) 3–26, [`hep-ph/9610449`].

[12] C. D. Froggatt, M. Gibson, and H. B. Nielsen, *Neutrino masses and mixings from an anomaly free $SMG \times U(1)^2$ model*, *Phys. Lett.* **B446** (1999) 256–266, [`hep-ph/9811265`].

[13] J. L. Chkareuli, C. D. Froggatt, and H. B. Nielsen, *Minimal mixing of quarks and leptons in the $SU(3)$ theory of flavour*, *Nucl. Phys.* **B626** (2002) 307–343, [hep-ph/0109156].

[14] S. F. King and G. G. Ross, *Fermion masses and mixing angles from $SU(3)$ family symmetry*, *Phys. Lett.* **B520** (2001) 243–253, [hep-ph/0108112].

[15] J. Kubo, A. Mondragon, M. Mondragon, and E. Rodriguez-Jauregui, *The flavor symmetry*, *Prog. Theor. Phys.* **109** (2003) 795–807, [hep-ph/0302196].

[16] G. L. Kane, S. F. King, I. N. R. Peddie, and L. Velasco-Sevilla, *Study of theory and phenomenology of some classes of family symmetry and unification models*, *JHEP* **08** (2005) 083, [hep-ph/0504038].

[17] M.-C. Chen and K. T. Mahanthappa, *From CKM matrix to MNS matrix: A model based on supersymmetric $SO(10) \times U(2)_F$ symmetry*, *Phys. Rev.* **D62** (2000) 113007, [hep-ph/0005292].

[18] G. Altarelli, F. Feruglio, and I. Masina, *From minimal to realistic supersymmetric $SU(5)$ grand unification*, *JHEP* **11** (2000) 040, [hep-ph/0007254].

[19] K. Agashe and C. D. Carone, *Supersymmetric flavor models and the $B \to \phi K_S$ anomaly*, *Phys. Rev.* **D68** (2003) 035017, [hep-ph/0304229].

[20] G. G. Ross, L. Velasco-Sevilla, and O. Vives, *Spontaneous CP violation and non-Abelian family symmetry in SUSY*, *Nucl. Phys.* **B692** (2004) 50–82, [hep-ph/0401064].

[21] R. Dermisek and S. Raby, *Bi-large neutrino mixing and CP violation in an $SO(10)$ SUSY GUT for fermion masses*, *Phys. Lett.* **B622** (2005) 327–338, [hep-ph/0507045].

[22] S. Antusch, S. F. King, and M. Malinsky, *Solving the SUSY Flavour and CP Problems with $SU(3)$ Family Symmetry*, *JHEP* **06** (2008) 068, [arXiv:0708.1282].

[23] L. Calibbi *et al.*, *FCNC and CP Violation Observables in a $SU(3)$-flavoured MSSM*, *Nucl. Phys.* **B831** (2010) 26–71, [arXiv:0907.4069].

[24] M. Albrecht, W. Altmannshofer, A. J. Buras, D. Guadagnoli, and D. M. Straub, *Challenging $SO(10)$ SUSY GUTs with family symmetries through FCNC processes*, *JHEP* **10** (2007) 055, [arXiv:0707.3954].

[25] W. Altmannshofer, D. Guadagnoli, S. Raby, and D. M. Straub, *SUSY GUTs with Yukawa unification: a go/no-go study using FCNC processes*, *Phys. Lett.* **B668** (2008) 385–391, [arXiv:0801.4363].

[26] L. Randall and R. Sundrum, *A large mass hierarchy from a small extra dimension*, *Phys. Rev. Lett.* **83** (1999) 3370–3373, [hep-ph/9905221].

[27] A. Pomarol, *Gauge bosons in a five-dimensional theory with localized gravity*, *Phys. Lett.* **B486** (2000) 153–157, [hep-ph/9911294].

[28] H. Davoudiasl, J. L. Hewett, and T. G. Rizzo, *Bulk gauge fields in the Randall-Sundrum model*, *Phys. Lett.* **B473** (2000) 43–49, [hep-ph/9911262].

[29] S. Chang, J. Hisano, H. Nakano, N. Okada, and M. Yamaguchi, *Bulk standard model in the Randall-Sundrum background*, *Phys. Rev.* **D62** (2000) 084025, [hep-ph/9912498].

[30] K. Agashe, A. Delgado, M. J. May, and R. Sundrum, *RS1, custodial isospin and precision tests*, *JHEP* **08** (2003) 050, [hep-ph/0308036].

[31] S. L. Glashow, J. Iliopoulos, and L. Maiani, *Weak Interactions with Lepton-Hadron Symmetry*, *Phys. Rev.* **D2** (1970) 1285–1292.

[32] M. E. Albrecht, M. Blanke, A. J. Buras, B. Duling, and K. Gemmler, *Electroweak and Flavour Structure of a Warped Extra Dimension with Custodial Protection*, *JHEP* **09** (2009) 064, [arXiv:0903.2415].

[33] M. Blanke, A. J. Buras, B. Duling, S. Gori, and A. Weiler, $\Delta F = 2$ *Observables and Fine-Tuning in a Warped Extra Dimension with Custodial Protection*, *JHEP* **03** (2009) 001, [arXiv:0809.1073].

[34] M. Blanke, A. J. Buras, B. Duling, K. Gemmler, and S. Gori, *Rare K and B Decays in a Warped Extra Dimension with Custodial Protection*, *JHEP* **03** (2009) 108, [arXiv:0812.3803].

[35] A. J. Buras, B. Duling, and S. Gori, *The Impact of Kaluza-Klein Fermions on Standard Model Fermion Couplings in a RS Model with Custodial Protection*, *JHEP* **09** (2009) 076, [arXiv:0905.2318].

[36] B. Duling, *A Comparative Study of Contributions to ϵ_K in the RS Model*, arXiv:0912.4208.

[37] G. Nordström, *Über die Möglichkeit, das elektromagnetische Feld und das Gravitationsfeld zu vereinigen*, *Phys. Z.* **15** (1914) 504–506.

[38] T. Kaluza, *On the Problem of Unity in Physics*, *Sitzungsber. Preuss. Akad. Wiss. Berlin (Math. Phys.)* **1921** (1921) 966–972.

[39] O. Klein, *Quantum theory and five-dimensional theory of relativity*, *Z. Phys.* **37** (1926) 895–906.

[40] J. Polchinski, *String theory. Vol. 1: An introduction to the bosonic string*, . Cambridge, UK: Univ. Pr. (1998) 402 p.

[41] J. Polchinski, *String theory. Vol. 2: Superstring theory and beyond*, . Cambridge, UK: Univ. Pr. (1998) 531 p.

[42] C. D. Hoyle *et al.*, *Sub-millimeter tests of the gravitational inverse-square law*, *Phys. Rev.* **D70** (2004) 042004, [hep-ph/0405262].

[43] E. G. Adelberger, J. H. Gundlach, B. R. Heckel, S. Hoedl, and S. Schlamminger, *Torsion balance experiments: A low-energy frontier of particle physics*, *Prog. Part. Nucl. Phys.* **62** (2009) 102–134.

[44] W. D. Goldberger and M. B. Wise, *Modulus stabilization with bulk fields*, *Phys. Rev. Lett.* **83** (1999) 4922–4925, [hep-ph/9907447].

[45] J. M. Maldacena, *The large N limit of superconformal field theories and supergravity*, *Adv. Theor. Math. Phys.* **2** (1998) 231–252, [hep-th/9711200].

[46] B. Batell and T. Gherghetta, *Warped Phenomenology in the Holographic Basis*, *Phys. Rev.* **D77** (2008) 045002, [arXiv:0710.1838].

[47] B. Batell and T. Gherghetta, *Holographic Mixing Quantified*, *Phys. Rev.* **D76** (2007) 045017, [arXiv:0706.0890].

[48] R. Contino and A. Pomarol, *The holographic composite Higgs*, *Comptes Rendus Physique* **8** (2007) 1058–1067.

[49] R. Contino, T. Kramer, M. Son, and R. Sundrum, *Warped/Composite Phenomenology Simplified*, *JHEP* **05** (2007) 074, [hep-ph/0612180].

[50] R. Contino, L. Da Rold, and A. Pomarol, *Light custodians in natural composite Higgs models*, *Phys. Rev.* **D75** (2007) 055014, [hep-ph/0612048].

[51] R. Contino, *A holographic composite Higgs model*, hep-ph/0609148.

[52] C. Csaki, C. Grojean, L. Pilo, and J. Terning, *Towards a realistic model of Higgsless electroweak symmetry breaking*, *Phys. Rev. Lett.* **92** (2004) 101802, [hep-ph/0308038].

[53] K. Agashe, R. Contino, and A. Pomarol, *The Minimal Composite Higgs Model*, *Nucl. Phys.* **B719** (2005) 165–187, [hep-ph/0412089].

[54] G. Cacciapaglia, C. Csaki, G. Marandella, and J. Terning, *A New Custodian for a Realistic Higgsless Model*, *Phys. Rev.* **D75** (2007) 015003, [hep-ph/0607146].

[55] M. S. Carena, E. Ponton, J. Santiago, and C. E. M. Wagner, *Light Kaluza-Klein states in Randall-Sundrum models with custodial $SU(2)$*, *Nucl. Phys.* **B759** (2006) 202–227, [hep-ph/0607106].

[56] K. Agashe, A. Delgado, and R. Sundrum, *Grand unification in RS1*, *Ann. Phys.* **304** (2003) 145–164, [hep-ph/0212028].

[57] K. Agashe, R. Contino, and R. Sundrum, *Top compositeness and precision unification*, *Phys. Rev. Lett.* **95** (2005) 171804, [hep-ph/0502222].

[58] **UTfit** Collaboration, M. Bona *et al.*, *Model-independent constraints on $\Delta F = 2$ operators and the scale of New Physics*, *JHEP* **03** (2008) 049, [arXiv:0707.0636].

[59] T. Gherghetta and A. Pomarol, *Bulk fields and supersymmetry in a slice of AdS*, *Nucl. Phys.* **B586** (2000) 141–162, [hep-ph/0003129].

[60] Y. Grossman and M. Neubert, *Neutrino masses and mixings in non-factorizable geometry*, *Phys. Lett.* **B474** (2000) 361–371, [hep-ph/9912408].

[61] F. Goertz and T. Pfoh, *On the Perturbative Approach in the Randall-Sundrum Model*, *JHEP* **10** (2008) 035, [arXiv:0809.1378].

[62] M. E. Peskin and T. Takeuchi, *Estimation of oblique electroweak corrections*, *Phys. Rev.* **D46** (1992) 381–409.

[63] I. Maksymyk, C. P. Burgess, and D. London, *Beyond S, T and U*, *Phys. Rev.* **D50** (1994) 529–535, [hep-ph/9306267].

[64] G. Altarelli, R. Barbieri, and F. Caravaglios, *Nonstandard analysis of electroweak precision data*, *Nucl. Phys.* **B405** (1993) 3–23.

[65] C. P. Burgess, S. Godfrey, H. Konig, D. London, and I. Maksymyk, *A Global fit to extended oblique parameters*, *Phys. Lett.* **B326** (1994) 276–281, [hep-ph/9307337].

[66] C. P. Burgess, S. Godfrey, H. Konig, D. London, and I. Maksymyk, *Model independent global constraints on new physics*, *Phys. Rev.* **D49** (1994) 6115–6147, [hep-ph/9312291].

[67] Z. Han and W. Skiba, *Effective theory analysis of precision electroweak data*, *Phys. Rev.* **D71** (2005) 075009, [hep-ph/0412166].

[68] R. Barbieri, A. Pomarol, R. Rattazzi, and A. Strumia, *Electroweak symmetry breaking after LEP-1 and LEP-2*, *Nucl. Phys.* **B703** (2004) 127–146, [hep-ph/0405040].

[69] Z. Han, *Electroweak constraints on effective theories with $U(2) \times U(1)$ flavor symmetry*, *Phys. Rev.* **D73** (2006) 015005, [hep-ph/0510125].

[70] G. Cacciapaglia, C. Csaki, G. Marandella, and A. Strumia, *The minimal set of electroweak precision parameters*, *Phys. Rev.* **D74** (2006) 033011, [hep-ph/0604111].

[71] H. Flacher *et al.*, *Gfitter - Revisiting the Global Electroweak Fit of the Standard Model and Beyond*, *Eur. Phys. J.* **C60** (2009) 543–583, [arXiv:0811.0009].

[72] C. Csaki, J. Erlich, and J. Terning, *The effective Lagrangian in the Randall-Sundrum model and electroweak physics*, *Phys. Rev.* **D66** (2002) 064021, [hep-ph/0203034].

[73] S. J. Huber, C.-A. Lee, and Q. Shafi, *Kaluza-Klein excitations of W and Z at the LHC?*, *Phys. Lett.* **B531** (2002) 112–118, [hep-ph/0111465].

[74] J. L. Hewett, F. J. Petriello, and T. G. Rizzo, *Precision measurements and fermion geography in the Randall-Sundrum model revisited*, *JHEP* **09** (2002) 030, [hep-ph/0203091].

[75] M. S. Carena, A. Delgado, E. Ponton, T. M. P. Tait, and C. E. M. Wagner, *Precision electroweak data and unification of couplings in warped extra dimensions*, *Phys. Rev.* **D68** (2003) 035010, [hep-ph/0305188].

[76] **Particle Data Group** Collaboration, C. Amsler *et al.*, *Review of particle physics*, *Phys. Lett.* **B667** (2008) 1.

[77] N. Arkani-Hamed, M. Porrati, and L. Randall, *Holography and phenomenology*, *JHEP* **08** (2001) 017, [hep-th/0012148].

[78] K. Agashe, R. Contino, L. Da Rold, and A. Pomarol, *A custodial symmetry for $Zb\bar{b}$*, *Phys. Lett.* **B641** (2006) 62–66, [hep-ph/0605341].

[79] C. Csaki, C. Grojean, H. Murayama, L. Pilo, and J. Terning, *Gauge theories on an interval: Unitarity without a Higgs*, *Phys. Rev.* **D69** (2004) 055006, [hep-ph/0305237].

[80] C. Csaki, J. Hubisz, and P. Meade, *Electroweak symmetry breaking from extra dimensions*, hep-ph/0510275.

[81] K. Agashe *et al.*, *LHC Signals for Warped Electroweak Neutral Gauge Bosons*, *Phys. Rev.* **D76** (2007) 115015, [arXiv:0709.0007].

[82] C. Csaki, C. Grojean, J. Hubisz, Y. Shirman, and J. Terning, *Fermions on an interval: Quark and lepton masses without a Higgs*, *Phys. Rev.* **D70** (2004) 015012, [hep-ph/0310355].

[83] C. D. Froggatt and H. B. Nielsen, *Hierarchy of Quark Masses, Cabibbo Angles and CP Violation*, *Nucl. Phys.* **B147** (1979) 277.

[84] S. Casagrande, F. Goertz, U. Haisch, M. Neubert, and T. Pfoh, *Flavor Physics in the Randall-Sundrum Model: I. Theoretical Setup and Electroweak Precision Tests*, *JHEP* **10** (2008) 094, [arXiv:0807.4937].

[85] N. Arkani-Hamed and M. Schmaltz, *Hierarchies without symmetries from extra dimensions*, *Phys. Rev.* **D61** (2000) 033005, [hep-ph/9903417].

[86] K. Agashe, A. E. Blechman, and F. Petriello, *Probing the Randall-Sundrum geometric origin of flavor with lepton flavor violation*, *Phys. Rev.* **D74** (2006) 053011, [hep-ph/0606021].

[87] C. Csaki, C. Delaunay, C. Grojean, and Y. Grossman, *A Model of Lepton Masses from a Warped Extra Dimension*, *JHEP* **10** (2008) 055, [arXiv:0806.0356].

[88] K. Agashe, *Relaxing Constraints from Lepton Flavor Violation in 5D Flavorful Theories*, *Phys. Rev.* **D80** (2009) 115020, [arXiv:0902.2400].

[89] M. Byrd, *The Geometry of $SU(3)$*, physics/9708015.

[90] K. Fujikawa and A. Yamada, *Test of the chiral structure of the top - bottom charged current by the process $b \to s$ gamma*, *Phys. Rev.* **D49** (1994) 5890–5893.

[91] D. O. Carlson, E. Malkawi, and C. P. Yuan, *Probing the couplings of the top quark to gauge bosons*, *Phys. Lett.* **B337** (1994) 145–151, [hep-ph/9405277].

[92] E. Malkawi and C. P. Yuan, *A Global analysis of the top quark couplings to gauge bosons*, *Phys. Rev.* **D50** (1994) 4462–4477, [hep-ph/9405322].

[93] S. Dawson and G. Valencia, *Limits on Non-Standard Top Quark Couplings from Electroweak Measurements*, *Phys. Rev.* **D53** (1996) 1721–1724, [hep-ph/9510455].

[94] G. Burdman, M. C. Gonzalez-Garcia, and S. F. Novaes, *Anomalous couplings of the third generation in rare B decays*, *Phys. Rev.* **D61** (2000) 114016, [hep-ph/9906329].

[95] F. Larios, M. A. Perez, and C. P. Yuan, *Analysis of tbW and ttZ couplings from CLEO and LEP / SLC data*, *Phys. Lett.* **B457** (1999) 334–340, [hep-ph/9903394].

[96] B. Grzadkowski and M. Misiak, *Anomalous Wtb coupling effects in the weak radiative B- meson decay*, *Phys. rev.* **D78** (2008) 077501, [arXiv:0802.1413].

[97] X.-G. He, J. Tandean, and G. Valencia, *Probing New Physics in Charm Couplings with FCNC*, *Phys. Rev.* **D80** (2009) 035021, [arXiv:0904.2301].

[98] K. Agashe, G. Perez, and A. Soni, *Flavor structure of warped extra dimension models*, *Phys. Rev.* **D71** (2005) 016002, [hep-ph/0408134].

[99] C. Csaki, A. Falkowski, and A. Weiler, *The Flavor of the Composite Pseudo-Goldstone Higgs*, *JHEP* **09** (2008) 008, [arXiv:0804.1954].

[100] K. Agashe, A. Azatov, and L. Zhu, *Flavor Violation Tests of Warped/Composite SM in the Two- Site Approach*, *Phys. Rev.* **D79** (2009) 056006, [arXiv:0810.1016].

[101] D. Schaile *private correspondence*.

[102] S. Leone *Talk given at the WIN09 Workshop* (2009). Perugia, Italy.

[103] G. D'Ambrosio, G. F. Giudice, G. Isidori, and A. Strumia, *Minimal flavour violation: An effective field theory approach*, *Nucl. Phys.* **B645** (2002) 155–187, [hep-ph/0207036].

[104] L. J. Hall and L. Randall, *Weak scale effective supersymmetry*, *Phys. Rev. Lett.* **65** (1990) 2939–2942.

[105] A. J. Buras, P. Gambino, M. Gorbahn, S. Jäger, and L. Silvestrini, *Universal unitarity triangle and physics beyond the standard model*, *Phys. Lett.* **B500** (2001) 161–167, [hep-ph/0007085].

[106] A. J. Buras, *Minimal flavor violation*, *Acta Phys. Polon.* **B34** (2003) 5615–5668, [hep-ph/0310208].

[107] M. Bauer, S. Casagrande, L. Gruender, U. Haisch, and M. Neubert, *Little Randall-Sundrum models: ϵ_K strikes again*, arXiv:0811.3678.

[108] J. Hubisz and P. Meade, *Phenomenology of the littlest Higgs with T-parity*, *Phys. Rev.* **D71** (2005) 035016, [hep-ph/0411264].

[109] J. Hubisz, P. Meade, A. Noble, and M. Perelstein, *Electroweak precision constraints on the littlest Higgs model with T parity*, *JHEP* **01** (2006) 135, [hep-ph/0506042].

[110] M. Blanke, A. J. Buras, A. Poschenrieder, S. Recksiegel, C. Tarantino, S. Uhlig, and A. Weiler, *Another look at the flavour structure of the littlest Higgs model with T-parity*, *Phys. Lett.* **B646** (2007) 253–257, [hep-ph/0609284].

[111] M. Blanke, A. J. Buras, A. Poschenrieder, S. Recksiegel, C. Tarantino, S. Uhlig, and A. Weiler, *Rare and CP-violating K and B decays in the littlest Higgs model with T-parity*, hep-ph/0610298.

[112] P. H. Frampton, P. Q. Hung, and M. Sher, *Quarks and leptons beyond the third generation*, *Phys. Rept.* **330** (2000) 263, [hep-ph/9903387].

[113] F. del Aguila and J. Santiago, *Universality limits on bulk fermions*, *Phys. Lett.* **B493** (2000) 175–181, [hep-ph/0008143].

[114] C. Arzt, M. B. Einhorn, and J. Wudka, *Patterns of deviation from the standard model*, *Nucl. Phys.* **B433** (1995) 41–66, [hep-ph/9405214].

[115] F. del Aguila, M. Perez-Victoria, and J. Santiago, *Effective description of quark mixing*, *Phys. Lett.* **B492** (2000) 98–106, [hep-ph/0007160].

[116] A. Azatov, M. Toharia, and L. Zhu, *Higgs Mediated FCNC's in Warped Extra Dimensions*, *Phys. Rev.* **D80** (2009) 035016, [arXiv:0906.1990].

[117] M. Bauer, S. Casagrande, U. Haisch, and M. Neubert, *Flavor Physics in the Randall-Sundrum Model: II. Tree- Level Weak-Interaction Processes*, arXiv:0912.1625.

[118] G. Burdman, *Flavor violation in warped extra dimensions and CP asymmetries in B decays*, *Phys. Lett.* **B590** (2004) 86–94, [hep-ph/0310144].

[119] G. Moreau and J. I. Silva-Marcos, *Flavour physics of the RS model with KK masses reachable at LHC*, *JHEP* **03** (2006) 090, [hep-ph/0602155].

[120] M. Blanke, A. J. Buras, A. Poschenrieder, C. Tarantino, S. Uhlig, and A. Weiler, *Particle antiparticle mixing, ε_K, $\Delta\Gamma_q$, A^q_{SL}, $A_{CP}(B_d \to \psi K_S)$, $A_{CP}(B_s \to \psi\phi)$ and $B \to X_{s,d}\gamma$ in the littlest Higgs model with T- parity*, *JHEP* **12** (2006) 003, [hep-ph/0605214].

[121] S. Herrlich and U. Nierste, *Enhancement of the $K_L - K_S$ mass difference by short distance QCD corrections beyond leading logarithms*, *Nucl. Phys.* **B419** (1994) 292–322, [hep-ph/9310311].

[122] S. Herrlich and U. Nierste, *Indirect CP violation in the neutral kaon system beyond leading logarithms*, *Phys. Rev.* **D52** (1995) 6505–6518, [hep-ph/9507262].

[123] S. Herrlich and U. Nierste, *The Complete $\Delta S = 2$ Hamiltonian in the Next-To-Leading Order*, *Nucl. Phys.* **B476** (1996) 27–88, [hep-ph/9604330].

[124] A. J. Buras, M. Jamin, and P. H. Weisz, *Leading and Next-to-Leading QCD Corrections to ε Parameter and $B^0 - \bar{B}^0$ Mixing in the Presence of a Heavy Top Quark*, *Nucl. Phys.* **B347** (1990) 491–536.

[125] J. Urban, F. Krauss, U. Jentschura, and G. Soff, *Next-to-leading order QCD corrections for the $B^0 - \bar{B}^0$ mixing with an extended Higgs sector*, *Nucl. Phys.* **B523** (1998) 40–58, [hep-ph/9710245].

[126] M. Ciuchini *et al.*, *Next-to-leading order QCD corrections to $\Delta F = 2$ effective Hamiltonians*, *Nucl. Phys.* **B523** (1998) 501–525, [hep-ph/9711402].

[127] A. J. Buras, M. Misiak, and J. Urban, *Two-loop QCD anomalous dimensions of flavour-changing four-quark operators within and beyond the standard model*, *Nucl. Phys.* **B586** (2000) 397–426, [hep-ph/0005183].

[128] A. J. Buras, S. Jäger, and J. Urban, *Master formulae for $\Delta F = 2$ NLO-QCD factors in the standard model and beyond*, *Nucl. Phys.* **B605** (2001) 600–624, [hep-ph/0102316].

[129] L. B. Okun, *LEPTONS AND QUARKS*, . Amsterdam, Netherlands: North-Holland (1982) 361p.

[130] R. Babich *et al.*, *$K^0 - \bar{K}^0$ mixing beyond the standard model and CP- violating electroweak penguins in quenched QCD with exact chiral symmetry*, *Phys. Rev.* **D74** (2006) 073009, [hep-lat/0605016].

[131] D. Becirevic, V. Gimenez, G. Martinelli, M. Papinutto, and J. Reyes, *B-parameters of the complete set of matrix elements of $\Delta B = 2$ operators from the lattice*, *JHEP* **04** (2002) 025, [hep-lat/0110091].

[132] J. Laiho, R. S. Van de Water, and E. Lunghi, *Lattice QCD inputs to the CKM unitarity triangle analysis*, arXiv:0910.2928.

[133] **Particle Data Group** Collaboration, W. M. Yao *et al.*, *Review of particle physics*, *J. Phys.* **G33** (2006) 1–1232.

[134] A. J. Buras and D. Guadagnoli, *Correlations among new CP violating effects in $\Delta F = 2$ observables*, *Phys. Rev.* **D78** (2008) 033005, [arXiv:0805.3887].

[135] **UTfit** Collaboration, M. Bona *et al.*, *The UTfit collaboration report on the status of the unitarity triangle beyond the standard model. I: Model- independent analysis and minimal flavour violation*, *JHEP* **03** (2006) 080, [hep-ph/0509219].

[136] M. Ciuchini, E. Franco, V. Lubicz, F. Mescia, and C. Tarantino, *Lifetime differences and CP violation parameters of neutral B mesons at the next-to-leading order in QCD*, *JHEP* **08** (2003) 031, [hep-ph/0308029].

[137] Z. Ligeti, M. Papucci, and G. Perez, *Implications of the measurement of the $B_s^0 - \bar{B}_s^0$ mass difference*, *Phys. Rev. Lett* **97** (2006) 101801, [hep-ph/0604112].

[138] M. Blanke, A. J. Buras, D. Guadagnoli, and C. Tarantino, *Minimal Flavour Violation waiting for precise measurements of ΔM_s, $|V_{ub}|$, γ and $B^0_{s,d} \to \mu^+\mu^-$*, *JHEP* **10** (2006) 003, [hep-ph/0604057].

[139] A. J. Buras *et al.*, *Patterns of Flavour Violation in the Presence of a Fourth Generation of Quarks and Leptons*, arXiv:1002.2126.

[140] **E949** Collaboration, A. V. Artamonov *et al.*, *New measurement of the $K^+ \to \pi^+\nu\bar{\nu}$ branching ratio*, *Phys. Rev. Lett.* **101** (2008) 191802, [arXiv:0808.2459].

[141] A. J. Buras, M. Gorbahn, U. Haisch, and U. Nierste, *Charm quark contribution to $K^+ \to \pi^+ \nu\bar{\nu}$ at next-to-next-to-leading order*, *JHEP* **11** (2006) 002, [hep-ph/0603079].

[142] **E391a** Collaboration, J. K. Ahn *et al.*, *Search for the Decay $K_L^0 \to \pi^0 \nu\bar{\nu}$*, *Phys. Rev. Lett.* **100** (2008) 201802, [arXiv:0712.4164].

[143] J. Brod and M. Gorbahn, *Electroweak Corrections to the Charm Quark Contribution to $K^+ \to \pi^+ \nu\bar{\nu}$*, *Phys. Rev.* **D78** (2008) 034006, [arXiv:0805.4119].

[144] Y. Grossman and Y. Nir, *$K_L \to \pi^0 \nu\bar{\nu}$ beyond the standard model*, *Phys. Lett.* **B398** (1997) 163–168, [hep-ph/9701313].

[145] M. Blanke, *Insights from the Interplay of $K \to \pi\nu\bar{\nu}$ and ε_K on the New Physics Flavour Structure*, arXiv:0904.2528.

[146] G. Buchalla and A. J. Buras, *The rare decays $K \to \pi\nu\bar{\nu}$, $B \to X\nu\bar{\nu}$ and $B \to \ell^+\ell^-$: An update*, *Nucl. Phys.* **B548** (1999) 309–327, [hep-ph/9901288].

[147] A. J. Buras, M. Gorbahn, U. Haisch, and U. Nierste, *The rare decay $K^+ \to \pi^+ \nu\bar{\nu}$ at the next-to-next- to-leading order in QCD*, *Phys. Rev. Lett.* **95** (2005) 261805, [hep-ph/0508165].

[148] F. Mescia and C. Smith, *Improved estimates of rare K decay matrix-elements from $K_{\ell 3}$ decays*, *Phys. Rev.* **D76** (2007) 034017, [arXiv:0705.2025].

[149] G. Isidori, F. Mescia, and C. Smith, *Light-quark loops in $K \to \pi\nu\nu$*, *Nucl. Phys.* **B718** (2005) 319–338, [hep-ph/0503107].

[150] P. Colangelo, F. De Fazio, P. Santorelli, and E. Scrimieri, *Rare $B \to K^{(*)}$ neutrino anti-neutrino decays at B factories*, *Phys. Lett.* **B395** (1997) 339–344, [hep-ph/9610297].

[151] G. Buchalla, G. Hiller, and G. Isidori, *Phenomenology of non-standard Z couplings in exclusive semileptonic $b \to s$ transitions*, *Phys. Rev.* **D63** (2001) 014015, [hep-ph/0006136].

[152] M. Bona *et al.*, *SuperB: A High-Luminosity Asymmetric e^+e^- Super Flavor Factory. Conceptual Design Report*, arXiv:0709.0451.

[153] W. Altmannshofer, A. J. Buras, D. M. Straub, and M. Wick, *New strategies for New Physics search in $B \to K^*\nu\bar{\nu}$, $B \to K\nu\bar{\nu}$ and $B \to X_s\nu\bar{\nu}$ decays*, *JHEP* **04** (2009) 022, [arXiv:0902.0160].

[154] M. Bartsch, M. Beylich, G. Buchalla, and D. N. Gao, *Precision Flavour Physics with $B \to K\nu\bar{\nu}$ and $B \to K\ell^+\ell^-$*, *JHEP* **11** (2009) 011, [arXiv:0909.1512].

[155] G. D'Ambrosio, G. Ecker, G. Isidori, and J. Portoles, *The decays $K \to \pi\ell^+\ell^-$ beyond leading order in the chiral expansion*, *JHEP* **08** (1998) 004, [hep-ph/9808289].

[156] G. Buchalla, G. D'Ambrosio, and G. Isidori, *Extracting short-distance physics from $K_{L,S} \to \pi^0 e^+ e^-$ decays*, *Nucl. Phys.* **B672** (2003) 387–408, [hep-ph/0308008].

[157] G. Isidori, C. Smith, and R. Unterdorfer, *The rare decay $K_L \to \pi^0\mu^+\mu^-$ within the SM*, *Eur. Phys. J.* **C36** (2004) 57–66, [hep-ph/0404127].

[158] S. Friot, D. Greynat, and E. De Rafael, *Rare kaon decays revisited*, *Phys. Lett.* **B595** (2004) 301–308, [hep-ph/0404136].

[159] A. J. Buras, R. Fleischer, S. Recksiegel, and F. Schwab, *Anatomy of prominent B and K decays and signatures of CP- violating new physics in the electroweak penguin sector*, *Nucl. Phys.* **B697** (2004) 133–206, [hep-ph/0402112].

[160] A. J. Buras, M. E. Lautenbacher, M. Misiak, and M. Munz, *Direct CP violation in $K_L \to \pi^0 e^+ e^-$ beyond leading logarithms*, *Nucl. Phys.* **B423** (1994) 349–383, [hep-ph/9402347].

[161] F. Mescia, C. Smith, and S. Trine, *$K_L \to \pi^0 e^+ e^-$ and $K_L \to \pi^0\mu^+\mu^-$: A binary star on the stage of flavor physics*, *JHEP* **08** (2006) 088, [hep-ph/0606081].

[162] **KTeV** Collaboration, A. Alavi-Harati *et al.*, *Search for the Rare Decay $K_L \to \pi^0 e^+ e^-$*, *Phys. Rev. Lett.* **93** (2004) 021805, [hep-ex/0309072].

[163] **KTeV** Collaboration, A. Alavi-Harati *et al.*, *Search for the Decay $K_L \to \pi^0\mu^+\mu^-$*, *Phys. Rev. Lett.* **84** (2000) 5279–5282, [hep-ex/0001006].

[164] J. Prades, *ChPT Progress on Non-Leptonic and Radiative Kaon Decays*, *PoS* **KAON** (2008) 022, [arXiv:0707.1789].

[165] C. Bruno and J. Prades, *Rare Kaon Decays in the $1/N_c$-Expansion*, *Z. Phys.* **C57** (1993) 585–594, [hep-ph/9209231].

[166] G. Isidori and R. Unterdorfer, *On the short-distance constraints from $K_{L,S} \to \mu^+\mu^-$*, *JHEP* **01** (2004) 009, [hep-ph/0311084].

[167] M. Gorbahn and U. Haisch, *Charm quark contribution to $K_L \to \mu^+\mu^-$ at next-to-next-to-leading order*, *Phys. Rev. Lett.* **97** (2006) 122002, [hep-ph/0605203].

[168] **CDF** Collaboration, T. Aaltonen *et al.*, *Search for $B_s^0 \to \mu^+\mu^-$ and $B_d^0 \to \mu^+\mu^-$ decays with $2fb^{-1}$ of $p\bar{p}$ collisions*, *Phys. Rev. Lett.* **100** (2008) 101802, [arXiv:0712.1708].

[169] **D0** Collaboration, V. M. Abazov *et al.*, *Search for $B_s \to \mu^+\mu^-$ at D0*, *Phys. Rev.* **D76** (2007) 092001, [arXiv:0707.3997].

[170] J. Shigemitsu *et al.*, *Recent results on B mixing and decay constants from HPQCD*, arXiv:0910.4131.

[171] C. Jarlskog, *Commutator of the Quark Mass Matrices in the Standard Electroweak Model and a Measure of Maximal CP Violation*, *Phys. Rev. Lett.* **55** (1985) 1039.

[172] R. Barbieri and G. F. Giudice, *Upper Bounds on Supersymmetric Particle Masses*, *Nucl. Phys.* **B306** (1988) 63.

[173] **Heavy Flavor Averaging Group (HFAG)** Collaboration, E. Barberio *et al.*, *Averages of b-hadron properties at the end of 2006*, arXiv:0704.3575.

[174] **HPQCD** Collaboration, I. Allison *et al.*, *High-Precision Charm-Quark Mass from Current-Current Correlators in Lattice and Continuum QCD*, *Phys. Rev.* **D78** (2008) 054513, [arXiv:0805.2999].

[175] K. G. Chetyrkin *et al.*, *Charm and Bottom Quark Masses: An Update*, arXiv:0907.2110.

[176] G. Buchalla, *Renormalization of $\Delta B = 2$ transitions in the static limit beyond leading logarithms*, *Phys. Lett.* **B395** (1997) 364–368, [hep-ph/9608232].

[177] **Tevatron Electroweak Working Group** Collaboration, *Combination of CDF and D0 Results on the Mass of the Top Quark*, arXiv:0903.2503.

[178] V. Lubicz and C. Tarantino, *Flavour physics and Lattice QCD: averages of lattice inputs for the Unitarity Triangle Analysis*, *Nuovo Cim.* **123B** (2008) 674–688, [arXiv:0807.4605].

[179] O. Gedalia, G. Isidori, and G. Perez, *Combining Direct & Indirect Kaon CP Violation to Constrain the Warped KK Scale*, *Phys. Lett.* **B682** (2009) 200–206, [arXiv:0905.3264].

[180] A. L. Fitzpatrick, G. Perez, and L. Randall, *Flavor from Minimal Flavor Violation & a Viable Randall- Sundrum Model*, arXiv:0710.1869.

[181] J. Santiago, *Minimal Flavor Protection: A New Flavor Paradigm in Warped Models*, *JHEP* **12** (2008) 046, [arXiv:0806.1230].

[182] C. Csaki, A. Falkowski, and A. Weiler, *A Simple Flavor Protection for RS*, arXiv:0806.3757.

[183] C. Csaki, G. Perez, Z. Surujon, and A. Weiler, *Flavor Alignment via Shining in RS*, arXiv:0907.0474.

[184] **Heavy Flavor Averaging Group** Collaboration, E. Barberio *et al.*, *Averages of b−hadron and c−hadron Properties at the End of 2007*, arXiv:0808.1297.

[185] **CDF** Collaboration, T. Aaltonen *et al.*, *First Flavor-Tagged Determination of Bounds on Mixing- Induced CP Violation in $B_s \to J/\psi\,\phi$ Decays*, *Phys. Rev. Lett.* **100** (2008) 161802, [arXiv:0712.2397].

[186] **D0** Collaboration, V. M. Abazov *et al.*, *Measurement of B_s^0 mixing parameters from the flavor-tagged decay $B_s^0 \to J/\psi\phi$*, arXiv:0802.2255.

[187] M. Blanke, *The custodially protected Randall-Sundrum model: theoretical aspects and flavour phenomenology*, (2009).

[188] H. Georgi and A. Pais, *Calculability and naturalness in gauge theories*, *Phys. Rev.* **D10** (1974) 539.

[189] H. Georgi and A. Pais, *Natural stepwise breaking of gauge and discrete symmetries*, *Phys. Rev.* **D16** (1977) 3520.

[190] N. Arkani-Hamed, A. G. Cohen, and H. Georgi, *(de)constructing dimensions*, *Phys. Rev. Lett.* **86** (2001) 4757–4761, [hep-th/0104005].

[191] N. Arkani-Hamed, A. G. Cohen, and H. Georgi, *Electroweak symmetry breaking from dimensional deconstruction*, *Phys. Lett.* **B513** (2001) 232–240, [hep-ph/0105239].

[192] N. Arkani-Hamed, A. G. Cohen, E. Katz, and A. E. Nelson, *The littlest higgs*, *JHEP* **07** (2002) 034, [hep-ph/0206021].

[193] H.-C. Cheng and I. Low, *TeV symmetry and the little hierarchy problem*, *JHEP* **09** (2003) 051, [hep-ph/0308199].

[194] H.-C. Cheng and I. Low, *Little hierarchy, little Higgses, and a little symmetry*, *JHEP* **08** (2004) 061, [hep-ph/0405243].

[195] I. Low, *T parity and the littlest Higgs*, *JHEP* **10** (2004) 067, [hep-ph/0409025].

[196] A. J. Buras, A. Poschenrieder, and S. Uhlig, *Particle antiparticle mixing, ε_K and the unitarity triangle in the littlest Higgs model*, *Nucl. Phys.* **B716** (2005) 173–198, [hep-ph/0410309].

[197] A. J. Buras, A. Poschenrieder, S. Uhlig, and W. A. Bardeen, *Rare K and B decays in the littlest Higgs model without T- parity*, *JHEP* **11** (2006) 062, [hep-ph/0607189].

[198] J. Hubisz, S. J. Lee, and G. Paz, *The flavor of a little Higgs with T-parity*, *JHEP* **06** (2006) 041, [hep-ph/0512169].

[199] I. I. Bigi, M. Blanke, A. J. Buras, and S. Recksiegel, *CP Violation in $D^0 - \bar{D}^0$ Oscillations: General Considerations and Applications to the Littlest Higgs Model with T-Parity*, *JHEP* **07** (2009) 097, [arXiv:0904.1545].

[200] M. Blanke, A. J. Buras, S. Recksiegel, and C. Tarantino, *The Littlest Higgs Model with T-Parity Facing CP-Violation in B_s - $\bar{B}_s$ Mixing*, arXiv:0805.4393.

[201] M. Blanke, A. J. Buras, S. Recksiegel, C. Tarantino, and S. Uhlig, *Correlations between ε'/ε and Rare K Decays in the Littlest Higgs Model with T-Parity*, *JHEP* **06** (2007) 082, [arXiv:0704.3329].

[202] T. Goto, Y. Okada, and Y. Yamamoto, *Ultraviolet divergences of flavor changing amplitudes in the littlest Higgs model with T-parity*, *Phys. Lett.* **B670** (2009) 378–382, [arXiv:0809.4753].

[203] F. del Aguila, J. I. Illana, and M. D. Jenkins, *Precise limits from lepton flavour violating processes on the Littlest Higgs model with T-parity*, *JHEP* **01** (2009) 080, [arXiv:0811.2891].

[204] M. Blanke, A. J. Buras, B. Duling, A. Poschenrieder, and C. Tarantino, *Charged lepton flavour violation and $(g-2)_\mu$ in the littlest Higgs model with T-parity: A clear distinction from supersymmetry*, hep-ph/0702136.

[205] M. Blanke, A. J. Buras, S. Recksiegel, C. Tarantino, and S. Uhlig, *Littlest Higgs Model with T-Parity Confronting the New Data on $D^0 - \bar{D}^0$ Mixing*, *Phys. Lett.* **B657** (2007) 81–86, [hep-ph/0703254].

[206] M. Blanke, A. J. Buras, B. Duling, S. Recksiegel, and C. Tarantino, *FCNC Processes in the Littlest Higgs Model with T-Parity: a 2009 Look*, arXiv:0906.5454.

[207] M. Maltoni, V. A. Novikov, L. B. Okun, A. N. Rozanov, and M. I. Vysotsky, *Extra quark-lepton generations and precision measurements*, *Phys. Lett.* **B476** (2000) 107–115, [hep-ph/9911535].

[208] H.-J. He, N. Polonsky, and S.-f. Su, *Extra families, Higgs spectrum and oblique corrections*, *Phys. Rev.* **D64** (2001) 053004, [hep-ph/0102144].

[209] J. Alwall *et al.*, *Is $V_{tb} \simeq 1$?*, *Eur. Phys. J.* **C49** (2007) 791–801, [hep-ph/0607115].

[210] G. D. Kribs, T. Plehn, M. Spannowsky, and T. M. P. Tait, *Four generations and Higgs physics*, *Phys. Rev.* **D76** (2007) 075016, [arXiv:0706.3718].

[211] M. S. Chanowitz, *Bounding CKM Mixing with a Fourth Family*, *Phys. Rev.* **D79** (2009) 113008, [arXiv:0904.3570].

[212] V. A. Novikov, A. N. Rozanov, and M. I. Vysotsky, *Once more on extra quark-lepton generations and precision measurements*, arXiv:0904.4570.

[213] M. Hashimoto, *Constraints on Mass Spectrum of Fourth Generation Fermions and Higgs Bosons*, arXiv:1001.4335.

[214] P. Q. Hung, *Minimal $SU(5)$ resuscitated by long-lived quarks and leptons*, *Phys. Rev. Lett.* **80** (1998) 3000–3003, [hep-ph/9712338].

[215] W.-S. Hou, *CP Violation and Baryogenesis from New Heavy Quarks*, *Chin. J. Phys.* **47** (2009) 134, [arXiv:0803.1234].

[216] Y. Kikukawa, M. Kohda, and J. Yasuda, *The strongly coupled fourth family and a first-order electroweak phase transition (I) Quark sector*, *Prog. Theor. Phys.* **122** (2009) 401–426, [arXiv:0901.1962].

[217] R. Fok and G. D. Kribs, *Four Generations, the Electroweak Phase Transition, and Supersymmetry*, *Phys. Rev.* **D78** (2008) 075023, [arXiv:0803.4207].

[218] B. Holdom, *Heavy quarks and electroweak symmetry breaking*, *Phys. Rev. Lett.* **57** (1986) 2496.

[219] C. T. Hill, M. A. Luty, and E. A. Paschos, *Electroweak symmetry breaking by fourth generation condensates and the neutrino spectrum*, *Phys. Rev.* **D43** (1991) 3011–3025.

[220] S. F. King, *Is electroweak symmetry broken by a fourth family of quarks? *, *Phys. Lett.* **B234** (1990) 108–112.

[221] G. Burdman and L. Da Rold, *Electroweak Symmetry Breaking from a Holographic Fourth Generation*, *JHEP* **12** (2007) 086, [arXiv:0710.0623].

[222] P. Q. Hung and C. Xiong, *Renormalization Group Fixed Point with a Fourth Generation: Higgs-induced Bound States and Condensates*, arXiv:0911.3890.

[223] P. Q. Hung and C. Xiong, *Renormalization Group Fixed Point with a Fourth Generation: Solution to the hierarchy problem*, arXiv:0911.3892.

[224] W.-S. Hou, M. Nagashima, and A. Soddu, *Enhanced $K_L \to \pi^0 \nu\bar{\nu}$ from direct CP violation in $B \to K\pi$ with four generations*, *Phys. Rev.* **D72** (2005) 115007, [hep-ph/0508237].

[225] W.-S. Hou, M. Nagashima, and A. Soddu, *Large time-dependent CP violation in B_s^0 system and finite D^0 - $\bar{D}^0$ mass difference in four generation standard model*, *Phys. Rev.* **D76** (2007) 016004, [hep-ph/0610385].

[226] A. Soni, A. K. Alok, A. Giri, R. Mohanta, and S. Nandi, *The Fourth family: A Natural explanation for the observed pattern of anomalies in B–CP asymmetries*, arXiv:0807.1971.

[227] G. Burdman, L. Da Rold, and R. D. Matheus, *The Lepton Sector of a Fourth Generation*, arXiv:0912.5219.

[228] J. A. Herrera, R. H. Benavides, and W. A. Ponce, *Flavor changing neutral currents with a fourth family of quarks*, *Phys. Rev.* **D78** (2008) 073008, [arXiv:0810.3871].

[229] M. Bobrowski, A. Lenz, J. Riedl, and J. Rohrwild, *How much space is left for a new family of fermions?*, *Phys. Rev.* **D79** (2009) 113006, [arXiv:0902.4883].

[230] A. Soni, A. K. Alok, A. Giri, R. Mohanta, and S. Nandi, *SM with four generations: Selected implications for rare B and K decays*, arXiv:1002.0595.